ELUCIDATION OF THE IMPACT OF N-GLYCAN STRUCTURE ON PHYSICAL STABILITY AND LOCAL FLEXIBILITY OF WELL-DEFINED IgG1-Fc GLYCOFORMS FROM A PHARMACEUTICAL DEVELOPMENT PERSPECTIVE

By

Apurva More
M.S., Pharmaceutical Chemistry, 2014, The University of Kansas, Lawrence, KS
B.Pharm., Pharmacy, 2011, Institute of Chemical Technology, Mumbai, India

Submitted to the graduate degree program in Pharmaceutical Chemistry and the Graduate Faculty of the University of Kansas in partial fulfillment of the requirements for the degree of Doctor of Philosophy.

Chair: David B. Volkin, Ph.D.

Thomas J. Tolbert, Ph.D.

David D. Weis, Ph.D.

C. Russell Middaugh, Ph.D.

Eric J. Deeds, Ph.D.

Date Defended: 29 June 2017

The dissertation committee for Apurva More certifies that this is the approved version of the following dissertation:

ELUCIDATION OF THE IMPACT OF N-GLYCAN STRUCTURE ON PHYSICAL STABILITY AND LOCAL FLEXIBILITY OF WELL-DEFINED IgG1-Fc GLYCOFORMS FROM A PHARMACEUTICAL DEVELOPMENT PERSPECTIVE

_____

Chair: David B. Volkin, Ph.D.

Date Approved: 29 June 2017

ABSTRACT

Therapeutic efficacies of IgG monoclonal antibodies (mAbs) depend on their physicochemical structural integrity, stability, flexibility and biological functionality. IgG-Fc glycosylation at Asn-297 is important for the structural integrity and effector function activities of IgG mAb therapeutics and is a key contributor of their heterogeneity. Molecular heterogeneities (like glycosylation) must be closely monitored and assessed during development of mAbs from drug candidate to marketed product and during biosimilar development. A variety of techniques are being developed to monitor chemical structure and glycosylation profiles of mAbs, however, novel analytical techniques are needed to better understand the effects of glycosylation on their complex higher order structures and dynamics for their effective development. In comparability and biosimilarity exercises, analytical characterization tools serve as the foundation for establishing similarity between pre change versus post change products and biosimilar versus innovator product. Hence, better tools are needed for drawing comparisons between the results. In this study, four highly purified, well-defined recombinant IgG1-Fc glycoform variants (High-mannose-Fc (HM-Fc), Man5-Fc (truncated glycoform), GlcNAc-Fc (truncated glycoform), and non-glycosylated-Fc (N297Q-Fc) were produced which served as model glycoproteins to study the effect of IgG1-Fc N-linked glycosylation on various pharmaceutical properties. This work explores the utility of yeast expression along with *in vitro* enzymatic digestion for obtaining homogenous glycoform profiles of IgG Fc glycans; which is extremely challenging to achieve considering the observed inherent glycan heterogeneity in expression hosts. We developed and utilized various orthogonal analytical techniques to explore the relationship between glycosylation and physical stability of these IgG1-Fc glycoforms and compared their physical stability in two different formulations to mimic follow on therapeutics or biosimilars that might

be formulated differently. Hence, this study contributed towards the ongoing development of data visualization and mathematical modeling tools for comparability and biosimilarity assessments. To simulate a more practical biosimilar comparability scenario, various mixtures of the four glycoforms were made to mimic heterogeneity found in biosimilars. The physical stability of these mixtures was evaluated by combination of high-throughput biophysical techniques. The ability of various biophysical techniques to demonstrate the estimated differences between the physical stability of the mixtures was examined. Even though the biophysical techniques utilized in this study are the most commonly used tools in the industry, these are low in resolution and only show the average conformational outcome. Hence, to obtain high-resolution peptide-level information on changes in local dynamics because of changes in IgG1-Fc glycans, hydrogen exchange (HX-MS) in combination with pepsin proteolytic digestion and liquid chromatography-mass spectrometry (LC-MS) was utilized. Previous HX-MS studies on IgG mAbs in our laboratory showed an increased flexibility of a particular peptide segment in the Fc region in the presence of excipients and salts. This result was attributed to the disruption in packing of the heterogeneous glycan structures with the Fc region. Another goal of this dissertation was to explore the mechanisms of interactions between glycans and IgG1-Fc. The correlations between glycosylation and physicochemical structure, stability and flexibility of well-defined IgG1-Fc glycoforms in this dissertation, will serve as important tools to enable rational design and optimization of stable IgG formulation conditions to avoid conformational destabilization and aggregation issues during their manufacture, long-term storage and administration. The extensive analytical characterization approach utilized in this dissertation will contribute towards the ongoing development of statistical tools as required by the US Food

and Drug Administration (FDA), for similarity analysis between biosimilar and innovator therapeutics.

Dedicated to:

My parents

Swati and Shirish More

ACKNOWLEDGEMENTS

The accomplishments in this dissertation would not have been possible without the immense support and guidance of my research advisor, Professor David Volkin. I thank him for giving me an opportunity to work in his laboratory and giving me a collaborative project, which involved working with the FDA and multiple laboratories at the University of Kansas (KU). I would like to thank him for believing in me, having faith in my capabilities and constantly motivating me to improve my scientific research and communication skills. Along with learning scientific research skills and protein characterization techniques in his laboratory, I have learnt the importance of keeping deadlines, organization and making good scientific presentations.

I would like to thank my dissertation co-advisors, Professor Thomas Tolbert and Professor David Weis for their scientific guidance and giving me the opportunity to perform research in their laboratories. I would like to thank Professor Thomas Tolbert for his enthusiasm in guiding me about protein production, glycosylation and providing an immense array of resources for carrying out research in his laboratory. I admire his passion for science along with his kind and student friendly nature, which makes working in his laboratory fun. I would like to thank Professor David Weis for his encouragement in training me to use the instruments in his laboratory, which required a lot of time and expertise. I also thank for him for providing valuable inputs towards editing this dissertation.

I would like to thank Dr. C. Russell Middaugh for his lessons on protein biophysics, stability and solubility in the Advanced Biotechnology and Equilibrium courses. Throughout my graduate study at KU, I have learnt immensely by interacting with him, not only about science, but also about life in general. I admire his positive outlook towards life, lively and cheerful nature that

creates a fun environment at the workplace. I want to thank Dr. Sangeeta Joshi for her immense scientific support and friendship throughout my time at KU. I thank her for giving me courage and motivating me throughout my PhD to be more confident in performing and presenting my research work. She is a role model for women in science.

I have learnt a lot from the past and present members of the Macromolecule and Vaccine Stabilization Center (MVSC). I would like to thank my current lab members Vishal Toprani, Sanjeev Agarwal, Dr. Ronald Toth and Dr. Ying Wan for their constant support, scientific guidance, and encouragement for doing research. I thank past members of MVSC Dr. Neha Sahni, Harshit Khasa and Dr. Jayant Arora for laboratory training, friendship, and support whenever needed. The wide variety of resources at MVSC resulted in obtaining extensive amount of data for this dissertation and helped learning about protein characterization. I acknowledge financial support from Siegfried Lindenbaum Fellowship for my tuition throughout the course of my graduate studies.

I would like to thank all the professors from Pharmaceutical Chemistry Department for their support and setting up an excellent foundation of the coursework. I like to thank all my schoolteachers from Jnana Prabodhini Prashala, and Fergusson College, Pune, India for their training in basic science. I would like to thank my best friend Renuka Kulkarni for always being supportive and listening to me throughout my PhD. It has been possible for me to pursue this research in the United States because of the support of my parents Swati and Shirish More and I dedicate this achievement to them.

TABLE OF CONTENTS

LIST OF TABLES

LIST OF FIGURES

LIST OF SUPPLEMENTARY FIGURES

LIST OF SUPPLEMENTARY TABLES

Chapter 1 Introduction

1.1 Role of Sugars in Nature

Monosaccharide sugar molecules (or more generally as carbohydrates), when linked together via glycosidic bonds to form multimers referred to as glycans or oligosaccharides (2-20 monosaccharides) or polysaccharides (or more generally as carbohydrate)[1], are one of the major macromolecular building blocks of life along with nucleic acids, proteins and lipids. The biological roles of glycans are vast and complex and could be broadly classified into three categories, first being structural and modulatory roles, second being extrinsic/intrinsic interspecies recognition and third being molecular mimicry of host glycans by microorganisms.[2,3] The roles of glycans specifically in modulating functions of proteins to which they are attached are very important topics biologically, as well as for pharmaceutical development of glycoproteins as therapeutic drugs or vaccine antigens. Structural and regulatory roles of glycans with respect to glycoproteins include contribution to aqueous solubility, glycoprotein folding, protection against proteases, and modulation of membrane receptor binding and signaling along with tuning a wide range of biological functions of proteins. Extrinsic and intrinsic recognition roles of glycans include binding of proteins like viral agglutins (e.g., influenza virus), bacterial and plant toxins to enter cells and evade immune responses, mediating recognition, uptake and processing of antigenic proteins containing terminal mannose (Man) or N-acetyl glucosamine (GlcNAc) glycans through C-type lectin interactions and acting as antigenic epitopes to trigger immune reactions. Lastly, molecular mimicry functions include evolution of glycan patterns of microorganisms to mimic glycans that are present in the host system.[2,4]

Majority of protein molecules in clinical development as therapeutic drug candidates are glycosylated. To extract the potential of glycoproteins as therapeutic molecules, it is important to

better understand the underlying mechanisms that affect these functions by developing systematic approaches and techniques to analyze them.[2] In recent years, there has been a huge increase in development and regulatory approvals of monoclonal antibody (mAb) therapeutics firstly, due to their specific action and secondly their use as vehicles for targeted delivery of other therapeutic entities (e.g., small molecules in case of antibody drug conjugates (ADCs) and proteins in case of Fc-fusion therapeutics) that lead to fewer side effects.[5] Biologically, five classes/isotypes of antibodies (which are IgG, IgM, IgA, IgD and IgE) mediate the adaptive immune response in humans for long-term protection against potential environmental pathogens. The combined effects of all the antibody isotypes result in removal and destruction of pathogens during an attack towards the immune system. However, the IgG class of antibodies is the popular choice for antibody molecules for therapeutic development due to their high abundance (~75%) in human serum as compared to the other types. Hence, the primary focus of our work will be on the IgG type of antibodies, especially the fragment crystallizable (Fc) which is glycosylated.

1.2 Structure and Function of IgG1 Antibodies

IgG1, IgG2, IgG3 and IgG4 are four subclasses of IgG antibodies having unique profiles of biological activities.[6] The IgG1 subclass is not only the abundant subclass present in the human serum, but also is the most well studied and the most popular choice for development as therapeutic antibody drug candidates. In addition, when developing a recombinant monoclonal antibody (rmAb) therapy, the selection of IgG subclass depends on the required biological effect these proteins can produce. The IgG1 glycoprotein (similar to other IgG subclasses) is a homodimer containing two heavy chains and two light chains connected by intra and intermolecular disulfide linkages which are folded to form two fragment antigen-binding (Fab) domains and one fragment crystallizable (Fc) domain. Each Fab domain is a heterodimer of light

chain linked to the heavy chain by a disulfide bond while the Fc domain is made of two heavy chains that exist as a dimer held together by two disulfide bonds in a hinge region as seen in Figure 1.1. Each Fab domain consists of two variable domains and two constant C_H1 domains, while the Fc has each of two constant C_H3 and C_H2 domains. The C_H2 domains have two N-linked-glycans attached to Asn-297 residue at each side and are packed together with N-glycans that fill the horseshoe shaped pocket between two C_H2 domains. The two C_H3 domains form multiple noncovalent interactions with one another.[7] The Fab domains of IgG1 antibodies neutralize antigens by specific binding and the glycosylated Fc domain is responsible for removal and destruction of antigens by governing biological functions like antibody-dependent cellular cytotoxicity (ADCC), complement dependent cytotoxicity (CDC), and clearance.[8] The N-glycans modulate binding of the Fc to different Fc ɣ receptors (FcɣR/FcR) to govern ADCC and CDC activities. It was commonly believed that FcRn binding is unaffected by glycosylation, however, in a recent study it was shown that glycans might affect FcRn binding which could ultimately affect antibody clearance.[9]

1.3 Glycosylation in IgG1 Antibodies

Protein glycosylation is the ubiquitous post-translational modification (PTM) and governs an immense array of biological functions due to their remarkable complexity and diversity between various organisms.[2-4,10-12] Almost 50 % of human genes encode a conserved site for glycan attachment comprising of an amino acid sequence –N-X-S/T- (X can be any AA other than proline) which is called an N-liked glycosylation site. This attachment takes place as co and/or post-translational events in the endoplasmic reticulum (ER) and the Golgi apparatus. Another site of glycan attachment lies in the oxygen of hydroxyl groups of side chains of amino acids (AA) serine, threonine and tyrosine which is called as O-linked glycosylation site, and this

attachment takes place in the Golgi.[13] Antibodies are glycoproteins and contain predominantly N-linked glycans at different Asn residues in the conserved sequence of both Fab and Fc domains.[6] Further, in IgG1 class of antibodies, the conserved N-liked glycosylation site lies on the Asn-297 residue in the Fc domain and is extremely crucial for the non-antigen binding biological functions of antibodies via the Fc. However, N-glycosylation in the Fab domains is variable (~15–25%),[14] and may or may not be present, depending on the presence of the conserved glycosylation AA sequence.

1.4 Structure and Type of N-linked Glycans in Human Serum IgG1

There are three broad classes of N-linked oligosaccharides associated with antibodies, which are the complex, the high-mannose and the hybrid type (as seen in Figure 1.1). Neither the high-mannose type nor the hybrid type glycans occur naturally on human IgG1 antibodies. The high-mannose type has been detected in antibodies expressed in yeast cell lines along with some minor amounts produced in rodent mammalian cell lines such as Chinese hamster ovary (CHO) and mouse myeloma (NS0).[15] As seen in Figure 1.1, glycans present on the human serum IgG1 Fc of polyclonal IgG, attached at Asn297, consists of complex biantennary types that have a core heptasaccharide that is conserved throughout all the glycoforms. Macro-heterogeneity exists due to the site of glycan attachment and can be symmetric or asymmetric depending on whether same or different glycans are attached to both the glycosylation sites on each of the Fc C_H2 domains. Micro-heterogeneity exists due to the type of glycan attachments to the core. For example, the attachment of glycans like fucose (Fuc), galactose (Gal), bisecting N-acetylglucosamine (GlcNAc) and N-acetylneuraminic acid (NANA or sialic acid) to the heptasaccharide core can cause heterogeneity. All the different combinations of these glycans attached to the core produce a heterogeneous pool of IgG1 glycoforms in the human serum[16]. Compared to Fc N-

glycosylation, the Fab glycans (if present) consists of high amounts of bisecting GlcNAc, galactose, and sialic acid and low core fucose. In human serum, around 4% of the polyclonal IgG Fabs have high-mannose glycans, however, they are rarely present in the Fc regions.[14]

1.5 Altered glycosylation in disease states

In humans, protein glycosylation plays an important role in growth and development and it has been observed that the glycoform profile of IgG varies with age, gender, over the term of pregnancy and disease conditions.[17] Changed glycosylation pattern is especially observed in many chronic and inflammatory autoimmune diseases[18] like rheumatoid arthritis, Crohn's disease and vasculitis, different types of cancers and hypercholesterolemia.[16,19,20] Previous studies have shown that decreased galactosylation of total serum IgG was observed in rheumatoid arthritis, Crohn's disease and cancer as compared with healthy individual.[16,20] The amounts and types of Fab glycans too can vary during certain physiological and pathological conditions, suggesting that N-glycosylation on polyclonal IgG might contribute to immune suppression or pathophysiology and potentially serve as biomarkers.[14]

1.6 Structure and Type of N-linked Glycans in Recombinantly Produced IgG Therapeutics

For mAb therapeutics to be fully biologically active, it is essential that they have fully occupied N-glycosylation sites in the C_H2 domain of the Fc (aglycosylated mAbs can still bind antigen and in some cases are very active since Fc effector function not required).[16,21,22] Figure 1.2 shows the common types of N-glycans found in therapeutic mAbs. Mammalian cells (CHO) and murine cells (NS0 or SP2/0) are the most commonly used expression hosts for production of rmAbs. The glycoforms of IgG mAbs produced in CHO cells are very similar to those present in

human serum IgGs, except for the bisecting GlcNAc and terminal sialic acid (NANA) which are present in relatively low amounts in human serum IgGs.[23] NS0 or SP2/0 cells produce rmAbs with have low levels of galactose-α1, 3-galactose and N-glycolylneuraminic acid (NGNA) instead of NANA which could be immunogenic in humans. All the production vessels above may add a α2, 3-linked N-glycylneuraminic acid which is not present in humans (α2, 6-linked N-glycylneuraminic acid in humans).[16] E. *coli* is also used for production of non-glycosylated mAbs or Fab fragments in the cases where Fc effector functions are not needed.

1.7 Influence of Glycosylation on Physicochemical Properties and Stability of IgG

Therapeutic antibodies are proteins, which are structurally complex high molecular weight molecules that are sensitive to their environment. Certain change during their production, purification, manufacturing, storage and delivery might lead to changes to their primary structure (also post-translational modification) or higher order structure (HOS). Primary structural changes occur to amino acid residues which are known as chemical instabilities in mAbs are deamidation (Asn to Asp, Gln to Glu), oxidation (Cys, His, Met, Tyr, Trp), isomerization (Asp to isoAsp), racemization (L and D), formation of acidic species (e.g. glycation with reducing sugars, deamidation by aspartic acid formation, addition of sialic acid glycans), formation of basic species (e.g., pyroGlu formation and succinimide formation during deamidation), proteolytic degradation, C-terminal clipping, fragmentation and disulfide bond heterogeneity (shuffling, thioether and trisulfide formation). Another aspect of primary structure changes are changes in glycosylation profiles which can occur during the production and commercial manufacturing of mAbs. Glycosylation is highly dependent upon the type of expression host, cell culture conditions and parameters, which could change during process development, large-scale manufacturing and biosimilar development.

Changes in higher order structures of proteins (secondary, tertiary and quaternary structures) known as physical instabilities are aggregation, denaturation, precipitation and surface adsorption. All these structural instabilities pose the biggest challenges for mAb pharmaceutical development and can negatively influence their therapeutic efficacies by decreasing dose, causing immunogenicity and lowering target binding.[5,24] In case of traditional small molecule drugs, the physicochemical instabilities are easier to predict and control due their much simpler structures than proteins. Even though protein drugs show well-defined chemical instabilities, the additional layers of their secondary, tertiary and quaternary structures lead to complicated higher order structures. Thus, overall, the rate and extent of chemical and physical degradations of proteins become interdependent. Additionally, glycosylation is a natural chemical modification to the Asn297 residue in both the C_H2 domains of the IgG antibodies, and is known to affect the chemical and physical structure of antibodies as discussed below.

1.7.1 Oxidation

His, Met, Cys, Trp, and Tyr amino acids are prone to oxidation. Many studies have identified oxidation prone residues in antibodies and their effect on thermal stability, aggregation and antigen and/or receptor binding capacities. For example, Trp-277 was identified as an oxidation site during acid-induced unfolding and aggregation of IgG1 and IgG2 containing G2F complex glycoform.[25] Another study showed that the oxidation of Met-252 and Met-428 affected the thermal stability of the C_H2 domain and FcRn binding of an IgG1.[26] Additionally, oxidation of residues within the complementarity-determining regions (CDRs) affected the antigen binding properties of antibodies.[27,28] In another study, the impact of Met oxidation was highly dependent on its location and the type of glycosylation state of the protein, where Met oxidation in the variable regions and C_H3 domains had no detectable impact on mAb conformation, but oxidation

of Met-252 and Met-428 in the C_H2 domain caused a large decrease in thermal stability and an increase in aggregation rate that was more prominent in aglycosylated mAb than the complex glycoform.[29] However, correlation with decrease or increase in size of N-linked glycans on oxidation of antibodies is yet to be made and it is not known which Met site in the C_H2 domain is affected predominantly by glycosylation. Also, whether the stabilizing effect of glycans towards oxidation is due to their attachment to the protein or due to their radical scavenging capabilities is not yet addressed.[24]

1.7.2 Deamidation and Isomerization

Asn deamidation is an important chemical destabilization pathway of proteins that could affect their overall stability and therapeutic efficacy during development and storage. There are deamidation prone NG motifs at Asn-315 and Asn-384 and DG motifs at Asp-280 and Asp-401 located in the Fc constant region and in the CDR regions of antibodies.[30] Isomerization in the CDRs of a mAbs impaired the binding affinity of an antibody for its target antigen resulting in reduced drug potency.[28] However, the ability of N-linked glycosylation to affect these deamidation prone sites along with other chemical instabilities of IgG antibodies remains to be tested.

1.7.3 Proteolytic Degradation

Glycosylation is known to affect the proteolytic degradation of antibodies. It was found that high-mannose, hybrid and sialyl glycoforms of IgG1 and IgG2 antibodies were more susceptible to enzymatic degradation by trypsin as compared to complex glycoforms (G0F) of IgG1 and IgG2 antibodies.[31,32] Not only the type of glycan (hybrid, high-mannose, complex, sialyl), but also isoforms of hybrid and sialyl glycoforms showed different susceptibility to trypsin degradation. It was also shown that upon deglycosylation, IgG1 antibodies showed

increased susceptibility towards papain.[33] Another study showed that terminal mannose provided stability against papain due to local stearic exclusion effects in high mannose glycoform of IgG1. Pepsin digestion showed afucosylated form to be more stable than high mannose and deglycosylated IgG1 glycoforms while HNE digestion showed no differences in digestion rates of these glycoforms, except the deglycosylated form.[34] Mechanistically, it was proposed that proteolytic stability of glycoproteins arises due to the fact that the glycan's presence provides a steric hindrance around the peptide backbone of the amino acids adjacent to the glycosylation site by preventing contact between the glycoprotein's surfaces.[24] However, different higher order structures and localized conformational changes in the C_H2 domains of IgG antibodies, depending on their type and size of glycoform was shown to be the cause of different susceptibilities of these antibodies towards enzymatic degradation.[31-33]

1.7.4 Secondary, Tertiary and Quaternary Structure

To investigate influence of N-glycans on IgG-Fc, crystal structures of four truncated glycoforms were generated and the results showed sequential collapse of C_H2 domains as the glycan size was decreased.[7] Secondary and tertiary structural changes were not observed upon deglycosylation of IgG1 antibodies, however, increased hydrodynamic radius and increased Sypro Orange binding (due to increased hydrophobic exposure) upon deglycosylation was observed by size exclusion chromatography (SEC) and extrinsic Sypro Orange fluorescence respectively.[33] At neutral pH and physiological salt concentration, *E. coli* derived Fc (aglycosylated) showed smaller hydrodynamic radius as measured by dynamic light scattering (DLS)[35] than a CHO-derived Fc(glycosylated) in spite of having two glycans, indicating of a more compact structure of the glycosylated Fc. Another study on G0F, afucosylated (G0), high mannose and deglycosylated IgG1 mAbs showed no measurable secondary or tertiary structure

changes after *in vivo* or *in vitro* glycan modification as observed by various spectroscopic techniques.[34] These studies also indicated that spectroscopic techniques might not be sensitive enough to detect structural changes upon glycan variation.

1.7.5 Solubility/Precipitation

Adequate protein solubility is an important property not only for chemistry, manufacturing and control (CMC) activities during process and formulation development of a mAb therapeutic drug candidate, but also for patient administration of protein based drugs. Antibody therapeutics requires high solubility that is generally greater than 100 mg/ml which allows for their reduced dosing intervals and self-administration. Further, subcutaneous delivery requires mAbs to be formulated at small volume (<1.5 mL) with high concentration (> 10 mg/ kg dose).[36] It is generally observed that glycosylation increases the solubility of proteins, by possibly increasing interactions between the glycoprotein surface and the surrounding solvent[24], but exceptions to this general observation have been reported. Solubility studies on hybridoma antibodies showed that neither the N-glycosylation at Fab nor extreme isoelectric points contributed to the high solubility of these proteins.[36] It was observed that introducing an N-linked glycan within a complementarity determining region (CDR) in Fab led to improved solubility of an anti-IL-13 monoclonal antibody CNTO607 by shielding an aggregation hotspot on the surface of the antibody by the glycans.[37] However, another study on an IgG monoclonal cryoimmunoglobulin showed dramatic decrease in solubility due to glycosylation in the variable region.[38] As there were previous attempts to understand the impact of Fab glycosylation on solubility of antibodies, there is need for a detailed study to know the contribution of Fc N-glycosylation on their solubility.

1.7.6 Conformational Stability

1.7.6.1 *Thermal induced structural alterations*

Protein higher order structures are sensitive to environmental temperature fluctuations, which might cause challenges during development and their storage. Initial studies conducted by differential scanning calorimetry to assess the thermal stability of IgG-Fc proteins revealed decreased thermal stability of the C_H2 domain on deglycosylation suggesting contribution of glycosylation for stabilization of secondary and tertiary structures of the C_H2 domain.[39] Another study on serially truncated native (G2F), G0F, truncated (Man3GlcNAc2, ManGlcNAc2) and deglycosylated glycoforms of IgG1 showed the highest thermal stability by native and degalctosylated with no difference between them, M3N2 and MN2 showed similar and decreased stabilities while the deglycosylated was the least thermally stable by DSC.[40] Thermal stability of the C_H2 domain by DSC and intrinsic fluorescence was the highest and similar for G0 and G0F glycoforms (complex), slightly lower for high mannose forms and the least for non-glycosylated.[34]The stabilities of the C_H3 domains and Fab regions of IgG1 were not affected as dramatically as C_H2 domains.[33,34,39,40] Along with destabilization at higher temperatures, protein higher order structure is sensitive to cold temperatures and may undergo denaturation at ambient pressures which could create challenges during production and development involving repeated freeze-thaw cycles.[24] Effect of glycosylation on cold denaturation of IgG antibodies has not been studied in detail. Various studies showing effect of glycosylation on thermal stability of proteins showed no correlation with the type of linkage (N or O link) but with the glycan content.

1.7.6.2 *pH induced structural alterations*

Exposure to various pH conditions during production, purification, storage and administration can result in protein destabilization by disruption of various intramolecular and intermolecular charge-charge interactions. pH denaturation studies on various proteins revealed a

general trend of increased stability against pH changes as a consequence of glycosylation, probably due to increased internal electrostatic interactions of the proteins, as well as decreased intermolecular and solvent interactions. Similarly, stabilities of native (G2F), high mannose and non-glycosylated IgG antibodies over a wide pH rage of 4.0-7.5 were tested by DSC and showed that the domain stability was related to the solution pH. High mannose and non-glycosylated forms had lower stability of the C_H2 domain over all the pH conditions studied (more prominent at low pH conditions), while the C_H3 and Fab regions did not show substantial changes.[34]

1.7.6.3 *Chemical induced structural alterations*

In addition to electrostatic forces, various noncovalent interactions like hydrophobic interaction and hydrogen bonding are responsible for the stabilization of native higher order structure of proteins. Glycosylation was observed to increase the stability of various proteins towards chemical unfolding by guanidine hydrochloride (GdnHCl), urea or sodium dodecyl sulfate (SDS).[24] Similarly, IgG antibody unfolding induced by GdnHCl studied by second derivative ultraviolet (UV) spectroscopy showed less resistance of deglycosylated mAbs towards unfolding which were consistent with the DSC thermal stability results.[33]

1.7.7 Aggregation

Proteins molecules can agglomerate irreversibly as a consequence of covalent and non-covalent interactions that are triggered by pH, temperature excursions, high concentration, excipients, mechanical forces and interaction with surfaces during their production, purification, manufacturing, storage, transport and administration. Proteins can aggregate due to their intrinsic colloidal properties in an environment or presence of certain sticky/hydrophobic patches, which usually lie buried in the protein, might be exposed during these stresses and become available to interact with other hydrophobic patches on another protein molecule.[41,42] The aggregation prone

regions also called motifs or hot spot regions can be predicted with some success[43] and other studies have showed compelling evidence of the involvement of C_H2 domain and CDRs in Fab domains (especially in residues Phe, Tyr or Trp[44]) in determining the aggregation rate and extent in IgG antibodies.[25,41] It is believed that glycans can cause an increase in steric repulsions between aggregation prone regions and reduce or prevent aggregation between proteins.[24] In IgG antibodies, aggregation in glycosylated and de-glycosylated antibodies was studied and it was shown that aglycosylated antibodies were more prone to aggregation especially at lower pH conditions and higher temperatures.[33,35,42,45,46] It was shown than several aggregation prone regions near the glycosylation site (Val-282, Pro-291, Tyr-296, Val-308, Leu-309)[33,43] underwent localized changes in conformation and/or a hydrophobic segment 249-259 became more solvent accessible upon deglycosylation which might be due to decreased protein-glycan interactions.[42,44,47,48] One study showed that IgG Fc aggregation strongly correlated with degree of C_H2 domain glycosylation which increased with decrease in size of glycan in the following order glycosylated< partially glycosylated < non-glycosylated, however, the effect of various sizes and types of N-liked glycans on protein aggregation was not probed in detail in this work.[25]

1.7.8 Long term storage stability

Understanding the forced or accelerated physicochemical stability results in the light of long-term storage stability of antibodies is a critical aspect during their therapeutic formulation development. N-glycosylation affects the chemical, physical and dynamic properties of antibodies and particularly deglycosylation leads to dramatic decreases in stability of these molecules. No substantial monomer loss was observed in complex (G2F, G0F), high mannose and deglycosylated glycoforms of IgG1 mAbs at 5°C (storage temperature), 30°C and 40°C (stressed temperatures) in low ionic strength buffer at pH 5.5 indicating that glycosylation had no

substantial effect on storage stability of IgG1 mAbs.[34]Another study showed similar results in which no substantial difference in aggregates were observed between antibody products containing low and high high-mannose glycans over accelerated and real time stability conditions.[49] This indicated that decreased stability of non-glycosylated IgGs observed during forced degradation stability might not reflect their true long-term stability.

1.7.9 Influence of Glycosylation on Flexibility of IgG

In order to better understand the structure-function relationship of antibodies, it is essential to consider an additional aspect of protein structure that is dynamics and flexibility.[50] It is seen that an IgG antibody shows intrinsic molecular motions and can exist in multiple conformations, which are essential for its function, for example, allowing antibodies to span a wider range to search for antigens and to be able to bind various FcγRs during binding events.[50-52] In addition, understanding the effect of glycosylation on flexibility of antibody is not very well understood with respect to physicochemical stability and biological functions. Various methods, both experimental and simulations, are required to understand the range of motions shown by antibodies.[50] X-ray crystallography is one of the most sensitive techniques to study antibody structure and flexibility at atomic resolution[53] however, it gives snapshot of a particular conformation present during the crystallization which also could get distorted by crystal packing forces and may not be a true representation of the solution state of the protein. In addition, only a limited number of crystal structures of different glycoforms of antibody are available which might not represent all the conformations sampled by the IgG in solution. As glycosylation is heterogeneous, it is challenging to get good resolution of a particular glycan in an X-ray crystal structure making it important to have a homogenous glycan distribution, which might be practically difficult to achieve. Another technique known as nuclear magnetic resonance (NMR)

used to probe dynamics of various proteins has been challenging for studying large proteins like antibodies, but has shown great success in studying antibody fragments. Solution NMR allows studying the flexibility of both the oligosaccharide chain and the protein chain around the glycan site. NMR analysis of G2F glycosylated mAbs revealed that the terminal glycans of both α1,3 and α1,6 arms are exposed and highly dynamic along with the additional tumbling motion of the Fc molecule.[54] Studies on multiple IgG and Fc fragments showed that the overall trend of increase in their thermal stability upon glycosylation was attributed to decrease in overall dynamics of the structure studied by hydrogen deuterium exchange mass spectrometry (HX-MS) and NMR.[7,24,55-59] It was also observed that reduction in structural mobility due to glycosylation occurred in regions that were far from the glycosylation site suggesting transfer of these local effects throughout the entire protein.[24]

Previous studies in our laboratory examined the effect of different additives on an IgG1 mAb backbone flexibility using HX-MS. The results showed increased local flexibility of a certain hydrophobic segment in the C_H2 domain of the mAb was seen in presence of Hofmeister salts such as thiocyanate (as anion) and pharmaceutical excipients such as arginine (as an amino acid excipient) that was correlated with decreased thermal stability of the C_H2 domain and increase in aggregation propensity.[47,60] This was attributed to disruption in packing of the heterogeneous glycan structures within this hot spot region and the glycans.[47] As a continuation of this research, the nature of interactions between glycan chains and regions of the C_H2 domain should be explored to gain more mechanistic insights into changes in physical stability of mAbs. As flexibility is an important aspect of the protein structure, the impact of IgG glycosylation on flexibility with regard to physicochemical stability, storage stability and biologic property has

not be addressed in detail and is often limited by the complexity and heterogeneous distribution of glycoforms of antibody.

1.8 Influence of Glycosylation on Pharmacodynamics (PD) and Pharmacokinetics (PK)

Evidence of glycosylation is essential for Fc effector function biological activities like ADCC and CDC was observed when deglycosylation of various antibodies led to loss of binding to Fc ɣ receptors and failed to activate complement (C1q).[61] This result suggested the importance of N-glycans for governing the biological activities related to Fc receptors and the complement. The type (fucose, galactose, sialic acid, bisecting GlcNAc) and branching (complex verses high mannose) of N-glycosylation is shown to affect the Fc effector functions and is extensively studied. Presence of core fucosylation showed ~ 50-fold increase in FcɣRIIIa receptor binding of IgG mAbs, which enhanced their ADCC both in vitro and in vivo, however binding to FcɣRI, C1q and FcRn, were unaffected.[62-65] Bisecting GlcNAc was shown to enhance the binding affinity to FcɣRIIIa resulting in higher ADCC activities; however, core fucose was shown to be more critical for ADCC activity of mAbs.[66] Terminal Gal (G2) increased the affinity to C1q two fold and increased the CDC activity of IgG mAbs,[67,68] however terminal galactosylation did not affect ADCC activity.[67-69] High mannose glycans (Man5/8/9) on IgG mAbs showed higher binding affinity to FcɣRIIIa and hence higher ADCC than non-fucosylated forms probably due to lack of fucose.[15,70-72] However, high-mannose glycans on IgG mAb also reduced their binding to C1q, leading to lower CDC activities.[70-72] Terminal sialylation of IgG interfered the binding of mAbs to FcɣRIIIa, which lead to decreased ADCC.[73] It has also been shown that antibody glycosylation in the variable region of Fabs can affect the neutralizing function of mAbs. Significant reduction or enhancement of antigen-binding activities of antibodies was observed upon deglycosylation of N-glycan in Fabs.[14]

The PK properties of IgG mAbs are primarily governed by binding to neonatal Fc receptor (FcRn) which recycles the mAbs intracellularly and thus avoids destruction in the lysozymes; this process gives the antibody its long serum half-life.[61,74] Different composition, branching or removal of glycans does not cause a meaningful impact on the PK properties of IgG *in vivo,* suggesting that glycosylation is not required for IgG antibody's long half-life.[75] An aglycosylated IgG1 antibody (mAb ALD518) demonstrated normal human serum half-life of around 20-32 days in Phase I clinical trial.[76] However, a recent HX-MS study revealed that deglycosylation increased the flexibility of the FcγR binding site of an antibody.[9] IgG mAbs having high mannose glycans (M5-M9) showed faster clearance than mAbs with complex glycans (G0F, G1F and G2F).[77,78] However, it was seen that binding affinity towards human FcRn of high mannose IgGs was similar to complex and hybrid IgGs.[15,74] Another study showed that Man5 and Man8/9 IgG glycoforms had similar clearance.[79] Thus, high mannose glycoforms can have the ability to affect clearance, which makes them critical quality attributes that need to be monitored during production of mAbs. The increased ADCC activities of IgG having HM N-glycans (Man5, Man8 and Man9), their substantial influence on clinical efficacy and pharmacokinetics, methods for their modulation and understanding underlying mechanisms are important for their future development.[80] Additionally, Fab domains can also impact the clearance of IgG mAbs depending upon their location of glycosylation.[61] The above findings demonstrate the ability of glycosylation to affect the PK/PD that could ultimately affect the biological outcome of mAb therapeutics. Hence, during novel bio-therapeutic or biosimilar development, challenges are associated with PK and PD evaluations, which could affect the clinical efficacy or clinical similarity, respectively.

1.9 Influence of Glycosylation on Immunogenicity

Different mAb production vehicles show different glycosylation in terms of branching and types of glycans. Any production cell line that attaches glycans to mAbs, which are not native to those, found in human glycoforms of antibodies, might lead to immunogenicity when these mAbs are administered to humans. The most recognized immunogenic glycan linkages and glycans are galactose-α1, 3-galactose (α-Gal epitope), N-glycolylneuraminic acid (Neu5Gc epitope), β1, 2-xylose (core-xylose epitope), and α1, 3-fucose (core-α1, 3-fucose epitope).[81,82] Cetuximab showed that presence of α-Gal and/or Neu5Gc in Fabs developed severe hypersensitivity reactions in patients within minutes after first exposure due to development of IgE anti-α-Gal antibodies.[81-84] However, α-Gal epitopes in the Fc linked glycans of Infliximab were not recognized by IgE anti-α-Gal antibodies, possibly due to the relative low abundance of α-Gal epitopes.[81,82,84] Additionally, mannose and N-acetyglucosamine glycan can be attached to mannose receptor on macrophages, dendritic cells and endothelial cells while fully galactosylated IgG glycoforms can undergo uptake by dendritic cells which might have the potential to be immunogenic.[16]

Humanization of therapeutic antibodies has reduced their risk for eliciting an anti-drug immune response compared to chimeric antibodies, but this effect is not absent entirely even in fully human mAbs (100% human sequences).[84] The potential of protein aggregates of humanized (95% human with 5% mouse in the CDRs) and fully human mAbs to cause immunogenicity is recognized even though the underlying mechanisms for their correlation are complex and not well understood.[85] It is an active area of research for mAbs to understand the impact of aggregation and immunogenicity. However, deglycosylation increased the propensity of mAbs for aggregation,[46] and this eventually might increase their propensity for immunogenicity reactions against the mAb in patients.

1.10 Glycoengineering of N-glycosylation of Therapeutic mAbs

Efficacy and stability of mAbs has been improved by various antibody engineering strategies.[86] As discussed above, since N-glycosylation significantly influences the PK, PD, antigen binding (Fab glycosylation), tissue targeting and stability of mAb therapeutics, glycoengineering can show promising improvement in their efficacy.[87] The main goal of glycoengineering is to control the heterogeneity of mAb glycosylation and obtain a glycoform distribution as homogenous as possible which will have enhanced biological activities.[88] Achieving the above goal is challenging, and can be done by the following ways: 1) genetic manipulation of expression host glycosylation pathway 2) addition of chemical inhibitors 3) optimizing cell culture conditions 4) *in vitro* glycan synthesis and remodeling, and 5) Expression of aglycosylated mAbs. CHO cells have been genetically engineered in a variety of ways and are widely used as production host for producing therapeutic antibodies that have no core fucose.[89] Although, CHO cells naturally produce non-fucosylated antibodies, their distribution is heterogeneous. Various preclinical and clinical studies showed that controlling glycosylation improved the efficacy of various mAbs like mogamulizumab (defucosylation), obinutuzumab (defucosylation with bisecting N-acetyglucosamine) and benralizumab.[90] Apart from glycan engineering, various attempts to increase therapeutic efficacy have been made by protein engineering of mAbs.[91]

1.10.1 Glycoengineering with Yeast Expressed mAbs

Yeast offers several advantages for production of recombinant mAbs such as ease of production, ease of genetic manipulation, stable expression, rapid cell growth, high protein yield, scalable fermentation processes, low-cost and no risk of human pathogenic virus contamination.[89] However, glycoproteins expressed in wild type yeast generally cannot be used

for therapeutic applications due to fungal type high-mannose glycans, which can result in immunogenicity and poor PK *in vivo*.[89] Glycoengineered *P. pastoris* platform can yield recombinant antibodies with human N-glycosylation that demonstrated increased FcγRIIIa binding and ADCC activities along with similar pharmacokinetic profiles in both mice and cynomolgus monkeys as compared to CHO expressed trastuzumab.[89] This was attributed to the loss of fucose in expression from this glycoengineered yeast strain.[89] Additionally, expression of mAbs in glycosylation deficient yeast along with *in vitro* enzymatic synthesis of N-glycans allows production of homogenous charge variants of IgG1-Fc as observed from a previous study in our labs.[92] This approach can be further utilized to obtain IgG mAbs with sequentially truncated well-defined homogenous glycans for studying their effect on different properties of IgG. Expression of aglycosylated mAbs have been carried out by site directed mutagenesis to get rid of the Asn-297 residue, expression in *E.coli* and treatment of fully glycosylated mAbs with PNGase-F (Peptide:N-Glycosidase F) enzyme. Engineered aglycosylated mAbs are beneficial when effector functions are unnecessary (e.g. in case of neutralizing antibodies and antibodies used to treat inflammatory diseases). Aglycosylated antibodies offer an advantage in circumventing the need for N-glycan control along with expression in bacteria of full-length mAbs is possible which could have higher yields and will be cost effective.[21,22,93]

1.11 Biologic (mAb) Drug Product Development, Comparability and Biosimilarity Assessments

Development of recombinant biological products (like mAbs) and their biosimilar counterparts to treat various diseases has many hurdles due to their inherent sensitive and complex structure especially, in their characterization, manufacturing, stabilization, formulation and delivery. N-glycan heterogeneity further adds to the complexity and technical challenges for

their pharmaceutical development. To meet the high demand of biologics, it is necessary to scale up their manufacturing or transfer their processes to another manufacturing site as summarized in Figure 1.3. The scale up and technology transfer might induce changes to the delicate structure of proteins along with changes in post-translational modifications like glycosylation, making it essential to analyze the pre- and post-manufacturing product for any differences in quality.[94,95] To ensure that changes do not affect the quality, it is the responsibility of the biologic's manufacturer to conduct extensive characterization of the pre and post changed products to convince regulatory agencies of the validity of their chosen approach.[95,96] As seen in Figure 1.3, depending on the level of risk of the change, comparability exercises need to be carried out that involves different steps. Extensive physicochemical characterization of the product structure is the foundation of comparability exercises and rarely includes the expensive clinical trials unless the change poses a high level of risk.[94,97-100]

The pharmaceutical market comprises of almost 30% biologics out of which mAbs are the fastest and largest growing segment.[101,102] Patents on the highest selling mAb therapeutics are expiring soon hence, currently; there are many biosimilars in development.[96,101,103,104] Biosimilars are copies of biotherapeutics just like generic version of small molecules drugs, which offer a comparatively affordable alternative therapy for patients. Manufacturing of protein therapeutics is challenging due to their inherently complex structure and production in living cells, which could affect the product quality, one of them being post-translational modifications like glycosylation as compared to simpler, robust structure and a well-designed manufacturing recipe of small molecule drugs. However, for biosimilar developers, where the manufacturing recipe for an innovator drug is unknown; the biosimilar developer has to figure out their own manufacturing procedure such that the biosimilar and the original protein drug are highly similar

in physicochemical structure, activity, safety and efficacy. Again, it is the responsibility of the biosimilar manufacturer to conduct comparative studies with the originator biologic and gather all the required data to prove biosimilarity.[96] Similarity is established at three levels as seen in Figure 1.4, where extensive analytical characterization and biological activity testing are the foundation of biosimilar development. If similarity is shown with high confidence at the first level then extent of clinical studies needed might be reduced which will ultimately lead to lower drug costs. Ongoing research areas in biologic development, comparability and biosimilarity include: 1) Structural integrity analysis 2) Assessment of physicochemical degradation pathways and their effect on biological activity and potency 3) Optimization of drug stability and delivery by formulation development 4) Analytical method development and novel analytical approach design, and 5) PK/PD and immunogenicity analysis.[95,105,106] Each of the above areas offer systematic development of mAb therapeutics during comparability and biosimilarity assessments however, there are challenges involved in every steps, which are further complicated by the inherent glycan heterogeneity of mAbs.

1.11.1 Analysis of N-glycosylation in mAbs: Glycan Profiling (Primary Structure) and Conformation for Comparability and Biosimilarity Assessments

It is difficult to predict and control mAb glycosylation patterns as they are highly dependent on process manufacturing variables.[107] As N-glycosylation of mAbs affects their stability, biological activity and efficacy, it is necessary to monitor glycosylation and characterize glycan structures in detail throughout the product lifecycle, and know which glycans might cause adverse events in humans.[108] Various orthogonal analytical tools are used for characterization of mAb glycosylation, which are high-performance liquid chromatography (HPLC), capillary electrophoresis (CE), mass spectrometry (MS), isoelectric focusing (IEF), and

lectin-based microarray (chromatography and mass spectrometry (MS) being the most popular).[109,110] It is also important that analytical characterization tools are able to characterize glycans for providing critical quality attributes.[108] Together, these analytical tools should provide a complete glycan fingerprint and identify possible glycosylation sites (macro-heterogeneity, ICH guidance Q6B), glycan content (micro-heterogeneity) and glycan structure that involve information regarding linkages between the constituting monosaccharides of glycans.[110] Another aspect of glycan analysis involves rapid glycan comparisons between batches is glycan profiling.

In addition to primary structure analysis of glycosylation, the effect of the glycan on conformation of the protein should also be tested especially during biosimilar comparisons.[111]. Higher order structure is essential for the binding of mAbs to its antigen as well as different Fc receptors for their biological activity. It has been recently shown that N-glycans on the C_H2 domain of mAbs are flexible, and show different motions depending on their size and structure.[54,112] NMR is a popular tool for structural characterization to study motions of different N-glycans of IgG Fc as well as the flexibility of the protein.[54,59,112-116] However, requirement of large amount of protein, slow data processing times and protein size limit have not made its use popular for comparability analysis.[117] HX-MS can provide useful information on the subtle higher-order changes with different glycosylation of IgG and has started being popular for comparability and biosimilar comparability analyses as a result of improved automation, faster data analysis, less interference from excipients, and requirement of small amounts of material.[31,47,48,56,57,111,118] The analysis of conformational effects is further complicated by the heterogeneous distribution of glycans.[119,120] It is difficult to attribute the conformational changes to a particular glycan type present in a heterogeneous pool. Additionally, low levels of

glycoforms need sensitive analytical techniques that are able to detect them and hence, no unique method is available for characterization.[117,121,122]

1.11.2 Assessment of Physicochemical Degradation Pathways of mAbs and their Effect on Biological Activity for Comparability and Biosimilarity Assessments

The main goal of forced degradation studies is to elucidate the physicochemical degradation pathway(s) of protein drug substances and products, by subjecting them to stresses that might be experienced by them during their production, purification, manufacturing, storage, transit and administration.[95] Any small amount of impurity or instability (specially the PTMs) could potentially lead to serious consequences on the overall stability and efficacy. In case of glycoforms, which affect the stability and efficacy of mAbs and are inherently heterogeneous, identifying a particular glycoform causing degradation will be extremely challenging. Long term and accelerated stability studies measure the rate of given degradation process over time while forced degradation studies generate degradants in a much shorter time so that degradants can be identified earlier and quicker.[123] However, it has been observed that even though accelerated and forced degradation studies of different IgG glycoforms showed differences with their N-glycosylation, the type of glycosylation did not affect their long-term stabilities.[34,49] Another advantage offered by forced degradation studies is to allow the development of stability indicating methods which can be used in later stages for the analysis of accelerated and long term stability studies.[123] This might be essential to develop analytical tools to detect subtle changes that occur due to N-glycosylation of mAbs. As seen in Figures 1.3 and 1.4, stress study also can provide timely recommendations for making improvements in the manufacturing process and might be useful to control the glycosylation of mAbs.[123] Comparing degradation profiles in biosimilar and referenced product is also a critical aspect of biosimilar development.

1.11.3 Formulation and Stability of mAbs for Comparability and Biosimilarity Assessments

A major objective of formulating antibodies as therapeutic agents is to control the rate of their degradation during their storage and shipping which will ensure their stability over their shelf life. Additionally, a robust formulation is required to support preclinical and clinical studies that need demonstration of safety, manufacturability and drug stability. Choice of proper formulation excipients and other conditions specific for a particular mAb will help achieve the above goals. As mAbs are growing in demand and many candidates are in discovery, it becomes critical to accelerate process and formulation development and move them rapidly into clinical manufacturing. Evaluating the effect of storage period, excipients and environmental stress on the accelerated (and long term) stability of protein drug products is an essential part of formulation development and comparability evaluations upon formulation change.[95,123] The dosage form could be changed from liquid to lyophilized or the drug delivery could be changed from IV to pre-filled syringes which again might require changes in formulation and extensive comparisons of stability of proteins.[95] In biosimilar development, the biosimilar developers have to implement a formulation, which might or might not be identical to the originator formulation, but does not show different degradation products as compared to the originator. Comparing stability profiles of proteins in their actual final dosage form formulations is a critical aspect of comparability and biosimilar development.

1.11.4 Development of Novel Data Visualization Tools for Comparability and Biosimilarity Assessments

In both comparability and biosimilarity exercises, changes occur to manufacturing processes and pre-change versus post change product (and originator versus biosimilar product)

must be characterized to demonstrate their similarity in terms of physicochemical structure, biological function, impurity profiles, safety and efficacy. As discussed above, mAbs are glycoproteins that show heterogeneous glycosylation, which is extremely sensitive to manufacturing conditions making it a critical quality attribute. Not only is glycosylation heterogeneous in nature, but also affect various pharmaceutical properties as we saw before, which could result in affecting the efficacy and safety of the products in comparability and biosimilarity scenarios. Ideally, having identical or homogenous glycosylation profile is desired but it is not practically possible as every batch of production might be different and difficult to control. Although significant advances have been made for glycosylation comparability analysis by various glyco-analysis techniques, the need for more sensitive approaches for the evaluation of higher order structures (HOS) of proteins remains an important challenge. Especially, for a biosimilar comparability exercise, where the foundation lies in extensive comparative physicochemical and biological characterization of the biosimilar and the originator, there is need for developing novel analytical approaches for comparability. Effect of N-linked glycosylation site occupancy and different charge states in various non-glycosylated forms within the C_H2 domain was examined which provided a sensitive analysis of subtle differences in the higher order structure (HOS) of these glycoproteins.[92,124] Various attempts have been made previously to develop novel data visualization approaches for accessing HOS of glycoproteins including mAbs and charge variants of IgG1-Fcs in the context of comparability.[92,95,124,125] These approaches include the utilization of empirical phase diagrams (EPD) and radar charts, which gives the information on the overall higher order structural stability profile of a protein in a holistic manner. This approach can be further investigated to study the effect of N-linked well-defined oligosaccharide structures on HOS of Fc region of antibodies.

In this work, we have utilized a set of well-defined IgG1 Fc glycoforms as a model for biosimilar comparability analysis by performing a series of comparative physical evaluations. These well-defined glycoforms differed only in glycosylation state or a single conservative amino acid mutation and they will be expected to exhibit a wide range of biophysical properties due to the effect of N-glycosylation on IgG1-Fc. Four IgG1-Fc glycoforms were produced using a combination of expression in genetically modified yeast and *in vitro* enzymatic truncation. They were extensively characterized for their purity, N-glycosylation structure, high molecular weight species and charge variants to ensure that these glycoforms differed only in glycosylation state or a single amino acid mutation. Subsequently, these different IgG1-Fc glycoforms were extensively characterized for solubility and physical stability properties using multiple low-resolution biophysical techniques to monitor different aspects of their higher-order structure across a wide range of pH and temperature conditions.

Another goal was to develop stability indicating assays that were sensitive to observe subtle differences between the HOS and physical stability of these glycoforms. To develop tools for comparability, these glycoforms were formulated in two different formulations (NaCl vs sucrose) to mimic mAb biosimilars that might be formulated in two different formulations. Further, large biophysical data sets obtained above were then used to construct data visualization tools based on EPDs and radar charts for structural comparison between different glycosylation states. Using this approach, differences in structural integrity and conformational stability were detected at stress conditions that could not be detected by using the same techniques under ambient conditions (i.e., no stress). Thus, an evaluation of conformational stability differences may serve as an effective surrogate to monitor differences in higher-order structure between protein samples. To mimic heterogeneity in biosimilars, mixtures of these four homogenous

glycoforms were prepared by combining them in defined ratios to produce well-defined batches of IgG1-Fc glycoforms with different physicochemical and biological attributes. Stability indicating assays developed before to characterize the solubility and physical stability of the four glycoforms were utilized to characterize the mixtures.

As a final aspect to this work, to gain a better mechanistic understanding of the physical stability changes as a function of N-glycosylation and to correlate these results with local flexibility, HX-MS was utilized. HX-MS offers higher resolution as compared to biophysical techniques for HOS characterization and monitoring flexibility of the IgG1-Fc glycoforms. This study contributes towards utilization of these homogenous glycoforms as a model for understanding impact of glycosylation on physical stability and flexibility, and their application in developing analytical tools for comparability and biosimilarity assessments.

1.12 Chapter Reviews

1.12.1 Correlating the Impact of Well-Defined Oligosaccharide Structures on Physical Stability Profiles of IgG1-Fc Glycoforms. (Chapter 2)

The focus of this work was to describe four well-defined IgG1-Fc glycoforms as a model system for biosimilarity analysis (High mannose-Fc, Man5-Fc, GlcNAc-Fc and N297Q-Fc aglycosylated) and to draw comparisons of their physical properties. A trend of decreasing apparent solubility (thermodynamic activity) by PEG precipitation (pH 4.5, 6.0) and lower conformational stability by differential scanning calorimetry (DSC) (pH 4.5) was observed with reducing size of the N297-linked oligosaccharide structures. Using multiple high-throughput biophysical techniques, the physical stability of the Fc glycoproteins was then measured in two formulations (NaCl and sucrose) across a wide range of temperatures (10-90˚C) and pH (4.0-7.5) conditions. The datasets were used to construct three-index empirical phase diagrams and radar

charts to visualize the regions of protein structural stability. Each glycoform showed improved stability in the sucrose (vs. salt) formulation. The HM-Fc and Man5-Fc displayed the highest relative stability, followed by GlcNAc-Fc, with N297Q-Fc being the least stable. Thus, the overall physical stability profiles of the four IgG1-Fc glycoforms also show a correlation with oligosaccharide structure. These datasets are used to develop a mathematical model for biosimilarity analysis.

1.12.2 Comparative Evaluation of Solubility and Physical Stability Profiles of Well-Defined Mixtures of IgG1-Fc Glycoforms as a Model for Biosimilar Comparability Analysis. (Chapter 3)

Four well-defined IgG1 Fc glycoforms (HM-Fc, Man5-Fc, GlcNAc-Fc, and N297Q-Fc) prepared previously were blended in specific ratios to produce well-defined mixtures to mimic biosimilar products. These mixtures had evident and subtle differences in physical and functional properties as expected from first studying homogenous glycoforms of IgG1-Fc. The mixtures were prepared by mixing HM-Fc with the three glycoforms in pre-defined proportion to make two sets of mixtures which were: 90%HM:10%X(subtle differences) and 50%HM:50%X(evident differences), in which X was N297Q-Fc, Man5-Fc, and GlcNAc-Fc. In addition, a more complex system was prepared by blending the four glycoforms (25 % each) to model heterogeneous systems typically encountered in monoclonal antibodies. Seven mixtures of IgG1-Fc glycoforms were prepared and utilized a model system for biosimilar comparability assesment. In addition, the four well-defined glycoforms were used as controls in each characterization techniques. The focus of this study was to evaluate the physical characteristics of these mixtures as a model system for biosimilar comparability analysis. Solubility and physical stability measurements were performed using high-throughput PEG precipitation assay

and biophysical techniques, including differential scanning calorimetry (DSC), intrinsic fluorescence, differential scanning fluorimetry (DSF), light scattering and turbidity, which were developed in the previous study. A trend in solubility and stability was observed, which depended on the type and composition of the mixtures. Mixtures containing Man5-Fc and HM-Fc showed higher stability, followed by mixtures of GlcNAc-Fc and HM-Fc and combinations of N297Q-Fc and HM-Fc showed the least stability. These datasets are being used to develop a mathematical model for biosimilarity analysis.

1.12.3 Correlating the Impact of Glycosylation on the Backbone Flexibility of Well-Defined IgG1-Fc Glycoforms Using Hydrogen Exchange-Mass Spectrometry (HX-MS). (Chapter 4)

We have utilized hydrogen/deuterium exchange mass spectrometry (HX-MS) for characterization of localized backbone flexibility of four well-defined homogenous N-linked Asn-297 glycoforms of an IgG1-Fc expressed and purified from *Pichia pastoris* cells, two of which were prepared using subsequent *in vitro* enzymatic treatments. A correlation was demonstrated between increased flexibility, especially of specific regions within C_H2 domains of the Fc and decreased N-linked oligosaccharide size from high mannose (Man8-Man12), Man5, GlcNAc and then non-glycosylated N297Q. These results were compared with previously published physicochemical stability, aggregation propensity, and Fcɣ receptor binding data with the same molecules allowing for more insightful correlations between N-glycosylation status and pharmaceutical properties of the IgG1-Fc glycoforms. We identified two potential aggregation hot spots where flexibility significantly increased upon glycan truncation. We also observed a correlation between increased backbone flexibility for Asn-315 containing peptides, increased deamidation rates, and decreased glycan size of the IgG1-Fc, while the opposite correlation was

noted for oxidation of Trp-277 residue. Finally, a trend of increasing C'E glycopeptide loop flexibility with decreasing glycan size was observed that correlated with FcγRIIIa binding data. These well-defined IgG1-Fc glycoforms serve as a model system not only to enable rational design and optimization of stable IgG formulation conditions, but also to identify physicochemical data sets potentially discriminating between various glycoforms for future biosimilarity assessments.

1.12.4 Conclusions and Future Work. (Chapter 5)

This final chapter summarizes what we learned about the structural integrity, conformational stability and flexibility of the various N-linked glycoforms of IgG1-Fc as a model system for comparability and biosimilarity assessments. The work from chapters 2-4 (assay development and characterization of physical properties and stability, characterization of mixtures, and correlating effect of glycosylation on physical stability and local flexibility) and potential utility of using HX-MS and the new data visualization methods for displaying HOS stability data (as discussed in the previous chapters) for comparability and biosimilarity are evaluated holistically. In addition, suggestions for future work are also discussed.

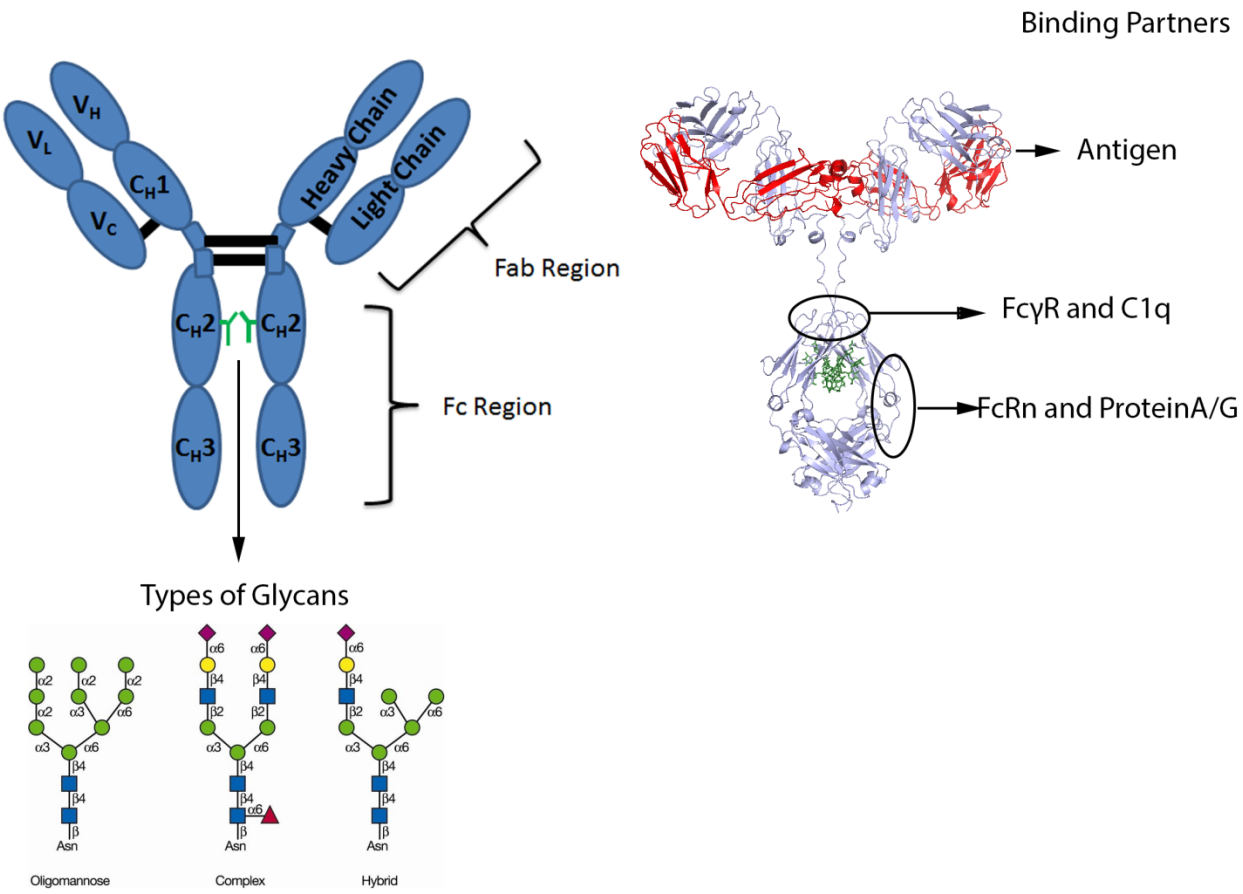

Figure 1.1: Structure of IgG1 antibody, Types of N-glycan and Binding Partners

Structure of IgG1 antibody and different regions involved with binding to different partners are shown. The types of N-glycan structures are shown at the bottom and are reproduced from the referred article with permission.[126]

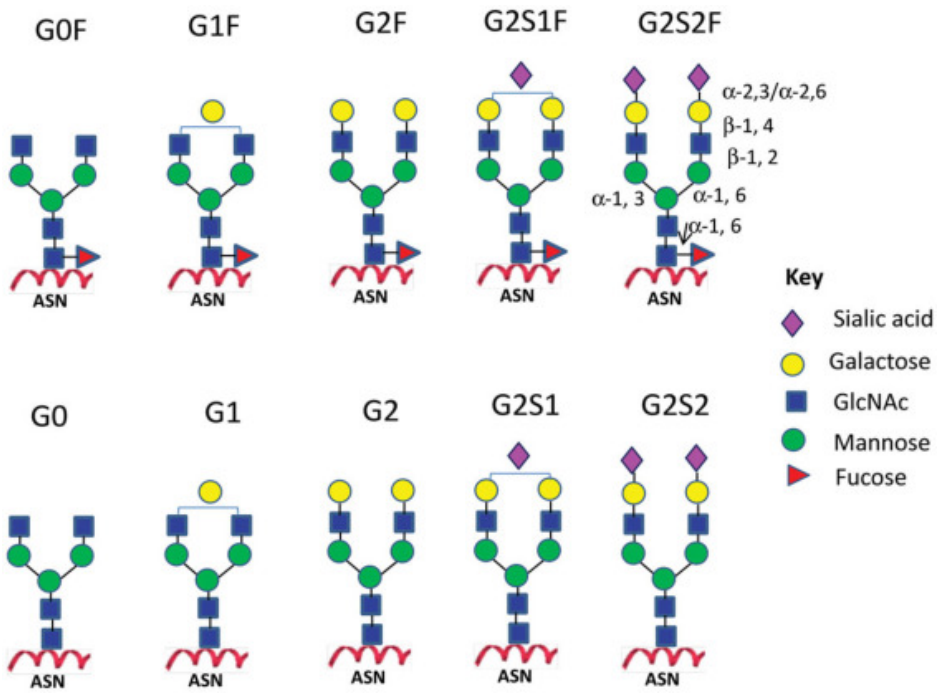

Figure 1.2: Types of N-glycans found in monoclonal antibody therapeutics. The figure is reproduced from the referred article with permission.[61]

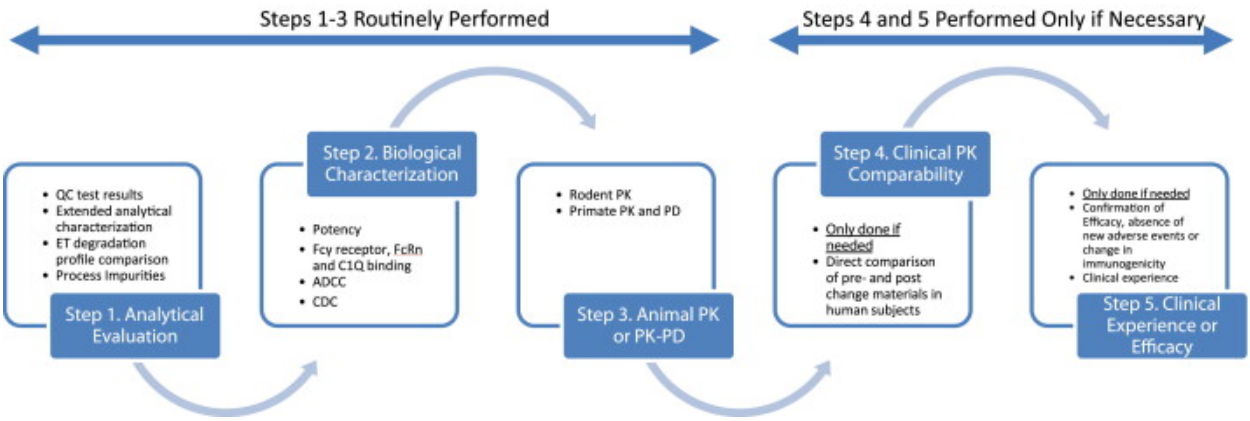

Figure 1.3: Analytical evaluations are the foundation of a comparability exercise in any nature of process change. Clinical comparability is performed only when uncertainty exists in demonstrating comparability in steps 1-3. The figure is reproduced from the referred article with permission.[97]

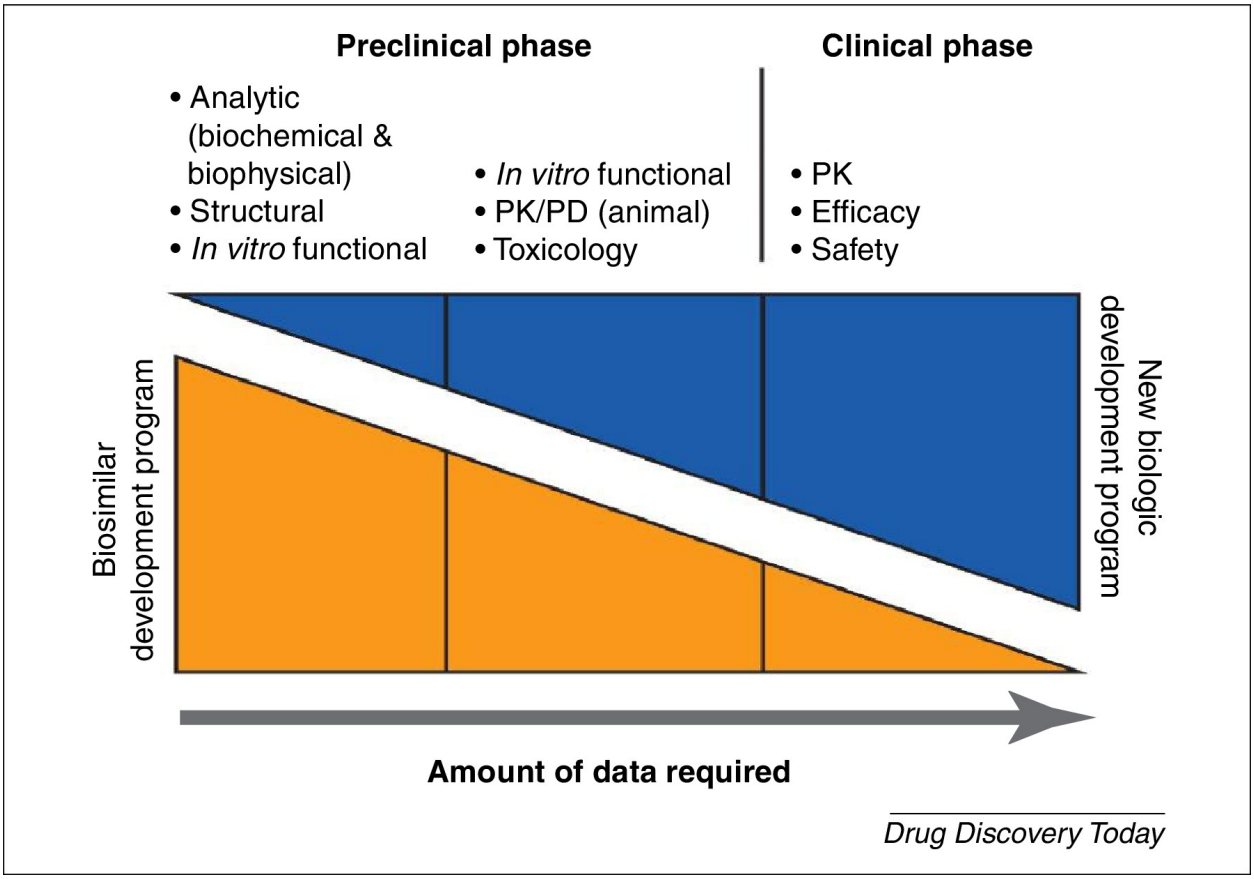

Figure 1.4: Amount of data required in biosimilar development versus new biologic development is shown. Three levels of data are required to demonstrate biosimilarity in which physicochemical analytical evaluations are the foundation of a biosimilarity exercise and clinical phase requires fewer data as seen above. The figure is reproduced from the referred article with permission. [127]

1.13 References

1. Bertozzi CR RD. 2009. Structural Basis of Glycan Diversity. In Varki A CR, Esko JD, et al., editor Essentials of Glycobiology, 2nd edition ed., Cold Spring Harbor (NY): Cold Spring Harbor Laboratory Press.

2. Varki A 2017. Biological roles of glycans. Glycobiology 27(1):3-49.

3. Moremen KW, Tiemeyer M, Nairn AV 2012. Vertebrate protein glycosylation: diversity, synthesis and function. Nature reviews Molecular cell biology 13(7):448-462.

4. Varki A 2011. Evolutionary forces shaping the Golgi glycosylation machinery: why cell surface glycans are universal to living cells. Cold Spring Harbor perspectives in biology 3(6).

5. Wang W, Singh S, Zeng DL, King K, Nema S 2007. Antibody structure, instability, and formulation. Journal of pharmaceutical sciences 96(1):1-26.

6. Vidarsson G, Dekkers G, Rispens T 2014. IgG subclasses and allotypes: from structure to effector functions. Frontiers in immunology 5:520.

7. Krapp S, Mimura Y, Jefferis R, Huber R, Sondermann P 2003. Structural Analysis of Human IgG-Fc Glycoforms Reveals a Correlation Between Glycosylation and Structural Integrity. Journal of Molecular Biology 325(5):979-989.

8. Schroeder HW, Jr., Cavacini L 2010. Structure and function of immunoglobulins. The Journal of allergy and clinical immunology 125(2 Suppl 2):S41-52.

9. Jensen PF, Larraillet V, Schlothauer T, Kettenberger H, Hilger M, Rand KD 2015. Investigating the interaction between the neonatal Fc receptor and monoclonal antibody variants by hydrogen/deuterium exchange mass spectrometry. Molecular & cellular proteomics : MCP 14(1):148-161.

10. Khoury GA, Baliban RC, Floudas CA 2011. Proteome-wide post-translational modification statistics: frequency analysis and curation of the swiss-prot database. Scientific reports 1:90.

11. Duan G, Walther D 2015. The Roles of Post-translational Modifications in the Context of Protein Interaction Networks. PLoS Computational Biology 11(2):e1004049.

12. Audagnotto M, Dal Peraro M 2017. Protein post-translational modifications: In silico prediction tools and molecular modeling. Computational and Structural Biotechnology Journal 15:307-319.

13. Jefferis R 2016. Glyco-engineering of human IgG-Fc to modulate biologic activities. Current pharmaceutical biotechnology.

14. Van de Bovenkamp FS, Hafkenscheid L, Rispens T, Rombouts Y 2016. The Emerging Importance of IgG Fab Glycosylation in Immunity. The Journal of Immunology 196(4):1435-1441.

15. Kanda Y, Yamada T, Mori K, Okazaki A, Inoue M, Kitajima-Miyama K, Kuni-Kamochi R, Nakano R, Yano K, Kakita S, Shitara K, Satoh M 2007. Comparison of biological activity among nonfucosylated therapeutic IgG1 antibodies with three different N-linked Fc oligosaccharides: the high-mannose, hybrid, and complex types. Glycobiology 17(1):104-118.

16. Jefferis R 2009. Glycosylation as a strategy to improve antibody-based therapeutics. Nature reviews Drug discovery 8(3):226-234.

17. Jefferis R 2009. Glycosylation of antibody therapeutics: optimisation for purpose. Methods in molecular biology 483:223-238.

18. Kailemia MJ, Park D, Lebrilla CB 2017. Glycans and glycoproteins as specific biomarkers for cancer. Analytical and bioanalytical chemistry 409(2):395-410.

19. Bai L, Li Q, Li L, Lin Y, Zhao S, Wang W, Wang R, Li Y, Yuan J, Wang C, Wang Z, Fan J, Liu E 2016. Plasma High-Mannose and Complex/Hybrid N-Glycans Are Associated with Hypercholesterolemia in Humans and Rabbits. PloS one 11(3):e0146982.

20. Zhang D, Chen B, Wang Y, Xia P, He C, Liu Y, Zhang R, Zhang M, Li Z 2016. Disease-specific IgG Fc N-glycosylation as personalized biomarkers to differentiate gastric cancer from benign gastric diseases. Scientific reports 6:25957.

21. Jung ST, Kang TH, Kelton W, Georgiou G 2011. Bypassing glycosylation: engineering aglycosylated full-length IgG antibodies for human therapy. Current opinion in biotechnology 22(6):858-867.

22. Hristodorov D, Fischer R, Linden L 2013. With or without sugar? (A)glycosylation of therapeutic antibodies. Molecular biotechnology 54(3):1056-1068.

23. Beck A, Reichert JM 2012. Marketing approval of mogamulizumab: a triumph for glyco-engineering. mAbs 4(4):419-425.

24. Sola RJ, Griebenow K 2009. Effects of glycosylation on the stability of protein pharmaceuticals. Journal of pharmaceutical sciences 98(4):1223-1245.

25. Latypov RF, Hogan S, Lau H, Gadgil H, Liu D 2012. Elucidation of acid-induced unfolding and aggregation of human immunoglobulin IgG1 and IgG2 Fc. The Journal of biological chemistry 287(2):1381-1396.

26. Gao X, Ji JA, Veeravalli K, Wang YJ, Zhang T, McGreevy W, Zheng K, Kelley RF, Laird MW, Liu J, Cromwell M 2015. Effect of individual Fc methionine oxidation on FcRn binding: Met252 oxidation impairs FcRn binding more profoundly than Met428 oxidation. Journal of pharmaceutical sciences 104(2):368-377.

27. Qi P, Volkin DB, Zhao H, Nedved ML, Hughes R, Bass R, Yi SC, Panek ME, Wang D, Dalmonte P, Bond MD 2009. Characterization of the photodegradation of a human IgG1 monoclonal antibody formulated as a high-concentration liquid dosage form. Journal of pharmaceutical sciences 98(9):3117-3130.

28. Yan Y, Wei H, Fu Y, Jusuf S, Zeng M, Ludwig R, Krystek SR, Jr., Chen G, Tao L, Das TK 2016. Isomerization and Oxidation in the Complementarity-Determining Regions of a Monoclonal Antibody: A Study of the Modification-Structure-Function Correlations by Hydrogen-Deuterium Exchange Mass Spectrometry. Analytical chemistry 88(4):2041-2050.

29. Zhang A, Hu P, MacGregor P, Xue Y, Fan H, Suchecki P, Olszewski L, Liu A 2014. Understanding the conformational impact of chemical modifications on monoclonal antibodies with diverse sequence variation using hydrogen/deuterium exchange mass spectrometry and structural modeling. Analytical chemistry 86(7):3468-3475.

30. Sinha S, Zhang L, Duan S, Williams TD, Vlasak J, Ionescu R, Topp EM 2009. Effect of protein structure on deamidation rate in the Fc fragment of an IgG1 monoclonal antibody. Protein science : a publication of the Protein Society 18(8):1573-1584.

31. Fang J, Richardson J, Du Z, Zhang Z 2016. Effect of Fc-Glycan Structure on the Conformational Stability of IgG Revealed by Hydrogen/Deuterium Exchange and Limited Proteolysis. Biochemistry 55(6):860-868.

32. Falck D, Jansen BC, Plomp R, Reusch D, Haberger M, Wuhrer M 2015. Glycoforms of Immunoglobulin G Based Biopharmaceuticals Are Differentially Cleaved by Trypsin Due to the Glycoform Influence on Higher-Order Structure. Journal of proteome research 14(9):4019-4028.

33. Zheng K, Bantog C, Bayer R 2011. The impact of glycosylation on monoclonal antibody conformation and stability. mAbs 3(6):568-576.

34. Zheng K, Yarmarkovich M, Bantog C, Bayer R, Patapoff TW 2014. Influence of glycosylation pattern on the molecular properties of monoclonal antibodies. mAbs 6(3):649-658.

35. Li CH, Narhi LO, Wen J, Dimitrova M, Wen ZQ, Li J, Pollastrini J, Nguyen X, Tsuruda T, Jiang Y 2012. Effect of pH, temperature, and salt on the stability of Escherichia coli- and Chinese hamster ovary cell-derived IgG1 Fc. Biochemistry 51(50):10056-10065.

36. Spencer S, Bethea D, Raju TS, Giles-Komar J, Feng Y 2012. Solubility evaluation of murine hybridoma antibodies. mAbs 4(3):319-325.

37. Wu S-J, Luo J, O'Neil KT, Kang J, Lacy ER, Canziani G, Baker A, Huang M, Tang QM, Raju TS, Jacobs SA, Teplyakov A, Gilliland GL, Feng Y 2010. Structure-based engineering of a monoclonal antibody for improved solubility. Protein Engineering, Design and Selection 23(8):643-651.

38. Middaugh C, Litman G 1987. Atypical glycosylation of an IgG monoclonal cryoimmunoglobulin. Journal of Biological Chemistry 262(8):3671-3673.

39. Ghirlando R, Lund J, Goodall M, Jefferis R 1999. Glycosylation of human IgG-Fc: influences on structure revealed by differential scanning micro-calorimetry. Immunology Letters 68(1):47-52.

40. Mimura Y, Church S, Ghirlando R, Ashton PR, Dong S, Goodall M, Lund J, Jefferis R 2000. The influence of glycosylation on the thermal stability and effector function expression of human IgG1-Fc: properties of a series of truncated glycoforms. Molecular Immunology 37:697-706.

41. Wu H, Kroe-Barrett R, Singh S, Robinson AS, Roberts CJ 2014. Competing aggregation pathways for monoclonal antibodies. FEBS letters 588(6):936-941.

42. Iacob RE, Bou-Assaf GM, Makowski L, Engen JR, Berkowitz SA, Houde D 2013. Investigating monoclonal antibody aggregation using a combination of H/DX-MS and other biophysical measurements. Journal of pharmaceutical sciences 102(12):4315-4329.

43. Chennamsetty N, Helk B, Voynov V, Kayser V, Trout BL 2009. Aggregation-prone motifs in human immunoglobulin G. J Mol Biol 391(2):404-413.

44. Voynov V, Chennamsetty N, Kayser V, Helk B, Forrer K, Zhang H, Fritsch C, Heine H, Trout BL 2009. Dynamic fluctuations of protein-carbohydrate interactions promote protein aggregation. PloS one 4(12):e8425.

45. Yageta S, Shibuya R, Imamura H, Honda S 2017. Conformational and Colloidal Stabilities of Human Immunoglobulin G Fc and Its Cyclized Variant: Independent and

Compensatory Participation of Domains in Aggregation of Multidomain Proteins. Molecular pharmaceutics 14(3):699-711.

46. Kayser V, Chennamsetty N, Voynov V, Forrer K, Helk B, Trout BL 2011. Glycosylation influences on the aggregation propensity of therapeutic monoclonal antibodies. Biotechnology Journal 6(1):38-44.

47. Majumdar R, Manikwar P, Hickey JM, Samra HS, Sathish HA, Bishop SM, Middaugh CR, Volkin DB, Weis DD 2013. Effects of salts from the Hofmeister series on the conformational stability, aggregation propensity, and local flexibility of an IgG1 monoclonal antibody. Biochemistry 52(19):3376-3389.

48. Majumdar R, Middaugh CR, Weis DD, Volkin DB 2015. Hydrogen-deuterium exchange mass spectrometry as an emerging analytical tool for stabilization and formulation development of therapeutic monoclonal antibodies. Journal of pharmaceutical sciences 104(2):327-345.

49. Lu Y, Westland K, Ma YH, Gadgil H 2012. Evaluation of effects of Fc domain high-mannose glycan on antibody stability. Journal of pharmaceutical sciences 101(11):4107-4117.

50. Teilum K, Olsen JG, Kragelund BB 2009. Functional aspects of protein flexibility. Cellular and molecular life sciences : CMLS 66(14):2231-2247.

51. Sandin S, Ofverstedt LG, Wikstrom AC, Wrange O, Skoglund U 2004. Structure and flexibility of individual immunoglobulin G molecules in solution. Structure 12(3):409-415.

52. Zhang X, Zhang L, Tong H, Peng B, Rames MJ, Zhang S, Ren G 2015. 3D structural fluctuation of IgG1 antibody revealed by individual particle electron tomography. Scientific reports 5:9803.

53. Saphire EO, Stanfield RL, Max Crispin MD, Parren PWHI, Rudd PM, Dwek RA, Burton DR, Wilson IA 2002. Contrasting IgG Structures Reveal Extreme Asymmetry and Flexibility. Journal of Molecular Biology 319(1):9-18.

54. Barb AW, Prestegard JH 2011. NMR analysis demonstrates immunoglobulin G N-glycans are accessible and dynamic. Nature chemical biology 7(3):147-153.

55. Mimura Y, Church S, Ghirlando R, Ashton PR, Dong S, Goodall M, Lund J, Jefferis R 2000. The influence of glycosylation on the thermal stability and effector function expression of human IgG1-Fc: properties of a series of truncated glycoforms. Mol Immunol 37(12-13):697-706.

56. Houde D, Arndt J, Domeier W, Berkowitz S, Engen JR 2009. Characterization of IgG1 Conformation and Conformational Dynamics by Hydrogen/Deuterium Exchange Mass Spectrometry. Analytical chemistry 81(7):2644-2651.

57. Houde D, Peng Y, Berkowitz S, Engen J 2010. Post-translational Modifications Differentially Affect IgG1 Conformation and Receptor Binding. Molecular and Cellular Proteomics.

58. Yamaguchi Y, Nishimura M, Nagano M, Yagi H, Sasakawa H, Uchida K, Shitara K, Kato K 2006. Glycoform-dependent conformational alteration of the Fc region of human immunoglobulin G1 as revealed by NMR spectroscopy. Biochimica et biophysica acta 1760(4):693-700.

59. Subedi GP, Hanson QM, Barb AW 2014. Restricted motion of the conserved immunoglobulin G1 N-glycan is essential for efficient FcgammaRIIIa binding. Structure 22(10):1478-1488.

60. Manikwar P, Majumdar R, Hickey JM, Thakkar SV, Samra HS, Sathish HA, Bishop SM, Middaugh CR, Weis DD, Volkin DB 2013. Correlating excipient effects on conformational and storage stability of an IgG1 monoclonal antibody with local dynamics as measured by hydrogen/deuterium-exchange mass spectrometry. Journal of pharmaceutical sciences 102(7):2136-2151.

61. Liu L 2015. Antibody Glycosylation and Its Impact on the Pharmacokinetics and Pharmacodynamics of Monoclonal Antibodies and Fc-Fusion Proteins. Journal of pharmaceutical sciences 104(6):1866-1884.

62. Yamane-Ohnuki N, Kinoshita S, Inoue-Urakubo M, Kusunoki M, Iida S, Nakano R, Wakitani M, Niwa R, Sakurada M, Uchida K, Shitara K, Satoh M 2004. Establishment of FUT8 knockout Chinese hamster ovary cells: an ideal host cell line for producing completely defucosylated antibodies with enhanced antibody-dependent cellular cytotoxicity. Biotechnology and bioengineering 87(5):614-622.

63. Satoh M, Iida S, Shitara K 2006. Non-fucosylated therapeutic antibodies as next-generation therapeutic antibodies. Expert opinion on biological therapy 6(11):1161-1173.

64. Iida S, Misaka H, Inoue M, Shibata M, Nakano R, Yamane-Ohnuki N, Wakitani M, Yano K, Shitara K, Satoh M 2006. Nonfucosylated therapeutic IgG1 antibody can evade the inhibitory effect of serum immunoglobulin G on antibody-dependent cellular cytotoxicity through its high binding to FcγRIIIa. Clinical Cancer Research 12(9):2879-2887.

65. Shields RL, Lai J, Keck R, O'Connell LY, Hong K, Meng YG, Weikert SH, Presta LG 2002. Lack of fucose on human IgG1 N-linked oligosaccharide improves binding to human

Fcgamma RIII and antibody-dependent cellular toxicity. The Journal of biological chemistry 277(30):26733-26740.

66. Shinkawa T, Nakamura K, Yamane N, Shoji-Hosaka E, Kanda Y, Sakurada M, Uchida K, Anazawa H, Satoh M, Yamasaki M, Hanai N, Shitara K 2003. The absence of fucose but not the presence of galactose or bisecting N-acetylglucosamine of human IgG1 complex-type oligosaccharides shows the critical role of enhancing antibody-dependent cellular cytotoxicity. The Journal of biological chemistry 278(5):3466-3473.

67. Raju TS 2008. Terminal sugars of Fc glycans influence antibody effector functions of IgGs. Current opinion in immunology 20(4):471-478.

68. Boyd PN, Lines AC, Patel AK 1995. The effect of the removal of sialic acid, galactose and total carbohydrate on the functional activity of Campath-1H. Mol Immunol 32(17-18):1311-1318.

69. Hodoniczky J, Zheng YZ, James DC 2005. Control of Recombinant Monoclonal Antibody Effector Functions by Fc N-Glycan Remodeling in Vitro. Biotechnology progress 21(6):1644-1652.

70. Zhou Q, Shankara S, Roy A, Qiu H, Estes S, McVie-Wylie A, Culm-Merdek K, Park A, Pan C, Edmunds T 2008. Development of a simple and rapid method for producing non-fucosylated oligomannose containing antibodies with increased effector function. Biotechnology and bioengineering 99(3):652-665.

71. Yu M, Brown D, Reed C, Chung S, Lutman J, Stefanich E, Wong A, Stephan JP, Bayer R 2012. Production, characterization, and pharmacokinetic properties of antibodies with N-linked mannose-5 glycans. mAbs 4(4):475-487.

72. Kanda Y, Yamane-Ohnuki N, Sakai N, Yamano K, Nakano R, Inoue M, Misaka H, Iida S, Wakitani M, Konno Y, Yano K, Shitara K, Hosoi S, Satoh M 2006. Comparison of cell lines for stable production of fucose-negative antibodies with enhanced ADCC. Biotechnology and bioengineering 94(4):680-688.

73. Scallon BJ, Tam SH, McCarthy SG, Cai AN, Raju TS 2007. Higher levels of sialylated Fc glycans in immunoglobulin G molecules can adversely impact functionality. Mol Immunol 44(7):1524-1534.

74. Liu L, Stadheim A, Hamuro L, Pittman T, Wang W, Zha D, Hochman J, Prueksaritanont T 2011. Pharmacokinetics of IgG1 monoclonal antibodies produced in humanized Pichia pastoris with specific glycoforms: a comparative study with CHO produced materials. Biologicals : journal of the International Association of Biological Standardization 39(4):205-210.

75. Salgia R, Patel P, Bothos J, Yu W, Eppler S, Hegde P, Bai S, Kaur S, Nijem I, Catenacci DV, Peterson A, Ratain MJ, Polite B, Mehnert JM, Moss RA 2014. Phase I dose-escalation study of onartuzumab as a single agent and in combination with bevacizumab in patients with advanced solid malignancies. Clinical cancer research : an official journal of the American Association for Cancer Research 20(6):1666-1675.

76. Clarke SJ, Smith JT, Gebbie C, Sweeney C, Olszewski N 2009. A phase I, pharmacokinetic (PK), and preliminary efficacy assessment of ALD518, a humanized anti-IL-6 antibody, in patients with advanced cancer. Journal of Clinical Oncology 27(15S):3025-3025.

77. Wright A, Morrison SL 1994. Effect of altered CH2-associated carbohydrate structure on the functional properties and in vivo fate of chimeric mouse-human immunoglobulin G1. The Journal of experimental medicine 180(3):1087-1096.

78. Wright A, Sato Y, Okada T, Chang K, Endo T, Morrison S 2000. In vivo trafficking and catabolism of IgG1 antibodies with Fc associated carbohydrates of differing structure. Glycobiology 10(12):1347-1355.

79. Yu M, Brown D, Reed C, Chung S, Lutman J, Stefanich E, Wong A, Stephan J-P, Bayer R 2012. Production, characterization and pharmacokinetic properties of antibodies with N-linked Mannose-5 glycans. mAbs 4(4):475-487.

80. Shi HH, Goudar CT 2014. Recent advances in the understanding of biological implications and modulation methodologies of monoclonal antibody N-linked high mannose glycans. Biotechnology and bioengineering 111(10):1907-1919.

81. Kuriakose A, Chirmule N, Nair P 2016. Immunogenicity of Biotherapeutics: Causes and Association with Posttranslational Modifications. Journal of immunology research 2016:1298473.

82. van Beers MM, Bardor M 2012. Minimizing immunogenicity of biopharmaceuticals by controlling critical quality attributes of proteins. Biotechnol J 7(12):1473-1484.

83. Padler-Karavani V, Varki A 2011. Potential impact of the non-human sialic acid N-glycolylneuraminic acid on transplant rejection risk. Xenotransplantation 18(1):1-5.

84. van Schie KA, Wolbink GJ, Rispens T 2015. Cross-reactive and pre-existing antibodies to therapeutic antibodies--Effects on treatment and immunogenicity. mAbs 7(4):662-671.

85. Ratanji KD, Derrick JP, Dearman RJ, Kimber I 2014. Immunogenicity of therapeutic proteins: Influence of aggregation. Journal of immunotoxicology 11(2):99-109.

86. Chen W, Kong L, Connelly S, Dendle JM, Liu Y, Wilson IA, Powers ET, Kelly JW 2016. Stabilizing the CH2 Domain of an Antibody by Engineering in an Enhanced Aromatic Sequon. ACS chemical biology 11(7):1852-1861.

87. Krasnova L, Wong CH 2016. Exploring human glycosylation for better therapies. Molecular aspects of medicine 51:125-143.

88. Giddens JP, Wang LX 2015. Chemoenzymatic Glyco-engineering of Monoclonal Antibodies. Methods in molecular biology 1321:375-387.

89. Zhang N, Liu L, Dumitru CD, Cummings NR, Cukan M, Jiang Y, Li Y, Li F, Mitchell T, Mallem MR, Ou Y, Patel RN, Vo K, Wang H, Burnina I, Choi BK, Huber HE, Stadheim TA, Zha D 2011. Glycoengineered Pichia produced anti-HER2 is comparable to trastuzumab in preclinical study. mAbs 3(3):289-298.

90. Niwa R, Satoh M 2015. The current status and prospects of antibody engineering for therapeutic use: focus on glycoengineering technology. Journal of pharmaceutical sciences 104(3):930-941.

91. Chan AC, Carter PJ 2010. Therapeutic antibodies for autoimmunity and inflammation. Nature reviews Immunology 10(5):301-316.

92. Alsenaidy MA, Okbazghi SZ, Kim JH, Joshi SB, Middaugh CR, Tolbert TJ, Volkin DB 2014. Physical stability comparisons of IgG1-Fc variants: effects of N-glycosylation site occupancy and Asp/Gln residues at site Asn 297. Journal of pharmaceutical sciences 103(6):1613-1627.

93. Crispin M 2013. Therapeutic potential of deglycosylated antibodies. Proceedings of the National Academy of Sciences of the United States of America 110(25):10059-10060.

94. Lubiniecki A, Volkin DB, Federici M, Bond MD, Nedved ML, Hendricks L, Mehndiratta P, Bruner M, Burman S, Dalmonte P, Kline J, Ni A, Panek ME, Pikounis B, Powers G, Vafa O, Siegel R 2011. Comparability assessments of process and product changes made during development of two different monoclonal antibodies. Biologicals : journal of the International Association of Biological Standardization 39(1):9-22.

95. Alsenaidy MA, Jain NK, Kim JH, Middaugh CR, Volkin DB 2014. Protein comparability assessments and potential applicability of high throughput biophysical methods and data visualization tools to compare physical stability profiles. Frontiers in Pharmacology 5:39.

96. McCamish M, Woollett G 2011. Worldwide experience with biosimilar development. mAbs 3(2):209-217.

97. Federici M, Lubiniecki A, Manikwar P, Volkin DB 2013. Analytical lessons learned from selected therapeutic protein drug comparability studies. Biologicals : journal of the International Association of Biological Standardization 41(3):131-147.

98. 2016. U.S. Food and Drug Administration. Guidance for Industry- Clinical Pharmacology Data to Support a Demonstration of Biosimilarity to a Reference Product.

99. 2015. U.S. Food and Drug Administration. Guidance for Industry-Quality Considerations in Demonstrating Biosimilarity of a Therapeutic Protein Product to a Reference Product.

100. 2015. U.S. Food and Drug Administration. Guidance for Industry- Scientific Considerations in Demonstrating Biosimilarity to a Reference Product.

101. Blackstone EA, Joseph PF 2013. The Economics of Biosimilars. American Health & Drug Benefits 6(8):469-478.

102. Geng X, Kong X, Hu H, Chen J, Yang F, Liang H, Chen X, Hu Y 2015. Research and development of therapeutic mAbs: An analysis based on pipeline projects. Human Vaccines & Immunotherapeutics 11(12):2769-2776.

103. Udpa N, Million RP 2016. Monoclonal antibody biosimilars. Nature reviews Drug discovery 15(1):13-14.

104. Kumar R, Singh J 2014. Biosimilar drugs: Current status. International Journal of Applied and Basic Medical Research 4(2):63-66.

105. Volkin DB, Hershenson S, Ho RJY, Uchiyama S, Winter G, Carpenter JF 2015. Two Decades of Publishing Excellence in Pharmaceutical Biotechnology. Journal of pharmaceutical sciences 104(2):290-300.

106. Berkowitz SA, Engen JR, Mazzeo JR, Jones GB 2012. Analytical tools for characterizing biopharmaceuticals and the implications for biosimilars. Nature reviews Drug discovery 11(7):527-540.

107. Reusch D, Haberger M, Kailich T, Heidenreich AK, Kampe M, Bulau P, Wuhrer M 2014. High-throughput glycosylation analysis of therapeutic immunoglobulin G by capillary gel electrophoresis using a DNA analyzer. mAbs 6(1):185-196.

108. Prien JM, Stöckmann H, Albrecht S, Martin SM, Varatta M, Furtado M, Hosselet S, Wang M, Formolo T, Rudd PM. 2015. Orthogonal Technologies for NISTmAb N-Glycan Structure Elucidation and Quantitation. State-of-the-Art and Emerging Technologies for Therapeutic Monoclonal Antibody Characterization Volume 2 Biopharmaceutical Characterization: The Nistmab Case Study, ed.: ACS Publications. p 185-235.

109. Huhn C, Selman MH, Ruhaak LR, Deelder AM, Wuhrer M 2009. IgG glycosylation analysis. Proteomics 9(4):882-913.

110. Zhang L, Luo S, Zhang B 2016. Glycan analysis of therapeutic glycoproteins. mAbs 8(2):205-215.

111. Fang J, Doneanu C, Alley WR, Jr., Yu YQ, Beck A, Chen W 2016. Advanced assessment of the physicochemical characteristics of Remicade(R) and Inflectra(R) by sensitive LC/MS techniques. mAbs 8(6):1021-1034.

112. Barb AW, Meng L, Gao Z, Johnson RW, Moremen KW, Prestegard JH 2012. NMR characterization of immunoglobulin G Fc glycan motion on enzymatic sialylation. Biochemistry 51(22):4618-4626.

113. Subedi GP, Barb AW 2016. The immunoglobulin G1 N-glycan composition affects binding to each low affinity Fc gamma receptor. mAbs 8(8):1512-1524.

114. Subedi GP, Barb AW 2015. The Structural Role of Antibody N-Glycosylation in Receptor Interactions. Structure 23(9):1573-1583.

115. Barb AW 2015. Intramolecular N-glycan/polypeptide interactions observed at multiple N-glycan remodeling steps through [(13)C,(15)N]-N-acetylglucosamine labeling of immunoglobulin G1. Biochemistry 54(2):313-322.

116. Marchetti R, Perez S, Arda A, Imberty A, Jimenez-Barbero J, Silipo A, Molinaro A 2016. "Rules of Engagement" of Protein-Glycoconjugate Interactions: A Molecular View Achievable by using NMR Spectroscopy and Molecular Modeling. ChemistryOpen 5(4):274-296.

117. Marino K, Bones J, Kattla JJ, Rudd PM 2010. A systematic approach to protein glycosylation analysis: a path through the maze. Nature chemical biology 6(10):713-723.

118. Pan J, Zhang S, Chou A, Borchers CH 2016. Higher-order structural interrogation of antibodies using middle-down hydrogen/deuterium exchange mass spectrometry. Chem Sci 7(2):1480-1486.

119. An Y, Zhang Y, Mueller H-M, Shameem M, Chen X 2014. A new tool for monoclonal antibody analysis: Application of IdeS proteolysis in IgG domain-specific characterization. mAbs 6(4):879-893.

120. Chen CL, Hsu JC, Lin CW, Wang CH, Tsai MH, Wu CY, Wong CH, Ma C 2017. Crystal Structure of a Homogeneous IgG-Fc Glycoform with the N-Glycan Designed to Maximize the Antibody Dependent Cellular Cytotoxicity. ACS chemical biology 12(5):1335-1345.

121. Patwa T, Li C, Simeone DM, Lubman DM 2010. Glycoprotein Analysis Using Protein Microarrays and Mass Spectrometry. Mass spectrometry reviews 29(5):830-844.

122. Reusch D, Haberger M, Maier B, Maier M, Kloseck R, Zimmermann B, Hook M, Szabo Z, Tep S, Wegstein J, Alt N, Bulau P, Wuhrer M 2015. Comparison of methods for the analysis of therapeutic immunoglobulin G Fc-glycosylation profiles—Part 1: Separation-based methods. mAbs 7(1):167-179.

123. Blessy M, Patel RD, Prajapati PN, Agrawal YK 2014. Development of forced degradation and stability indicating studies of drugs—A review. Journal of Pharmaceutical Analysis 4(3):159-165.

124. Alsenaidy MA, Kim JH, Majumdar R, Weis DD, Joshi SB, Tolbert TJ, Middaugh CR, Volkin DB 2013. High-throughput biophysical analysis and data visualization of conformational stability of an IgG1 monoclonal antibody after deglycosylation. Journal of pharmaceutical sciences 102(11):3942-3956.

125. Alsenaidy MA, Wang T, Kim JH, Joshi SB, Lee J, Blaber M, Volkin DB, Middaugh CR 2012. An empirical phase diagram approach to investigate conformational stability of "second-generation" functional mutants of acidic fibroblast growth factor-1. Protein science : a publication of the Protein Society 21(3):418-432.

126. Stanley P SH, Taniguchi N. 2009. N-Glycans. In Varki A CR, Esko JD, et al., editor Essentials of Glycobiology, 2nd edition ed., Cold Spring Harbor (NY): Cold Spring Harbor Laboratory Press.

127. Bui LA, Hurst S, Finch GL, Ingram B, Jacobs IA, Kirchhoff CF, Ng CK, Ryan AM 2015. Key considerations in the preclinical development of biosimilars. Drug Discov Today 20 Suppl 1:3-15.

Chapter 2 Correlating the Impact of Well-Defined Oligosaccharide Structures on Physical Stability Profiles of IgG1-Fc Glycoforms

(More AS, Toprani VM, Okbazghi SZ, Kim JH, Joshi SB, Middaugh CR, Tolbert TJ, Volkin DB 2016. Correlating the Impact of Well-Defined Oligosaccharide Structures on Physical Stability Profiles of IgG1-Fc Glycoforms. Journal of pharmaceutical sciences 105(2):588-601.)

2.1 Introduction

Post-translational modifications such as glycosylation and their effect on the structure, function and pharmaceutical properties of antibody molecules have been a topic of interest for many years.[1,2] With the popularity of monoclonal antibody (mAb) therapeutics (primarily IgG), and the development of more affordable biosimilars, the interest in evaluating antibody glycosylation has greatly increased.[3,4,5,6] Glycosylation of IgGs plays an important biological role in maintaining pharmacokinetic attributes (circulation half lives in blood, clearance and bioavailability) and controlling biological activity (by affecting the IgG affinity to bind various Fc receptors *in vivo).*[7,8,9,10,11,12,13,14,15] For example, mAbs with high mannose N-linked glycans show increased clearance (decreased serum half-life) leading to reduced exposure and lower efficacy,[16] while IgGs containing bisecting GlcNAc glycans show enhanced antibody dependent cell mediated cytotoxicity (ADCC) and stronger binding to FcγRIIIa receptors. [13,16,17,18,19,20]

The IgG1 glycoprotein is a homodimer containing two antigen binding Fab regions connected to a Fc region by flexible linkers.[21] The IgG1-Fc is a disulfide-bonded homodimer that comprises of two non-covalently paired C_H2-C_H3 domains.[22] The N-linked glycosylation site lies at the asparagine 297 (Asn^{297}) residue of the consensus sequence Asn-X-Ser/Thr of the C_H2 domain. The two C_H2 domains do not pair directly but are bridged together by the complex di-antennary glycans, which occupy the inside of a horseshoe-shaped pocket between these domains.[23] The glycans form various non-covalent interactions with the Fc domains contributing to the formation of a stable conformation.[7] Structural analysis by X-ray crystallography in combination with molecular dynamic simulations have shown that full or partial removal of the glycan residues cause conformational changes in the C_H2 domain resulting in loss of both glycan-glycan and glycan-protein backbone non-covalent interactions.[24] The aglycosylated Fc

displays a larger radius of gyration (Rg) than glycosylated Fc in solution suggesting a more open conformation (as measured by small-angle X-ray scattering).[23] Numerous studies on natural, truncated and aglycosylated glycoforms of mAbs have shown that changes in glycosylation affect protease susceptibility, flexibility, physicochemical stability and aggregation, often in a complex manner.[10,17,25-34]

Protein glycosylation is a heterogeneous post-translational modification which includes glycosylation site occupancy variation (macro-heterogeneity) and variations in type, length, and branching of glycans (micro-heterogeneity).[35] During recombinant expression of mAb therapeutics, variation in glycosylation occurs as the result of the type of expression hosts, scales of manufacturing, and culture conditions.[7,13,36-37] Because of these effects, ensuring tight limits of glycan heterogeneity during manufacturing is a challenge, and is a critical aspect of mAb development, both for innovator and biosimilar protein-drugs.[38] Although glycosylation engineering holds tremendous potential in improving the efficacy of antibody therapeutics,[39,40,35] more systematic studies are needed to better understand their effects on pharmaceutical properties to develop a stable and efficacious glycoprotein formulation.

Developing new analytical approaches and techniques to better determine and compare the complexity of post-translational modifications (such as glycosylation) of protein drugs, and to elucidate their higher-order structural integrity, is currently an urgent need for both comparability[41,42] and biosimilarity assessments.[43,44] Extensive analytical characterization can serve as a key tool to minimize the extent to which expensive, time consuming clinical trials are required to ensure that the safety and efficacy of protein drugs is maintained after process changes (comparability) or when made by different manufacturers (biosimilarity).[41-44] Previous work in our labs has utilized a variety of biophysical techniques combined with data

visualization tools such as empirical phase diagrams and radar charts to show that enzymatic removal of glycans from the Fc region of an IgG1 mAb decreased physical stability.[45] In addition, site occupancy and amino acid changes at the Asn297 site within IgG1-Fc molecules was shown to affect their physical stability profile by the same experimental approach.[45-46] Similarly, Yageta et al[47] has recently used empirical phase diagrams to compare the conformational and colloidal stability of isolated constant domains of human IgGs (including aglycosylated C_H2 domains) under acidic conditions. One key goal of these types of studies is to assess the utility of physical stability profiles in protein comparability assessments.[41]

In this work, we report the use of four well-defined IgG1-Fc glycoforms (HM-Fc, Man5-Fc, GlcNAc-Fc and N297Q-Fc) as a comparative model system for developing a mathematical approach for biosimilarity analysis. The purpose of this study is to compare the apparent solubility (thermodynamic activity) and physical stability profiles of these model Fc glycoforms under a variety of solution conditions. This was a collaborative project which involved other laboratories at KU which carried out (1) thorough biological characterization of these IgG1-Fc glycoforms,[48] (2) chemical stability evaluations of the four IgG1-Fc glycoforms,[49] and (3) mathematical modeling of physical stability data presented in this work for the purpose of biosimilarity assessments.[50]

We have determined the effect of oligosaccharide structure on the relative apparent solubility (thermodynamic activity) of the Fc glycoforms using a PEG precipitation assay. We then evaluated the structural integrity and conformational stability using a variety of biophysical techniques including intrinsic and extrinsic fluorescence spectroscopy, turbidity measurements and differential scanning calorimetry across a variety of pH, temperature and formulation conditions. Comparative information on the structure and stability of these Fc glycoforms with

regard to differences in glycosylation is generated by the use of data visualization tools including three-index empirical phase diagrams and radar charts. These results are not only useful as part of preformulation characterization studies during formulation development (as described in this chapter), but also provide large datasets for mathematical modeling for biosimilarity assessments using data mining and machine learning tools.[50]

2.2 Materials and Methods

2.2.1 Materials

IgG1-Fc glycoforms (HM-Fc, Man5-Fc, GlcNAc-Fc) were produced using a combination of expression in a glycosylation deficient strain of *Pichia pastoris* (yeast), protein purification and *in-vitro* enzymatic synthesis as described elsewhere (see Okbazghi et al, 2016 and Alsenaidy et al, 2014).[48,51] The non-glycosylated variant of the IgG1-Fc (N297Q-Fc) was made by mutating the N-linked glycosylation site at Asn-297 (EU numbering) to Gln 297 and was produced as described elsewhere (see Okbazghi et al, 2016 and Alsenaidy et al, 2014).[48,51] After expression and purification, the four well-defined IgG1-Fc glycoproteins were concentrated and dialyzed into a storage buffer (10% sucrose, 20 mM histidine, pH 6.0) and frozen at −80°C at a concentration of 0.2 mg/mL.[51] A pictorial summary of the four well-defined IgG1-Fc glycoforms used in this work is provided in Figure 2.1.

For PEG precipitation studies and differential scanning calorimetry (DSC), the four IgG1-Fc glycoforms were concentrated to 3 mg/mL using a Millipore Amicon Ultra (EMD Millipore, Billerica, MA) with 0.5 mL centrifugal filter device and a 10 kDa MW cut off. All the glycoforms were then dialyzed at 4°C overnight in a 20 mM citrate phosphate buffer with ionic strength adjusted to 0.15 by NaCl at pH 4.5 and 6.0 to obtain final protein stock solutions of 1 mg/mL. For the biophysical characterization studies, samples were thawed and dialyzed into one

of two different formulations: (1) 20 mM citrate phosphate buffer adjusted to an ionic strength of 0.15 with NaCl (pH 4.0-7.5, at 0.5 pH unit increments), and (2) 20 mM citrate phosphate buffer containing 10% sucrose (w/v) (pH 4.0-7.5, 0.5 pH unit increments). Dialysis was performed at 4°C using Slide-A-Lyzer dialysis cassettes (Life technologies, Grand Island, NY) with a 10 kDa molecular weight cut off, with three buffer exchanges; two exchanges at 4h intervals and one overnight. Components of all buffers including L-Histidine, sodium phosphate and sodium chloride as well as PEG-10,000 were purchased from Sigma-Aldrich (St Louis, MO) while citric acid anhydrous and citric acid monohydrate were purchased from Fisher Scientific at the highest purity grade. Sucrose was obtained from Pfansteihl, Inc. (Waukegan, IL).

2.2.2 Methods

2.2.2.1 *PEG Precipitation Assay*

The experimental protocol was adapted from Gibson et al[52] and Toprani et al.[53] Stock solutions of PEG-10,000 ranging from 0 to 40% w/v PEG were prepared in 20 mM citrate phosphate buffer with ionic strength adjusted to 0.15 by NaCl at pH 4.5 and pH 6.0. A volume of 40 µL of each of the PEG-10,000 solutions (from 0 to 40% w/v PEG) were added to wells of a 96-well polystyrene filter plate (Corning#3504, Corning Life Sciences, Corning, NY). Ten µL of the protein stock solutions (1 mg/mL) was then added to each well to achieve a final protein concentration of 0.2 mg/mL. The plates were incubated at room temperature overnight and then were centrifuged at 548 (x g) for 15 min. The filtrate was collected in a clear 96 well collection plate (Greiner Bio-One#655001, Greiner Bio-One North America Inc., Monroe, NC). The protein concentration was determined on a NanoDrop 2000 spectrophotometer (NanoDrop Products, Wilmington, DE) using 2 µL of filtrate by measuring absorbance at 280 nm. The concentrations of all four IgG1-Fc proteins vs % PEG-10,000 data were fit to a standard four-

parameter, modified Hill-slope sigmoidal curve equation (Eq.1), using Python (x,y) v.2.7.6.0, an open source scientific software based on python language. The % PEG_{midpt} values and apparent solubility value parameters were then calculated from the resulting curve fit[52] where t= top plateau, b= bottom plateau, mid= x-axis midpoint, and s=slope. The % PEG_{midpt} values were determined by noting the x-axis midpoints.

$$y = b + \left(\frac{t-b}{1+ e^{\,s(mid-x)}}\right) \qquad (1)$$

The apparent solubility values were determined[54] by first plotting the same data sets on a logarithmic scale from the transition region and then fitting them using equation (2) to extrapolate the data to zero % PEG concentrations.

$$\log Sp = \log a_o - A_{12}[PEG] \qquad (2)$$

Under certain assumptions, including non-interaction of PEG with protein, the y intercept of the linear fit is the apparent thermodynamic activity (or apparent solubility) of the protein. The p values for all four IgG1-Fc samples were determined using the student t-test in Microsoft Excel 2010 software. All the truncated glycoforms (Man5-Fc, GlcNAc-Fc, and N297Q-Fc) were compared to the HM-Fc as a control. A p value of < 0.05 was accepted as significant.

2.2.2.2 *Differential Scanning Calorimetry (DSC)*

DSC experiments were performed using a MicroCal VP-AutoDSC instrument with an autosampler (MicroCal, LLC, Northampton, MA). Thermograms of protein samples (at 0.4 mg/mL concentration formulated in 20 mM citrate phosphate buffer adjusted to an ionic strength of 0.15 by NaCl at pH 4.5 and 6.0) were obtained from 10°C to 100°C with a scanning rate of 60°C/h. Data analysis was performed using the MicroCal LLC DSC plug-in for the Origin 7.0 software package. The raw thermograms of the protein samples were buffer subtracted using the corresponding buffer system thermograms, baseline fitted and normalized by concentration to

obtain the final thermograms. The final thermograms were fit to a non-two-state unfolding model with four transitions to calculate the heat capacity peak maximum (T_m values) of the four transitions. The onset temperature (T_{onset}) of the transitions was determined by identifying the point where the heat capacity (Cp) value for the thermal transition reached 500 cal $mol^{-1}°C^{-1}$.[29, 55]

2.2.2.3 *Intrinsic (Trp) fluorescence spectroscopy*

The fluorescence spectrum of each of the IgG1 Fc glycoforms was measured in triplicate using a Photon Technology International (PTI) Quantum master fluorometer (New Brunswick, New Jersey) with 200 µL of 0.2 mg/mL protein solution in 0.2 cm path length quartz cuvettes. Samples were excited at 295 nm (>95% Trp emission) and the emission spectra at 10°C were recorded from 305 to 405 nm. For thermal stability measurements, the temperature was raised in increments of 1.25°C from 10 to 90°C with a heating rate of 15°C/h. Data were collected and spectra were buffer subtracted and analyzed using an in-house software (MiddaughSuite). The maximum peak position (λ_{max}) values were calculated using a "spectral center of mass" method (MSM) that results a red shift in the peak position by 10–14 nm compared with the actual value, but produces a more reproducible measure of spectral shift and a higher signal to noise ratio.[51]

2.2.2.4 *Extrinsic fluorescence spectroscopy*

The extrinsic fluorescence measurements were performed using a MX3005P QPCR system (Agilent Technologies). Samples contained 0.2 mg/mL protein in a total sample volume of 100 µL. The Sypro™ orange dye was purchased from Invitrogen, Inc. (Carlsbad, CA) and was supplied in a concentrated form (5000x) and dissolved in dimethyl sulfoxide (DMSO). The stock was diluted to 40x in water and then added to the protein samples to achieve 1x dye concentration for measurements. Using custom filter sets, the mixture was excited at 492 nm,

and the emission intensity change with temperature at 610 nm was followed. The temperature was raised from 25 to 90°C using 60°C/h heating rate and 1˚C as a step size. Data were transferred to Excel software (Microsoft, Redmond, Washington) for data analysis. Protein samples were run in triplicate and corresponding buffer blanks were run and subtracted from each sample spectrum. The fluorescence intensity was plotted against temperature as described previously.[51]

2.2.2.5 *OD 350 nm measurements*

Turbidity measurements were performed using a Cary 100 UV-Visible spectrophotometer (Varian medical Systems, Inc., Palo Alto, California) equipped with a 12 cell holder with a peltier type temperature controller. Samples contained 0.2 mg/mL protein with a total volume of 250 µL in 1 cm path length quartz cells. Optical density at 350 nm was monitored as the temperature was raised in increments of 1.25˚C from 10 to 90˚C with a heating rate of 60˚C/h. Protein samples were run in triplicate and corresponding buffer blanks were run and subtracted from each sample. The OD at 350nm was plotted against temperature as described previously. [51]

2.2.2.6 *Construction of EPDs and Radar Charts*

Three-index Empirical Phase Diagrams (EPDs) and Radar Charts were employed to visualize the biophysical stability of the four IgG1-Fc glycoforms using in-house software (MiddaughSuite). Detailed descriptions of the construction of both three-index EPDs and radar charts are published elsewhere.[56,57] Briefly, the 3-index EPDs display structural changes in proteins as color changes, based on data sets obtained from three biophysical techniques as a function of solution pH and temperature. The three biophysical data sets in this work are extrinsic fluorescence intensity using a Sypro Orange dye, intrinsic Trp fluorescence peak

position, and optical density at 350 nm. For the 3-index EPDs, each dataset was mapped to three color components – red, green, and blue, respectively. For each of the four IgG1-Fc glycoforms, and their corresponding extrinsic Sypro Orange fluorescence and turbidity measurements, the minimum value in a dataset was mapped to the loss of the color component (e.g., black), and the maximum value to the full color intensity. For Trp fluorescence peak position, however, the maximum value was mapped to the loss of color component and minimum value to the full color component for better visualization. The combination of these RGB values produced a single color at each point in pH and temperature space indicating overall structural changes due to the applied environmental stress. The individual RGB components were displayed in a separate panel alongside the three-index EPDs (see Supplemental Figures 2.4 and 2.5) since the explicit display of its RGB components can be helpful in better understanding the interpretation of color changes. The color green from intrinsic Trp fluorescence indicates protein structure closest to the native state (least amount of structural change). The color red appears as the Sypro Orange binding increases indicating structural alterations in the protein. The blue color appears when higher turbidity is measured by optical density values at 350 nm indicating protein aggregation.

To better define regions of structural similarities and differences, a *k*-means clustering algorithm was applied to the three datasets for identifying boundaries of similar color regions. The *k*-means clustering algorithm calculates *k* central points (or centroids) in which all samples belong to each cluster whose mean is the calculated centroid. The number of clusters (*k*) was selected in advance by visual assessment of the 3-index EPDs and raw biophysical data stability profiles.[51]

Radar charts were generated to display average readouts of three biophysical datasets within a cluster. Each biophysical dataset was represented as a separate radial axis where the

minimum value in an averaged dataset for a cluster was mapped to the center of the radar chart and the maximum value to the outer circumference. Connecting values in each axis yields a final polygon to represent a specific structural state.[51,56,57] Polygons in a radar chart have smaller areas if the protein stays closer to its native state; thus less change is observed from a baseline of the analytical readouts from each technique.

2.3 Results

2.3.1 Initial Comparisons of Relative Solubility and Conformational Stability

An assessment of the apparent solubility (thermodynamic activity) of the four IgG1-Fc glycoform variants was performed using PEG precipitation as described previously[52-54](see Methods section). As shown in Figure 2.2, protein vs. % PEG concentration plots were generated at pH 4.5 (Figure 2.2A, 2.2B and 2.2C) and pH 6.0 (Figure 2.2D, 2.2E and 2.2F) for various glycoforms in a NaCl containing formulation. For ease of comparison, each of the Fc glycoform variants (Man5-Fc, GlcNAc-Fc, and N297Q-Fc) were plotted versus the high mannose HM-IgG1-Fc glycoform. The plots show a sigmoidal curve, demonstrating that as the crowding agent PEG concentration increases; there is a point at which a decrease in the amount of the protein in solution occurs in a quantifiable manner. The N297Q-Fc at pH 4.5 begins to precipitate rapidly as the PEG concentration is increased, and deviates from the typical sigmoidal curve, possibly indicating structural alterations in the protein and/or direct interaction between the PEG and protein.

As shown in Figure 2.3A and 2.3B, the % PEG_{midpt} value is the weight % PEG required to reduce the protein concentration by 50% of its initial value. For each of the glycoforms, a trend of decreasing % PEG_{midpt} values with increasing solution pH was observed. More subtle differences were observed at pH 6.0 while at pH 4.5 the differences were more prominent (see

Figures 2.2D, E, F and 2.2A, B, C). In terms of general trends, the HM-Fc showed the highest % PEG_{midpt} values followed by Man5-Fc, GlcNAc-Fc and then the non-glycosylated N297Q IgG1-Fc. Differences in % in PEG_{midpt} values between the HM-Fc vs. Man5-Fc and GlcNAc-Fc were statistically significant at pH 4.5, but at pH 6.0, the differences between HM-Fc vs. Man5-Fc were not significant. Significant differences in % PEG_{midpt} values between the HM-Fc vs. either GlcNAc-Fc or N297Q-Fc were observed at both pH values.

As shown in Figure 2.3C and 2.3D, the apparent solubility (thermodynamic activity) values can be calculated by extrapolation to zero PEG concentration[53,54] (see Methods section). These values showed trends similar to those found with % PEG_{midpt} in terms of Fc oligosaccharide structure and solution pH. At both pH values, the apparent activity values between HM-Fc vs. Man-5 glycoforms showed no statistically significant differences. The apparent activity values of HM-Fc vs. either GlcNAc-Fc or N297Q-Fc showed statistical significant differences at both pH 4.5 and 6.0.

The overall conformational stability of all the four IgG1-Fc glycoforms at pH 4.5 and pH 6.0 in a NaCl containing buffer was probed by DSC. Representative thermograms of HM-Fc, Man5-Fc, GlcNAc-Fc and N297Q-Fc are shown in Figure 2.4 A-D, respectively. Each of the four IgG1-Fc glycoforms showed two major endothermic peaks which could be mathematically fit to two T_{onset} values ($T_{onset}1$, $T_{onset}2$) and four T_m values (T_m1 , T_m2, T_m3 and T_m4) as summarized in Table 2.1. Based on previous studies with human IgG Fc glycoforms from the Jefferis lab,[58] the $T_{onset}1$, T_m1 and T_m2 values correspond to the unfolding of the C_H2 domain of the IgG1-Fc, while the $T_{onset}2$, T_m3 and T_m4 values correspond to the unfolding of the IgG1-Fc C_H3 domain. In general, these values were lower at pH 4.5 than 6.0 for each of the four IgG1-Fc glycoforms. A trend of decreasing conformational stability with the truncation of carbohydrate

units was observed for the $T_{onset}1$, T_m1 and T_m2 values, which correspond to the C_H2 domain containing the N-linked glycosylation site at pH 4.5 condition: highest values were observed for HM-Fc and Man5-Fc, intermediate for GlcNAc-Fc and the lowest for N297Q-Fc (See Table 2.1). At the higher pH 6.0 conditions, differences in conformational stability (the T_{onset} 1, T_m1 and T_m2 values) versus type of glycosylation were observed when comparing the aglycosylated versus the glycosylated forms.

2.3.2 Physical Stability of IgG1-Fc Proteins as a Function of pH and Temperature using High Throughput Biophysical Analyses

To evaluate the structural integrity and physical stability of the four different IgG1-Fc glycoforms over a wider range of conditions, high throughput biophysical analyses were utilized using relatively small amounts of material (compared to PEG and DSC analysis). First, the structural integrity of the overall tertiary structure of the four IgG1-Fc glycoforms was evaluated by measurement of intrinsic Trp fluorescence at 10°C, at pH values from 4.0-7.5 (increments of 0.5) in formulations containing either NaCl (formulation 1) or Sucrose (formulation 2). For each Fc glycoform, the wavelength of maximum intensity (λ_{max}) at each pH was calculated and found to be in the range of 328 to 334 nm with standard deviations calculated from triplicate measurements of up to ~2 nm (see Supplemental Figure 2.1). These results indicated that the four glycoforms were overall similar (with some minor differences noted).

The stability of the overall tertiary structure of the four glycoforms was evaluated by collecting the intrinsic Trp fluorescence spectra, and plotting the changes in λ_{max}, as a function of increasing temperature at each pH condition in the two formulations as shown in Figure 2.5A (NaCl) and Figure 2.6A (Sucrose). Note that the λ_{max} values in Figures 2.5A and 2.6A are red shifted due to the use of a spectral center of mass (MSM) method (see also Supplemental Figures

2.2A and 2.3A with the same physical stability data shown with corresponding standard deviation (SD) error bars from triplicate measurements). In formulation 1 (NaCl) with increases in temperature, all of the Fc glycoforms showed a subtle increase in peak positions followed by a more sudden increase (transition) before plateauing (Figure 2.5A). Similar trends were observed in formulation 2 (sucrose) in Figure 2.6A.

The T_m values of thermal transitions were calculated for each of the four IgG1-Fc glycoforms at each of the eight pH values in both formulations (see plot of values in the thermal stability panel in Figures 2.5A and 2.6A). In general, the T_m values of the intrinsic fluorescence thermal transitions for the four glycoforms followed trends dependent upon the type of glycoform, the solution pH, and the formulation (NaCl and sucrose). First, the T_m values of thermal transitions were the highest for HM-Fc and Man5-Fc followed by intermediate values for GlcNAc-Fc and the lowest values for N297Q-Fc under all pH conditions examined and in both formulations. Second, for each of the four glycoforms and in both of formulations, the T_m values increased with increases in solution pH. These results suggest that the HM-Fc and Man5-Fc glycoforms display similar, yet distinct, physical stability of the tertiary structure, followed by the GlcNAc-Fc with intermediate stability, with the N297Q-Fc aglycosylated form the least thermally stable. Each of the IgG1-Fc glycoforms showed lower tertiary structure stability at acidic pH values, with increasing thermal stability as the solution pH increased. Finally, the T_m values for each of the IgG-Fc glycoforms at each solution pH were relatively higher in formulation 2 (sucrose) than in formulation 1 (NaCl). To better display this latter effect, the differences in T_m values (ΔT_m) between formulations (sucrose versus NaCl) at each pH condition, and for each of the four Fc proteins, are also shown in Figure 2.7A. These differences in the T_m values due to formulation excipients were more prominent at lower pH values (e.g., pH

4.0, 4.5 and 5.0). Each of the four glycoforms is more stable with respect to the overall tertiary structure in formulation 2 (sucrose) than in formulation 1 (NaCl).

A similar set of experiments were performed with extrinsic fluorescence analysis (see Figures 2.5B and 2.6B), where Sypro Orange was used as a probe for detecting protein structural alterations seen as increased fluorescence intensity upon exposure of the dye to increased apolar environments (presumably as a result of structural changes and/or aggregate formation by the protein). Alterations in apolar nature of the four IgG1-Fc glycoforms vs. temperature were monitored by following changes in Sypro Orange fluorescence intensity in the two formulations. (See Supplementary Figures 2.2B and 2.3B for the same physical stability data with corresponding SD error bars from triplicate measurements). The Sypro Orange fluorescence peak intensity at the starting temperature (10°C) in the N297Q-Fc in both formulations trended relatively higher, and showed more variability across the pH range, compared to other three forms. The GlcNAc-Fc also displayed similar elevated signals at low pH, but to somewhat lesser extent than the aglycosylated Fc protein.

The T_m values of the transitions in the Sypro Orange fluorescence intensity versus temperature curves were calculated and plotted for the four Fc glycoforms at all 8 pH conditions in both formulations; see thermal stability panels in Figures 2.5B and 2.6B. As certain proteins at some pH conditions exhibited multiple thermal transitions, T_m values of the major thermal transition were calculated for simplicity for these initial comparisons. The T_m values of extrinsic Sypro Orange fluorescence thermal transitions for the four IgG1-Fc glycoforms again followed specific trends dependent upon the type of glycoform, the solution pH, and the formulation composition (NaCl and sucrose). First, the T_m values of major transitions in peak intensity versus temperature curves were the highest for HM-Fc and Man5-Fc glycoforms followed by

intermediate values for GlcNAc-Fc and lowest values for N297Q-Fc in both formulations. Second, for each of the four IgG1-Fc glycoforms, the T_m values increased with increases in the solution pH in both the formulations. Additionally, in both formulations for all four proteins, two thermal transitions were observed at lower pH values (e.g., pH 4.0, 4.5, 5.0) (see Figures 2.5B and 2.6B). Finally, the T_m values for each of the glycoforms were relatively higher in formulation 2 (sucrose) than in formulation 1 (NaCl). The differences in Tm values (ΔT_m) between the sucrose and NaCl formulations for the four IgG1-Fc proteins are plotted in Figure 2.7B. Note that the differences are more prominent at lower pH values (e.g., pH 4.0, 4.5 and 5.0). These results indicate that with respect to their tertiary structure stability as measured by extrinsic Sypro orange fluorescence measurements, the N297Q aglycosylated form is least thermally stable, followed by the GlcNAc-Fc glycoform with intermediate stability, and the highest thermal stability seen with the HM-Fc and Man5-Fc glycoforms. These trends in the physical stability profiles are similar to the intrinsic fluorescence spectroscopy results. For the less stable glycoforms, the lower pH values (4.0 and 4.5), trended toward an apparent higher surface hydrophobicity even at lower temperatures, suggesting some level of structural alteration under these conditions. Each of the glycoforms is more thermally stable in sucrose than in NaCl under most pH conditions tested, particularly at the lower pH values (e.g., 4.0, 4.5 and 5.0).

As final set of experiments, the temperature-induced aggregation was evaluated by monitoring optical density (OD) changes at 350 nm (average of 3 replicates) as a function of increasing temperature from pH 4.0-7.5 (at intervals of 0.5) and in the two formulations (see Figures 2.5C and 2.6C). (See Supplementary Figures 2.2C and 2.3C with the same physical stability data with corresponding SD error bars from triplicate measurements.) Differences in aggregation pattern were observed with the type of glycoform, the solution pH, and the two

formulation conditions. The HM-Fc and Man5-Fc glycoforms did not show any notable increases in OD350 values as the temperature increased across all of the pH conditions tested in both formulations. The GlcNAc-Fc and N297Q-Fc samples displayed single thermal transitions between pH 5.0 to 7.0 in both formulations. The GlcNAc-Fc glycoform showed two transitions at pH 6.0 in formulation 2 (sucrose), and a single thermal transition at pH 7.5 in formulation 1 (NaCl). At pH 4.0 and 4.5, no detectable changes in OD350 values versus temperature were observed for all of the four glycoforms in both the formulations.

The onset temperature values (T_{onset}), where a rapid increase in OD350 was observed, were calculated for each of the four glycoforms at all eight pH conditions and in both formulations (Figure 2.5C and 2.6C). The T_{onset} values were determined by noting the temperature at which the transition starts. The T_{onset} values for triplicate runs were in the range of 77-85°C with standard deviations (SD) from 0 to 2.6°C for the four Fc glycoforms. However, the GlcNAc-Fc at pH 6.0 in formulation 2 (sucrose) showed the first T_{onset} at 54.1°C and a second at 75.3°C. The results indicate that GlcNAc-Fc is the most aggregation prone glycoform followed by the N297Q-Fc. The HM-Fc and Man5-Fc Fc proteins are not prone to aggregation at any of the solution conditions tested here.

2.3.3 Physical Stability Evaluations and Comparisons between IgG1-Fc glycoform variants using Data Visualization Techniques

Using the physical stability data sets acquired from intrinsic fluorescence spectroscopy, extrinsic Sypro orange fluorescence, and turbidity measurements, 3-index empirical phase diagrams (EPDs) (left panels) and radar charts (right panels) were constructed for each of the individual IgG1-Fc glycoforms formulated in either NaCl (Figure 2.8) or sucrose (Figure 2.9). The corresponding individual RGB components generated as part of the three-index EPDs are

shown in Supplementary Figures 2.4 and 2.5. Analysis of the raw biophysical data, the 3-index EPDs, and their corresponding individual RGB color indices were then used as a basis to visually identify regions with similar structural characteristics. These numerical values were then used for clustering analysis to identify the primary structural regions for each protein (as a function of pH and temperature) as displayed in the radar chart diagrams on the right panels of Figure 2.8 and Figure 2.9.

In each of the four Fc proteins in 2 formulations, the 3-index EPDs show a green region that represents a state in which the IgG1-Fc glycoforms exist in their most native-like conformation. In this green region, minimal structural changes were observed in Trp fluorescence position, whereas other color components were suppressed on account of low signals from their corresponding techniques. In the radar charts, region A corresponds to this native-like green region in the EPD displayed as a polygon with the smallest area. Further, the percent areas of this native-like region A were calculated. The percent areas for region A in formulation 1 (NaCl) for both HM-Fc and Man5-Fc were 51%, GlcNAc-Fc 40% and N297Q-Fc 26%, while the percent areas for region A in formulation 2 (sucrose) were 56%, 55%, 51% and 48% for HM-Fc, Man5-Fc, GlcNAc-Fc and N297Q-Fc, respectively.

Similarly, regions B and C in the radar charts correspond to the bright red/orange and dark red colors in the 3-index EPDs. These regions represent structurally altered forms of the Fc glycoforms as indicated by increases in the Sypro orange fluorescence (region B) and fluorescence peak position (region C). Region D in the radar charts, observed in the GlcNAc-Fc and N297Q-Fc forms only, represents an aggregated state of the Fc glycoforms with increased optical density at 350nm. This region D in the radar chart corresponds to a blue color in the 3-index EPDs. The four IgG1-Fc glycoforms can be compared head to head by comparing the 3-

index EPDs and radar charts in both formulations across all pH conditions that were tested (Figures 2.8 and 2.9) as described in the discussion.

2.4 Discussion

The objective of this work was to examine the effect of the oligosaccharide structure occupying both of the N-linked 297 glycosylation sites in a series of four well-defined IgG1-Fc proteins on physical stability and solubility of these proteins under different solution conditions (pH, temperature and formulation additives). The HM-Fc, Man5-Fc, and GlcNAc-Fc glycoforms along with the N297Q-Fc aglycosylated protein were first evaluated by DSC and in a PEG precipitation assay, a previously described method to assess the relative apparent solubility of protein molecules by measuring the amount of PEG required to precipitate the protein from solution.[51,56,57] Because these 2 methods require relatively large amounts of protein (several milligrams), the 4 proteins were evaluated in only 1 formulation (citrate-phosphate buffer with NaCl) at 2 pH values (4.5 and 6.0). In the next set of experiments, 3 different high-throughput biophysical analyses were utilized since relatively small amounts of protein are required (~0.1-0.2 mg per condition). This allowed us to assess the physical stability of the four IgG1-Fc proteins under a range of solution conditions, including a wider range of temperature (10 ˚C - 90˚C), solution pH (4.0-7.5) and different formulation additives (NaCl vs sucrose). The latter not only permitted more extensive evaluations to compare the effect of oligosaccharide structure on IgG1-Fc physical stability, but provided much larger datasets required for the modeling of biosimilarity described by Kim JH et al.[50]

Solubility of mAbs is a crucial aspect of formulation development and can affect stability, activity, and potentially immunogenicity. Glycosylation is known to affect protein solubility in general, but more systematic studies are essential to draw further correlations with

glycosylation type with mAbs. For example, 1 previous report demonstrated an additional glycosylation within the Fab region of a mAb greatly increased solubility[59], while another showed dramatic decreased solubility due to additional glycosylation of the variable region of an isolated human IgG cryoimmunoglobulin.[60] In this work, we examined the effect of oligosaccharide structure occupying both of the N297 sites in the C_H2 domain in an IgG1-Fc. Relative apparent solubility (thermodynamic activity) profiles of IgG1-Fc glycoforms were determined using PEG precipitation assay measured by a combination of the curve shape (PEG versus protein concentrations), PEG midpoint numbers, and apparent solubility (thermodynamic activity) values. A trend of oligosaccharide structure vs. IgG-Fc apparent solubility (thermodynamic activity) was established with the HM-Fc and Man5-Fc glycoforms displaying the highest (yet distinct) relative values, GlcNAc-Fc glycoform showing intermediate, and the N297Q-Fc aglycosylated form having the lowest relative values at both pH 4.5 and pH 6.0.

Similarly, when conformational stability of the four Fc glycoforms was initially assessed by DSC at pH 4.5 in the NaCl-containing formulation, the thermal onset (T_{onset1}) and thermal melting temperatures (T_{m1} and T_{m2}), corresponding to the C_H2 domain of IgG-Fc proteins, displayed higher temperatures with increasing the glycan size. HM-Fc and Man5-Fc glycoforms had the highest relative thermal stability, intermediate stability was shown by the GlcNAc-Fc glycoform, and the N297Q-Fc aglycosylated form displayed the lowest stability. At pH 6.0, notable differences in $T_{onset1,}$ T_{m1} and T_{m2} values were noted only between the glycosylated vs. the aglycosylated Fc proteins. Differences in DSC thermal melting values between glycosylated (G2 form) and aglycosylated (peptide-N-glycosidase [PNGase] treated) human IgG1-Fc at pH 7.4 (PBS buffer) have been reported previously.[58]

These initial experiments established a key role of Fc glycosylation oligosaccharide structure in the apparent solubility and conformational stability of the IgG-Fc glycoproteins under the limited experimental conditions. The physical stability profiles of the four IgG1-Fc proteins under a wider range of solution conditions, including temperatures (10 ˚C-90˚C), solution pH (4.0-7.5) and different formulation additives (NaCl vs sucrose), were then examined. As shown in Figures 2.5 and 2.6, large physical stability data sets, consisting of thousands of data points, were generated and then analyzed by data visualization techniques developed previously in our labs[56,57] including three-index empirical phase diagrams and radar charts (Figures 2.8 and 2.9). These data visualization tools permit a direct comparison of the physical stability profiles of each of the 4 IgG1-Fc proteins across a wide range of environmental conditions.

As a starting point in these comparisons, the different structural alterations in the proteins that occur due to exposure to different temperature and pH were identified by analysis the data from the three biophysical methods as summarized in the radar chart displays in Figures 2.8 and 2.9. For example, the 4 glycoforms of IgG1-Fc show different physical stability profiles by comparing the areas of region A (native-like) in the radar charts. In formulation 1 (NaCl) and 2 (sucrose), the temperatures at which the transitions from the native region (A) to the structurally altered regions (B and C) occur at the highest values (across the pH range) in the HM-Fc and Man5-Fc glycoforms, intermediate in the GlcNAc-Fc glycoform and the lowest in the N297Q-Fc aglycosylated form. Furthermore, the percent area of native like region A (green colored region) is the highest in the HM-Fc and Man5-Fc glycoforms, intermediate in the GlcNAc-Fc glycoform and least in the N297Q-Fc glycoform as described above. These results reveal that the HM-Fc and Man5-Fc glycoforms are the most thermally stable, followed by the GlcNAc-Fc glycoform,

with the aglycosylated N297Q-Fc form being the least thermally stable. There is also an increase in the intensity and area of region B (orange and red color) from HM-Fc, Man5, GlcNAc to N297Q-Fc glycoforms, which indicates that the HM-Fc and Man5-Fc manifest overall lower exposure of hydrophobic surfaces than the GlcNAc-Fc and N297Q-Fc forms, with the N297Q-Fc having the highest overall exposed apolar areas. The presence of region D in the radar charts in the GlcNAc-Fc and N297Q-Fc samples shows the increased aggregation propensity of these 2 samples compared to the HM-Fc and Man5-Fc glycoforms.

In both formulations, each of the IgG1-Fc glycoforms show decreased thermal stability at lower pH values. The physical stability profile increases with increases in pH, as indicated by the temperatures at which the structural transitions from the native-like region (A) to the structurally altered regions (B ,C, D) occur in the radar charts. We observed similar trends previously with the di-glycosylated HM-Fc and aglycosylated N297Q-Fc molecules in a NaCl buffer when used as controls to evaluate the effect site occupancy and Asn/Asp residues at site N297.[51] In addition, the effect of the formulation conditions on the physical stability of each IgG1-Fc glycoform is also evident. The areas of the native like region A (green region) in the radar charts are higher in the formulation 2 (with sucrose) compared to region A in formulation 1 (with salt). In the presence of sucrose, the temperatures at which the transitions from the native region (A) to the structurally altered regions (B and C) occur are higher in all four glycoforms than in formulation 1 (with salt). These results indicate that sucrose offers improved thermal physical stability profiles for each of the four glycoforms of IgG1-Fc compared to NaCl, particularly at the lower pH conditions.

It is of interest to compare our results with recent studies from other labs examining other IgG mAbs and Fc molecules by similar and different analytical methods. A recent study by

Zheng et al[18] compared glycosylation variants of a Chinese Hamster Ovary (CHO) produced IgG1 full-length mAb which included a G0 form, an afucosylated variant of G0 (that exhibits enhanced ADCC), a high mannose form, and a deglycosylated form (from PNGase treatment). Through a comparison of higher order structure, thermal unfolding, protease digestion and stability between these glycosylation variants, it was concluded that deglycosylated and high mannose IgG1 forms were relatively less stable (e.g., as shown by DSC in a pH range of 4.0-7.5), while the G0 and afucosylated G0 forms showed higher thermal stability. The high mannose and deglycosylated forms also showed more rapid pepsin digestion.[18] In another study by Zheng et al (2011)[61], a comparison between fully glycosylated forms and PNGase-cleaved deglycosylated forms of IgG1 mAbs showed decreased thermal stability of the C_H2 domains of the deglycosylated forms by DSC at pH 5.5. In our studies, we have seen similar trends with decreased conformational stability (DSC) and physical stability profiles of non-glycosylated N297Q IgG1-Fc compared to the HM-Fc and Man5-Fc forms. However, the HM-Fc and Man-5-Fc were shown to be overall similar by DSC and their physical stability profiles, with some minor differences noted between the 2 forms depending on the analytical method, solution pH and formulation. This could reflect differences between IgG1-Fc versus a full-length IgG1 mAb as well as differences in HM content in the two studies (Man9 vs. this study with HM glycoforms having distributions of Man8-Man12, with the majority in Man8 forms).

Zheng et al.[61] showed by SEC that deglycosylated IgG1 mAbs had higher aggregation rates than their glycosylated counterparts as a result of an accelerated stability study at pH 5.5. These results correlate with our studies that show the GlcNAc-Fc and the non-glycosylated N297Q-Fc (glycoforms with 1 GlcNAc sugar and no sugar, respectively) have the highest aggregation tendencies by turbidity measurements from pH 5.0 to pH 7.0 (compared to the HM-

Fc and Man5-Fc which showed no aggregation). Similar findings regarding the non-aggregating tendencies of high-mannose IgG1 mAbs were shown as a result of real time and accelerated stability studies.[20] Finally, the effect of pH, temperature and salt on the stability, acid induced unfolding and aggregation of CHO (glycosylated) and *Escherichia coli* (aglycosylated) derived IgG1 Fc molecules has also been examined.[19,62] An interesting observation was made regarding a critical role of the C_H2 domain in determining the rate and extent of Fc aggregation, which correlated with the presence or absence glycosylation at the Asn-297.[62] It has been proposed that the presence of glycosylation in the C_H2 domain masks hydrophobic aggregation motifs and is crucial in preventing aggregation of IgG mAbs.[63] It was also demonstrated that CHO derived (glycosylated) IgG1-Fc protein is not only more compact and more thermally stable than the *E. coli* derived (aglycosylated) protein at neutral pH, but the thermal stability was pH and salt dependent where lower pH and higher salt conditions were more unfavorable. Similar effects of solution conditions were observed in our studies where IgG1-Fc glycoform stability increased with increasing solution pH and in presence of sucrose (instead of NaCl).

This work not only demonstrates the effect of oligosaccharide structure of IgG1-Fc on pharmaceutical properties (e.g., apparent solubility and physical stability) under different solution conditions, but also contributes towards the development of new analytical approaches and data visualization tools to assess structural integrity and conformational stability and makes comparisons between different versions of the same biopharmaceutical molecule (using well-defined IgG1-Fc glycoforms as a model system). This systematic approach of using EPDs and radar charts to compare physical stability profiles successfully recognizes subtle similarities and differences among different versions of the same protein (as would be done in comparability or biosimilarity studies). As a result of changes in post-translational modifications (glycosylation

pattern) or formulation composition (NaCl vs. sucrose), physical stability differences between the 8 different samples (4 different Fc glycoforms in 2 different formulations) was established. Thus, this model system shows proof of concept of an efficient protocol to evaluate the effect of process and product changes on the structural integrity and physical stability as part of comparability assessments.[41,42,64] Future applications could also address potential stability differences between different batches of the same process due to lot-to-lot variability of process and product impurities. Similar challenges now exist for establishing similarity between biopharmaceuticals produced by innovator versus biosimilar manufacturers. Comparative data sets of molecules containing information on post-translational modifications, higher-order structures and accelerated stability are an important part of formulation development and biosimilarity assessments. As described by (Kim JH et al)[50], these large physical stability data sets are used as a model system to establish a new method of mathematical modeling for biosimilarity assessments using machine-learning approaches.

Table 2.1: Summary of Thermal Onset Temperatures (T_{onset1}, T_{onset2}) and Thermal Melting Temperatures (T_{m1}, T_{m2}, T_{m3}, T_{m4}) for the four IgG1-Fc glycoforms (HM-Fc, Man5-Fc, GlcNAc-Fc and N297Q-Fc) at two different pH conditions (pH 4.5 and pH 6.0) measured by DSC. Samples were prepared at 0.4 mg/mL in 20 mM citrate–phosphate buffer and adjusted to an ionic strength of 0.15 by addition of NaCl. Results are reported in °C as average and standard deviation of triplicate measurements

	T_{onset1}	T_{onset2}	T_{m1}	T_{m2}	T_{m3}	T_{m4}
pH 6.0						
HM-Fc	55.0±0.8	72.4±0.3	61.7±0.3	66.0±0.2	80.7±2.6	82.1±2.4
Man5-Fc	56.7±0.6	71.9±0.3	62.7±0.3	66.0±0.0	78.4±0.1	83.4±0.1
GlcNAc-Fc	58.5±0.4	72.1±0.3	62.9±0.8	65.5±0.5	77.7±0.3	83.2±0.1
N297Q-Fc	52.5±0.2	71.2±0.7	57.2±1.1	61.0±0.4	79.0±0.0	83.4±0.0
pH 4.5						
HM-Fc	42.8±1.7	64.0±3.4	49.8±0.4	53.9±0.2	73.8±1.1	78.9±0.2
Man5-Fc	42.0±2.1	60.5±0.7	50.1±0.2	53.5±0.1	71.7±0.2	77.8±0.2
GlcNAc-Fc	39.9±0.3	65.4±0.4	45.9±0.6	50.0±0.3	73.0±0.1	78.6±0.0
N297Q-Fc	34.6±1.0	66.1±0.5	40.8±0.6	44.1±1.2	74.2±0.1	78.5±0.1

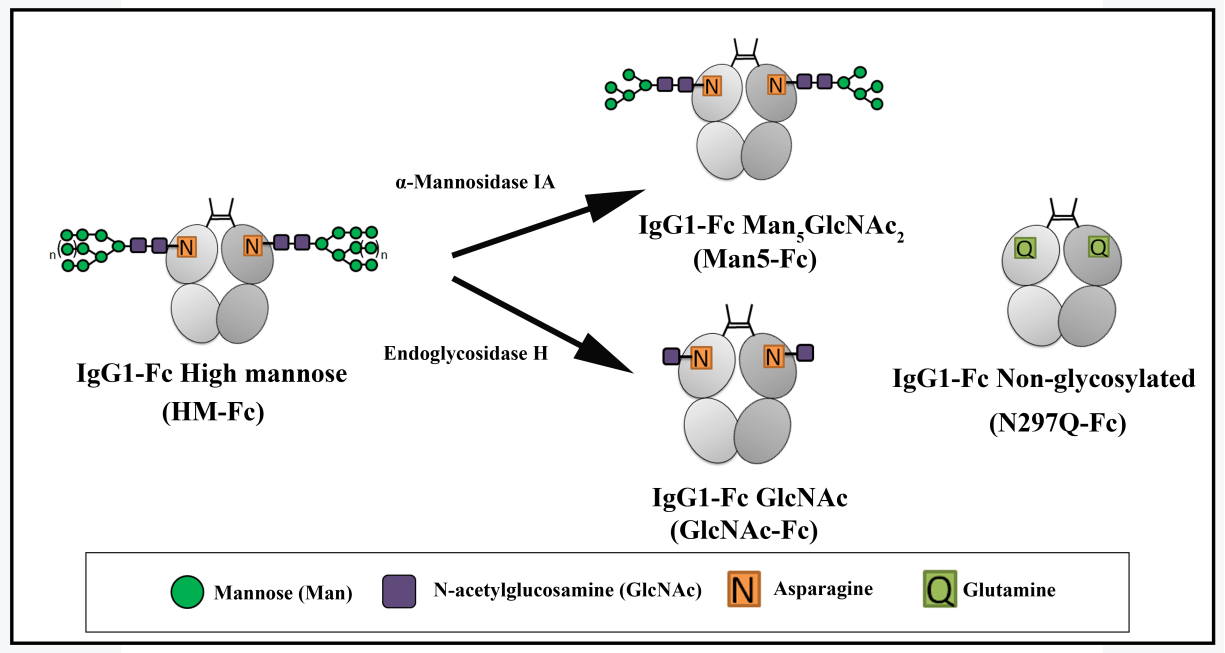

Figure 2.1: Schematic representation of the four well-defined IgG1-Fc glycoforms characterized in this work in terms of physical stability profiles. The high mannose IgG1-Fc (HM-Fc) was expressed in yeast and purified, and upon treatment with enzymes α-mannosidase 1A and endoglycosidase-H, produced two fully homogeneous glycoforms IgG1-Fc $Man_5GlcNAc_2$ (Man5-Fc) and IgG1-Fc GlcNAc (GlcNAc-Fc), respectively. Site-directed mutagenesis was used to produce the non-glycosylated mutant of IgG1-Fc (N297Q-Fc).

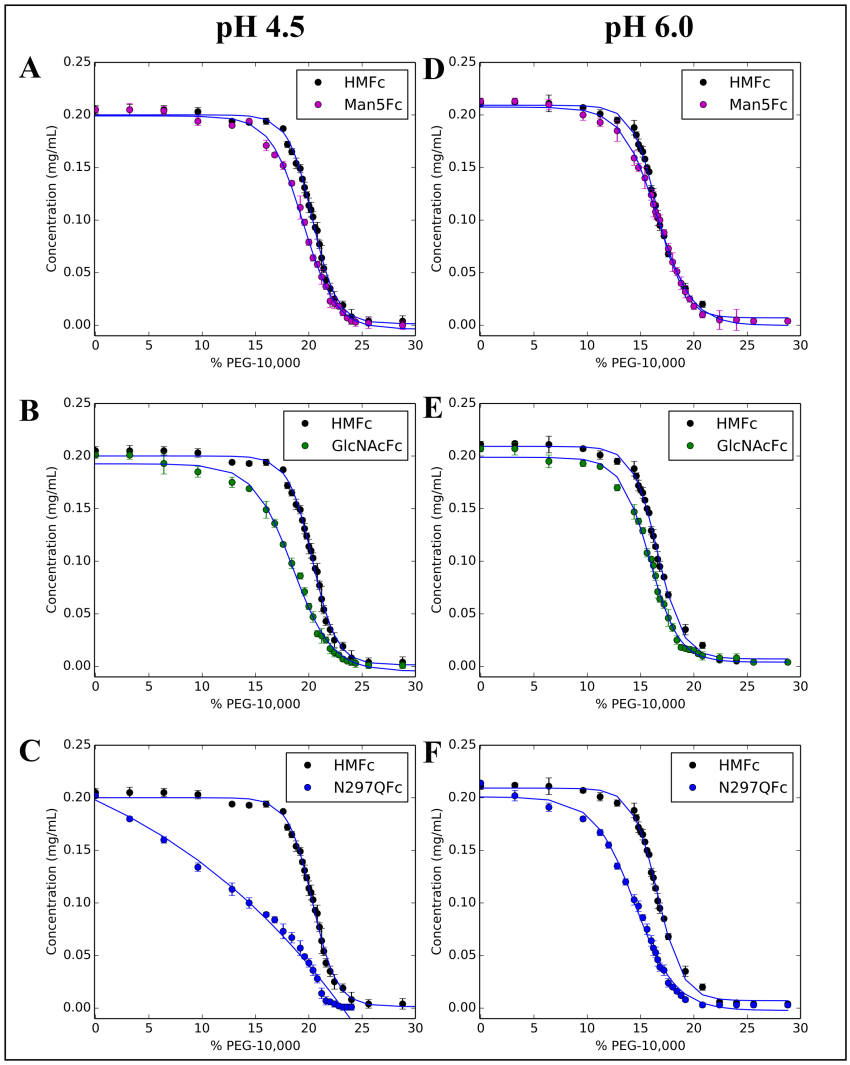

Figure 2.2: Concentration of each IgG1-Fc glycoform (HM-Fc, Man5-Fc, GlcNAc-Fc and N297Q-Fc) versus amount of PEG added to solution. Each panel shows results of HM-Fc for ease of comparison. Samples were formulated in citrate-phosphate buffer with ionic strength adjusted to 0.15 by NaCl at pH 4.5 (A,B,C) and pH 6.0 (Panel D,E,F), respectively. The error bars denote standard deviation for n = 3 replicates at each % PEG concentration.

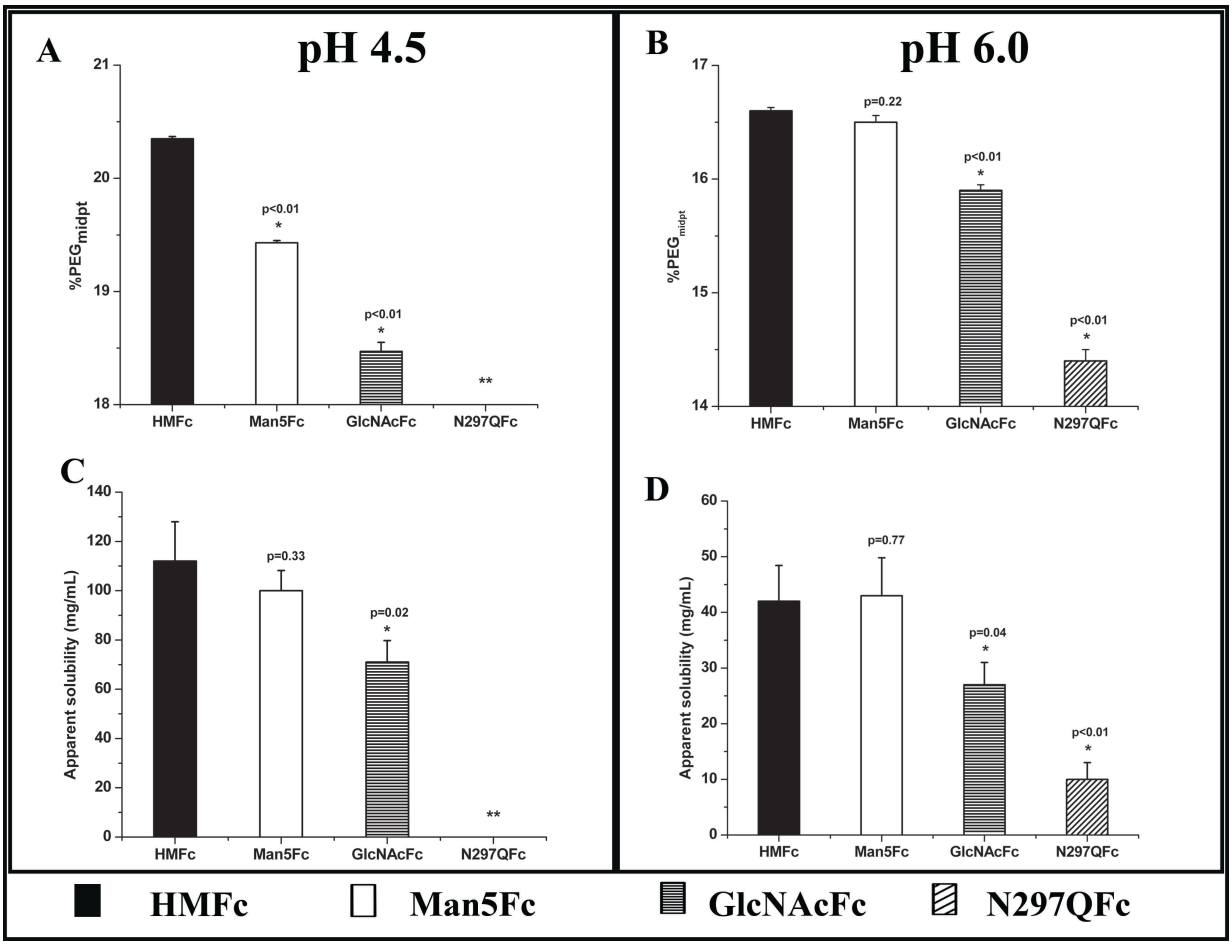

Figure 2.3: Comparison of apparent solubility (thermodynamic activity) parameters of the each of IgG1-Fc glycoforms (Man5-Fc, GlcNAc-Fc and N297Q-Fc) to HM-Fc glycoform by PEG precipitation assay at pH 4.5 and pH 6.0. A and B show the comparison of PEG_{midpt} values (w/v) at pH 4.5 and pH 6.0, respectively. C and D show the comparison of the apparent solubility (activity) values at pH 4.5 and pH 6.0, respectively. Error bars indicate the standard deviation of 3 replicates. * Statistical significance compared to the HM-Fc with a p value <0.05 is indicated. **No calculated parameters for N297Q-Fc at pH 4.5 were possible due to the non-ideal nature of the %PEG curve (see Figure 2.2).

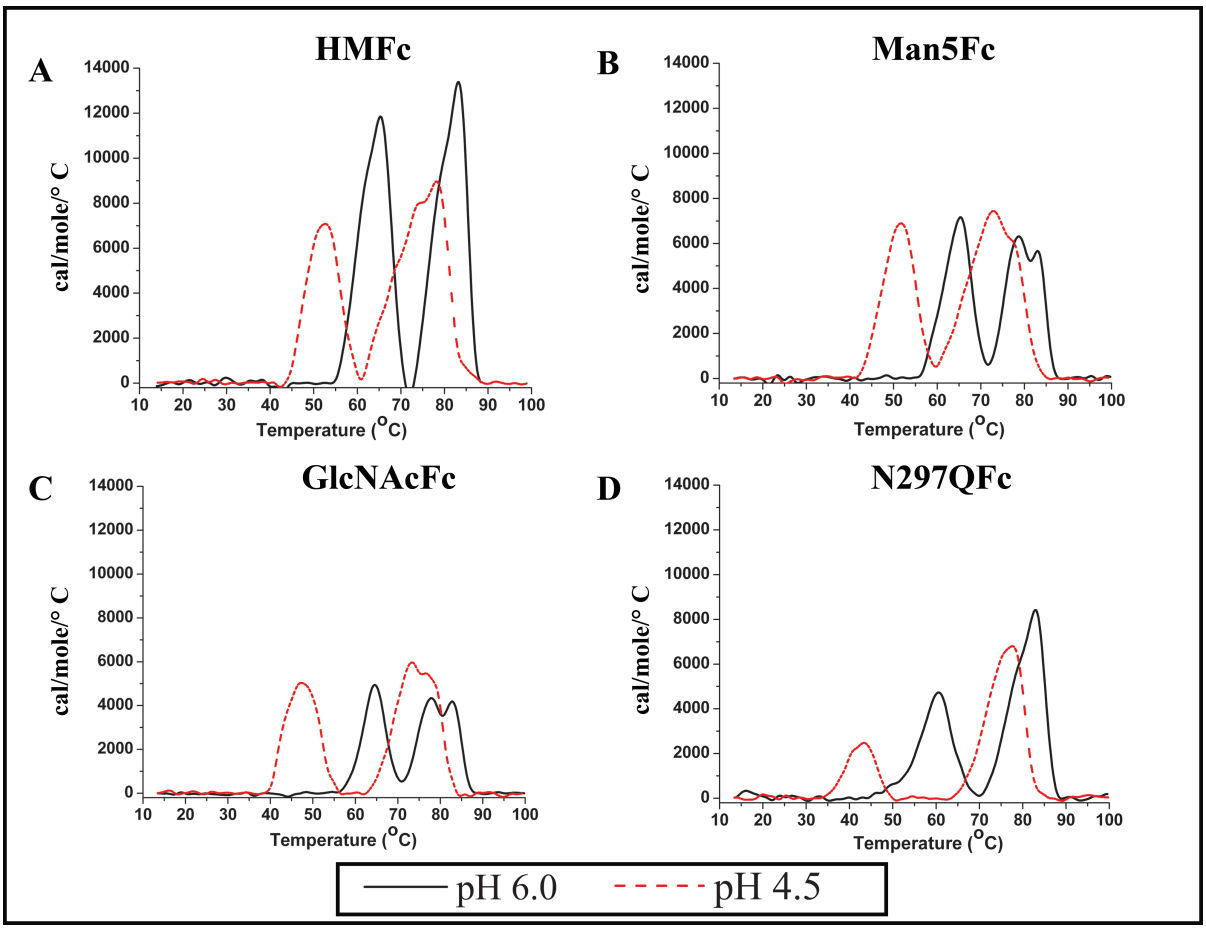

Figure 2.4: Comparison of representative curve-fitted DSC thermograms of 4 IgG1-Fc glycoforms; HM-Fc (Panel A), Man5-Fc (Panel B), GlcNAc-Fc (Panel C) and N297Q-Fc (Panel D) at two different pH conditions (pH 4.5 and pH 6.0). Samples were a 0.4 mg/mL in 20 mM citrate–phosphate buffer, adjusted to an ionic strength of 0.15 by addition of NaCl.

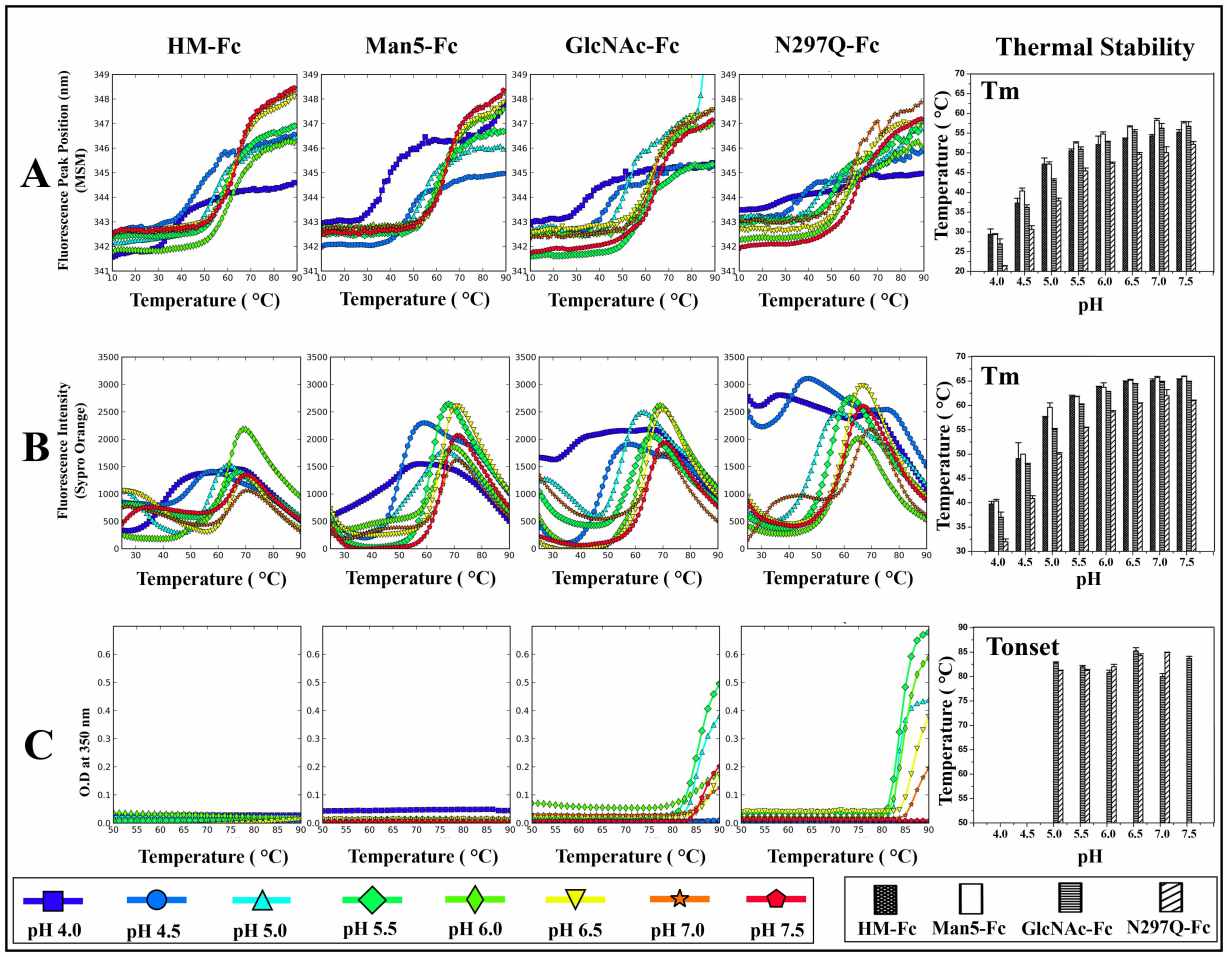

Figure 2.5: Biophysical characterization of four well-defined glycoforms of IgG1-Fc (HM-Fc, Man5-Fc, GlcNAc-Fc and N297Q-Fc) vs. temperature across the pH range of 4.0–7.5 in a solution containing NaCl (formulation 1). Biophysical measurements include (A) intrinsic Trp fluorescence, (B) extrinsic Sypro Orange fluorescence spectroscopy, and (C) optical density at 350 nm. Thermal stability panel displays T_m values obtained from intrinsic Trp fluorescence and extrinsic Sypro orange fluorescence thermal melting curves, and T_{onset} values obtained from turbidity (O.D. at 350 nm versus temperature) measurements. Samples were prepared at 0.2 mg/mL in 20 mM citrate phosphate buffer with NaCl added to I=0.15 at the indicated pH values.

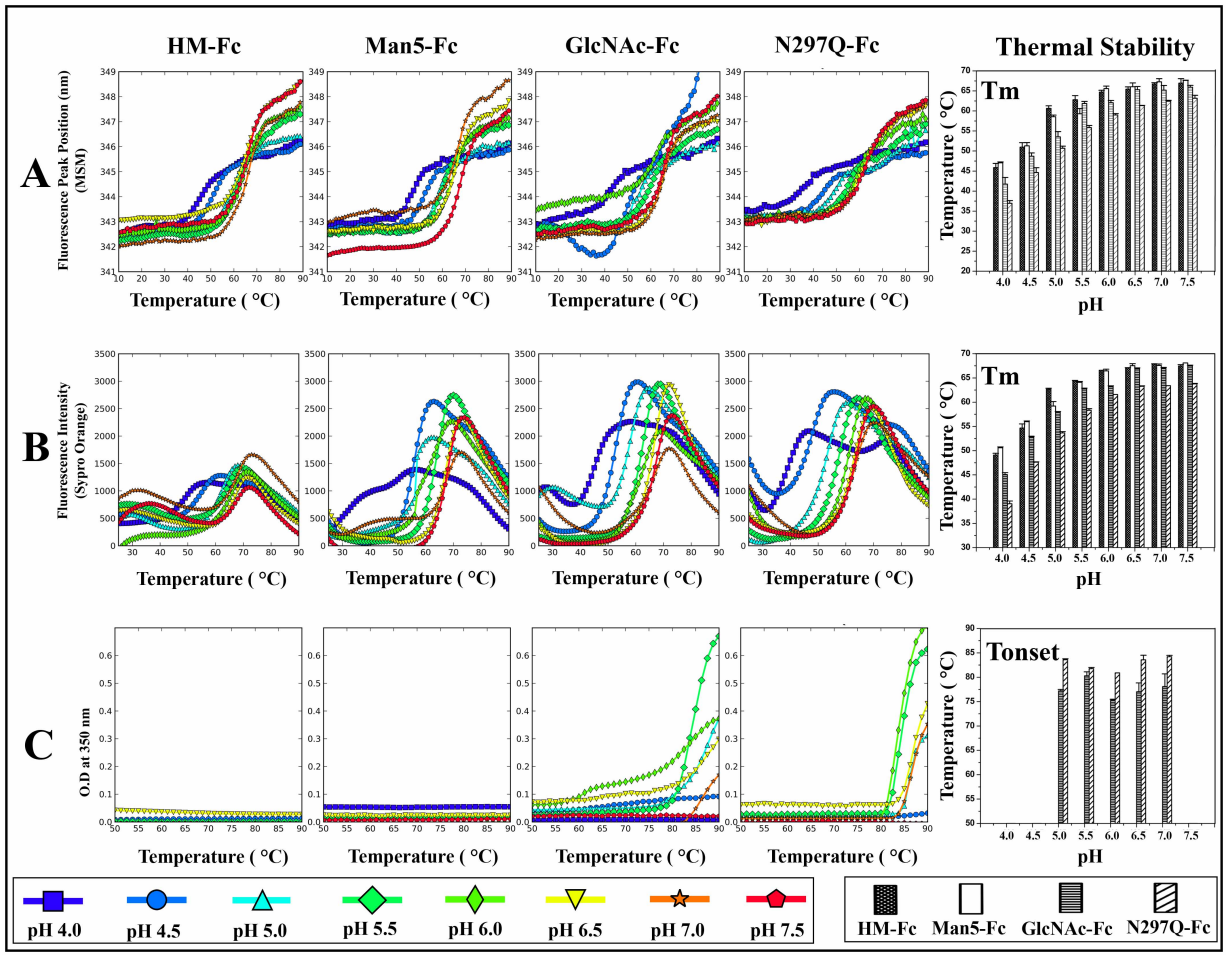

Figure 2.6: Biophysical characterization of four glycoforms of IgG1-Fc (HM-Fc, Man5-Fc, GlcNAc-Fc and N297Q-Fc) vs. temperature across the pH range of 4.0–7.5 in a solution containing sucrose (formulation 2). Biophysical measurements include (A) intrinsic Trp fluorescence, (B) extrinsic Sypro Orange fluorescence spectroscopy, and (C) optical density at 350 nm. Thermal stability panel displays T_m values obtained from intrinsic Trp fluorescence and extrinsic Sypro orange fluorescence thermal melting curves, and T_{onset} values obtained from turbidity (O.D. at 350 nm versus temperature) measurements. Samples were prepared at 0.2 mg/mL in 20 mM citrate-phosphate buffer, 10% sucrose (w/v) at the indicated pH values.

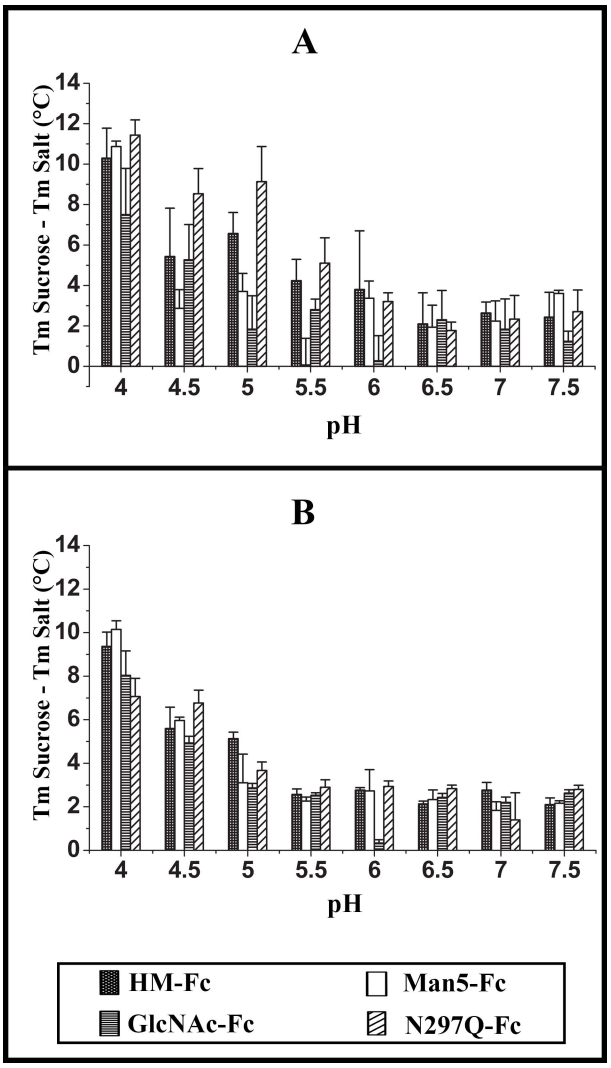

Figure 2.7: Summary of thermal stability trends vs. solution pH for the 4 well-defined IgG1-Fc glycoforms in sucrose vs. NaCl containing formulations. Bar chart displays of ΔT_m values of each protein in sucrose versus NaCl, ΔT_m = (T_m sucrose–T_m NaCl), as obtained from (A) intrinsic fluorescence and (B) extrinsic Sypro orange fluorescence thermal melting curves. The IgG1-Fc glycoforms (HM-Fc, Man5-Fc, GlcNAc-Fc and N297Q-Fc) were formulated in 20 mM citrate phosphate buffer at the indicated pH values with either NaCl added to I=0.15 (formulation 1) or 10% sucrose (w/v; formulation 2).

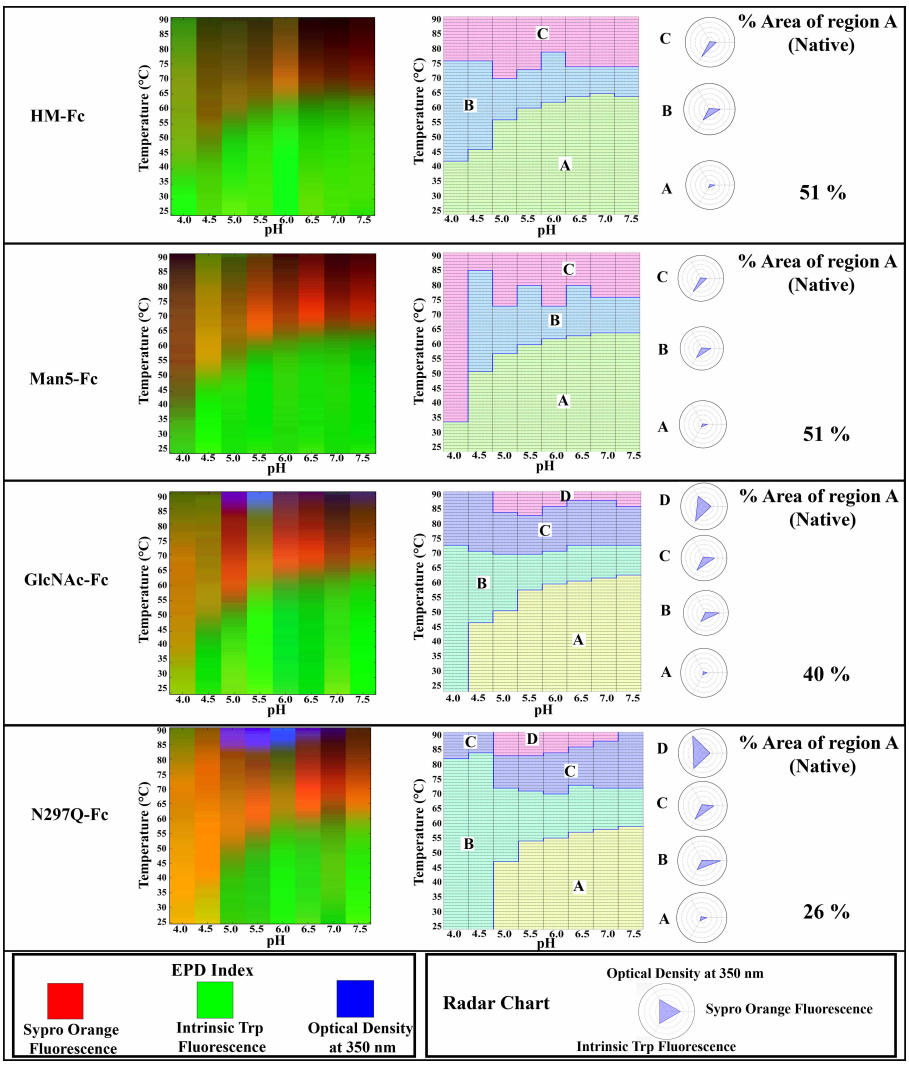

Figure 2.8: Data visualization of the physical stabilty data sets (see Figure 2.5) of the 4 well-defined IgG1-Fc glycoforms in formulation 1 (NaCl). 3-index empirical phase diagrams (left panels) and radar charts (right panels) for each IgG1-Fc protein (HM-Fc, Man5-Fc, GlcNAc-Fc and N297Q-Fc) across the pH range of 4.0–7.5 and temperature range of 25°C-90°C are shown. Biophysical measurements include intrinsic Trp and extrinsic Sypro Orange fluorescence spectroscopy, as well as optical density at 350 nm. Samples contained 0.2 mg/mL in 20 mM citrate phosphate buffer at indicated pH with NaCl added to I=0.15 (formulation 1).

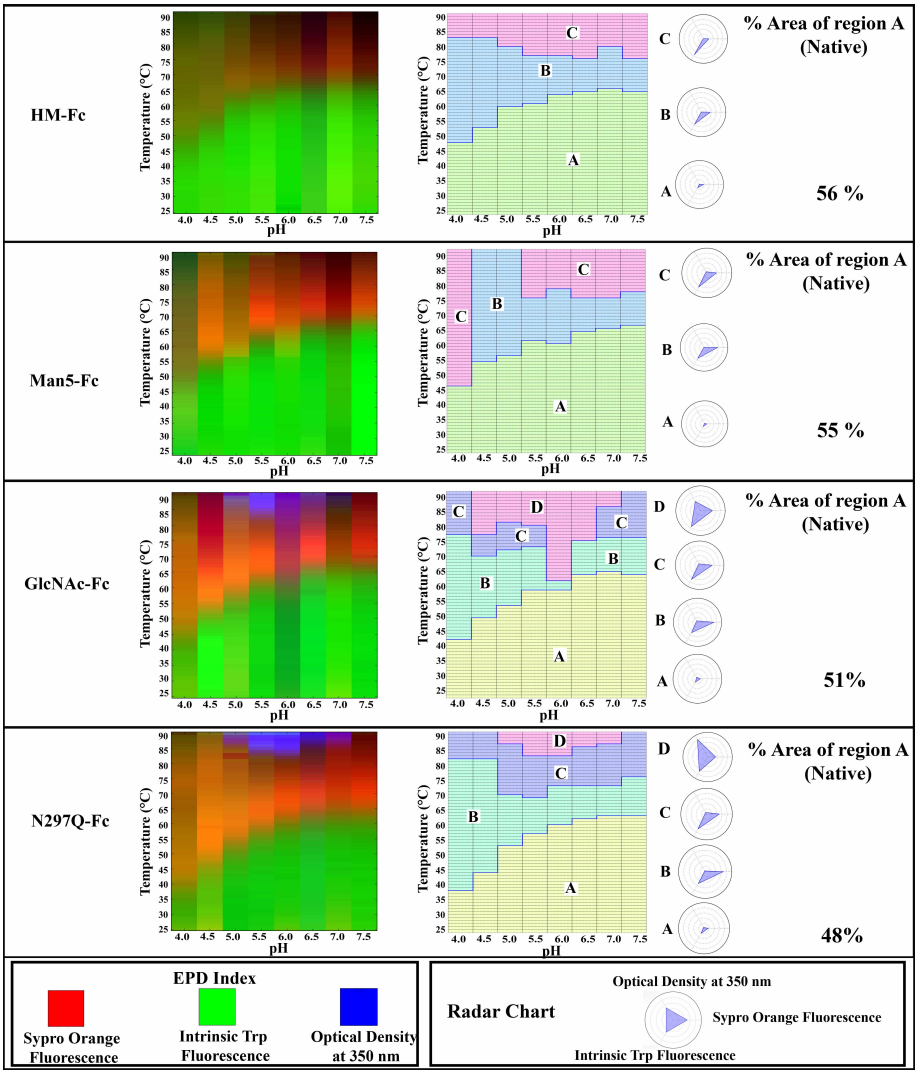

Figure 2.9: Data visualization of the physical stabilty data sets (see Figure 2.6) of the four well-defined IgG1-Fc glycoforms in formulation 2 (sucrose). Three-index empirical phase diagrams (left panels) and radar charts (right panels) for each of the IgG1-Fc proteins (HM-Fc, Man5-Fc, GlcNAc-Fc and N297Q-Fc) across the pH range of 4.0–7.5 and temperature range of 25-90°C are shown. Biophysical measurements include intrinsic Trp and extrinsic Sypro Orange fluorescence spectroscopy as well as optical density at 350 nm. See Figure 2.5 legend for description of region A (Green), B (Orange), C (Brown) and D (Blue). Samples contained 0.2

mg/mL in 20 mM citrate-phosphate buffer at indicated pH with 10% sucrose (w/v; formulation 2).

In figures 2.8 and 2.9, Regions A (Green) represent regions where the IgG-Fc Fc proteins exist in the native-like conformation. Regions B (Orange) and C (Brown) represent regions where the same proteins exist at an altered structural state as seen from an increase in Sypro Orange and Trp fluorescence signals, respectively. Region D (Blue) represents a region where the Fc glycoproteins are in an aggregated state as seen by an increased optical density signal.

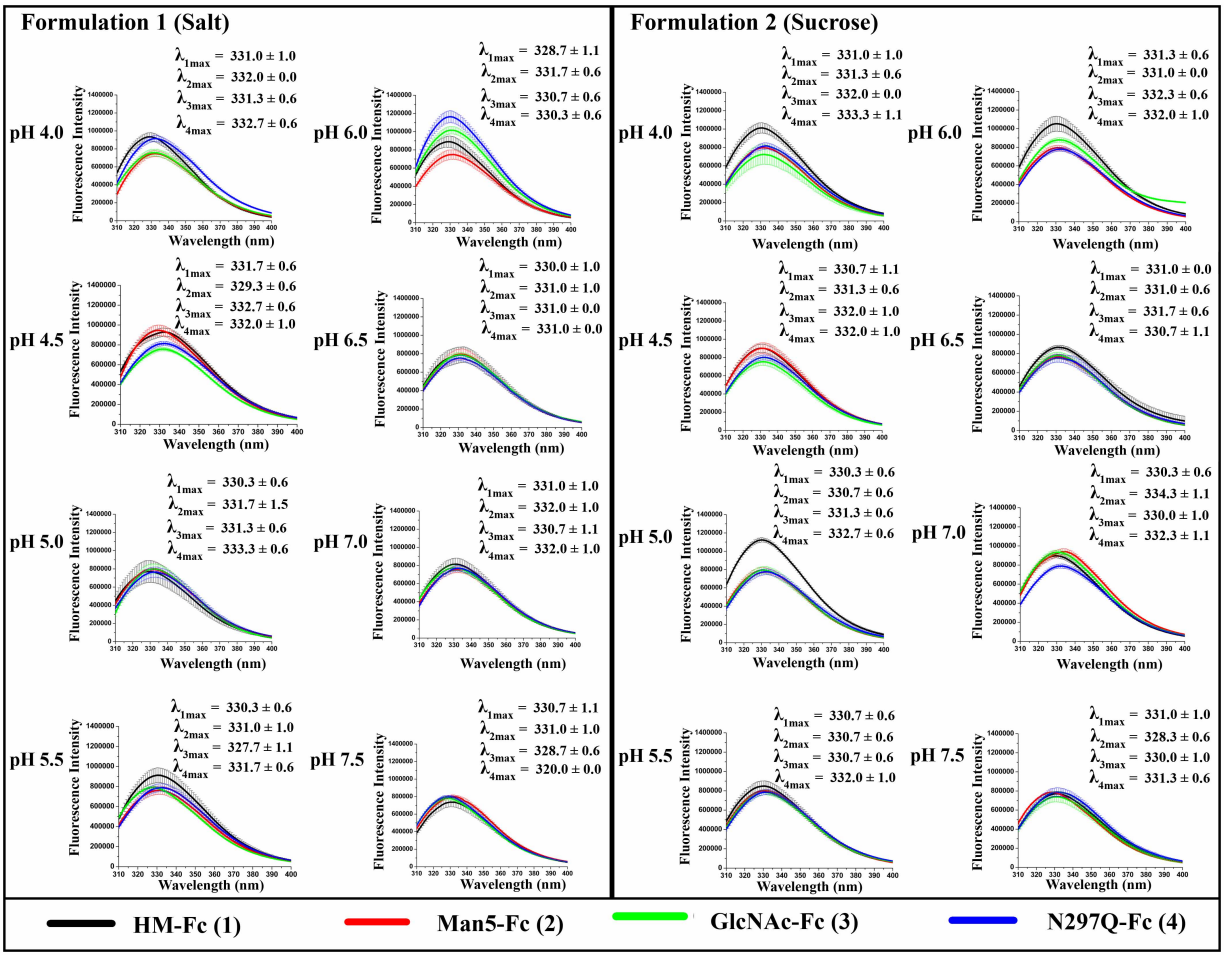

Supplementary Figure 2.1: Intrinsic (Trp) fluorescence spectra at 10°C of four well-defined glycoforms of IgG1-Fc (HM-Fc, Man5-Fc, GlcNAc-Fc and N297Q-Fc) across the pH range of 4.0–7.5 in 2 solutions containing either NaCl (formulation 1-NaCl) or sucrose (formulation 2-sucrose). The λ_{max} values are also shown for each protein at each pH condition. Each of the samples was run in triplicate with standard deviation (SD) of λ_{max} values ranging from 0 to 1.5 nm.

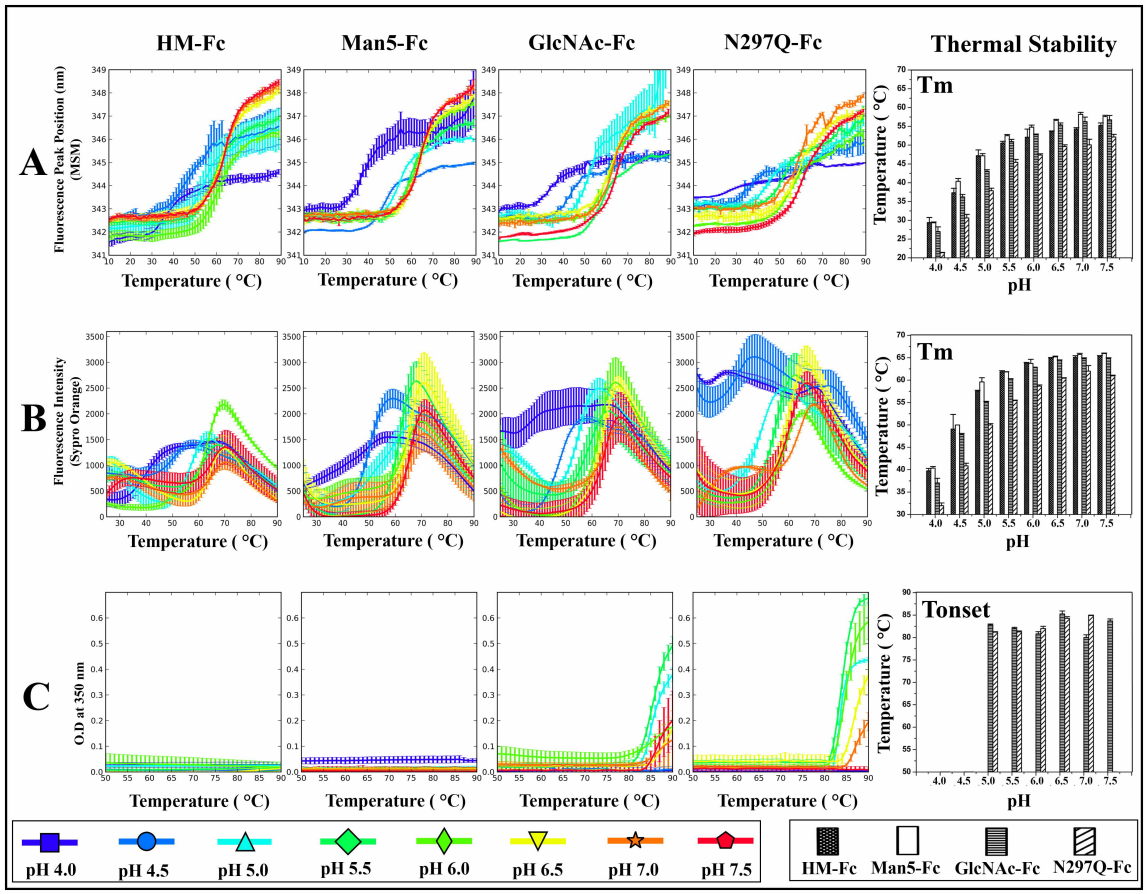

Supplementary Figure 2.2: Biophysical characterization of four well-defined glycoforms of IgG1-Fc (HM-Fc, Man5-Fc, GlcNAc-Fc and N297Q-Fc) versus temperature across the pH range of 4.0–7.5 in a solution containing NaCl (formulation 1). Biophysical measurements include (A) intrinsic Trp fluorescence, (B) extrinsic Sypro Orange fluorescence spectroscopy, and (C) optical density at 350 nm. Thermal Stability panel displays T_m values obtained from intrinsic Trp fluorescence and extrinsic Sypro orange fluorescence thermal melting curves, and T_{onset} values obtained from turbidity (O.D. at 350 nm vs. temperature) measurements. Samples were prepared at 0.2 mg/mL in 20 mM citrate phosphate buffer with NaCl added to I=0.15 at the indicated pH values. Each sample was run in triplicate, and the standard deviation (SD) of peak positions

ranged from 0-2 nm, the SD of Sypro orange fluorescence intensity ranged from 5-970 fluorescence intensity units, and the SD of optical density ranged from 0.001-0.07 OD. The SD of T_m values obtained from intrinsic Trp fluorescence ranged from 0.1-1.6°C, SD of T_m values obtained from extrinsic Sypro orange fluorescence thermal melting curves ranged from 0-4.0°C, and the SD of the T_{onset} values obtained from turbidity (O.D. at 350 nm vs. temperature) measurements ranged from 0-1.6°C.

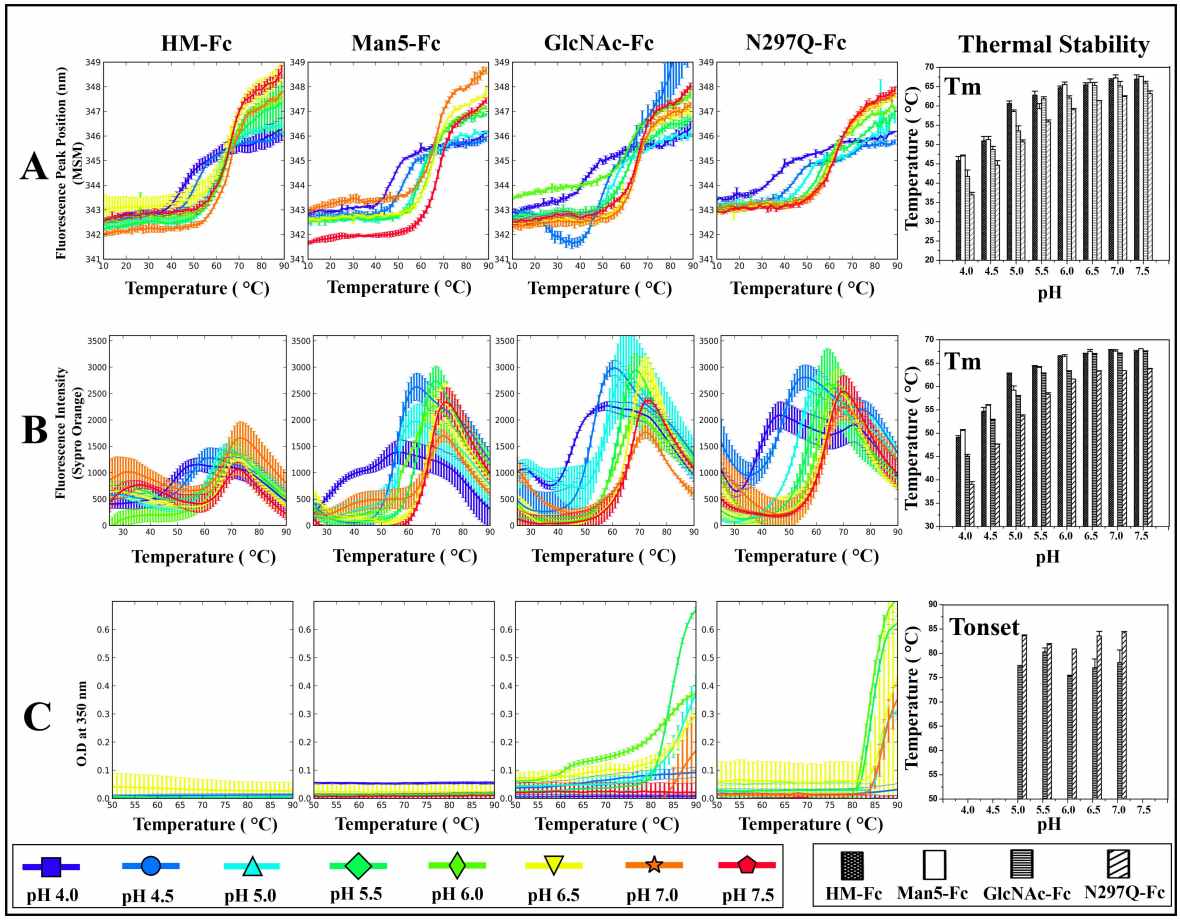

Supplementary Figure 2.3: Biophysical characterization of four glycoforms of IgG1-Fc (HM-Fc, Man5-Fc, GlcNAc-Fc and N297Q-Fc) vs. temperature across the pH range of 4.0–7.5 in a solution containing sucrose (formulation 2). Biophysical measurements include (A) intrinsic Trp fluorescence, (B) extrinsic Sypro Orange fluorescence, and (C) optical density at 350 nm. Thermal Stability panel displays T_m values obtained from intrinsic Trp fluorescence and extrinsic SYPRO orange fluorescence thermal melting curves, and T_{onset} values obtained from turbidity (O.D. at 350 nm vs. temperature) measurements. Samples were prepared at 0.2 mg/mL in 20 mM citrate-phosphate buffer, 10% sucrose (w/v) at the indicated pH values. Each sample was run in triplicate and the standard deviation (SD) of peak positions ranged from 0-2 nm, the SD of Sypro orange fluorescence intensity ranged from 20-840 fluorescence intensity units, and the SD

of optical density ranged from 0.001-0.07 OD. The SD of T_m values obtained from intrinsic Trp fluorescence ranged from 0.05-1.6°C, the SD of T_m values obtained from extrinsic Sypro orange fluorescence thermal melting curves ranged from 0.1°C -1.7°C, and the SD of T_{onset} values obtained from turbidity (O.D. at 350 nm versus temperature) measurements ranged from 0°C-1.8°C.

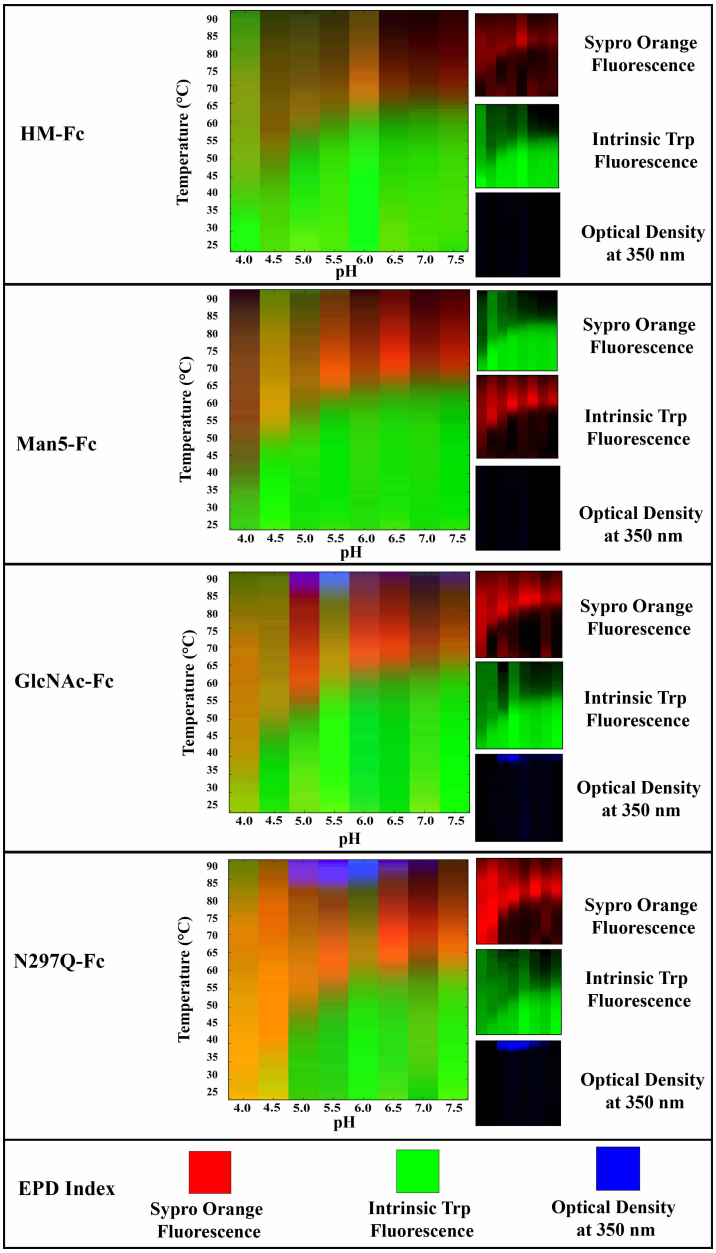

Supplementary Figure 2.4: Data visualization of the physical stabilty data sets (see Figure 2.5) of the four well-defined IgG1-Fc glycoforms in formulation 1 (NaCl). 3-index empirical phase diagrams (left panels) alongside readouts from individual RGB components (right panels) for each IgG1-Fc protein (HM-Fc, Man5-Fc, GlcNAc-Fc and N297Q-Fc) across the pH range of 4.0–7.5 and temperature range of 25°C 90°C are shown. Biophysical measurements include intrinsic Trp fluorescence (G), extrinsic Sypro Orange fluorescence (R), and optical density at

350 nm (B). The combination of these RGB values produces a single color at each pH and temperature point. In the three-index EPDs, green represent regions where the IgG-Fc Fc protein exists in the native-like conformation. Regions orange and brown represent regions where the same proteins exist at an altered structural state as seen from an increase in Sypro Orange and Trp fluorescence signals, respectively. Blue region represents a region where the Fc glycoproteins are in an aggregated state as seen by an increased optical density signal. See Methods section for description of preparation of 3-index EPDs. Samples contained 0.2 mg/mL in 20 mM citrate phosphate buffer at indicated pH with NaCl added to I=0.15 (formulation 1).

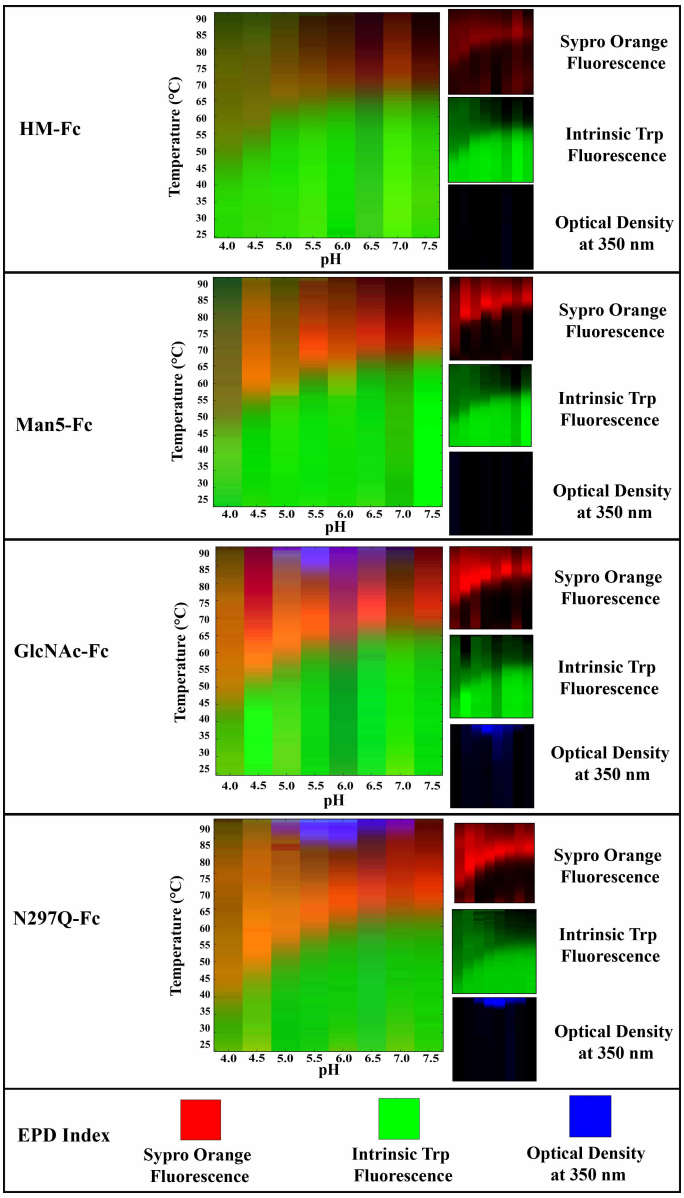

Supplementary Figure 2.5: Data visualization of the physical stabilty data sets (see Figure 2.6) of the four well-defined IgG1-Fc glycoforms in formulation 2 (sucrose). Three-Index Empirical Phase Diagrams (left panels) alongside readouts from individual RGB components (right panels) for each IgG1-Fc protein (HM-Fc, Man5-Fc, GlcNAc-Fc and N297Q-Fc) across the pH range of 4.0–7.5 and temperature range of 25°C-90°C are shown. Biophysical measurements include intrinsic Trp fluorescence(G), extrinsic Sypro Orange fluorescence spectroscopy(R), and optical density at 350 nm(B). The combination of these RGB values produces a single color at each pH

and temperature point. In the three-index EPDs, green represent regions where the IgG-Fc Fc protein exists in the native-like conformation. Regions orange and brown represent regions where the same proteins exist at an altered structural state as seen from an increase in Sypro Orange and Trp fluorescence signals, respectively. Blue region represents a region where the Fc glycoproteins are in an aggregated state as seen by an increased optical density signal. See Methods section for description of preparation of three-index EPDs. Samples contained 0.2 mg/mL in 20 mM citrate phosphate buffer at indicated pH with 10% sucrose (w/v; formulation 2)

2.5 References

1. Arnold JN, Wormald MR, Sim RB, Rudd PM, Dwek RA 2007. The impact of glycosylation on the biological function and structure of human immunoglobulins. Annual review of immunology 25:21-50.

2. Alain Beck TW, Christian Bailly and Nathalie Corvaia May 2010. Strategies and challenges for the next generation of therapeutic antibodies. Nature Reviews Immunology 10:345-352.

3. Dalziel M, Crispin M, Scanlan CN, Zitzmann N, Dwek RA 2014. Emerging Principles for the Therapeutic Exploitation of Glycosylation. Science 343(6166).

4. Ecker DM, Jones SD, Levine HL 2015. The therapeutic monoclonal antibody market. mAbs 7(1):9-14.

5. Beck A, Wagner-Rousset E, Ayoub D, Van Dorsselaer A, Sanglier-Cianferani S 2013. Characterization of therapeutic antibodies and related products. Analytical chemistry 85(2):715-736.

6. Niwa R, Satoh M 2015. The current status and prospects of antibody engineering for therapeutic use: focus on glycoengineering technology. Journal of pharmaceutical sciences 104(3):930-941.

7. Jefferis R 2009. Glycosylation as a strategy to improve antibody-based therapeutics. Nature reviews Drug discovery 8(3):226-234.

8. Mimura Y, Sondermann P, Ghirlando R, Lund J, Young SP, Goodall M, Jefferis R 2001. Role of oligosaccharide residues of IgG1-Fc in FcγRIIb binding. Journal of Biological Chemistry 276(49):45539-45547.

9. Krapp S, Mimura Y, Jefferis R, Huber R, Sondermann P 2003. Structural Analysis of Human IgG-Fc Glycoforms Reveals a Correlation Between Glycosylation and Structural Integrity. Journal of Molecular Biology 325(5):979-989.

10. Hristodorov D, Fischer R, Linden L 2013. With or without sugar? (A)glycosylation of therapeutic antibodies. Molecular biotechnology 54(3):1056-1068.

11. Yu X, Baruah K, Harvey DJ, Vasiljevic S, Alonzi DS, Song B-D, Higgins MK, Bowden TA, Scanlan CN, Crispin M 2013. Engineering Hydrophobic Protein–Carbohydrate Interactions to Fine-Tune Monoclonal Antibodies. Journal of the American Chemical Society 135(26):9723-9732.

12. Lin C-W, Tsai M-H, Li S-T, Tsai T-I, Chu K-C, Liu Y-C, Lai M-Y, Wu C-Y, Tseng Y-C, Shivatare SS, Wang C-H, Chao P, Wang S-Y, Shih H-W, Zeng Y-F, You T-H, Liao J-Y, Tu Y-C, Lin Y-S, Chuang H-Y, Chen C-L, Tsai C-S, Huang C-C, Lin N-H, Ma C, Wu C-Y, Wong C-H 2015. A common glycan structure on immunoglobulin G for enhancement of effector functions. Proceedings of the National Academy of Sciences 112(34):10611-10616.

13. Liu L 2015. Antibody Glycosylation and Its Impact on the Pharmacokinetics and Pharmacodynamics of Monoclonal Antibodies and Fc-Fusion Proteins. Journal of pharmaceutical sciences 104(6):1866-1884.

14. Anthony RM, Wermeling F, Ravetch JV 2012. Novel roles for the IgG Fc glycan. Ann N Y Acad Sci 1253:170-180.

15. Li H, d'Anjou M 2009. Pharmacological significance of glycosylation in therapeutic proteins. Current opinion in biotechnology 20(6):678-684.

16. Yu M, Brown D, Reed C, Chung S, Lutman J, Stefanich E, Wong A, Stephan JP, Bayer R 2012. Production, characterization, and pharmacokinetic properties of antibodies with N-linked mannose-5 glycans. mAbs 4(4):475-487.

17. Sola RJ, Griebenow K 2009. Effects of glycosylation on the stability of protein pharmaceuticals. Journal of pharmaceutical sciences 98(4):1223-1245.

18. Zheng K, Yarmarkovich M, Bantog C, Bayer R, Patapoff TW 2014. Influence of glycosylation pattern on the molecular properties of monoclonal antibodies. mAbs 6(3):649-658.

19. Li CH, Narhi LO, Wen J, Dimitrova M, Wen ZQ, Li J, Pollastrini J, Nguyen X, Tsuruda T, Jiang Y 2012. Effect of pH, temperature, and salt on the stability of Escherichia coli- and Chinese hamster ovary cell-derived IgG1 Fc. Biochemistry 51(50):10056-10065.

20. Lu Y, Westland K, Ma YH, Gadgil H 2012. Evaluation of effects of Fc domain high-mannose glycan on antibody stability. Journal of pharmaceutical sciences 101(11):4107-4117.

21. Wang W, Singh S, Zeng DL, King K, Nema S 2007. Antibody structure, instability, and formulation. Journal of pharmaceutical sciences 96(1):1-26.

22. Jefferis R 2012. Isotype and glycoform selection for antibody therapeutics. Archives of biochemistry and biophysics 526(2):159-166.

23. Borrok MJ, Jung ST, Kang TH, Monzingo AF, Georgiou G 2012. Revisiting the role of glycosylation in the structure of human IgG Fc. ACS chemical biology 7(9):1596-1602.

24. Buck PM, Kumar S, Singh SK 2013. Consequences of glycan truncation on Fc structural integrity. mAbs 5(6):904-916.

25. Yamaguchi Y, Nishimura M, Nagano M, Yagi H, Sasakawa H, Uchida K, Shitara K, Kato K 2006. Glycoform-dependent conformational alteration of the Fc region of human immunoglobulin G1 as revealed by NMR spectroscopy. Biochimica et biophysica acta 1760(4):693-700.

26. Houde D, Arndt J, Domeier W, Berkowitz S, Engen JR 2009. Characterization of IgG1 Conformation and Conformational Dynamics by Hydrogen/Deuterium Exchange Mass Spectrometry. Analytical chemistry 81(7):2644-2651.

27. Kameoka D, Masuzaki E, Ueda T, Imoto T 2007. Effect of buffer species on the unfolding and the aggregation of humanized IgG. Journal of biochemistry 142(3):383-391.

28. Wang T, Kumru OS, Yi L, Wang YJ, Zhang J, Kim JH, Joshi SB, Middaugh CR, Volkin DB 2013. Effect of ionic strength and pH on the physical and chemical stability of a monoclonal antibody antigen-binding fragment. Journal of pharmaceutical sciences 102(8):2520-2537.

29. Cheng W, Joshi SB, He F, Brems DN, He B, Kerwin BA, Volkin DB, Middaugh CR 2012. Comparison of high-throughput biophysical methods to identify stabilizing excipients for a model IgG2 monoclonal antibody: conformational stability and kinetic aggregation measurements. Journal of pharmaceutical sciences 101(5):1701-1720.

30. Kayser V, Chennamsetty N, Voynov V, Forrer K, Helk B, Trout BL 2011. Glycosylation influences on the aggregation propensity of therapeutic monoclonal antibodies. Biotechnology Journal 6(1):38-44.

31. Hristodorov D, Fischer R, Joerissen H, Muller-Tiemann B, Apeler H, Linden L 2013. Generation and comparative characterization of glycosylated and aglycosylated human IgG1 antibodies. Molecular biotechnology 53(3):326-335.

32. Raju TS. 2010. Impact of Fc Glycosylation on Monoclonal Antibody Effector Functions and Degradation by Proteases. In Shire SJ, Gombotz W, Bechtold-Peters K, Andya J, editors. Current Trends in Monoclonal Antibody Development and Manufacturing, ed., New York, NY: Springer New York. p 249-269.

33. Liu H, Bulseco GG, Sun J 2006. Effect of posttranslational modifications on the thermal stability of a recombinant monoclonal antibody. Immunol Lett 106(2):144-153.

34. Sedlak E, Schaefer JV, Marek J, Gimeson P, Pluckthun A 2015. Advanced analyses of kinetic stabilities of iggs modified by mutations and glycosylation. Protein science : a publication of the Protein Society 24(7):1100-1113.

35. Sola RJ, Griebenow K 2010. Glycosylation of therapeutic proteins: an effective strategy to optimize efficacy. BioDrugs : clinical immunotherapeutics, biopharmaceuticals and gene therapy 24(1):9-21.

36. Hayes JM, Cosgrave EF, Struwe WB, Wormald M, Davey GP, Jefferis R, Rudd PM 2014. Glycosylation and Fc receptors. Current topics in microbiology and immunology 382:165-199.

37. Sethuraman N, Stadheim TA 2006. Challenges in therapeutic glycoprotein production. Current opinion in biotechnology 17(4):341-346.

38. Schiestl M, Stangler T, Torella C, Cepeljnik T, Toll H, Grau R 2011. Acceptable changes in quality attributes of glycosylated biopharmaceuticals. Nature biotechnology 29(4):310-312.

39. Beck A, Reichert JM 2012. Marketing approval of mogamulizumab: a triumph for glyco-engineering. mAbs 4(4):419-425.

40. Wei Y, Li C, Huang W, Li B, Strome S, Wang LX 2008. Glycoengineering of human IgG1-Fc through combined yeast expression and in vitro chemoenzymatic glycosylation. Biochemistry 47(39):10294-10304.

41. Federici M, Lubiniecki A, Manikwar P, Volkin DB 2013. Analytical lessons learned from selected therapeutic protein drug comparability studies. Biologicals : journal of the International Association of Biological Standardization 41(3):131-147.

42. Lubiniecki A, Volkin DB, Federici M, Bond MD, Nedved ML, Hendricks L, Mehndiratta P, Bruner M, Burman S, Dalmonte P, Kline J, Ni A, Panek ME, Pikounis B, Powers G, Vafa O, Siegel R 2011. Comparability assessments of process and product changes made during development of two different monoclonal antibodies. Biologicals : journal of the International Association of Biological Standardization 39(1):9-22.

43. Bui LA, Hurst S, Finch GL, Ingram B, Jacobs IA, Kirchhoff CF, Ng CK, Ryan AM 2015. Key considerations in the preclinical development of biosimilars. Drug Discov Today 20 Suppl 1:3-15.

44. Crommelin DJ, Shah VP, Klebovich I, McNeil SE, Weinstein V, Fluhmann B, Muhlebach S, de Vlieger JS 2015. The similarity question for biologicals and non-biological complex drugs. European journal of pharmaceutical sciences : official journal of the European Federation for Pharmaceutical Sciences 76:10-17.

45. Alsenaidy MA, Kim JH, Majumdar R, Weis DD, Joshi SB, Tolbert TJ, Middaugh CR, Volkin DB 2013. High-throughput biophysical analysis and data visualization of conformational stability of an IgG1 monoclonal antibody after deglycosylation. Journal of pharmaceutical sciences 102(11):3942-3956.

46. Chaudhuri R, Cheng Y, Middaugh CR, Volkin DB 2014. High-throughput biophysical analysis of protein therapeutics to examine interrelationships between aggregate formation and conformational stability. The AAPS journal 16(1):48-64.

47. Yageta S, Lauer TM, Trout BL, Honda S 2015. Conformational and Colloidal Stabilities of Isolated Constant Domains of Human Immunoglobulin G and Their Impact on Antibody Aggregation under Acidic Conditions. Molecular pharmaceutics 12(5):1443-1455.

48. Okbazghi SZ, More AS, White DR, Duan S, Shah IS, Joshi SB, Middaugh CR, Volkin DB, Tolbert TJ 2016. Production, Characterization, and Biological Evaluation of Well-Defined IgG1 Fc Glycoforms as a Model System for Biosimilarity Analysis. Journal of pharmaceutical sciences 105(2):559-574.

49. Mozziconacci O, Okbazghi S, More AS, Volkin DB, Tolbert T, Schoneich C 2016. Comparative Evaluation of the Chemical Stability of 4 Well-Defined Immunoglobulin G1-Fc Glycoforms. Journal of pharmaceutical sciences 105(2):575-587.

50. Kim JH, Joshi SB, Tolbert TJ, Middaugh CR, Volkin DB, Smalter Hall A 2016. Biosimilarity Assessments of Model IgG1-Fc Glycoforms Using a Machine Learning Approach. Journal of pharmaceutical sciences 105(2):602-612.

51. Alsenaidy MA, Okbazghi SZ, Kim JH, Joshi SB, Middaugh CR, Tolbert TJ, Volkin DB 2014. Physical stability comparisons of IgG1-Fc variants: effects of N-glycosylation site occupancy and Asp/Gln residues at site Asn 297. Journal of pharmaceutical sciences 103(6):1613-1627.

52. Gibson TJ, McCarty K, McFadyen IJ, Cash E, Dalmonte P, Hinds KD, Dinerman AA, Alvarez JC, Volkin DB 2011. Application of a high-throughput screening procedure with PEG-induced precipitation to compare relative protein solubility during formulation development with IgG1 monoclonal antibodies. Journal of pharmaceutical sciences 100(3):1009-1021.

53. Toprani VM, Joshi SB, Kueltzo LA, Schwartz RM, Middaugh CR, Volkin DB 2016. A Micro-Polyethylene Glycol Precipitation Assay as a Relative Solubility Screening Tool for Monoclonal Antibody Design and Formulation Development. Journal of pharmaceutical sciences 105(8):2319-2327.

54. Walsh G 2014. Biopharmaceutical benchmarks 2014. Nat Biotech 32(10):992-1000.

55. Manikwar P, Majumdar R, Hickey JM, Thakkar SV, Samra HS, Sathish HA, Bishop SM, Middaugh CR, Weis DD, Volkin DB 2013. Correlating excipient effects on conformational and storage stability of an IgG1 monoclonal antibody with local dynamics as measured by hydrogen/deuterium-exchange mass spectrometry. Journal of pharmaceutical sciences 102(7):2136-2151.

56. Maddux NR, Joshi SB, Volkin DB, Ralston JP, Middaugh CR 2011. Multidimensional methods for the formulation of biopharmaceuticals and vaccines. Journal of pharmaceutical sciences 100(10):4171-4197.

57. Kim JH, Iyer V, Joshi SB, Volkin DB, Middaugh CR 2012. Improved data visualization techniques for analyzing macromolecule structural changes. Protein Science 21(10):1540-1553.

58. Ghirlando R, Lund J, Goodall M, Jefferis R 1999. Glycosylation of human IgG-Fc: influences on structure revealed by differential scanning micro-calorimetry. Immunology Letters 68(1):47-52.

59. Wu S-J, Luo J, O'Neil KT, Kang J, Lacy ER, Canziani G, Baker A, Huang M, Tang QM, Raju TS, Jacobs SA, Teplyakov A, Gilliland GL, Feng Y 2010. Structure-based engineering of a monoclonal antibody for improved solubility. Protein Engineering, Design and Selection 23(8):643-651.

60. Middaugh C, Litman G 1987. Atypical glycosylation of an IgG monoclonal cryoimmunoglobulin. Journal of Biological Chemistry 262(8):3671-3673.

61. Zheng K, Bantog C, Bayer R 2011. The impact of glycosylation on monoclonal antibody conformation and stability. mAbs 3(6):568-576.

62. Latypov RF, Hogan S, Lau H, Gadgil H, Liu D 2012. Elucidation of acid-induced unfolding and aggregation of human immunoglobulin IgG1 and IgG2 Fc. The Journal of biological chemistry 287(2):1381-1396.

63. Majumdar R, Manikwar P, Hickey JM, Samra HS, Sathish HA, Bishop SM, Middaugh CR, Volkin DB, Weis DD 2013. Effects of salts from the Hofmeister series on the conformational stability, aggregation propensity, and local flexibility of an IgG1 monoclonal antibody. Biochemistry 52(19):3376-3389.

64. Alsenaidy MA, Jain NK, Kim JH, Middaugh CR, Volkin DB 2014. Protein comparability assessments and potential applicability of high throughput biophysical methods and data visualization tools to compare physical stability profiles. Frontiers in Pharmacology 5:39.

Chapter 3 Comparative Evaluation of Well-defined Mixtures of IgG1-Fc Glycoforms as a Model for Biosimilar Comparability Analysis

3.1 Introduction

Monoclonal antibody therapeutics (mAbs) are one of the largest selling and fastest growing biological therapeutics used for treatment of diseases including various cancers and autoimmune disorders such as rheumatoid arthritis.[1,2] Their development process is complicated due to their complex and delicate structures and their production in living cells. Even though innovator mAb biologics show highest sales and clinical utility for providing life-altering therapies, they come with a high price tag especially for chronic conditions that require continuous long-time treatment.[1,2] Additionally, the top selling blockbuster mAb biologics like Rituxan and Humira have had their patents expire recently (in 2016 in the USA) while others (Xolair, Erbitux, Remicade, Avastin, Herceptin, Prolia) are on the verge of expiry in a couple of years. This has driven the pharmaceutical manufacturers to develop biosimilars as lower cost alternatives.[1,2] Biosimilars are approved copies or generic versions of a biologic therapeutic often known as innovator product that can be manufactured after the innovator's patent expires. It is estimated that cost of biosimilars will be 50–70% of the original manufacturer's price.[3] The approval of biosimilars is based on demonstrating that the biosimilar is "highly similar" to the licensed innovator product in terms of quality, safety and efficacy.

The primary and higher order structures (HOS) of biologics are very delicate in nature and further complicated by heterogeneity due to the addition of post-translational modifications like glycosylation. N-glycosylation is a conserved PTM on Asn-297 of the Fc region of antibodies and therapeutic mAbs, which results in significant structural heterogeneity of mAbs. Depending on the type of recombinant expression system, cell culture conditions and additives, the glycosylation pattern on the mAb can vary. Different types of N-glycan structures attached to the Fc of mAbs result in different effector functions. For example, high galactosylation increased the

binding of Fc region to C1q complement protein in serum and increased the CDC (complement dependent cytotoxicity) while having moderate effect on ADCC (antibody dependent cell mediated cytotoxicity).[4-6] The binding of non-fucosylated IgG Fc glycoforms to FcγRIIIa receptors increased significantly with increase in ADCC activity as compared to fucosylated complex glycoforms of IgG.[7] Apart from affecting effector functions of mAbs, glycosylation affects the pharmacokinetic properties and immunogenicity of mAbs as well. For example, mAbs having high mannose type of glycans (Man5/Man8/Man9) showed increased clearance and α1, 3-bound galactose, N-glycylneraminic acid (NGNA) showed adverse immune reactions.[8,9]

N-glycosylation is also known to affect the HOS structure, flexibility and stability of mAbs, and recently it was shown that the glycans are dynamic as well and affect various properties of mAbs by influencing the HOS. [5,10-16] Hence, when the mode of action of a therapeutic mAbs involves Fc effector function, glycosylation causes the main source of heterogeneity and can impact the purity, safety, efficacy of the product making it a critical quality attribute (CQA).[4] CQA is a property that should be maintained within appropriate limits to ensure desired product quality, safety and efficacy, which can be achieved by control of manufacturing procedures.[4,17] Similarly, in biosimilar development, the biosimilar developer has to develop novel manufacturing methods (owing to proprietary nature of innovator's manufacturing protocols) to attempt to duplicate the glycan heterogeneity that is found in the innovator product.[18] Practically, glycan heterogeneity between the biosimilar can be controlled by tight manufacturing procedures, but it is extremely challenging and near to impossible to reproduce glycans content exactly, thus the goal is to produce a glycan content that is "highly similar" to the innovator. Hence, an extensive analytical characterization of glycosylation is required, especially during biosimilar development making it critical to have improved, state of

the art analytical techniques. Similarly, when a manufacturing protocol is changed, for example, cell line change or expression parameter change, extensive analytical characterization is required to ascertain that the pre-change and the post-change products are highly similar and do not show meaningful clinical differences.

The Food and Drug Administration (FDA) guidance documents recommend a couple of approaches to demonstrate biosimilarity, in which analytical characterization is the most fundamental aspect. In the step-wise approach for demonstrating biosimilarity between a proposed biosimilar and innovator product, establishing analytical biosimilarity is the first step.[17] It is the responsibility of the biosimilar manufacturer to conduct extensive tests to demonstrate similarity. These characterizations involve physicochemical characterizations like molecular weight determination, analyzing complexity of the protein (higher order structure and posttranslational modifications), degree of heterogeneity, impurity profiles, and degradation profiles denoting stability.[19] Additionally, biological characterization is also required for example, if part of the mechanism of action of a particular mAb is ADCC or CDC, then FcγRIIIa receptor binding or C1q binding needs to be performed, respectively. When the biosimilar product attributes in terms of physicochemical structure and biological activity are not comparable to that of the innovator product, various process steps are modified to bring the attributes within the variability of the innovator product. This process is repeated until the attributes of biosimilar product match or are highly similar to those of innovator product.[1] Depending on the extent of similarity of these attributes between the biosimilar and the innovator product, the type and extent of preclinical and clinical trials can be modified. Thus, analytical characterization with respect to chemical, physical structure and biological activity is required to establish high similarity. Highly robust analytical characterizations will help make the expensive

pre-clinical and clinical trials more streamlined, which will cut down costs of biosimilars making them more affordable for patients. FDA guidance documents recommend that the CQAs obtained from analytical studies should be identified and classified according to the risk of their potential impact on product quality and the clinical outcomes using appropriate statistical models or methods.[20] Once identified, the CQA needs to be compared between various batches of innovator drug and biosimilar and the extent of uncertainty must be decided. However, the assessment of uncertainty can be relatively subjective and often lacks appropriate statistical reasoning or an approach of combining differences in each individual data set.[17]

An alternative approach to comparing each CQA, is a more holistic approach for comparison which can combine differences from individual data sets.[21] Recent FDA guidance refers to using a more holistic approach of fingerprint analysis which says "it may be useful to compare the quality attributes of the proposed biosimilar product with those of the reference product using a meaningful fingerprint-like analysis algorithm that covers a large number of product attributes and their combination with high sensitivity using orthogonal methods.[22] Previous work in our laboratory, as described in the introduction (Chapter 1), has shown that data visualization tools such as empirical phase diagrams (EPDs) and radar charts can be used to locate patterns of differences in HOS among different proteins and IgG1-Fc glycoforms. These tools can summarize multiple CQAs from multiple techniques between different samples and provide a qualitative evaluation of HOS and physical stability between different groups. Also, physical stability of different glycoforms in different formulations was tested to simulate follow-on biologics or biosimilars that might have different formulations than the originator.[23] These biophysical stability data sets can be utilized to establish a mathematical model based on machine learning approaches to further assess similarity in a more quantitative manner.[21]

The production of model proteins, extensive physicochemical characterization and stability profile of individual model IgG1-Fc glycoproteins was carried out as described in Chapter 2. To better understand the CQAs, development of holistic data visualization tools and development of initial mathematical model were performed on the four individual IgG Fc glycoforms as described in Chapter 2. The overall goal of this study was to simulate a more real world problem of biologics and innovator products by making mixtures of the four well-defined glycoforms of IgG1-Fc (HM-Fc, Man5-Fc, GlcNAc-Fc and N297Q-Fc), performing analytical characterization and using the data sets to develop mathematical models based on machine learning approaches to compare samples. To make the mixtures that would represent the heterogeneity in biosimilar and innovator products, the four well-defined homogenous glycoforms (HM-Fc had distribution of well-defined high mannose forms ranging from Man8-Man12; Man8 being the most abundant) were mixed in different ratios to achieve seven well-defined mixtures that showed a wide range of properties from subtle to evident. Mixtures that were anticipated to show evident differences were 50% mixtures of HM-Fc with 50% of Man5-Fc, GlcNAc-Fc or N297Q-Fc while those that would show subtle differences were mixtures of 90% HM-Fc with 10% Man5-Fc, GlcNAc-Fc or N297Q-Fc. Lastly, a more complex mixture was made which had 25% of each glycoform. The initial characterization of these mixtures showed no differences with respect to protein content, purity, charge heterogeneities, high molecular weight species and tertiary structure as assessed by ultraviolet (UV) spectroscopy, SDS-PAGE, capillary isoelectric focusing (cIEF), size exclusion chromatography (SEC) and intrinsic tryptophan fluorescence. As extensive physical characterization is the fundamental step in biosimilarity assessments, all the seven mixtures were characterized extensively for their physical stability and solubility by utilizing high-throughput spectroscopic tools and a relative solubility assay. Relative solubility, overall conformational

stability, tertiary structure stability, hydrophobic exposure and aggregation propensity of these seven mixtures were probed by assays developed in the Chapter 2: PEG precipitation assay, DSC, intrinsic tryptophan fluorescence spectroscopy, extrinsic Sypro Orange fluorescence spectroscopy and OD350 turbidity. The four well-defined IgG Fc glycoforms studied in Chapter 2 also served as controls in this study. A stressed pH condition of pH 4.5 was also used along with pH 6.0 to study the physical properties of these mixtures by the above techniques. The biophysical techniques showed similar stability profile trends of the mixtures as were anticipated based on the properties of the individual types. Mixtures containing Man5-Fc and HM-Fc showed higher physical stability, intermediate stability was seen in mixtures of GlcNAc-Fc and HM-Fc, and mixtures of HM-Fc and N297Q-Fc showed the least stable physical profile. Also, the 90% mixtures showed subtle differences compared to the 50% mixtures, as expected. DSC and PEG solubility methods, especially at stressed conditions (pH 4.5), were very successful at demonstrating subtle differences in the physical stability and relative solubility profiles of these mixtures. In addition, this study established correlations between the physical stability, chemical stability and biological activity of these well-defined mixtures (which were studied in Schöneich and Tolbert laboratories at KU, respectively). The large stability and solubility analytical data sets generated from these mixture studies are currently being utilized to refine and validate the machine learning based mathematical model to assess overall biosimilarity in the Deeds laboratory at KU.

3.2 Materials and Methods

3.2.1 Materials

For relative solubility and biophysical characterization and stability studies, all the samples were dialyzed at 4°C overnight in a 20 mM citrate phosphate buffer with ionic strength

adjusted to 0.15 by NaCl at pH 4.5 and 6.0. Dialysis was performed at 4°C using Slide-A-Lyzer dialysis cassettes (Life technologies, Grand Island, NY) with a 10 kDa molecular weight cutoff, with three buffer exchanges; two exchanges at 4 hour intervals and one overnight. All the samples were filtered by Millex-GV-0.22 uM syringe filter units (EMD Millipore, Billerica, MA) before measurements. For PEG solubility studies, samples were concentrated by Millipore Amicon Ultra-0.5 mL centrifugal device (EMD Millipore, Billerica, MA) with a MW cut off of 10 kDa to obtain a final protein stock concentration of 1 mg/mL. Components of all buffers including, sodium phosphate and sodium chloride as well as PEG-10,000 were purchased from Sigma-Aldrich (St Louis, MO) while citric acid monohydrate and citric acid anhydrous were purchased from Fisher Scientific at the highest purity grade.

3.2.2 Methods

3.2.2.1 *Preparation of Mixtures IgG1 Fc*

After producing and purifying the four IgG1-Fc glycoforms (the starting materials: HM-Fc, Man5-Fc, GlcNAc-Fc and N297Q-Fc) as mentioned previously,[24] these were dialyzed at 4°C overnight in a 20 mM citrate phosphate buffer with ionic strength adjusted to 0.15 by NaCl at pH 6.0. Dialysis was performed at 4°C using Slide-A-Lyzer dialysis cassettes (Life technologies, Grand Island, NY) with a 10 kDa molecular weight cutoff, with three buffer exchanges; two exchanges at 4h intervals and one overnight. After dialysis, the final concentration of the four IgG1-Fc proteins, also known as controls, were adjusted to 0.5mg/mL and were mixed in different ratios as seen in Figure 3.1 to obtain seven different mixtures. The final concentration of protein in the mixtures was 0.5 mg/mL and the seven mixtures and 4 controls were stored in aliquots of 5 mL at -80°C for further analysis.

3.2.2.2 *Sodium Dodecyl Sulfate-Polyacrylamide Gel Electrophoresis (SDS-PAGE)*

For the reduced samples, each of the IgG1 Fc proteins (7 µg) were mixed with 2X TrisHCl SDS loading dye containing 100 mM DTT and incubated at 70 °C for 2 min. The reduced IgG1 Fc samples were then separated by sodium dodecyl sulfate polyacrylamide gel electrophoresis using NuPAGE 4-12% Bis-Tris gradient gel (Life Technologies, Grand Island, NY) gels and a MES running buffer (Life Technologies).[24] A similar method was followed for non-reduced samples of IgG1 Fc proteins except DTT was omitted during the incubation step. The running time for all the gels was 60 min at 150 V. Protein bands were visualized by staining with Coomassie blue R250 (Teknova, Hollister, CA) and destained with a mixture of 30% methanol, 10% acetic acid, and 60% ultrapure water. Gel images were recorded using an Alphaimager (Protein Simple, Santa Clara, CA) gel imaging system.

3.2.2.3 *Size exclusion chromatography (SEC)*

Experiments were performed using a Shimadzu high-performance liquid chromatography system equipped with a photodiode array detector capable of recording UV absorbance spectra from 200 to 400 nm and a temperature controlled auto sampler. A Tosoh TSK-Gel Bioassist G3SWxL column (7.8 mm ID x 30.0 cm L) and a corresponding guard column (TOSOH Biosciences, King of Prussia, Pennsylvania) were used for Fc protein characterization. First, the SEC column was equilibrated for at least 10 column volumes (CV) with a mobile phase containing 200 mM sodium phosphate, pH 6.8, and a flow rate of 0.7 mL/min at 30 ^{0}C column temperature as mentioned previously.[24] Next, the column was calibrated using gel filtration MW standards (Bio-Rad, Hercules, CA) before and after the runs of IgG1-Fc glycoforms to ensure column and HPLC system integrity. All Fc samples were centrifuged at 14,000 g for 5 min before injection to remove insoluble protein aggregates. Protein samples at a concentration of 0.5

mg/mL were injected in a volume of 50 µL, and a 30 min run time was used for elution. Peak quantification was carried out using LC solutions software (Shimadzu, Kyoto, Japan). The errors for monomer percent for all the samples represent SD of triplicate measurements.

3.2.2.4 *Capillary isoelectric focusing (cIEF)*

The determination of isoelectric points (pIs) of all the IgG1-Fc glycoforms using capillary isoelectric focusing (cIEF) were performed with an iCE280 analyzer from Convergent Biosciences (now Protein Simple, Toronto, Canada) equipped with a microinjector. A FC Cartridge (Protein Simple, Toronto, Canada) with 50 mm, 100 µm I.D. fluorocarbon-coated capillary and built-in electrolyte tanks were used for focusing. The cartridge was calibrated by hemoglobin standard (Protein Simple, Toronto, Canada) before and after focusing of IgG1-Fc samples to ensure its integrity. For focusing, a sample mixture was prepared where each of the IgG1 Fc glycoforms were mixed with urea (Fischer Scientific), methyl cellulose (Protein Simple, Toronto, Canada), sucrose (Pfanstiehl Inc., Waukegan, IL), N,N,N',N'-Tetramethylethane-1,2-diamine (Sigma-Aldrich, St Louis, MO) and Pharmalyte 3–10 (GE Healthcare Biosciences, Pittsburgh, PA). The final protein concentration in the sample mixture was 0.2 mg/mL. All the IgG1 Fc glycoforms were resolved using a pre-focusing time of 1 minute at 1500 V and a focusing time of 7 minutes at 3000 V. Observed peaks were calibrated using two pI markers with values of 5.84 and 8.18. The separation was monitored at 280 nm by a CCD detector. Quantitation of the peaks was done using Chromperfect® software. The error bars for pI values of all the samples represent standard deviation (SD) of triplicate measurements.

3.2.2.5 *UV Spectroscopy*

Absorbance spectra were obtained over the wavelength range of 200–400 nm employing an Agilent 8453 UV-visible spectrophotometer equipped with a diode array detector. All samples

were analyzed in a quartz cuvette with a 1-cm path length and the absorbance value at 280 nm was used to calculate the concentration of proteins. Second-derivative spectra were calculated using Origin software to determine peak positions. Results are reported showing triplicate runs of all the samples.

3.2.2.6 *PEG Precipitation Assay*

The experimental protocol was adapted from Toprani et al.[25] Stock solutions of PEG-10,000 ranging from 0 to 40% w/v PEG were prepared in 20 mM citrate phosphate buffer with ionic strength adjusted to 0.15 by NaCl at pH 4.5 and pH 6.0. A volume of 40 µL of each of the PEG-10,000 solutions (from 0 to 40% w/v PEG) were added to wells of a 96-well polystyrene filter plate (Corning#3504, Corning Life Sciences, Corning, NY). Ten µL of the protein stock solutions (1 mg/mL) was then added to each well to achieve a final protein concentration of 0.2 mg/mL. The plates were incubated at room temperature overnight and then were centrifuged at 1233 (x g) for 15 min. The filtrate was collected in a clear 96 well collection plate (Greiner Bio-One#655001, Greiner Bio-One North America Inc., Monroe, NC). The protein concentration was determined on a NanoDrop 2000 spectrophotometer (NanoDrop Products, Wilmington, DE) using 2 µL of filtrate by measuring absorbance at 280 nm. Each samples were run in triplicates and the data was analyzed using Python (x,y) v.2.7.6.0, an open source scientific software based on python language and the % PEG_{midpt} values and apparent solubility value parameters were then calculated as described before.[23,25]

3.2.2.7 *Differential Scanning Calorimetry (DSC)*

DSC experiments were performed using a MicroCal VP-AutoDSC instrument with an autosampler (MicroCal, LLC, Northampton, Massachusetts). Triplicate measurements of all samples (at 0.4 mg/mL concentration) were obtained from 10°C to 100°C with a scanning rate of

60°C/h. Data analysis was performed using the MicroCal LLC DSC plug-in for the Origin 7.0 software package to obtain the final DSC thermograms and the onset temperature (T_{onset}) of the first transition for all the samples as described before.[23]

3.2.2.8 *Intrinsic (Trp) fluorescence spectroscopy*

The fluorescence spectra were measured in triplicate using a Photon Technology International (PTI) Quantum master fluorometer (New Brunswick, New Jersey) with 200 µL of 0.2 mg/mL protein solution in 0.2 cm path length quartz cuvettes. Samples were excited at 295 nm (>95% Trp emission) and the emission spectra from 10°C to 90°C in increments of 1.25°C were recorded from 305 to 405 nm. The spectra were analyzed and the maximum peak position (λ_{max}) values were calculated using a "spectral center of mass" method (MSM) as described before[1]. From the peak position (λ_{max}) versus temperature plots transition midpoint temperatures (T_m) were calculated for all the samples.

3.2.2.9 *Extrinsic fluorescence spectroscopy*

The extrinsic fluorescence measurements were performed in triplicates using a MX3005P QPCR system (Agilent Technologies). Samples contained 0.2 mg/mL protein in a total sample volume of 100 µL. The Sypro™ orange dye was purchased from Invitrogen, Inc. (Carlsbad, CA) and was diluted in water and then added to the protein samples to achieve 1x dye concentration as reported before[23]. Using custom filter sets, the samples was excited at 492 nm, and the emission intensity change with temperature at 610 nm was followed. The temperature was raised from 25°C to 90°C using 60°C/h heating rate and 1˚C as a step size. Data analysis was carried out to obtain fluorescence intensity against temperature plots and the transition midpoint temperatures (T_m) were calculated for all the samples as described previously.[23]

3.2.2.10 *Optical density (OD) 350 nm measurements*

Turbidity measurements were performed using a Cary 100 UV-Visible spectrophotometer (Varian medical Systems, Inc., Palo Alto, California) equipped with a 12 cell holder with a peltier type temperature controller. Samples contained 0.2 mg/mL protein with a total volume of 250 µL in 1 cm path length quartz cells. OD at 350 nm was monitored as the temperature was raised in increments of 1.25˚C from 10 to 90˚C with a heating rate of 60˚C/h. Protein samples were run in triplicate and corresponding buffer blanks were run and subtracted from each sample. The OD at 350 nm was plotted against temperature as described previously.[23]

3.3 Results

3.3.1 Initial comparisons of purity, high molecular weight species, charge heterogeneities and structural integrity of well-defined mixtures of IgG1-Fc glycoforms

Approximately 99% purity was achieved for each of the seven IgG1-Fc mixtures and four controls IgG1-Fc (individual glycoforms) as determined by both reduced and non-reduced SDS-PAGE gels (Figure 3.2). Size exclusion high performance liquid chromatography (SEC) was then used to evaluate purity (under non-denaturing conditions) to determine if aggregates were present in controls and mixtures before starting their biophysical and binding analysis. (Figure 3.3 shows representative SEC chromatograms of each of the controls and mixtures). The monomeric purity of mixtures and controls was determined by SEC, as shown in the Table 3.1, and the results indicate that all the IgG1-Fc mixtures and controls are monomeric (97-99 %) with small levels of aggregates present across the IgG1-Fc samples (1-3 %). Characterization of the isoelectric point (pI) range of the seven mixtures and controls of IgG1-Fc glycoforms by capillary isoelectric focusing (cIEF) showed pI of 7.2 in the base buffer. Figure 3.4 shows representative cIEF chromatograms and the pI values of the major species in the mixtures and

controls. Figure 3.5 A shows second derivative UV-visible absorption spectra of the four IgG1-Fc controls and seven mixtures. No changes in the ultraviolet absorption peak positions of the three aromatic amino acids (Phe, Tyr, Trp see Figure 3.5 B for the peak locations) were observed indicating no major differences in tertiary structure in the base buffer, across all the samples. The structural integrity of the overall tertiary structure of the four IgG1-Fc glycoform controls and the seven mixtures was evaluated by measurement of intrinsic Trp fluorescence at 10°C at pH values 4.5 and 6.0 (see Figure 3.6). For each sample, the wavelength of maximum intensity (λ_{max}) at 10°C at each pH was calculated and was found to be overall similar and in the range of 328 to 330 nm with standard deviations calculated from triplicate measurements of up to ~0.6 nm. These results indicated that the spectra for the controls and mixtures were overall similar at 10°C at both pH 4.5 and pH 6.0. The fluorescence intensity obtained for each protein represents the average values of all the tryptophan residues present in the protein.

3.3.2 Relative Apparent Solubility

An assessment of the apparent solubility (thermodynamic activity) of four IgG1-Fc glycoform controls (HM-Fc, Man5-Fc, GlcNAc-Fc and N297Q-Fc) and their seven mixtures was performed using PEG precipitation as described previously (see Methods section). Protein versus % PEG concentration plots were generated for all the samples at pH 4.5 and pH 6 respectively, in the formulation buffer as shown in Figure 3.7 (for mixtures) and Figure 3.8 A and D (for controls). The solubility curves of the mixtures (see Figure 3.7) show a sigmoidal curve, demonstrating that as the crowding agent (PEG) concentration increases; there is a point at which a decrease in the amount of the protein in solution occurs in a quantifiable manner. For ease of comparison, the protein versus % PEG concentration plots for the four controls were plotted together at both pH 4.5 (Figure 3.8 A) and pH 6 (Figure 3.8 D). These curves solubility

curves show differences between the controls with regard to glycosylation and pH as seen previously in Chapter 2. As seen in Figure 3.8 A, at pH 4.5 the N297Q-Fc begins to precipitate rapidly as the PEG concentration is increased, and deviates from the typical sigmoidal curve, possibly indicating structural alterations in the protein and/or direct interaction between the PEG and protein, which is consisent with the previous results.[23]

Figure 3.8 B and E show % PEG_{midpt} values (which is the weight % PEG required to reduce the protein concentration by 50% of its initial value) at pH 4.5 and pH 6 respectively, for all samples. For each sample, a trend of decreasing % PEG_{midpt} values with increasing solution pH from 4.5 to 6 was observed indicating decreasing solubility as the solution pH increased. In terms of general trends of the four controls, the HM-Fc showed the highest % PEG_{midpt} value followed by Man5-Fc, GlcNAc-Fc and lastly, the non-glycosylated N297Q-Fc at pH 4.5 (Figure 3.8 B) as seen previously[1]. At pH 6 (Figure 3.8 E), the HM-Fc and Man5-Fc did not show significant differences in the % PEG_{midpt} that was similar to previous results[1] while GlcNAc-Fc showed intermediate % PEG_{midpt} values followed by the N297Q-Fc showing the least.

Similarly with the mixture samples, subtle differences were observed in % PEG_{midpt} at pH 6 (Figure 3.8 E) than at pH 4.5 (Figure 3.8 B) where more prominent differences were observed. At both pH 4.5 and 6, 50% mixtures of HM-Fc (Mixtures 1, 2 and 3 which are 50% mixtures of HM-Fc with 50% Man5-Fc, 50% GlcNAc-Fc and 50% N297Q-Fc respectively) showed a similar trend with % PEG_{midpt} as observed in their respective controls from which they are made. For example, Mixture 1 showed the highest % PEG_{midpt} value, Mixture 2 intermediate and Mixture 3 the least which correlated with the trend observed in their respective controls which was in decreasing order of % $PEG_{midpt:}$ Man5-Fc control >GlcNAc-Fc control>N297Q-Fc control. All the 50% mixtures of HM-Fc showed lower % PEG_{midpt} values that the HM-Fc controls at both

the pH conditions. Also, Mixture 3 which had 50% N297Q-Fc with 50% HM-Fc did not precipitate as rapidly as the 100% N297Q-Fc control. At pH 4.5 (Figure 3.8 B) and 6 (Figure 3.8 E), % PEG_{midpt} values of the 90% mixtures of HM-Fc (Mixtures 4, 5 and 6 which are 90% mixtures of HM-Fc with 10% Man5-Fc, 10% GlcNAc-Fc and 10% N297Q-Fc respectively), showed subtle differences between their % PEG_{midpt} in the order of decreasing % PEG_{midpt}: Mixture 4> Mixture 5> Mixture 6. This trend was subtle but similar to the trend observed in the 50% mixtures (Mixture 1, 2 and 3), which is dependent on the trend observed in the controls from which they were prepared. All the 90% mixtures of HM-Fc showed slightly lower % PEG_{midpt} values than the HM-Fc control but were higher than their respective 50% mixtures at pH 4.5 while the trends were similar and differences were subtle at pH 6. Mixture 7 (which was 25% mixture of each of HM-Fc, Man5-Fc, GlcNAc-Fc and N297Q-Fc) showed similar % PEG_{midpt} values to Mixture 1 (HM: Man5::50:50) and 5 (HM:GlcNAc::90:10), but slightly higher values than Mixture 6 (90%HM-Fc:10%N297Q-Fc) at pH 4.5 and the differences were subtle at pH 6. To summarize, we can rank order the solubility profiles of IgG1-Fc glycoform mixtures from high to low by following the % PEG_{midpt} values that decreased in the following order: Mixture 4> Mixture 1> Mixture 5> Mixture 7> Mixture 6> Mixture 2> Mixture 3 at pH 4.5. However, at pH 6 even though the trend was similar it was difficult to rank order the solubility profiles of mixtures due to subtle differences between the % PEG_{midpt}. Mixture 3, which had a higher percent (50%) of the N297Q-Fc control, showed the lowest % PEG_{midpt}, while Mixture 4 which had high percent (90%) of the HM-Fc and 10% Man5-Fc showed the highest % PEG_{midpt} value at pH 4.5. The 50% (Mixture 1) and 90% (Mixture 4) mixtures of HM-Fc with Man5-Fc showed % PEG_{midpt} values lower than the HM-Fc control and higher than the Man5-Fc control. Similarly, the 50% (Mixture 2) and 90% (Mixture 5) mixtures of HM-Fc with GlcNAc-Fc

showed % PEG_{midpt} values lower than the HM-Fc control and higher than the GlcNAc-Fc control. In addition, similar results were seen for 50% (Mixture 3) and 90% (Mix 6) of HM-Fc with N297Q-Fc.

As shown in Figure 3.8 C and 3.8 F, the apparent solubility (thermodynamic activity) values were calculated by extrapolation to zero PEG concentration (see Methods section) in pH 4.5 and pH 6, respectively. These values showed trends similar to those found with % PEG_{midpt} in terms of Fc glycan structure of the controls and solution pH. At both pH values, the apparent activity values between HM-Fc vs. Man5-Fc glycoforms showed no significant differences. The apparent activity values of GlcNAc-Fc were lower than the HM-Fc and Man5-Fc at pH 4.5 and 6. The N297Q-Fc showed the lowest apparent activity value at pH 6. At both pH 4.5 (Figure 3.8 C) and 6 (Figure 3.8 F), the apparent solubility values all mixtures followed similar trends as % PEG_{midpt} values. Apparent solubility values for Mixture 3 (50%HM-Fc::50%N297Q-Fc) were lowest at both pH 4.5 and 6 but were higher than the N297Q-Fc control due to the presence of 50% of HM-Fc control. However, as the errors were higher in apparent solubility calculations, it was difficult to rank order the solubility profiles of the mixtures.

3.3.3 Overall Conformational Stability and Tertiary Structure Stability

Differential scanning calorimetry was used to assess the overall conformational stability of the four IgG1-Fc glycoform controls and their mixtures as the samples were heated from 10°C to 100 °C. Figure 3.9, shows representative DSC thermograms of all the samples obtained at both pH 4.5 and 6 which showed two major endothermic peaks, as seen previously.[23] For direct comparison between the samples, the T_{onset} values of the first transition were calculated and plotted as a bar chart representation at pH 4.5 (Figure 3.12 A) and pH 6 (Figure 3.12 B). Based on previous studies with human IgG-Fc glycoforms, the first and second transition corresponds

to the unfolding of the C_H2 and C_H3 domains of the IgG-Fc respectively[26]. The T_{onset} values calculated in this study represent the temperatures of onset of transition in the C_H2 domain of the IgG1-Fc of all samples. The thermal melting temperatures for C_H3 domain of controls did not show significant differences under pH 4.5 and pH 6 as observed before,[23] thus they were not shown here assuming subtle differences in the mixtures will not be observed.

Intrinsic Trp fluorescence spectroscopy and Sypro Orange fluorescence spectroscopy were utilized as two complementary techniques to evaluate the stability of the overall tertiary structure of the glycofrom controls and 7 mixtures. The intrinsic Trp fluorescence spectra were collected at pH 4.5 and 6 and the changes in λ_{max} (MSM peak position) as a function of increasing temperature (every 1.25°C starting from 10°C to 90°C) were plotted for all samples as shown in Figure 3.10. The λ_{max} is senitive to the environment around the tryptophan residues and as a result can be used as probe to study changes in the higher-order structure of proteins often accompanied by shift of λ_{max} to longer wavelengths (red shift). As seen in the representative peak position plots for all the samples at pH 4.5 and pH 6 (Figure 3.10), there is no change in λ_{max} values up to certain temperatures. However, more dramatic increase (transition) in λ_{max} is observed as the temperature increases before plateauing off. The melting temperatures (T_m, which is the midpoint temperature of a thermal transition) of thermal transitions were calculated as mentioned before[23] and plotted as bar chart at both pH 4.5 and 6 (see Figure 3.12 C and 3.12 D respectively). Sypro Orange was used as a probe for detecting protein structural alterations seen as increased fluorescence intensity upon exposure of the dye to increased apolar environments (presumably as a result of structural changes and/or aggregate formation by the protein). Sypro Orange fluorescence peak intensity was collected as a function of increasing temperature for all the samples at at pH 4.5 and 6 (see Figure 3.11). The melting

temperatures (T_m, which is the midpoint temperature of a thermal transition) of thermal transitions were calculated as mentioned before[23] and plotted as bar chart at both pH 4.5 and 6 (see Figure 3.12 E and 3.12 F, respectively).

In general, the T_{onset} and T_m values of the DSC and intrinsic/extrinsic fluorescence thermal transitions for all the controls and mixtures followed trends that depend upon the type of glycoform and the solution pH as noted previously.[1] The DSC results showed that T_{onset} values of all the samples were lower at pH 4.5 (Figure 3.12 A) than 6 (Figure 3.12 B). Similarly, T_m values obtained at pH 4.5 and pH 6 from intrinsic tryptophan fluorescence (Figure 3.12 C and 3.12 D) and extrinsic Sypro Orange fluorescence (Figure 3.12 E and 3.12 F) were lower in pH 4.5 than pH 6 demonstrating the lower conformational and tertiary structure stability of all the controls and mixtures at lower pH conditions. Also, the Sypro Orange fluorescence peak intensity at the starting temperature (25°C) for all samples was relatively higher at pH 4.5 than at pH 6 (Figure 3.11). For all the samples, higher fluorescence peak intensity at lower pH condition suggests relatively increased surface hydrophobicity and presumably some level of structural alteration even at lower temperatures.

For the IgG1-Fc glycoform controls, a trend of decreasing conformational stability with the truncation of carbohydrate units was observed for the T_{onset} values at pH 4.5 where the highest values were observed for HM-Fc and Man5-Fc controls (Man5 trended slightly higher than HM-Fc but within error), followed by GlcNAc-Fc and the lowest for N297Q-Fc control (Figure 3.12 A). Similarly, T_m values of thermal transitions obtained from intrinsic Trp fluorescence (Figure 3.12 C) and Sypro Orange fluorescence (Figure 3.12 E) were the highest for HM-Fc and Man5-Fc (Man5 trended slightly higher than HM-Fc in Sypro Orange) followed by intermediate values for GlcNAc-Fc and the lowest values for N297Q-Fc. At pH 6, T_{onset} from

DSC (Figure 3.12 B) showed similar trends as observed at pH 4.5, where N297Q-Fc was the least stable; however the differences between the other three controls were subtle. Also T_m values from Intrinsic Trp fluorescence (Figure 3.12 D) and Sypro Orange fluorescence (Figure 3.12 E) showed similar trends as pH 4.5. The Sypro Orange fluorescence peak intensity (Figure 3.11) at the starting temperature (25°C) for N297Q-Fc control in both pH conditions trended relatively higher as compared to the other three controls suggesting increased surface hydrophobicity of N297Q-Fc even at lower temperatures. These results suggest that the HM-Fc and Man5-Fc glycoforms display highest stability of the tertiary structure, followed by the GlcNAc-Fc with intermediate stability, and the N297Q-Fc aglycosylated form having the least thermal tertiary structure stability as seen before.[23] Interestingly, Man5-Fc trended a bit higher in stability than HM-Fc as observed by DSC and Sypro Orange which was not seen in a previous study that utilized different batches of controls and showed HM-Fc to have highest stability[23] by these techniques.

The 50% mixtures of HM-Fc (Mix 1, 2 and 3 which were which were 50% mixtures of HM-Fc with 50% Man5-Fc, 50% GlcNAc-Fc and 50% N297Q-Fc respectively) showed large differences in conformational stability following the trend from highest to lowest T_{onset} values at pH 4.5 (Figure 3.12 A) as shown; Mixture 1 (HM:Man5::50:50)> Mixture 2 (HM:GlcNAc::50:50)> Mixture 3 (HM:N297Q-FC::50:50). This trend was similar to the stability trend observed in their respective controls which was with decreasing order of stability Man5-Fc>GlcNAc-Fc>N297Q-Fc. Similarly at pH 4.5, Mixtures 1, 2 and 3 showed relatively large differences in T_m values obtained from intrinsic Trp fluorescence (Figure 3.12 C) and Sypro Orange fluorescence (see Figure 3.12 E), and followed the trend similar to their individual component controls. At pH 6 differences in conformational stability (see T_{onset} in Figure 3.12 B)

versus type of glycosylation in the mixtures were subtle than pH 4.5 and showed similar trends as observed at pH 4.5. Similarly, differences in tertiary structure stability (see T_m in Figure 3.12 D and 3.12 F) versus type of glycosylation in the mixtures were subtle at pH 6 than at pH 4.5. The 90% mixtures of HM-Fc (Mixtures 4, 5 and 6 which were 90% mixtures of HM-Fc with 10% Man5-Fc, 10% GlcNAc-Fc and 10% N297Q-Fc respectively) and Mixture 7 (which was 25% mixtures of each of HM-Fc, Man5-Fc, GlcNAc-Fc and N297Q-Fc) showed subtle differences in conformational stability by DSC and their T_{onset} values were almost similar to those of 100% HM-Fc controls at both pH conditions (see Figure 3.12 A and 3.12 B). This 10% mixture of Man5-Fc, GlcNAc-Fc and N297Q-Fc (Mixtures 4, 5 and 6 respectively) with 90% HM-Fc showed equivalent stability to the HM-Fc control as it is the most abundantly present in these mixtures. Similar results were observed by intrinsic Trp fluorescence (see Figure 3.12 C and 3.12 D) and Sypro Orange fluorescence (see Figure 3.12 E and 3.12 F) at both pH conditions; however, the T_m values obtained for Mixture 7 were slightly lower than 100% HM-Fc control.

Differences between the N297Q-Fc control and its mixtures with HM-Fc were observed easily at both pH 4.5 and pH 6 where 100% N297Q-Fc control that had the least conformational stability, showed increased stability as the % of HM-Fc increased from 50% (Mixture 3) to 90% (Mixture 6). Overall, Mixture 7 (which was 25% mixtures of all controls) showed intermediate stability between Mixture 3 and Mixture 6. The GlcNAc-Fc control also showed similar increase in conformational stability upon mixing with increasing amounts of HM-Fc, but the ability to distinguish between 50% and 90% mixtures was subtle at both pH 4.5 and 6. 50 % and 90% mixtures of HM-Fc with Man5-Fc, show similar conformational stabilities with HM-Fc and

Man5-Fc controls except Mixture 1, which can be distinguished at pH 4.5 where it showed highest stability as it had high amounts of the most stable Man5-Fc (50%).

3.3.4 Aggregation propensity by Turbidity

Temperature induced aggregation profile of the IgG1-Fc glycoform controls and seven mixture samples was evaluated by monitoring optical density (OD) changes of the samples at 350 nm as a function of increasing temperature at pH 4.5 and 6.0 (See Figure 3.13). Differences in aggregation pattern were observed with the type of glycoform and the solution pH. The HM-Fc and Man5-Fc IgG1-Fc controls did not show any notable increases in OD350 values as the temperature increased across both pH conditions tested as seen before.[23] These glycoforms did not show the tendency to aggregate by turbidity assay in the conditions tested. The GlcNAc-Fc control displayed a single thermal transition at pH 6.0 while the N297Q-Fc control displayed a single thermal transition at both pH 4.5 and pH 6.0 as observed before.[23] Mixtures 3 and 7 (that contained 50% HM-Fc::50% N27QFc and 25% of each HM-Fc, Man5-Fc, GlcNAc-Fc and N297Q-Fc, respectively) showed increase in OD 350 values with a single transition as the temperature increased at pH 6.0, but did not show any increase in OD350 values at pH 4.5. Mixture samples 1, 2, 4, 5 and 6 (that contained 50% HM-Fc::50 % Man5-Fc, 50% HM-Fc::50 % GlcNAc-Fc , 90% HM-Fc::10% Man5-Fc, 90% HM-Fc::10% GlcNAc-Fc, 90% HM-Fc::10% N297Q-Fc, respectively) however, did not show any increase in the OD 350 values with a rise in temperature at both the pH conditions. The onset temperatures (T_{onset}), where rapid increase in OD350 was observed, were calculated for all the samples (Figure 3.13). The T_{onset} values were determined by noting the temperature at which the transition starts. The T_{onset} values for triplicate runs were in the range of 82.0-90.0°C with standard deviations (SD) from 0.1°C -1.2°C for all samples that showed transition in OD 350nm. Both controls GlcNAc-Fc and N297Q-Fc

show T_{onset} at 82.7°C (SD ranging from 0.5°C -1.0°C) at pH 6.0, while N297Q-Fc shows T_{onset} at 82.0°C ± 0.1°C in pH 4.5. Mixtures 3 and 7 show T_{onset} values at 90.0°C±0.8°C, 85.5°C ±0.4°C and 87.3°C ± 1.2°C, respectively.

The results indicate that N297Q-Fc is the most aggregation prone of the IgG1-Fc glycoform, which shows transitions in both the pH conditions, followed by GlcNAc-Fc which showed transition at pH 6.0, while the T_{onset} of aggregation appears to be the same for both the controls. The HM-Fc and Man5-Fc are not prone to aggregation at either of the pH conditions tested here. Mixtures 3 and 7 (which have the high percent (50%) of the aggregation prone GlcNAc-Fc and N297Q-Fc proteins) show transitions at pH 6.0, while at pH 4.5; the N297Q-Fc containing mixtures do not show aggregation unlike the N297Q-Fc control.

3.4 Discussion

It is well established that comprehensive analytical characterization is the first step of biosimilarity assessments during manufacturing of biotherapeutics. Extensive analytical testing with respect to the primary and higher order structures of protein therapeutic candidates is essential in establishing the foundation of comparative biosimilarity.[27] Also, the first experimental key step in biosimilar approval process is assessing comparative structural and functional properties between the biosimilar and the reference product and emphasis of the use of "orthogonal methods" and "fingerprint-like methods" by the FDA.[28] The extensive biophysical techniques used in this study are shown to be useful in establishing differences in physical stability profile of mixtures of IgG1-Fc glycoforms. Initial characterization of the controls and mixtures did not show any significant differences in pI values and overall tertiary structure at pH 6.0 (without temperature stress) as assessed by cIEF (shown in Figure 3.4) and second-derivative UV spectroscopy (shown in Figure 3.5A). Also, the tertiary structure analyzed at pH 6.0 and pH

4.5 by intrinsic tryptophan fluorescence did not show any differences between the mixtures, and the controls at 10°C (see Figure 3.6). SEC was able to distinguish the N297Q-Fc control as it had a slightly higher content of high molecular weight species than the other controls and mixtures (Table 3.1). SDS-PAGE analysis showed differences between each of the four IgG1-Fc controls except, between HM-Fc and Man5-Fc as observed before.[23,24] As seen in Figure 3.2, the large sized glycoforms (HM-Fc and Man5-Fc) migrated nearest, GlcNAc-Fc which had intermediate size migrated to an intermediate distance, and the lowest sized N297Q-Fc migrated farthest on both reduced and non-reduced gels as observed previously.[24] Similarly, the components of 50% mixtures and 90% mixtures were identified by SDS-PAGE based on the intensities of each band and migration of the components within the mixture as compared to controls. However, the 50% and 90% mixtures of HM and Man-Fc were not resolved in SDS-PAGE and were analyzed by mass spectrometry in the Tolbert lab. Intact mass analysis of the controls and mixtures was performed to identify N-glycans in the controls and composition of glycoforms in the mixtures. The percentage of glycoform composition in the mixtures was examined using the mass spectrometry peak intensity as evaluated previously for identification of glycosylation profiles in the controls.[24] The results demonstrated that the estimated percentages of the mixture components (as shown in Figure 3.1) were accurately determined by mass spectrometry as described somewhere else. Other studies also showed that mass spectrometry has proved to be a very rapid and reliable tool in glycan content analysis in biosimilar comparability.[29,30] Even though the information on the chemical structure of glycans can be elucidated by mass spectrometry, yet the differences in HOS need a broad array of different analytical techniques.

It was evident from the results of PEG relative solubility and biophysical characterization techniques that the PEG_{midpt} and apparent solubility values, as well as T_{onset} and T_m values of the

pure IgG1-Fc controls are dependent on the type of glycoform and solution pH conditions. These techniques were able to distinguish structural and physical stability differences in homogenous glycoforms of differentially glycosylated IgG1-Fc (controls) and proved to be successful in distinguishing the various levels of differences between their mixtures as well. The % PEG_{midpt}, especially at pH 4.5 was most sensitive to monitor the differences between IgG1-Fc glycoform mixtures and also was able to successfully rank order their solubility profiles. As the results indicate, techniques like DSC, intrinsic and extrinsic fluorescence were successful in distinguishing between mixtures up to certain extent (controls and 50% mixtures) however, the ability to distinguish between the 90% mixtures (that were expected to show subtle changes) was lower. As seen in Figure 3.13, turbidity by OD 350 nm did not show any differences in all the mixtures and controls at pH 4.5, except N297Q-Fc, which showed significant increase in OD 350 signal. However, at pH 6.0 OD 350 was able to detect changes between GlcNAc-Fc and N297Q-Fc controls and their 50% mixtures (2 and 3) with HM-Fc, however it was not able to distinguish between any of the 90% mixtures. The 25 % mixture of all the glycoforms (Mixture 7) showed intermediate rise in OD 350 as compared to GlcNAc-Fc and N297Q-Fc controls at pH 6.0.

Although the above biophysical techniques are considered as low resolution techniques, they are high throughput, well established, commonly available and widely used in the industry. The use of higher resolution analytical techniques such as NMR, X-ray crystallography, cryo EM and H/D exchange mass spectrometry to gain higher order structural information is limited as part of analytical comparability studies as a result of certain drawbacks.[31] Hence, the biophysical techniques used in this work along with two pH conditions and temperature stresses prove useful in distinguishing between IgG1-Fc glycoform mixtures with regard to their solubility and physical stability. This again shows the importance of stress conditions to detect differences that

are not readily apparent when monitored under non-stressed conditions (i.e., at low temperatures under neutral pH conditions).[31]

In mutation prone diseases like infectious diseases or certain types of cancers it has been seen that the monospecific nature of mAbs makes them less effective in treatment. In such scenarios, recombinant polyclonal antibodies or antibody cocktails which can have a wide array of binding to complex target antigens and could show therapeutic potential.[32,33] In such therapeutics, it is essential to characterize the individual components of these antibody mixtures to gain clinical approval. These products will also show glycosylation variation as seen in mAbs and will further complicate their control and characterization. Several analytical tools have been used to characterize such mixtures of antibodies including cation exchange chromatography, ELISA and mass spectrometry.[33] However, not many studies have been conducted to understand their physical structure and stability. The biophysical characterization approach utilized in this study to characterize mixtures of IgG1-Fc glycoforms could be utilized for characterization of these antibody mixtures as well.

In summary, the four control IgG Fc glycoforms and seven mixtures were evaluated for their physical stability and relative solubility profiles using an array of biophysical characterization tools. Future work should involve comparing the chemical stability and biological functions (performed in other labs at KU) of these mixtures along with these results to get a complete idea of their properties so that the mathematical model can determine the extent of similarity (biosimilarity) between these mixtures. These analytical tools were successful in detecting subtle and major differences in physical properties of these mixtures. Some of these assays were redundant and yielded little information (like cIEF, SEC, second derivative UV and turbidity), and identifying these less informative assays can simplify the

overall analytical characterization approach by eliminating them or weighing the assays in the mathematical model. These studies have generated a large amount of stability and relative solubility data set, which will be utilized to develop a mathematical model for determining the level of biosimilarity between samples. It would be interesting to see if the developed mathematic model is capable of predicting the components of the individual mixtures.

Table 3.1: Percent monomer content by SEC analysis showed the following results: HM-Fc control, Man5-Fc Control, GlcNAc-Fc Control, Mixture 1, Mixture 2, Mixture 3, Mixture 4, Mixture 5, Mixture 6, Mixture 7 showed ~ 99.0 % monomer purity and N297Q-Fc Control showed 97.9 % monomer purity. The monomer percent values are average calculated from triplicate runs, and the standard deviation ranged from 0.0 to 0.1.

Mixture	Average Monomer Percent
HM-Fc control	99.7±0.0
Man5-Fc Control	99.7±0.1
GlcNAc-Fc Control	99.8±0.1
N297Q-Fc Control	97.8±0.0
Mixture 1	99.7±0.0
Mixture 2	99.6±0.1
Mixture 3	98.9±0.1
Mixture 4	99.6±0.1
Mixture 5	99.6±0.0
Mixture 6	99.4±0.1
Mixture 7	99.3±0.0

Glycoform Structure	Mixture Name	Mixture Components
	HM-Fc Control	100% HM-Fc
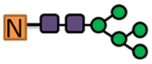	Man5-Fc Control	100% Man5-Fc
	GlcNAc-Fc Control	100% GlcNAc-Fc
	N297Q-Fc Control	100% N297Q-Fc
	Mixture 1	50% HM-Fc+50% Man5-Fc
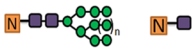	Mixture 2	50% HM-Fc+50% GlcNAc-Fc
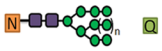	Mixture 3	50% HM-Fc+50% N297Q-Fc
	Mixture 4	90% HM-Fc+10% Man5-Fc
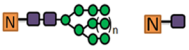	Mixture 5	90% HM-Fc+10% GlcNAc-Fc
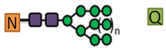	Mixture 6	90% HM-Fc+10% N297Q-Fc
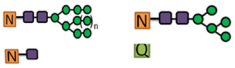	Mixture 7	25%HM-Fc+25%+Man5-Fc+ 25% GlcNAc-Fc+25% N297Q-Fc

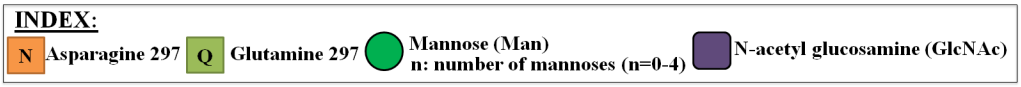

Figure 3.1: Schematic representation of percent of purified IgG1-Fc glycoforms for the preparation of various well-defined IgG1-Fc mixtures and the N-linked Asn-297 glycoform structure in each sample.

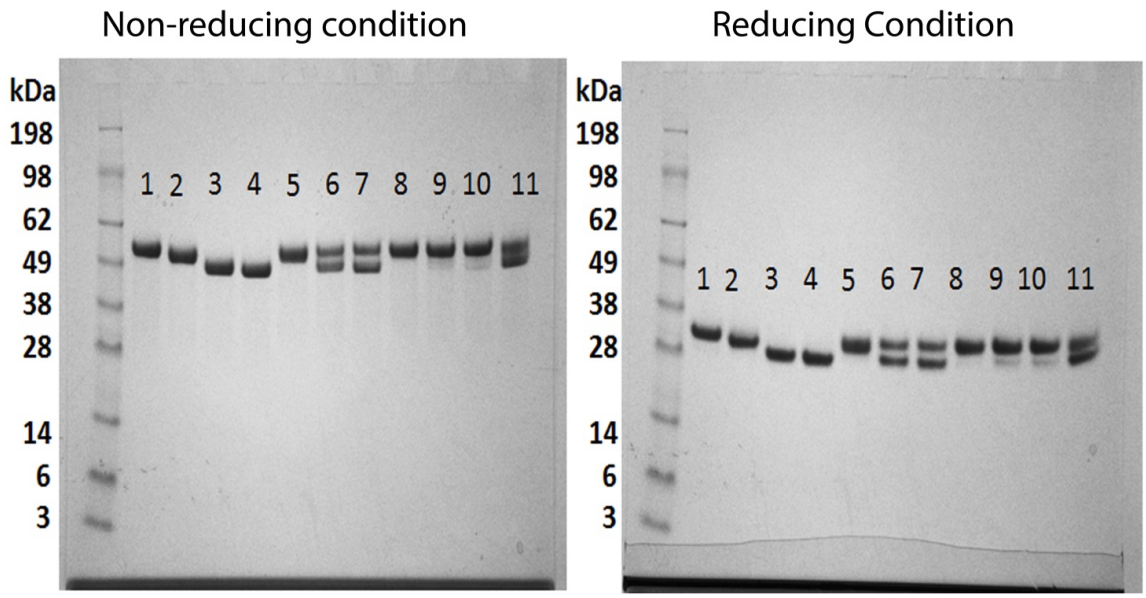

Figure 3.2: SDS-PAGE characterization of mixtures IgG1-Fc glycoforms under non-reduced and reduced conditions. Sample included (See Figure 3.1 for composition of mixtures):

1.HM-Fc Control;

2.Man5-Fc Control;

3.GlcNAc-Fc Control;

4.N297Q-Fc Control;

5.Mixture 1(HM-Fc:Man5-Fc::50:50);

6.Mixture 2(HM-Fc:GlcNAc-Fc::50:50);

7.Mixture 3(HM-Fc:N297Q-Fc::50:50);

8.Mixture 4(HM-Fc:Man5-Fc::90:10);

9.Mixture 5(HM-Fc:GlcNAc-Fc::90:10);

10.Mixture 6(HM-Fc:N297Q-Fc::90:10);

11.Mixture 7(HM-Fc:Man5-Fc:GlcNAc-Fc:N297Q-Fc::25:25:25:25)).

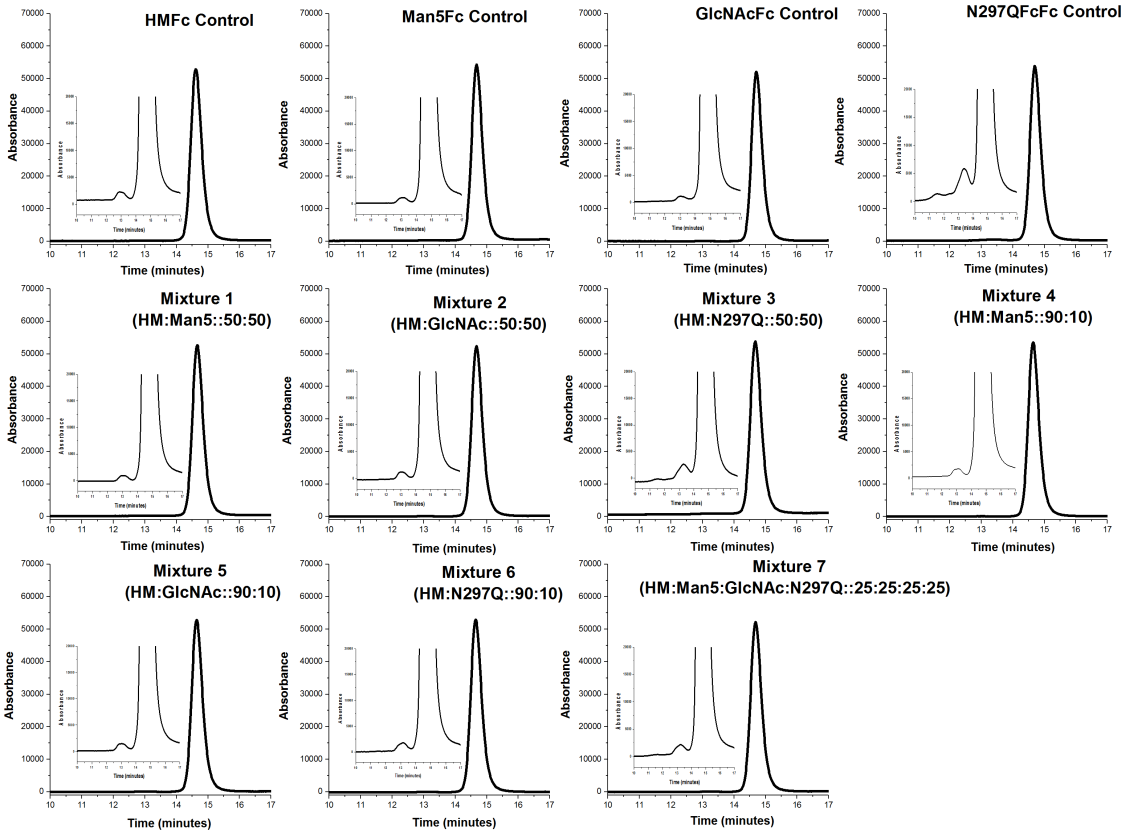

Figure 3.3: Representative size exclusion chromatography (SEC) characterization of mixtures IgG1-Fc glycoforms at 280nm and inset are the zoomed in plots. SEC analysis showed the following results: HM-Fc control, Man5-Fc Control, GlcNAc-Fc Control, Mixture 1, Mixture 2, Mixture 3, Mixture 4, Mixture 5, Mixture 6, Mixture 7 showed ~ 99.0 % monomer purity and N297Q-Fc Control showed 97.9 % monomer purity. The monomer percent values are average calculated from triplicate runs, and the standard deviation ranged from 0.0 to 0.1. See Table 3.1 for summary of percent monomer values. See Figure 3.1 for composition of mixtures.

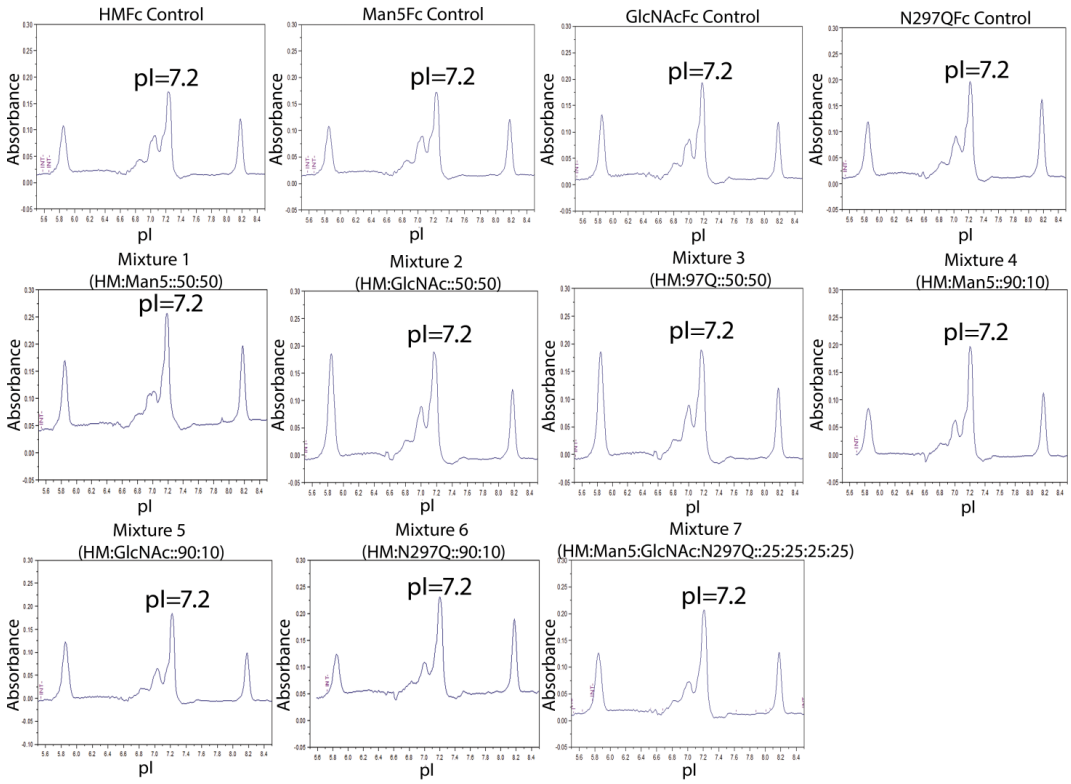

Figure 3.4: Representative characterization of the isoelectric pH (pI) of mixtures IgG1-Fc glycoforms as measured by capillary isoelectric focusing (cIEF). cIEF analysis showed the following results for the major species: All the controls and mixtures show pI of 7.2 in 20 mM citrate phosphate, 150 mM NaCl buffer, at pH 6.0. The pI values are average values calculated from triplicate runs, and the standard deviations are 0.0. See Figure 3.1 for composition of mixtures.

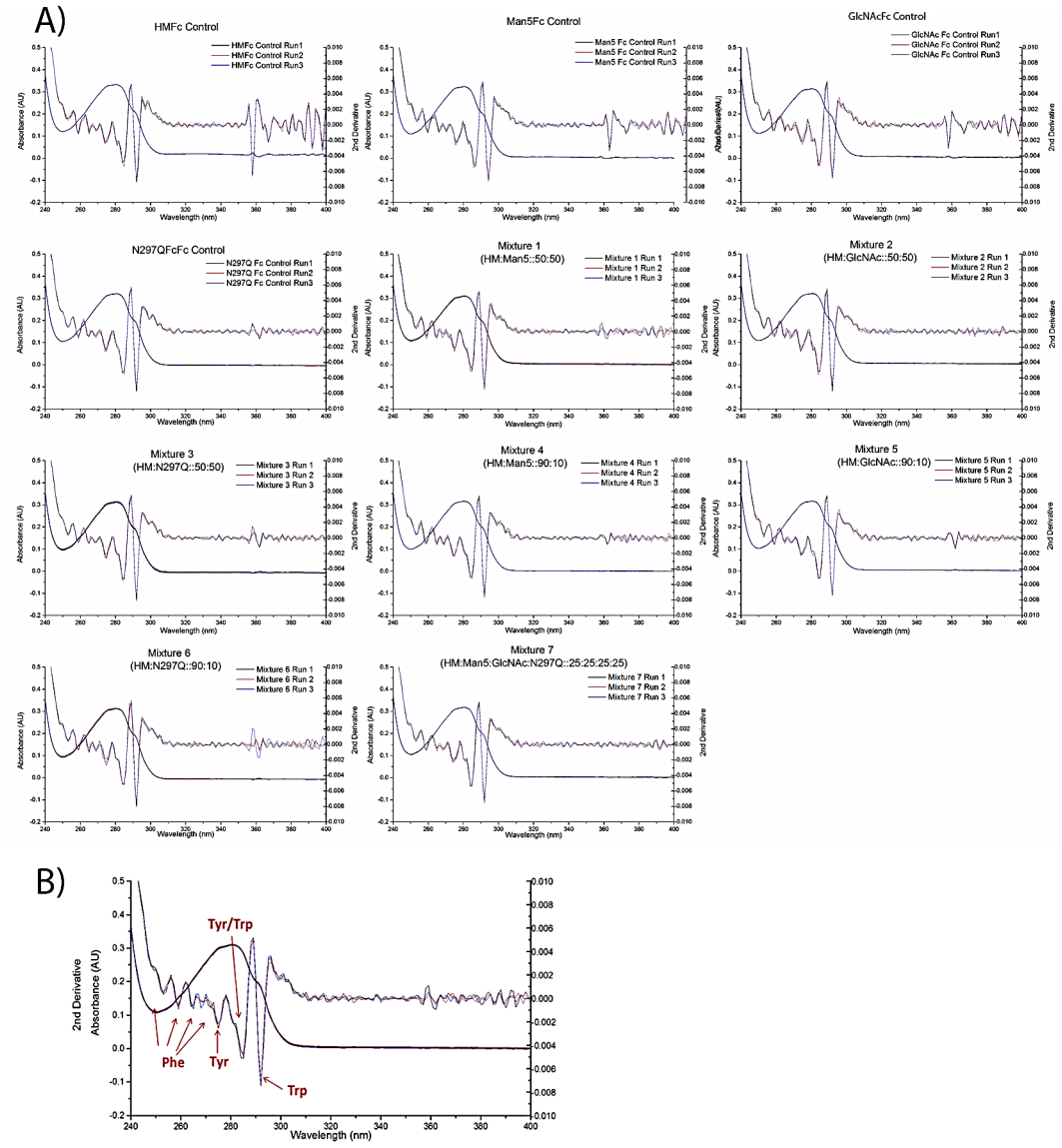

Figure 3.5: Absorbance spectra and Second derivative UV-visible absorption spectra.

A) Absorbance spectra and Second derivative UV-visible absorption spectra of triplicate runs of the four IgG1-Fc glycoform controls and seven mixtures from 240-400nm **B)** A representative 2nd derivative spectra showing ultraviolet absorption peak positions of the following three aromatic amino acids: Phe, Tyr, Trp. See Figure 3.1 for composition of mixtures.

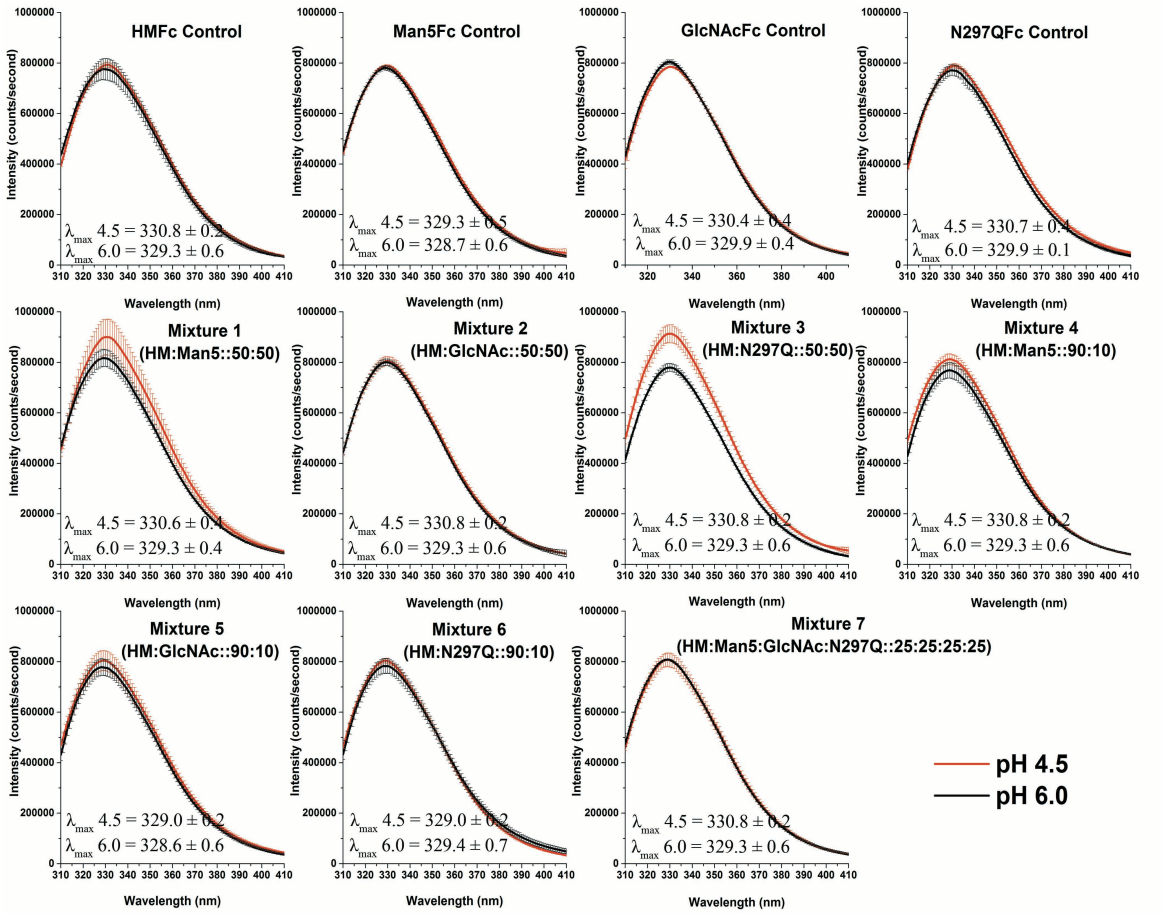

Figure 3.6: Intrinsic (Trp) fluorescence spectra at 10°C of four IgG1-Fc controls (HM-Fc, Man5-Fc, GlcNAc-Fc and N297Q-Fc) and seven mixtures at pH 4.5(red) and pH 6.0 (black). The λ_{max} values are also shown for each protein mixture at 10°C (pH 4.5 and pH 6.0). Each of the samples were run in triplicate with the standard deviation (SD) of λ_{max} values ranging from 0.2 to 0.6 nm. See Figure 3.1 for composition of mixtures.

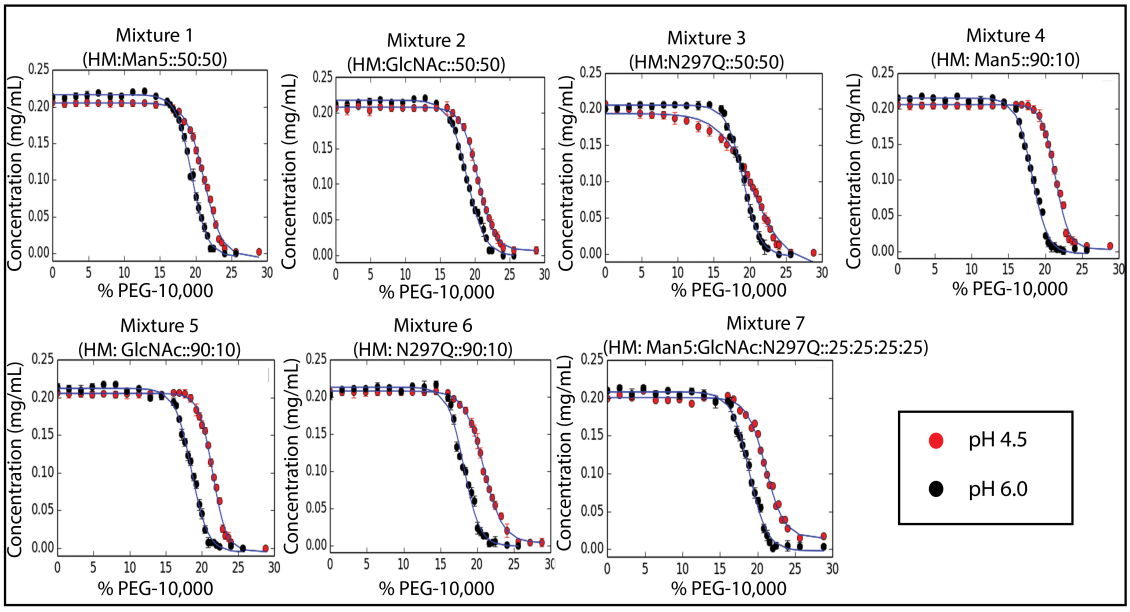

Figure 3.7: Concentration of IgG1-Fc glycoform mixtures versus amount of PEG added to solution at pH 4.5(red) and pH 6.0(black). The error bars denote standard deviation for n = 3 replicates at each % PEG concentration. See Figure 3.1 for composition of mixtures.

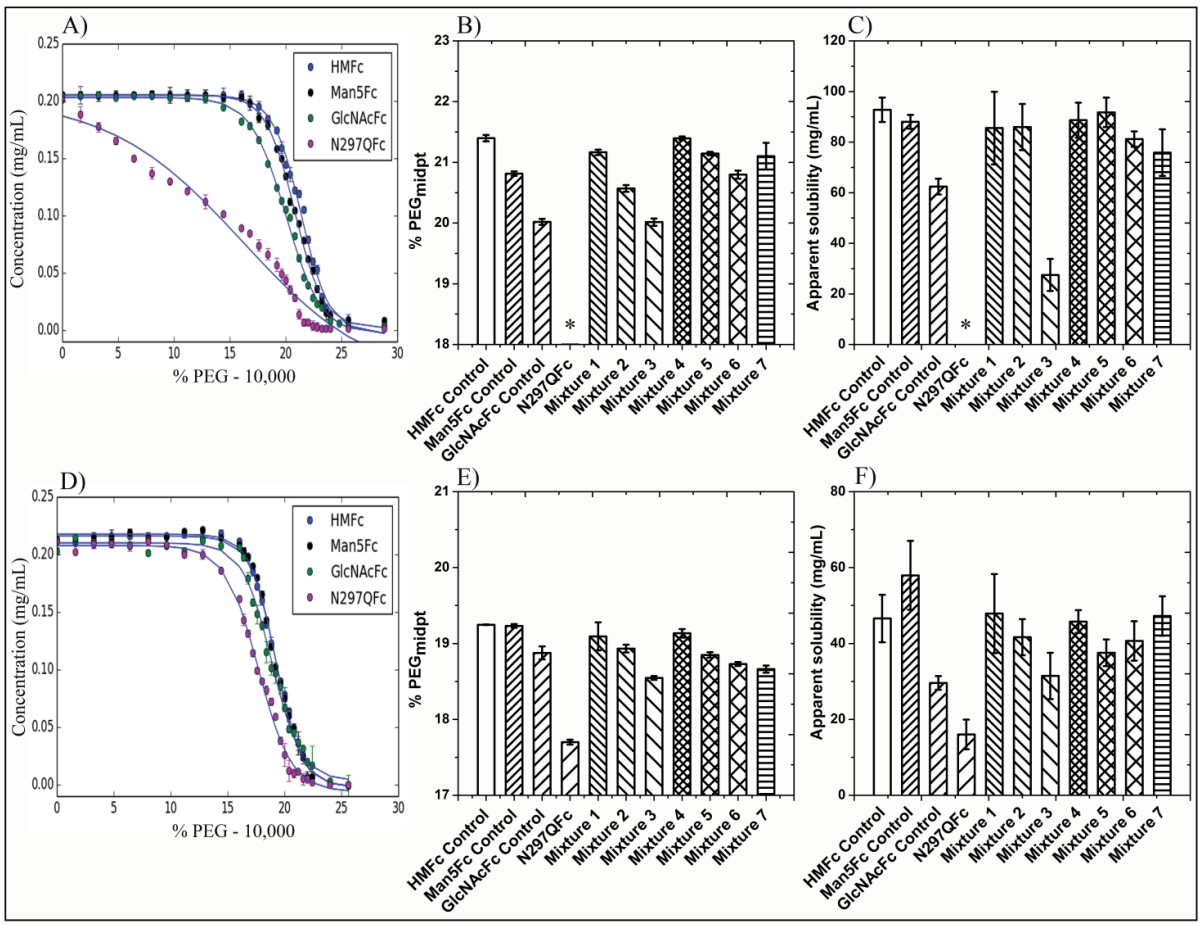

Figure 3.8: Comparison of % PEG midpoint and apparent solubility (thermodynamic activity) parameters of IgG1-Fc glycoform controls and mixtures by PEG precipitation assay at pH 4.5 (A, B, C) and pH 6.0 (D, E, F). A and D show concentration of IgG1-Fc glycoform controls (HM-Fc, Man5-Fc, GlcNAc-Fc and N297Q-Fc) versus amount of PEG added to solution at pH 4.5 and pH 6.0, respectively. B and E show the comparison of PEG midpoint (PEG_{midpt}) values (w/v) at pH 4.5 and pH 6.0, respectively. C and F show the comparison of apparent activity values at pH 4.5 and pH 6.0, respectively. Error bars indicate the standard deviation of three replicates.* No calculated parameters for N297Q-Fc at pH 4.5 were possible due to the non-ideal nature of the %PEG curve. See Figure 3.1 for composition of mixtures.

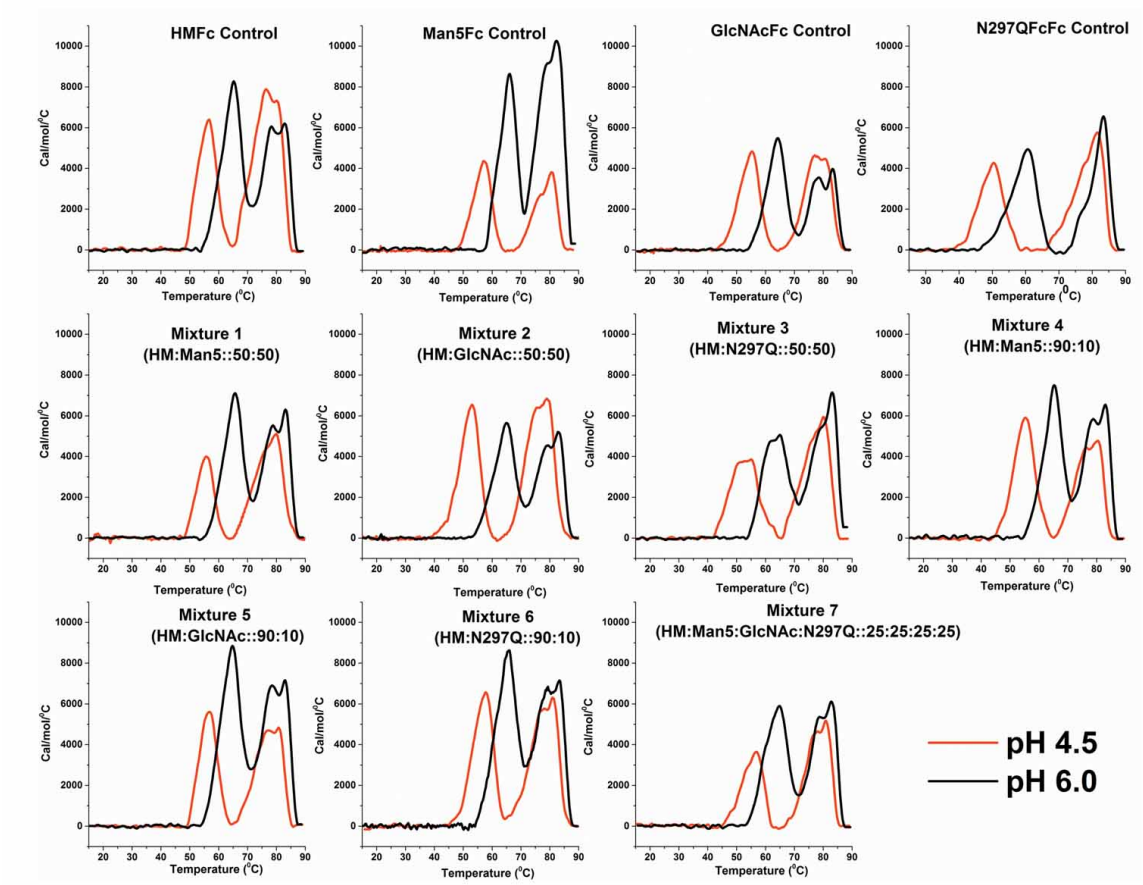

Figure 3.9: Comparison of representative curve-fitted DSC thermograms of IgG1-Fc glycoform controls and mixtures at pH 4.5 (red) and pH 6.0 (black). All samples were at 0.4 mg/mL. See Figure 3.1 for composition of mixtures.

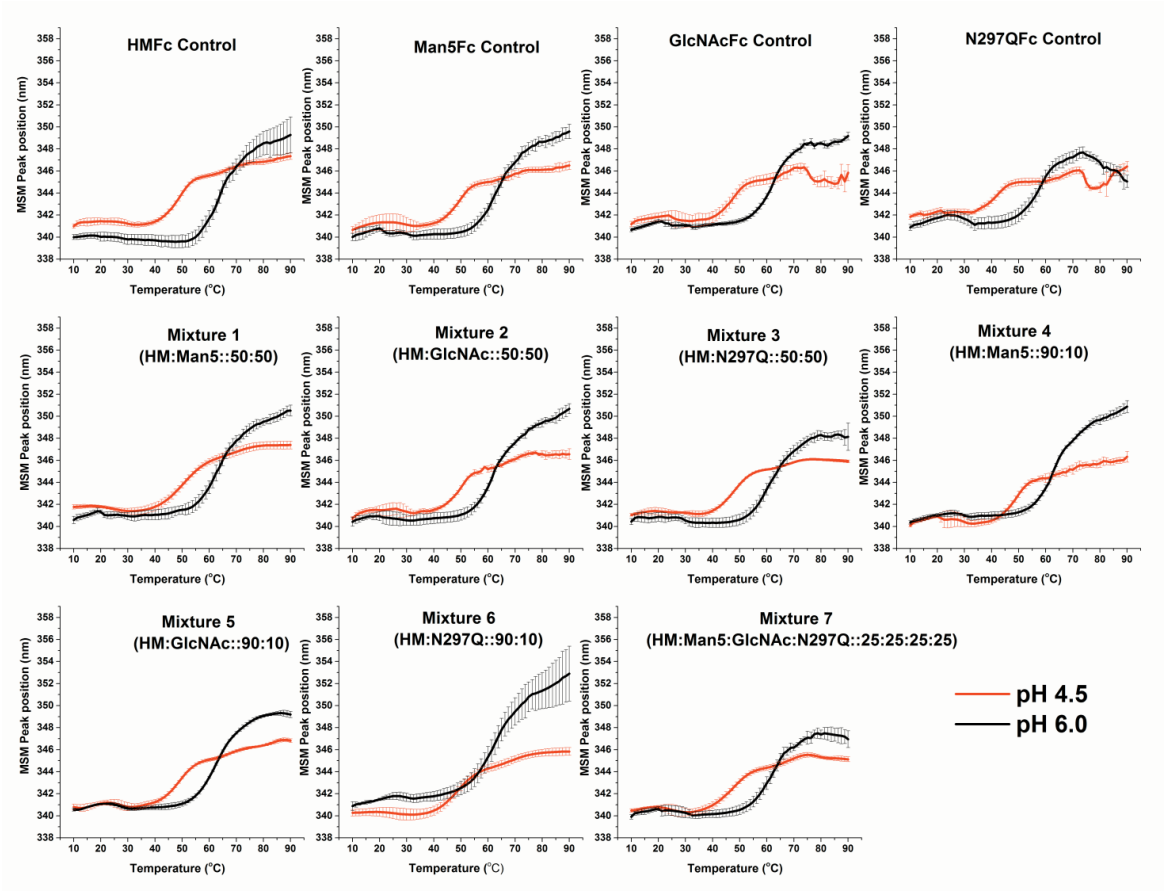

Figure 3.10: Intrinsic fluorescence spectroscopy thermal melting curves of the 4 different glycoform controls of IgG1-Fc and 7 mixtures across the pH 4.5 (red) and pH 6.0 (black). The average peak positions of triplicate measurements are shown and the error bars representing the standard deviations. See Figure 3.1 for composition of mixtures.

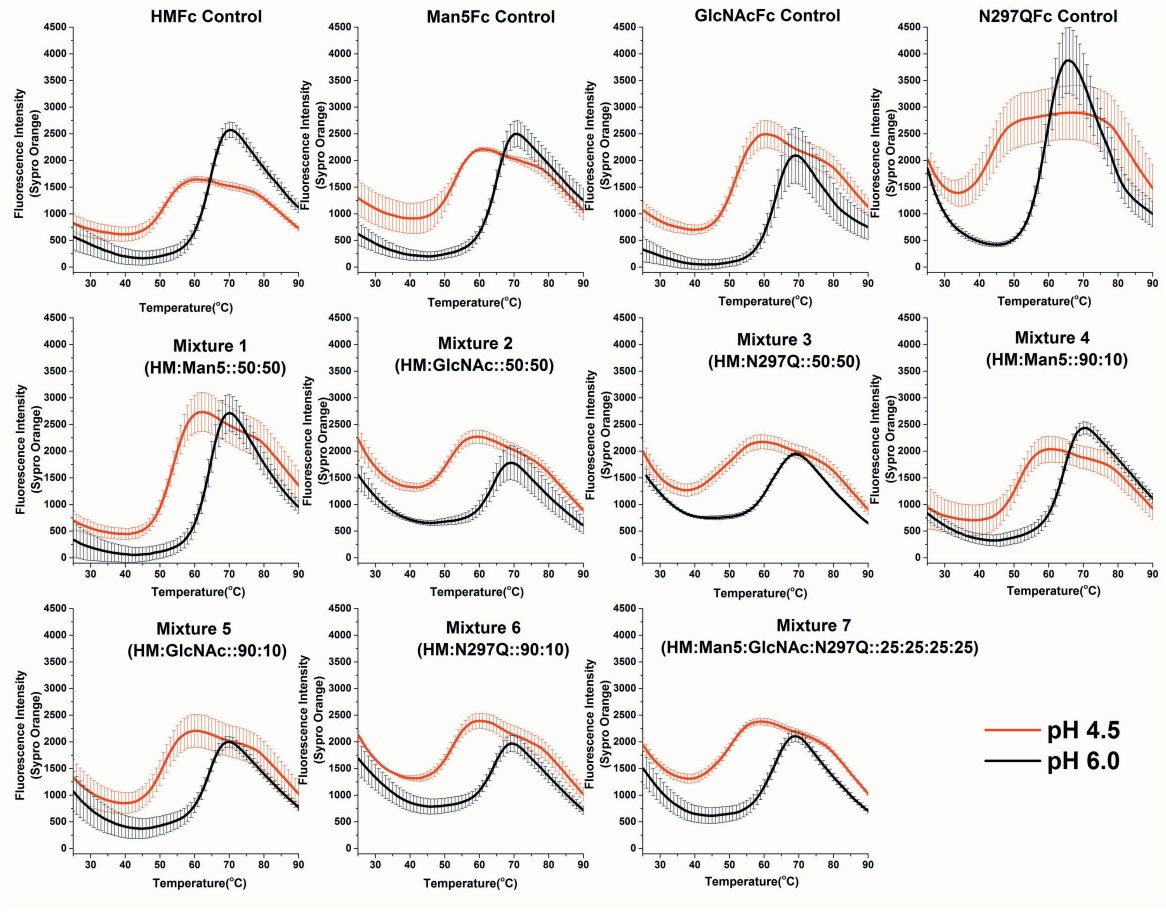

Figure 3.11: Extrinsic Sypro Orange fluorescence thermal melting curves in the presence of IgG1-Fc glycoform controls and mixture samples at pH 4.5 (red) and 6.0 (black). The average peak intensities of triplicate measurements are shown and error bars represent the standard deviations. See Figure 3.1 for composition of mixtures.

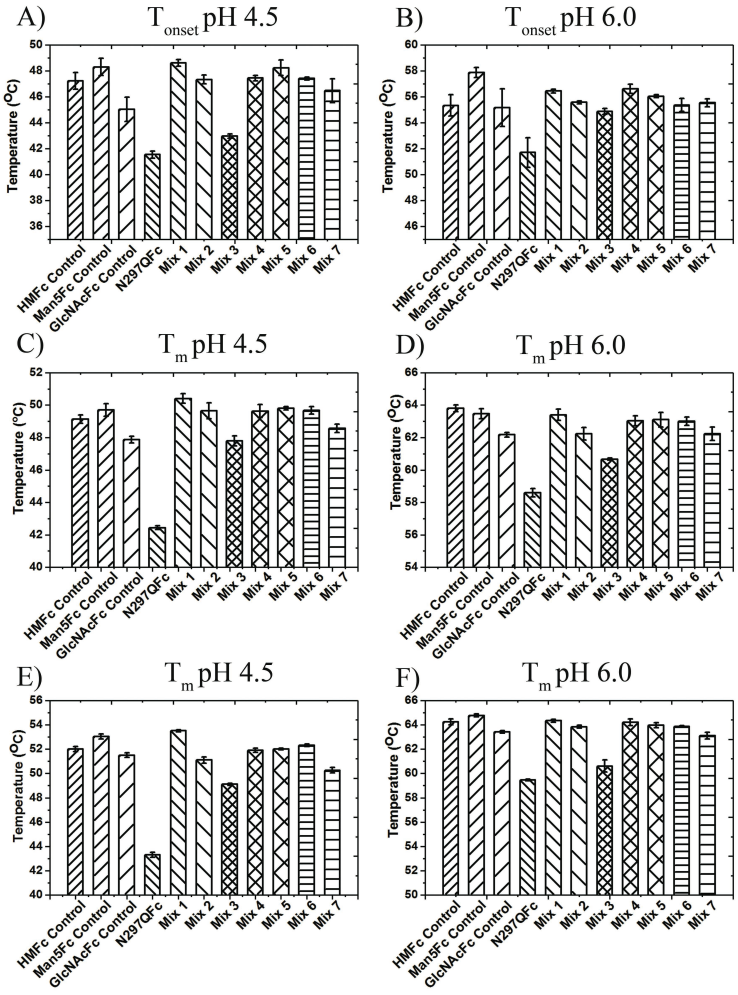

Figure 3.12: Thermal stability by DSC, intrinsic tryptophan fluorescence and extrinsic Sypro Orange fluorescence. A and B show bar chart representation of T_{onset} values of four controls and seven mixtures of IgG1-Fc glycoforms measured by DSC at pH 4.5 and pH 6.0, respectively. C and D show bar chart representation of T_m values of four controls and seven mixtures of IgG1-Fc glycoforms measured by intrinsic fluorescence thermal melting curves at pH 4.5 and pH 6.0, respectively. E and F show bar chart representation of T_m values of four controls and seven mixtures of IgG1-Fc glycoforms measured by extrinsic SYPRO Orange fluorescence thermal melting curves at pH 4.5 and pH 6.0, respectively. The error bars indicate the standard deviations of three replicates and the average T_{onset} and T_m values are shown. See Figure 3.1 for

composition of mixtures.

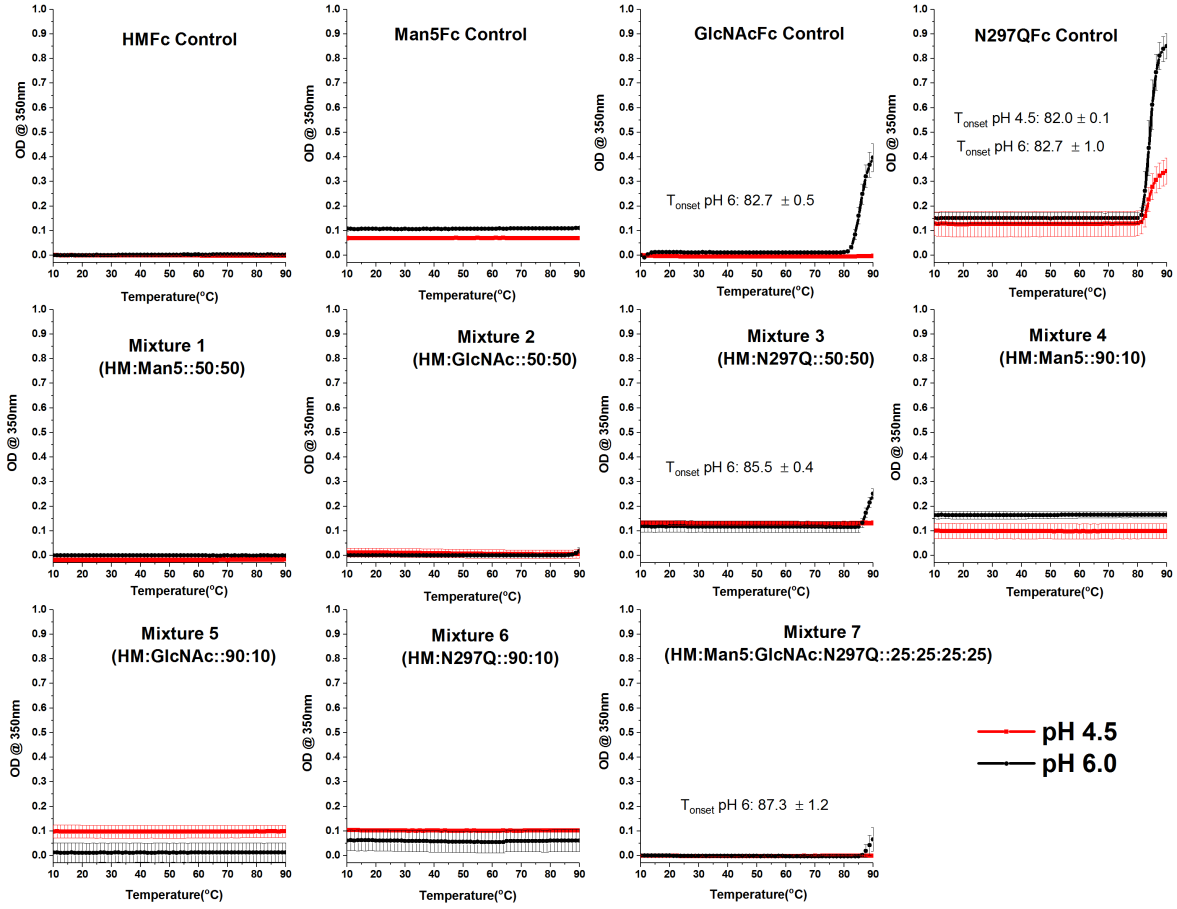

Figure 3.13: Optical density (OD) at 350nm as a function of temperature of the 4 IgG1-Fc glycoform controls (HM-Fc, Man5-Fc, GlcNAc-Fc and N297Q-Fc) and seven mixtures of the controls at pH 4.5 (red) and pH 6.0 (black). The average OD 350 nm values of triplicate measurements are shown with error bars. See Figure 3.1 for composition of mixtures.

3.5 References

1. McCamish M, Woollett G 2011. Worldwide experience with biosimilar development. mAbs 3(2):209-217.

2. Udpa N, Million RP 2016. Monoclonal antibody biosimilars. Nature reviews Drug discovery 15(1):13-14.

3. Grabowski H, Guha R, Salgado M 2014. Biosimilar competition: lessons from Europe. Nature reviews Drug discovery 13(2):99-100.

4. Reusch D, Tejada ML 2015. Fc glycans of therapeutic antibodies as critical quality attributes. Glycobiology 25(12):1325-1334.

5. Houde D, Peng Y, Berkowitz S, Engen J 2010. Post-translational Modifications Differentially Affect IgG1 Conformation and Receptor Binding. Molecular and Cellular Proteomics.

6. Hodoniczky J, Zheng YZ, James DC 2005. Control of Recombinant Monoclonal Antibody Effector Functions by Fc N-Glycan Remodeling in Vitro. Biotechnology progress 21(6):1644-1652.

7. Kanda Y, Yamada T, Mori K, Okazaki A, Inoue M, Kitajima-Miyama K, Kuni-Kamochi R, Nakano R, Yano K, Kakita S, Shitara K, Satoh M 2007. Comparison of biological activity among nonfucosylated therapeutic IgG1 antibodies with three different N-linked Fc oligosaccharides: the high-mannose, hybrid, and complex types. Glycobiology 17(1):104-118.

8. Yu M, Brown D, Reed C, Chung S, Lutman J, Stefanich E, Wong A, Stephan JP, Bayer R 2012. Production, characterization, and pharmacokinetic properties of antibodies with N-linked mannose-5 glycans. mAbs 4(4):475-487.

9. Jefferis R 2009. Glycosylation as a strategy to improve antibody-based therapeutics. Nature reviews Drug discovery 8(3):226-234.

10. Krapp S, Mimura Y, Jefferis R, Huber R, Sondermann P 2003. Structural Analysis of Human IgG-Fc Glycoforms Reveals a Correlation Between Glycosylation and Structural Integrity. Journal of Molecular Biology 325(5):979-989.

11. Zheng K, Yarmarkovich M, Bantog C, Bayer R, Patapoff TW 2014. Influence of glycosylation pattern on the molecular properties of monoclonal antibodies. mAbs 6(3):649-658.

12. Alsenaidy MA, Kim JH, Majumdar R, Weis DD, Joshi SB, Tolbert TJ, Middaugh CR, Volkin DB 2013. High-throughput biophysical analysis and data visualization of conformational stability of an IgG1 monoclonal antibody after deglycosylation. Journal of pharmaceutical sciences 102(11):3942-3956.

13. Majumdar R, Manikwar P, Hickey JM, Samra HS, Sathish HA, Bishop SM, Middaugh CR, Volkin DB, Weis DD 2013. Effects of salts from the Hofmeister series on the conformational stability, aggregation propensity, and local flexibility of an IgG1 monoclonal antibody. Biochemistry 52(19):3376-3389.

14. Houde D, Arndt J, Domeier W, Berkowitz S, Engen JR 2009. Characterization of IgG1 Conformation and Conformational Dynamics by Hydrogen/Deuterium Exchange Mass Spectrometry. Analytical chemistry 81(7):2644-2651.

15. Frank M, Walker RC, Lanzilotta WN, Prestegard JH, Barb AW 2014. Immunoglobulin G1 Fc domain motions: implications for Fc engineering. J Mol Biol 426(8):1799-1811.

16. Barb AW, Prestegard JH 2011. NMR analysis demonstrates immunoglobulin G N-glycans are accessible and dynamic. Nature chemical biology 7(3):147-153.

17. Chow SC, Song F, Bai H 2016. Analytical Similarity Assessment in Biosimilar Studies. The AAPS journal 18(3):670-677.

18. Azevedo V, Hassett B, Fonseca JE, Atsumi T, Coindreau J, Jacobs I, Mahgoub E, O'Brien J, Singh E, Vicik S, Fitzpatrick B 2016. Differentiating biosimilarity and comparability in biotherapeutics. Clinical rheumatology 35(12):2877-2886.

19. 2015. U.S. Food and Drug Administration. Guidance for Industry- Scientific Considerations in Demonstrating Biosimilarity to a Reference Product.

20. Tsong Y, Dong X, Shen M 2017. Development of statistical methods for analytical similarity assessment. Journal of biopharmaceutical statistics 27(2):197-205.

21. Kim JH, Joshi SB, Tolbert TJ, Middaugh CR, Volkin DB, Smalter Hall A 2016. Biosimilarity Assessments of Model IgG1-Fc Glycoforms Using a Machine Learning Approach. Journal of pharmaceutical sciences 105(2):602-612.

22. 2016. U.S. Food and Drug Administration. Guidance for Industry- Clinical Pharmacology Data to Support a Demonstration of Biosimilarity to a Reference Product.

23. More AS, Toprani VM, Okbazghi SZ, Kim JH, Joshi SB, Middaugh CR, Tolbert TJ, Volkin DB 2016. Correlating the Impact of Well-Defined Oligosaccharide Structures on Physical Stability Profiles of IgG1-Fc Glycoforms. Journal of pharmaceutical sciences 105(2):588-601.

24. Okbazghi SZ, More AS, White DR, Duan S, Shah IS, Joshi SB, Middaugh CR, Volkin DB, Tolbert TJ 2016. Production, Characterization, and Biological Evaluation of Well-Defined IgG1 Fc Glycoforms as a Model System for Biosimilarity Analysis. Journal of pharmaceutical sciences 105(2):559-574.

25. Toprani VM, Joshi SB, Kueltzo LA, Schwartz RM, Middaugh CR, Volkin DB 2016. A Micro-Polyethylene Glycol Precipitation Assay as a Relative Solubility Screening Tool for Monoclonal Antibody Design and Formulation Development. Journal of pharmaceutical sciences 105(8):2319-2327.

26. Ghirlando R, Lund J, Goodall M, Jefferis R 1999. Glycosylation of human IgG-Fc: influences on structure revealed by differential scanning micro-calorimetry. Immunology Letters 68(1):47-52.

27. Federici M, Lubiniecki A, Manikwar P, Volkin DB 2013. Analytical lessons learned from selected therapeutic protein drug comparability studies. Biologicals : journal of the International Association of Biological Standardization 41(3):131-147.

28. Berkowitz SA, Engen JR, Mazzeo JR, Jones GB 2012. Analytical tools for characterizing biopharmaceuticals and the implications for biosimilars. Nature reviews Drug discovery 11(7):527-540.

29. Reusch D, Haberger M, Falck D, Peter B, Maier B, Gassner J, Hook M, Wagner K, Bonnington L, Bulau P, Wuhrer M 2015. Comparison of methods for the analysis of therapeutic immunoglobulin G Fc-glycosylation profiles-Part 2: Mass spectrometric methods. mAbs 7(4):732-742.

30. Xie H, Chakraborty A, Ahn J, Yu YQ, Dakshinamoorthy DP, Gilar M, Chen W, Skilton SJ, Mazzeo JR 2010. Rapid comparison of a candidate biosimilar to an innovator monoclonal antibody with advanced liquid chromatography and mass spectrometry technologies. mAbs 2(4):379-394.

31. Alsenaidy M, Jain NK, Kim J, Middaugh C, Volkin D 2014. Protein comparability assessments and potential applicability of high throughput biophysical methods and data visualization tools to compare physical stability profiles. Frontiers in Pharmacology 5(39).

32. Haurum JS 2006. Recombinant polyclonal antibodies: the next generation of antibody therapeutics? Drug Discov Today 11(13-14):655-660.

33. Thompson NJ, Hendriks LJA, de Kruif J, Throsby M, Heck AJR 2014. Complex mixtures of antibodies generated from a single production qualitatively and quantitatively evaluated by native Orbitrap mass spectrometry. mAbs 6(1):197-203.

Chapter 4 Correlating the Impact of Glycosylation on the Backbone Flexibility of Well-Defined IgG1-Fc Glycoforms Using Hydrogen Exchange-Mass Spectrometry (HX-MS)

4.1 Introduction

Glycosylation is a widespread and complex post-translational modification occurring naturally in human proteins as well as in therapeutic proteins that introduces structural heterogeneity.[1-4] Development and regulatory approvals of glycosylated monoclonal antibodies (mAbs) as well as Fc-fusion proteins, antibody–drug conjugates (ADCs) and antibody fragments have increased dramatically over the past three decades.[5,6] The IgG1 subclass of antibodies, which are the most abundant form found in human serum as well as the most popular subclass for approved mAb therapeutics, show N-linked-glycosylation (glycan attached to the amide group of asparagine) at Asn-297[7-10] located in a conserved amino acid sequence of Asn-X-Ser/Thr (X: any AA except Pro) in the constant heavy chain of the Fc region.[11] The Fc sequence is highly conserved in subclasses of IgG (except a few amino acid residues)[10] and the heterogeneous N-glycan structures are known to modulate different effector functions of IgG antibodies like antibody-dependent cellular cytotoxicity (ADCC) and complement dependent cytotoxicity (CDC) as well as antibody clearance by affecting FcɣR, C1q and FcRn (observed recently) binding, respectively.[10,12,13] Naturally occurring N-glycans of IgG1 antibody in the human serum are complex, biantennary (consists two arms: one α-1, 3 arm and one α-1, 6 arm) type containing a common seven glycan core (4 N-acetyl glucosamine (GlcNAc), and 3 mannose (Man)).[14,15] Glycan heterogeneity in antibodies exists depending upon the site occupancy (symmetric or asymmetric) and type of glycans attached to the common core which governs the binding to various receptors affecting the antibody biological functions.[16-18] For example, presence of terminal and bisecting GlcNAc and absence of Fuc(fucose) increased ADCC by increasing receptor affinity, increasing terminal sialylation reduced ADCC, and presence of Gal(galactosylation) promoted CDC by increasing interaction with C1q. [19-21] Hence, it an active

area of research to better understand mechanisms underlying these glycosylation effects so that antibodies can be engineered to improve and obtain the desired therapeutic effects.[16,19,22-24]

Therapeutic efficacy of IgG mAbs depends on their structural integrity and conformational stability, local flexibility and biological functionality.[24-27] N-glycosylation at Asn-297 of C_H2 domain is important for the structural integrity, flexibility, physicochemical stability, aggregation stability and PK/PD properties of therapeutic mAbs.[19,28-31] Hence, it is necessary to closely monitor the molecular heterogeneities like glycosylation and evaluate their consequences on product quality, stability, and efficacy during development of mAbs products and their corresponding biosimilar candidates.[24,32-36] Recombinant therapeutic mAbs that require N-glycosylation are produced in mammalian expression hosts (like CHO, SP20 and NSO cells) that have the ability to produce human like glycosylation patterns.[37,38] Additionally, attempts have been made to achieve a high degree of control over glycan heterogeneity and achieving glycan reproducibility by ensuring tight controls of the manufacturing protocols.[39] However, heterogeneity still exists in mAbs produced in these expression systems that could affect the product quality, for example, mAbs having unnatural glycans such as the presence of N-glycolylneuraminic acid (NGNA) when expressed by mouse cell lines (instead of N-acetylneuraminic acid, NANA), or presence of small amounts (ranging from 1%-20%) of high-mannose (Man5-Man9) type of glycans.[39-42] For example, high mannose (HM) glycoforms of IgG showed reduced serum half-life by binding to mannose receptor, increased ADCC and reduced CDC activities as compared with complex fucosylated or hybrid glycan antibodies.[19,43] Hence, monitoring glycan content and heterogeneity is a critical product quality attribute during therapeutic mAb production, when manufacturing changes (comparability) are made or during biosimilar development,[44] since monitoring glycosylation effects on stability and biological

activity of monoclonal antibodies will help to obtain the desired therapeutic outcome.[19,45,46] Ensuring protein stability within a pharmaceutical dosage form, from manufacturing through patient administration, is a critical aspect of therapeutic protein development, where physicochemical degradation may lead to loss of potency, aggregation and immunogenicity.[24,26,47] To improve long-term stability of glycoproteins during pharmaceutical development, various glycoengineering strategies have become popular due to stability increasing effects of glycans on proteins.[48,49] Also, monitoring the impact of glycosylation on stability is critical during comparability and biosimilar development due to heterogeneous nature of glycosylation and their subtle effects on the physicochemical structure.[24,50-52] Hence, it is important to understand how glycosylation affects protein stability of antibodies, and in addition, the inter-relationships between stability versus the desired biological activity need to be established.

To this end, we generated a series of well defined, near homogenous IgG1-Fc glycoforms with serially truncated glycan residues and analyzed them using the physical, chemical and receptor binding assays as described previously (resulting in a series of four manuscripts which appeared in the February 2016 issue of Journal of Pharmaceutical Sciences).[28,29,31,53] For example, results showed that different IgG1-Fc glycans not only affect chemical degradation differently (especially deamidation of Asn-315 and transformation of Trp-277 into glycine hydroperoxide), but also can lead to different impurity profiles.[29] Also, correlations of physical stability with the size of glycans between HM, Man5, GlcNAc and N297Q IgG1-Fc glycoforms was observed, where HM and Man5-Fcs had higher physical stabilities, apparent solubility values and stronger receptor binding than the GlcNAc and non-glycosylated N297Q-Fc as measured by various biophysical techniques, PEG solubility assay and FcγRIIIA binding assays,

respectively.[28,31] These results showed a correlation of decreased length of glycan with decreased physical stability and binding. These large biophysical data sets of these samples generated at various pH and temperature conditions were further utilized to develop an integrated mathematical model for biosimilarity analysis.[53]

In this chapter, we measure the local flexibility of four well-defined glycoproteins by pepsin digestion followed by hydrogen deuterium exchange mass spectrometry (HX-MS). HX-MS provides information on in higher order structure (HOS) by monitoring the protein's backbone amide hydrogen exchange, which is an indicator of solvent exposure and hydrogen bonding in the protein. Peptic peptides are analyzed by LC-MS to assess the deuteration level of each peptide, so that localized differences in higher order structure is obtained at peptide level. HX-MS has been used extensively to investigate subtle higher order structural changes and dynamics in mAbs as a consequence of aggregation, reversible self-association, oxidation, excipients and mutation.[25,54-61] However, only a few extensive HX studies have been carried to study the effects of glycosylation on flexibility in different IgG1 and IgG2 antibodies, and correlating the impact of a certain glycan to flexibility differences in the Fc were often limited by glycan heterogeneities present in the sample, not considering the effects of exchangeable hydrogens in glycans and the possibility of glycan effects on the intrinsic kinetics of HX.[32,54,55,62] In this work, we correlate the local structural flexibility alterations, especially in the C_H2 domain, with IgG1-Fc glycoform's overall conformational stability, chemical stability and receptor binding profiles a previously reported in our laboratories. [28,29,31,53]

4.2 Materials and Methods

4.2.1 Materials

4.2.1.1 Preparation and initial characterization of IgG1-Fc glycoforms

The IgG1-Fc glycoforms (high-mannose-Fc (HM-Fc), Man5-Fc, GlcNAc-Fc and N297Q-Fc) were prepared by expression of HM-Fc in glycosylation-deficient strain of *Pichia pastoris* followed by *in-vitro* enzymatic digestion of HM-Fc by α-1, 2-mannosidase and endoglycosidase H (Endo H) to obtain the truncated Man5-Fc and GlcNAc-Fc, respectively as discussed in previous work.[31] For the N297Q non-glycosylated IgG1-Fc, mutagenesis was used to remove the N-linked glycosylation site as described before.[31] The proteins showed high purity, and no significant proteolysis products, high molecular weight species (HMWS) and charge heterogeneities were present after purification and enzyme truncation as described previously.[31] The HM-Fc was heterogeneous, with N-glycans containing 8 to 12 mannose residues (Man8-Man12) at each N297 site, with the major glycan being the $Man_8GlcNAc_2$ form as characterized previously.[31] The truncated Man5-Fc, GlcNAc-Fc glycoforms and the non-glycosylated N297Q-Fc were well-defined and highly homogenous.[31] With decreasing glycan size, the HM, Man5, and GlcNAc glycoforms IgG1-Fc form a well-defined series of model glycoproteins. The non-glycosylated N297Q-Fc mutant was used as a negative control in these studies.

4.2.1.2 Sample preparation for hydrogen exchange mass spectrometry (HX-MS)

For hydrogen exchange mass spectrometry studies, all four Fc glycoforms were dialyzed at 4°C in a 20 mM citrate phosphate buffer with ionic strength adjusted to 0.15 by NaCl at pH 6.0. Dialysis was performed at 4°C and subsequently, the proteins were concentrated as described elsewhere.[28] The final adjusted protein stock concentration of 1 mg/mL was determined by absorbance at 280 nm as measured by an Agilent 8453 UV–visible spectrophotometer (Palo Alto, California). Components of all buffers including, sodium

phosphate and sodium chloride were purchased from Sigma-Aldrich (St Louis, MO) while citric acid anhydrous and citric acid monohydrate were purchased from Fisher Scientific all at the highest purity grade. Liquid chromatography grade acetic acid and phosphoric acid, tris (2-carboxyethyl) phosphine hydrochloride (TCEP), porcine pepsin, guanidine hydrochloride, and deuterium oxide (99+%D) were purchased from Fluka/Sigma–Aldrich (St. Louis, Missouri). Liquid chromatography–mass spectrometry (LC–MS)-grade formic acid (+99%) was purchased from Thermo Scientific (Rockford, Illinois). LC-MS-grade water, acetonitrile, and isopropanol were purchased from Fisher Scientific (Fair Lawn, New Jersey).

4.2.1.3 Deuterated labelling buffer preparation

Deuterium-based labelling buffer contained 0.15 M sodium chloride, and 20 mM citrate-phosphate at pH 6.0 in 99.9 atom % D_2O. The pH of the buffer was then measured and adjusted by adding 0.4 units to the pH meter reading which takes into account the correction for the deuterium isotope effect when measuring pD with a pH meter.[63] The same batch of buffer was used for HX experiments for all the four IgG1-Fc glycoforms to avoid any variation in the buffer properties.

4.2.2 Methods

4.2.2.1 *Homology model*

The The X-ray structure of the Fc from Thr108-Lys330 (PDB ID: 1HZH)[64] was used as the template for the Fc homology models. The sequence identity was 100%, except for N297Q-Fc which had N297 substituted by Q.

4.2.2.2 *HX-MS*

Hydrogen Hydrogen exchange was performed using an H/DX PAL robot (LEAP Technologies, Carrboro, North Carolina) and MS measurements were conducted using a QTOF mass spectrometer (Agilent 6530, Santa Clara, California) with Agilent 1260 Infinity LC System. For HX, deuterium labelling of Fc glycoproteins was performed in triplicates as published previously. Exchange reactions were quenched after incubation for 5 labeling times: 15 s, 10^2 s, 10^3 s, 10^4 s and 86400 s and the quenched samples were digested by an immobilized pepsin column, prepared in-house as published before.[65] As previously described elsewhere, a standard LC-MS procedure for HX-MS[66,67] was used and the carry-over from the pepsin column between samples was removed using a two-wash cocktail method.[68] All HX-MS measurements were made relative to HM-Fc, so this form was run in parallel in the same day with each of the three glycoforms (Man5-Fc, GlcNAc-Fc and N297Q-Fc) to control for day-to-day variability.

4.2.2.3 *Peptide mapping and glycopeptide identification*

Prior to HX-MS analysis, combination of accurate mass measurements and collision induced dissociation (CID) with tandem MS was used to identify a total of 51 peptides listed in Supplementary Table 4.1. Identified peptides covered 100% of the primary sequence of the heavy chain of the IgG1-Fc glycoforms. Different fragmentation strategies were utilized by using different collision energies for fragmentation of the glycopeptides to be able to confidently confirm their identities. A preferred list of glycopeptides which had very low MS/MS scores and no MS/MS data was made and the glycopeptides in the list were then subjected to fragmentation by modifying the collision energy. The following collision energy equation by Agilent was used to optimize the collision energy for fragmentation by changing the offset values.

$$\text{Collision Energy} = \frac{\text{Slope} \times {}^{\text{m}}/_{\text{z}}}{100} + \text{Offset}$$

Glycopeptides tend to undergo glycan fragmentation during collision induced dissociation (CID) and hence the energy of fragmentation needs to be optimized so that ideally, the glycans undergo minimal fragmentation without hindering the peptide backbone (amide bond) fragmentation. It is not possible to prevent glycan fragmentation in CID and thus oxoniuim ions that are characteristic ions of their respective glycopeptides were utilized to confirm the identity of each glycopeptides for the four IgG1-Fc glycoforms.[69,70]

4.2.2.4 *Deuteration controls*

Deuterium recovery was estimated separately using highly deuterated peptides. The deuteration controls of each peptide belonging to each glycoform (HM-Fc, Man5-Fc, GlcNAc-Fc and N297Q-Fc) were prepared separately by first collecting peptic peptides following pepsin column digestion. The peptides were subsequently dried on a vacuum concentrator and reconstituted in H_2O buffer, at pH 6.0. Afterwards, the peptides were deuterium labeled for 4 hr and analyzed like standard samples. Based on the deuteration controls, the deuterium recovery ranged between 30.74% and 80.84%. The deuterium contents in 3 glycopeptide (17, 18, and 19) controls of all the 4 IgG1-Fc glycoforms are provided in the Supplementary Table 4.2.

4.2.2.5 *HX-MS data analysis*

Initial peptide LC-MS feature extraction and centroid calculations were carried out using HDExaminer (Sierra Analytics, Modesto, CA). All MS results were individually inspected to insure reliability. Retention time window adjustments were manually applied as needed. Additional numerical and statistical analysis was carried out in Excel (Microsoft, Redmond, WA). The extent of HX was quantified on a percentage basis after back-exchange correction:

$$\%D_t = \frac{\bar{m}_t - m_0}{\bar{m}_\infty - m_0} \times 100\% \qquad (1)$$

where m denotes peptide centroid mass and t is the HX time. $\bar{m}_t$ is the mean of the centroid value from triplicate measurements, m_0 is the theoretical centroid mass of the undeuterated peptide, and $\bar{m}_\infty$ is mean of the centroids obtained from the deuteration control.

Differential exchange, $\Delta\mathrm{HX}_t$ values at each HX time, representing the difference in HX for each peptide of IgG1-Fc glycoform (subscript g) relative to the same peptide in the HM-Fc (subscript HM-Fc) is given by:

$$\Delta\mathrm{HX}_t = \%D_{\mathrm{g,t}} - \%D_{\mathrm{HM},t} \qquad (2)$$

For mapping HX effects onto an Fc homology model, HX data from all time points for each peptide were averaged into a single value, $\Delta\overline{\mathrm{HX}}$, representing the average difference in HX between Man5-Fc, GlcNAc-Fc and N297Q-Fc relative to HM-Fc:

$$\Delta\overline{\mathrm{HX}} = \frac{\sum_{i=1}^{n} \%D_{\mathrm{g},t_i} - \%D_{\mathrm{HM},t_i}}{n} \qquad (3)$$

where the index i covers the range of discrete HX times t_i. For overlapping peptides covering the same residues, statistically significant differences, defined subsequently, took precedence over insignificant results. There were no cases of significant differences of opposite sign, i.e., no cases where both significantly faster and slower exchange were observed in overlapping peptides.

Standard error was propagated assuming random, uncorrelated error based on conventional error analysis methods applied to equations (1), (2) and (3). Standard error, denoted here as ε, in

individual technical replicates was estimated based on the sample standard deviation of *n* repeated measurements:

$$\varepsilon = \frac{s}{\sqrt{n}} \qquad (4)$$

where *s* denotes the sample standard deviation i.e., $\sqrt{\sum (x-\bar{x})^2 / (n-1)}$. Significant differences were identified using the criterion that the measured differential exchange was three-fold greater than the propagated standard error (i.e., $|\Delta\overline{\mathrm{HX}}| > 3\varepsilon$). More specifically, the propagated standard errors in $\Delta\overline{\mathrm{HX}}_t$ and $\Delta\overline{\mathrm{HX}}$ of all peptides except glycopeptides are:

$$\varepsilon_{\Delta HX_t} = \frac{1}{(\bar{m}_\infty - m_0)} \sqrt{\varepsilon^2_{\bar{m}_{t,g}} + \varepsilon^2_{\bar{m}_{t,HM}} + \left(\frac{\bar{m}_{t,g} - \bar{m}_{t,HM}}{\bar{m}_\infty - m_0} \times \varepsilon_{\bar{m}_\infty} \right)^2} \times 100 \qquad (5)$$

$$\varepsilon_{\Delta \overline{HX}} = \frac{1}{n\left(\bar{m}_\infty - m_0\right)} \sqrt{\varepsilon^2_{\bar{m}_g} + \varepsilon^2_{\bar{m}_{HM}} + \left(\frac{\bar{m}_g - \bar{m}_{HM}}{n\left(\bar{m}_\infty - m_0\right)} \times \varepsilon_{\bar{m}_\infty} \right)^2} \times 100 \qquad (6)$$

The propagated standard errors in $\Delta\mathrm{HX}$ and $\Delta\overline{\mathrm{HX}}$ of glycopeptides are:

$$\varepsilon_{\Delta HX_t} = \sqrt{\left(\frac{\varepsilon_{\bar{m}_{t,g}}}{\bar{m}_{\infty,g} - m_0} \right)^2 + \left(\frac{\varepsilon_{\bar{m}_{t,HM}}}{\bar{m}_{\infty,HM} - m_0} \right)^2 + \left(\frac{\bar{m}_{t,g}}{\left(\bar{m}_{\infty,g} - m_0\right)^2} \times \varepsilon_{\bar{m}_{\infty,g}} \right)^2 + \left(\frac{\bar{m}_{t,HM}}{\left(\bar{m}_{\infty,HM} - m_0\right)^2} \times \varepsilon_{\bar{m}_{\infty,HM}} \right)^2} \times 100 \qquad (7)$$

$$\varepsilon_{\Delta \overline{HX}} = \frac{1}{n} \sqrt{\left(\frac{\varepsilon_{\bar{m}_g}}{\bar{m}_{\infty,g} - m_0} \right)^2 + \left(\frac{\varepsilon_{\bar{m}_{HM}}}{\bar{m}_{\infty,HM} - m_0} \right)^2 + \left(\frac{\bar{m}_g}{\left(\bar{m}_{\infty,g} - m_0\right)^2} \times \varepsilon_{\bar{m}_{\infty,g}} \right)^2 + \left(\frac{\bar{m}_{HM}}{\left(\bar{m}_{\infty,HM} - m_0\right)^2} \times \varepsilon_{\bar{m}_{\infty,HM}} \right)^2} \times 100 \qquad (8)$$

Where $\bar{m}_\infty$ is mean of the centroids obtained from the deuteration control for each glycopeptide of each IgG1-Fc glycoform (subscript g) and the HM-Fc (subscript HM-Fc).

4.3 Results

4.3.1 Proximal effects of N-glycosylation on the Fc backbone flexibility

The backbone flexibility of IgG1-Fc as a function of N-linked glycosylation was analyzed by incubating four Fc constructs with well-defined glycosylation: High Mannose (HM), Man5, GlcNAc and N297Q in D_2O buffer containing 20 mM citrate-phosphate buffer and 0.15 M NaCl (pH 6.0) for varying periods of time. The labeled samples were subsequently quenched, digested, and analyzed by LC-MS. A total of 51 IgG1-Fc peptides were reproducibly generated by pepsin digestion, resulting in sequence coverage of 100% for the constant heavy chain of IgG1-Fc of the four glycoforms. For convenience, the peptides are indexed sequentially from the N-terminus (peptide 1) to C-terminus (peptide 51) as listed in Supplemental Table 4.1. Figure 4.1 shows the progression of HX, a readout of the Fc backbone flexibility, in three peptic peptides 17, 18 and 19 that span heavy chain (HC) residues 278-299, 278-300 and 282-300 respectively, and include the C'E loop and glycosylation site. As seen in Figure 4.1, the rate of hydrogen exchange in these three glycopeptides showed an inverse trend of faster HX with decreasing glycan size: HX was fastest in non-glycosylated N297Q-Fc, intermediate in GlcNAc-Fc, and slowest in Man5-Fc and Man8-Fc (HM-Fc). The Man5 form exchanged faster than Man8 in glycopeptides 17 and 18, but similar exchange was observed between these forms in glycopeptide 19. Although there are interesting trends in the glycopeptide data in Figure 4.1, several factors make more direct and quantitative comparisons of HX rates between these three glycopeptides problematic (see Discussion section).

The HX kinetics for three glycopeptide segments of the individual high mannose forms (Man8-Man12) are shown in Figure 4.2. The high mannose glycopeptides 17 and 18 cover residues 278-299 and 278-300 similar to results shown for other glycoforms in Figure 4.1, however an additional glycopeptide covering residues 278-306 was identified in the high mannose glycoforms. Peptide 19 (HC residues 282-300) was not observed in the digestion of the

high mannose Fc suggesting that differences in glycosylation might alter pepsin digestion specificity. There are subtle, but statistically significant, differences in hydrogen exchange kinetics observed in glycopeptide 17. In general, the Man8 form exchanges more slowly than the Man5 (as seen in Figure 4.1) and Man9-Man12 glycoforms (as seen in Figure 4.2). The HX rate trends in Man5 and HM glycopeptides 18, 19 and 278-306 (as seen in Figures 4.1 and 4.2) are similar to peptide 17, but more subtle. The above results indicate that the degree of change in HX depended on the degree of glycan size, suggesting that backbone flexibility near the glycosylation site is minimized by glycans of intermediate length. This result suggests that higher mannose forms might promote greater flexibility in the backbone in regions proximal to the glycosylation site, but such conclusions based on these trends should be viewed as tentative, given the many limitations in the more direct and quantitative analysis of the HX results on the glycopeptides (see Discussion section).

4.3.2 Glycosylation has distal effects on Fc Backbone Flexibility

The hydrogen exchange kinetics for eight peptides representing regions distal from the glycosylation site for each of the four IgG1-Fc glycoforms are shown in Figure 4.3. Peptide 2 (HC residues 225-240) covers the hinge and proximal C_H2 domain, peptide 4 (HC residues 235-252), peptide 12 (HC residues 262-277), peptide 23 (HC residues 301-306) and peptide 24 (HC residues 306-318) all cover the C_H2 domain, peptide 27 (HC residues 334-348) covers the C_H2 and C_H3 domain interface, and peptide 34 (HC residues 359-367) and peptide 48 (HC residues 424-447) cover the C_H3 domain. The rates of HX in these regions give a qualitative readout of the backbone dynamics. For example, peptide 23 (HC residues 301-306) and peptide 34 (HC residues 359-367) in the C_H2 and C_H3 domain respectively, exchange slowly, indicating that these regions are rigid. In contrast, peptide 2 (HC residues 225-240), in the hinge region,

exchanges rapidly, indicating that the protein backbone is dynamic in this region. The data in Figure 4.3 also show that the HX rate is affected by the glycans. For example, the HX rate of peptide 2 is much faster in the non-glycosylated N297Q-Fc compared to HM-Fc, Man5-Fc and GlcNAc-Fc. This result indicates higher flexibility of the hinge and proximal C_H2 domain regions in the deglycosylated Fc. Hydrogen exchange kinetics for HM and Man5-Fcs were similar in the regions spanned by peptides 4 and 23 from the C_H2 domain. However, in peptide 12, exchange by Man5-Fc was slightly slower than HM-Fc (differences are apparent at 10^4 s and 86400 s) while in peptide 24 HX was faster (differences at 10 s, 10^2 s and 10^3 s) than HM-Fc. In the C_H2 domain peptides 4,12,23,24, and 27, there is a trend from fastest HX in the aglycosylated (N297Q) form, to intermediate HX by the GlcNAc-Fc to equal, slow HX by HM-Fc and Man5-Fc. These results indicate that as the size of the glycan attached to N297 is truncated from HM or Man5 down to GlcNAc or is completely removed (in N297Q-Fc), the flexibility in these C_H2 domain regions increases. In contrast, the extent of glycosylation did not have a substantial effect on C_H3 domain peptides 34 and 48, except that HX was slightly faster in these regions for N297Q-Fc suggesting that complete removal of the glycan causes increased flexibility of the C_H3 domain as well, distal from the glycosylation site in the quaternary Fc structure.

4.3.3 Flexibility Differences in IgG1-Fc glycoforms (focusing on aggregation hot spots, deamidation hot spots and glycopeptide C'E loop)

HX difference plots in Figure 4.4 show the effects of altered glycosylation in the IgG1-Fc glycoforms (Man-5 Fc, GlcNAc-Fc and aglycosylated N297Q) relative to high mannose species for all 51 peptides covering the IgG1-Fc at each individual HX time. The vertical axes are the HX differences (ΔHX_t, as defined by equation 2) between each Fc glycoform species and the

HM-Fc glycoform, used as the baseline. For calculating differential HX in glycopeptides 17-19, Man8 was used as the baseline, as it showed the slowest HX among the different HM form glycopeptides (see Figure 4.2). The peptides are indexed from the N- to C-terminus and represented on the horizontal axes. The locations of each peptide are provided in Supplemental Table 4.1. A positive value indicates faster exchange by the glycoform than by high mannose while a negative value indicates slower exchange. The dashed lines in Figure 4.4 indicate the limits for statistical significance as calculated by equation 5. Overall, the HX difference or ΔHX_t values indicate that backbone flexibility increases in the order of Man5 < GlcNAc < N297Q, as shown in Figure 4.4. All of the large significant changes were positive, meaning that the backbone flexibility increased in Man5, GlcNAc and N297Q IgG1-Fc states compared to the HM-Fc. However, there were also some small, but significant, decreases in HX, meaning that some regions exchanged slightly more slowly relative to the baseline HM-Fc. These small decreases in HX were in peptides 12 (HC residues: 262-277), 13 (HC residues: 263-277) and 14 (HC residues: 264-277) of Man5-Fc, in the C_H2 domain, peptides 36 (HC residues: 368-380), 38 (HC residues: 369-379), 41 (HC residues: 377-390) and 46 (HC residues: 405-423) of Man5-Fc, in the C_H3 domain, and peptides 36 and 46 in the C_H3 domain of GlcNAc-Fc.

Several regions of interest in the C_H2 domain (see Discussion section) are denoted in Figure 4.4: two aggregation hot spots (as determined by correlation to aggregation propensity shown in previous work[25,60]), a deamidation prone NG site at Asn-315 (shown previously[29]), and the glycopeptide containing C'E loop (the C'E site is essential for the Fc receptor binding, also shown in previous work[71,72]). Changing the glycan from HM to either GlcNAc or aglycosylated caused substantial increases in the rate of HX in both aggregation hotspots and in the deamidation hotspot (see Figure 4.4). In contrast, changing to Man5 did not significantly alter

HX in these regions. Overall, Figure 4.4 shows that decreasing glycan size results in faster HX.

For each of the peptides spanning the regions of interest denoted in in Figure 4.4, the HX difference plots, relative to the high mannose control, show that Man5-Fc exchanges more slowly than either GlcNAc-Fc or N297Q-Fc. HX is generally faster in GlcNAc-Fc and fastest in N297Q-Fc. Decreasing the glycan size from HM to GlcNAc or removal of the glycan (N297Q-Fc) caused significant increases in backbone flexibility in the peptides covering the aggregation hot spot regions. The effects of glycan removal were stronger (i.e., greater increases in HX rate) than simply decreasing the glycan to GlcNAc (see the annotated regions in Figure 4.4). Less obvious, but still statistically significant increases in HX occurred in some of these regions when the glycan was decreased from HM to Man5. For example, peptide 8 spanning the aggregation hot spot region #1 of Man5-Fc showed a significant increase in flexibility at 10^4 s.

The Fc contains a deamidation hotspot, NG, at 315-316, which is covered by peptides 24 and 25. Decreasing the glycan from HM to GlcNAc or removal of the glycan caused significantly faster HX exchange in the region of the deamidation hotspot, most evident at 10^4 s. HX by Man5-Fc also was significantly faster in this region than HM-Fc, but the degree of increase was smaller than GlcNAc and N297QFc.

Several glycopeptides, 17-19, cover the C'E loop region. Here, the high mannose form is heterogeneous, Man8-Man12. Man8 was selected as the baseline to represent HX by the HM-Fc in this region. Here, all the Man5, GlcNAc, and N297Q glycoforms exchanged faster than the Man8 glycoform except for glycopeptide 19 where there was no significant difference between HX by Man5 and Man8. This effect extends into another region, peptide 16 (HC residues 278-293), that begins on the N-terminal side of the C'E loop. There are other regions, such as the C_H2/C_H3 interface and some regions in the C_H3 domain that also become more flexible when the

glycan is shortened or removed. These trends must be viewed with caution, however, because of potential artifacts arising in the HX kinetics of glycopeptides.[73] We will return to this point in the Discussion.

4.3.4 Homology Mapping of Flexibility Differences in IgG1-Fc glycoforms

Figure 4.5 shows the difference plots of HX effects as a function of glycosylation, using the average HX difference across all time points compared to the high mannose Fc control and also displays the results as mapped onto a homology model of the IgG1-Fc. Additionally, regions of interest are mapped on to a homology model as seen in Figure 4.5, panel A. The vertical axis in Figure 4.5, panel B shows the average HX difference ($\Delta\overline{HX}$, as defined by equation 3) across all HX time points for all 51 peptides between each IgG1-Fc glycoform versus the HM-Fc baseline. In this representation, the changes in backbone flexibility (increases or decreases) presented in Figure 4.4 are averaged over all the five HX time points. The significant differences in $\Delta\overline{HX}$ were mapped onto the homology model (Figure 4.5, panel C). For overlapping peptides with conflicting results, significant changes were given priority (see Materials and Methods for more details). Regions with strongly increased HX ($\Delta\overline{HX}$ > 5%) and weakly increased HX ($\Delta\overline{HX}$ < 5%) as compared to HM-Fc were mapped in dark blue and cyan colors on the homology model, respectively. While, regions with decreased HX as compared to HM-Fc are colored pink, regions with no significant difference in HX with respect to HM-Fc are colored gray and the glycans are colored green. There were significant differences in the glycopeptides (17-18) and a trend that correlated with the size of N-glycan attached. However, as already noted, direct and quantitative comparison of glycopeptides is complicated (see Discussion section). In general, there was an overall increase in HX rate in the Fc molecules as the glycans were truncated from high mannose to aglycosylated. As the relative HX effects are averaged over all the five time

points, the weak Man5-Fc effects are more obvious than in Figure 4.4, especially for the aggregation and deamidation hot spot regions. In peptide 8, covering aggregation hot spot #1, there was a significant increase in HX by Man5-Fc, but no significant increases in HX in peptides 20-23, spanning aggregation hot spot # 2. In the deamidation hotspot, spanned by peptides 24 and 25, there was a significant increase in flexibility as compared to HM-Fc not apparent in the individual time points shown in Figure 4.4. The C_H2 and C_H3 domain peptides that exchanged more slowly than HM-Fc, as noted for 10^4 s of labeling in Man5-Fc and GlcNAc-Fc in Figure 4.4, were not significantly different when averaged over all HX times in Figure 4.5B, except for one peptide number 12 in Man5-Fc, which showed significant decrease in backbone flexibility as compared to HM-Fc (shown in pink region in the homology map in Figure 4.5C). The degree of increase in $\Delta\overline{HX}$ values as well as the number of peptides with significant increases in flexibility increased with truncation of glycans from Man5 to GlcNAc and N297Q (as compared to the high mannose IgG1-Fc control). As seen in Figure 4.5 panel C, a few peptides in C_H2 and C_H3 domains showed significant increase in $\Delta\overline{HX}$ values and flexibility of Man5-Fc as compared to HM-Fc. The degree of increase was weak ($\Delta\overline{HX}$ < 5%). One region also showed decrease in $\Delta\overline{HX}$ values and flexibility as compared to HM-Fc. In GlcNAc-Fc, all the peptides in the C_H2 domain and a few peptides in the C_H3 domain showed significant increase in $\Delta\overline{HX}$ and flexibility as compared to the HM-Fc. While majority of these peptides showed a weak degree of increase, a few peptides in the C_H2 domain showed strong degree ($\Delta\overline{HX}$ > 5%) of increase in HX which was not observed in the Man5-Fc. The largest increase in $\Delta\overline{HX}$ values and flexibility were seen upon de-glycosylation where essentially the entire IgG1-Fc became more flexible. In general, largest $\Delta\overline{HX}$ values and strongest increase ($\Delta\overline{HX}$ > 5%) in

flexibility were observed in all the peptides of C_H2 domains and few peptides in the C_H3 domains of N297Q-Fc as compared to HM-Fc.

4.4 Discussion

The goal of this work was to examine the effect of glycan size on the local flexibility of four well-defined IgG1-Fc glycoforms in order to correlate these results with known chemical stability, conformational stability, aggregation propensity and FcγRIIIa receptor binding studies that were published recently as a series of papers.[28,29,31] The hydrogen exchange results in this work revealed a trend of increasing backbone flexibility with decreasing N-glycan size (relative to high mannose) in the IgG1-Fc molecules. Decreasing the glycan size to Man5 caused smallest increase in backbone flexibility (mostly in the C_H2 domain and C_H2/C_H3 interface) relative to HM-Fc. Further decreasing the glycan to a single GlcNAc at both Asn-297 sites caused more widespread and larger increases in backbone flexibility. Finally, removal of the glycan (N297Q-Fc) caused the largest increase in backbone flexibility across the entire IgG1-Fc molecule. The differences in flexibility were more prominent in the C_H2 domain; however, flexibility differences in some regions of the C_H3 domains were also observed among these four glycoforms.

The overall physical stability, chemical stability and receptor binding profiles of the four IgG1-Fc glycoforms were studied previously, and showed a correlation with oligosaccharide structure: HM-Fc and Man5-Fc displayed the highest relative physical stability, followed by GlcNAc-Fc, with N297Q-Fc being the least stable.[28] Also, apparent solubility values (thermodynamic activity) measured by PEG precipitation assay, of these IgG1-Fc glycoforms decreased as the glycans were sequentially truncated from HM to non-glycosylated N297Q.[28] Under thermal stress, the aggregation propensity of GlcNAc-Fc and N297Q-Fc was greater than

the aggregation propensity of the HM-Fc and Man5-Fc, as measured by a turbidity assay.[28] Additionally, HM-Fc and Man5-Fc both had similar high affinities for FcγRIIIa, GlcNAc-Fc had relatively low affinity, and the non-glycosylated N297Q-Fc had no measurable affinity for FcγRIIIa.[31] Similarly, HM-Fc and Man5-Fc showed higher susceptibility for Trp-277 oxidation and lower susceptibility towards Asn-315 deamidation than GlcNAc and non-glycosylated N297Q IgG1-Fc.[29] It is important to see the overall flexibility results of the various IgG1-Fc glycoforms in the light of conformational stability, aggregation propensity and receptor binding of mAbs in general, as these comparisons should ultimately provide insight into their pharmaceutical development as discussed below.

4.4.1 Correlation of previous aggregation propensity results of IgG1-Fc glycoforms with HX Results

Aggregation is a complex, multi-step process involving both local hot spots (areas of local structural alterations and/or enhanced flexibility) and global factors including overall conformational and colloidal stability.[74] Hydrophobic, aggregation-prone sites in IgG antibodies have been identified in both the variable and constant regions of IgG molecules by *in silico* analysis.[75] HX-MS studies have identified a particular segment near the Phe-243 in HC residues 241–252, FLFPPKPKDTLM (peptides 3-8 in this study) in C_H2 domain of the Fc that became more flexible in response to a variety of stresses including destabilizing additives (thiocyanate and arginine), anti-microbial agents, methionine oxidation, deglycosylation and point mutations in C_H2.[25,54,58,60,66,76] Previously, two separate studies from our lab identified this region as the aggregation hotspot (referred to as aggregation hotspot # 1 in this study, see Figure 4.4).[25,60] Additionally, we observed changes in backbone flexibility in another region across the four IgG1-Fc glycoforms, which included HC residues Y300-L306 (peptides 20-23) of the C_H2

domain. This result was consistent to previously seen increases in flexibility of this region of an IgG1 mAb in presence of thiocyanate [25]. This particular region exchanges quite slowly, so that differences only become apparent after long HX times, as seen in our study and in the previous study.[25] Increases in backbone flexibility in residues V273-L306 upon substitution of complex glycans with high-mannose glycans in an IgG2 antibody have been reported recently by HX-MS.[32] In this region (Y300-L306), the N297Q mutation caused greatest increase in flexibility, the GlcNAc-Fc form caused intermediate increase, while Man5-Fc did not cause a significant change compared to HM-Fc. Here, we denote this second region as aggregation hot spot # 2 (peptides 20-23, see Figure 4.4). The extent of change in the backbone flexibility (of these two aggregation hot spots in the C_H2 domain), conformational instability (studied in Chapter 2), and increased aggregation propensity (studied in Chapter 2) of IgG1-Fc glycoforms correlate well with decreased size of N-linked glycan.[28] As seen in Chapter 2, we have found that under thermal stress, both the non-glycosylated N297Q-Fc and GlcNAc-Fc both aggregated at the same onset temperature at pH 6.0 in 150 mM NaCl formulation, but the extent of N297Q-Fc aggregation was more extensive as seen the OD 350 values. However, GlcNAc-Fc was more aggregation prone in another formulation that contained 10% sucrose instead of NaCl.[28] In this same assay, HM-Fc and Man5-Fc showed no aggregation under any of the experimental conditions tested (see Chapter 2).[28] Two phenylalanine residues in this region (Phe-241 and Phe-243) pack against the glycans in the crystal structure,[64] and these interactions would expected to be absent in the GlcNAc and non-glycosylated C_H2. Although comparisons between HX kinetics at the glycan site itself are qualitative in nature (See Figures 4.1 and 4.2, and discussion below), the trend of increase in HX rate shown in Figure 4.1 upon removal of first GlcNAc glycan (in the

core) at the Asn-297 underscores the importance of this core residue in stabilization of the IgG backbone, presumably through side chain-glycan interactions.

4.4.2 Correlation of previous Asn-315 deamidation and Trp-277 oxidation of IgG1-Fc glycoforms results with HX results

It was previously observed that the deamidation of Asn-315 of HM-Fc, Man5-Fc, GlcNAc-Fc and N297Q-Fc during a 3-month accelerated stability study at 40°C was dependent on the size of N-glycans.[29] It was observed that the rate and extent of deamidation of Asn-315 was faster for GlcNAc-Fc and N297Q-Fc than HM-Fc and Man5-Fc, indicating that trimming or removal of the N-glycan promotes deamidation of Asn-315.[29] A direct correlation between the rate of Asn-315 deamidation and the local flexibility of peptides (24 and 25) containing the Asn-315 was observed with the four IgG1-Fc glycoforms. We saw that backbone flexibility of the C_H2 domain in peptides 24 and 25 (containing Asn-315) significantly increased as the size of glycan was truncated from HM-Fc, to Man5-Fc, GlcNAc-Fc and non-glycosylated N297Q-Fc (see Figure 4.3 for uptake plot of peptide 24, and Figures 4.4 and 4.5 for difference plots of peptides 24 and 25). Previous studies have reported deamidation of Asn-315 in IgG mAbs, both *in vivo* and *in vitro,* and attributed this result to changes in flexibility near Asn-315 region.[18,77-82] We are also examining this intriguing correlation by HX-MS in greater detail elsewhere.[83] The role of N-glycan size in governing the rate of Asn-315 deamidation by affecting the flexibility in this region has not been reported before to best of our knowledge with IgG1-Fc molecules.

Additionally, an accelerated stability study of the above four IgG1-Fc glycoforms at 40°C for 4 weeks showed a different correlation of glycosylation with the rate of degradation of Trp-277 to glycine hydroperoxide (Gly-277).[29] The HM-Fc and Man5-Fc showed higher rate of conversion of Trp-277 into glycine hydroperoxide than GlcNAc-Fc and non-glycosylated

N297Q-Fc, indicating that the decrease in size of N-glycan decreases the degradation of Trp-277.[29] In this HX study, we observed that peptide 12 (HC 262-277) containing Trp-277 in the C_H2 domain showed highest flexibility in N297Q-Fc (see Figure 4.3), intermediate flexibility in GlcNAc-Fc, and least flexibility in HM-Fc and Man5-Fc. In fact, Man5-Fc showed slightly lower flexibility in this peptide than HM-Fc at 10^4s and 10^5s (see in Figure 4.4 and as seen in the homology model in Figure 4.5). Other overlapping peptides containing Trp-277 (peptides 13, 14 and 15) showed similar overall trends in flexibility with the size of glycans as seen in peptide 12, but were subtle and non-significant for Man-Fc (as seen in Figure 4.5). Our results indicate that as the glycans were sequentially truncated, the flexibility in peptide 12 increased significantly. Thus, there appears to be an inverse correlation of local flexibility, and a direct correlation to glycan size, for increasing Trp-277 degradation in this IgG1-Fc.[29] In contrast to Asn-315 deamidation results described above, this result indicates that Trp-277 oxidation rates do not correlate with local backbone flexibility of this residue within the backbone structure of the IgG1-Fc glycoforms.

4.4.3 Correlation of previous Fc receptor binding with IgG1-Fc glycoforms with HX Results

A number of studies report the effects of carbohydrate composition on binding affinity of mAbs with various Fcγ receptors.[84] FcγRIIIa receptor is the primary target for most therapeutic mAbs requiring ADCC action and is the most studied interaction.[19,84] X-ray crystallography and Fc engineering have identified different regions of IgG1-Fc that are essential for interactions with FcγRIIIa receptors which are the lower hinge (HC residues L235-S239), the BC segment (HC residues D265-269E), the C'E segment (residues Q295 and Y296), and the FG segment (HC residues A327-I332).[55,85] The C_H2 domain orientation of the Fc region is also an important

component of mAb binding affinity to FcγRIIIa. An "open" IgG-Fc structure is the most favored conformation for interaction with FcγRIIIa, as seen in the IgG-Fc–FcγRIIIa complex. FcγRIIIa is sensitive to the type of glycosylation present on the Fc region of antibodies; such as removing core fucose increased the affinity of Fc for receptor binding but still maintain an open conformation while truncation of or removal of other core oligosaccharides resulted in a "closed" conformation (collapse) that was unfavorable for binding.[71,86] In addition to the conformation of the C_H2 domain, previous studies have identified an important role for C'E loop dynamics and glycan motions in receptor binding.[84,87,88] In our previous Fc receptor binding studies with these four well-defined IgG1-Fc glycoforms, it was observed that HM-Fc and Man5-Fc had highest affinities for FcγRIIIa, GlcNAc-Fc showed lower affinity, while N297Q-Fc did not show any binding to the receptor by two different binding formats as measured by BLI.[31]

In this work, we saw a correlation of HX in peptides 17-19 (which include C'E loop, and residues Q295 and Y296), peptides 3-4 (containing residues L235-S239), peptides 12-15 (containing residues D265-269E) and peptides 26-27 (containing residues A327-I332) with the size of glycans. We observed that HM-Fc and Man5-Fc show similar HX trends overall, but Man5-Fc showed relatively faster HX as compared to HM-Fc in C'E loop peptides 17 and 18 (see Figure 4.1) and peptides 26-27 which were shown to be significant (see Figures 4.4 and 4.5). GlcNAc-Fc showed intermediate rise in HX, while the N297Q-Fc showed the fastest HX as compared to HM-Fc in all the peptides. Additionally, we saw significant increase in HX over all glycoforms in peptide 16 (residues: Y278-E293) which lies just before the C'E loop which could be important for FcγRIIIa binding, as reported by a HX-MS study on fucose depleted complex glycoforms in presence of FcγRIIIa (residues 279-301).[55] We observed that as the glycans were truncated from Man5 to the core GlcNAc and finally removal of all glycans (N297Q-Fc),

sequential increase in HX was observed in these peptides as compared to HM-Fc (See Figures 4.4 and 4.5). Additionally, residues F241-K246 (aggregation hot spot #1 in our study) were found important for modulation of glycan motions as studied by NMR,[88] and impacted the FcγRIIIa binding affinity of Fc fragment. Similarly, we see increased HX in peptides 5-8 (containing residues 241-246) with decreases in the size of N-glycan in the series of four well-defined glycoforms of IgG1-Fc.

In other studies, Man5-Fc and Man8/9-Fc showed enhanced affinity for FcγRIIIa as compared to the complex G0F glycoforms of an IgG;[89] however, another study showed higher rate of HX in the C'E loop glycopeptide (Y278-L306) of Man5 IgG1 than G0F IgG1 and IgG2.[32] These results indicate the importance and involvement of regions other than the C'E loop for receptor binding.[32] Additionally, GlcNAc-Fc showed intermediate binding to FcγRIIIa in our previous studies, even though it does not provide enough backbone interactions to maintain the open structure of the C_H2 domains (that is favorable to receptor binding) and also showed an overall increase in flexibility across the entire C_H2 domain by HX-MS. This result again is consistent with the notion that importance of the first core GlcNAc in sampling conformations that are essential for the binding of Fc to these receptors, which are absent in non-glycosylated Fcs. Overall, these results point out towards complex correlations between IgG-Fc conformational integrity, local flexibility and strength of interaction with the FcγRIIIa receptors that are modulated by the oligosaccharide size for N-glycosylation. Future work in better understanding the mechanism of the receptor binding by N-glycan modulation in the context of local flexibility measurements of well-defined IgG glycoforms will provide opportunities for improved IgG therapeutics.

4.4.4 Effects of different glycoforms on local flexibility of mAbs by HDX

Backbone flexibility observations within HM, Man5, GlcNAc and non-glycosylated IgG1-Fc glycoforms reported in our work show differences in similar regions of Fc as described previously in studies on complex and deglycosylated glycoforms of mAbs.[32,54,55,62] Although direct, quantitative comparisons across these HX studies are impeded by slight differences in peptide coverage, glycan heterogeneities, labelling conditions and data representation methods, qualitative comparisons of backbone flexibility trends in different glycoforms of mAbs can be drawn. We note that the deuterium uptake curves in this work show a trend with glycan size, particularly near the Phe-243 region (peptides 3-8) and at the glycopeptide region Y278-Y300 (peptides 16-19), similar to several other HX-MS studies on IgG mAbs.[32,54,55] Additionally, we see other regions that show differences in HX such as residues 300-306 (peptides 20, 21, 22, 23), C_H2-C_H3 interface (peptides 24-27) and the C_H3 domain (limited in Man5-Fc, widespread in GlcNAc and N297Q-Fcs) in our studies with IgG-Fc molecules, locations which was believed to be unaffected by N-glycosylation and was not seen previously in HX studies of mAbs.[32,54,55] The Phe-243 region is notable because the side chains in this region of the Fc make contact with the glycan in X-ray crystal structures.[64] The flexibility trends in terms of increased or decreased protection are dependent on the presence of N-glycan (deglycosylated vs. glycosylated) and type and size of N-linked glycan (complex, hybrid and high mannose).

A previous study comparing HX of glycosylated (mostly G0F) and deglycosylated IgG1 antibodies found increased flexibility in residues L236-253M containing the Phe-243 upon deglycosylation[54] which is similar to our observations in this work with these corresponding amino acid residues (in our case residues L235-M252 and peptides 2-8) in N297Q-Fc compared to HM-Fc (Man8-Man12). Similarly, another HX-MS study of IgG2 molecules containing HM (mostly Man9) and hybrid glycans (A1G1M4F and A1G1M5F) found greater backbone

flexibility in the C_H2 domain, especially near the Phe-243 residue, as compared to the shorter complex glycans (mostly A2G0F).[32] The difference in increased backbone flexibility in the Man9 glycoform at the Phe-243 residue was attributed to the possibility of removal of contacts between complex glycans and Fc residues that were absent in HM.[32] Finally, an additional HX-MS study showed that differential galactosylation affected backbone motion in an IgG1 in residues F242-I254 (containing the Phe-243). Hypergalactosylation (G2) caused slower HX compared to non-galactosylated (G0) or partially-galactosylated (G1). These differences were attributed to a hydrogen bond between galactose and Lys-246. The presence of fucose (G0F, G1F, G2F vs G0, G1, G2) however, did not alter HX in this region.[55] For the four IgG1-Fc glycoforms studied in the present work, there were no significant backbone flexibility differences between HM-Fc and Man5-Fc. This result indicates that the Man5 structure is essential for the relatively lower backbone flexibility of these IgG1-Fc glycoforms (Man5 and HM), and upon truncation of the glycan size in the other two IgG1-Fc (in GlcNAc and N297Q), the flexibility of this region increases further, likely due to the loss of stabilizing interactions between the glycan and the polypeptide backbone.

Differences in flexibility were observed at the glycopeptides Y278-L306 and Y278-F300 in IgG1 and IgG2 mAbs respectively, where HX was faster in high-mannose (Man9, Man5-7) and hybrid glycopeptides than in complex glycopeptides (mostly A2G0F) suggesting similar backbone flexibility patterns between these two different subclasses of IgG.[32] In our studies, sequential glycan truncation caused an increase in backbone flexibility at or near the site of glycosylation, where truncation from HM (mostly Man8) to Man5 appears to cause a slight increase, GlcNAc-Fc caused an intermediate increase while N297Q-Fc caused the greatest increase (although HX artifacts in glycopeptides cannot be completely discounted as discussed

subsequently). However, in a previous study by Houde et al, glycopeptide residues P292-T308 showed significant decrease in backbone flexibility upon deglycosylation.[54] A couple of observations for this contrast effect in the glycopeptide region could be due to the different deglycosylation approaches utilized or different techniques utilized for studying the structure and flexibility. The previous HX study used PNGase-F treatment for deglycosylation of a fully glycosylated antibody[54], while, we have utilized a non-glycosylated IgG1-Fc mutant where Asn-297 was replaced by Gln. The increased protection of the glycopeptide in the PNGase-F treated mAb is consistent with the observed collapse and increased compactness of C_H2 domains upon glycan truncation and deglycosylation as seen before.[71,90] However, discrepancy exists in the case where an aglycosylated Fc (expressed in *E. coli*) showed increased radius of gyration in solution by SAXS.[72] Secondly, crystal structure studies have shown that even though C_H2 domain distances were reduced or increased in aglycosylated Fcs, the C'E loop becomes flexible[71,72,91] which is inconsistent with the observed decrease in flexibility in the glycopeptide region in the HX study by Houde et al. Our results support the observed increases in C'E loop flexibility upon glycan truncation (in Man5-Fc and GlcNAc-Fc) and non-glycosylated N297Q-Fc.

Another interesting observation in our study is that within the high mannose glycoforms of the IgG1-Fc, the Man8 glycopeptide appeared to be relatively the most rigid and that backbone flexibility increased as the mannose content increased sequentially to Man12 (see Figure 4.2). It was observed previously that sialylated glycoforms of IgG1 and IgG2 showed similar enzymatic degradation susceptibility as HM glycoforms and this was related to the weakening of interactions between glycans and C_H2 domains due to steric effects of bulky sialylated groups.[32] Thus, faster HX upon increasing the glycan size from Man8 to Man12

observed in this work with IgG1-Fc might be due to steric effects caused by the sequential addition of bulky mannose units. The Man9 crystal structure also showed increased inter C_H2 domain distance, attributed to the need to accommodate a large, multiply branched glycan in the C_H2 pocket.[92] Interestingly, we observed that when Man8 was truncated to Man5, flexibility in the glycopeptide C'E loop appeared to be slightly increased (but was still less than Man12) for these IgG1-Fc molecules. However in another study, differences in the glycopeptide region (Y278–F300) between Man5-Man7 and Man9 of both full length IgG1 and IgG2 were not seen.[32]

In HX, glycoform enrichment is not necessary when comparing HX effects in the glycopeptides. However, there are a few limitations in direct comparisons of glycopeptides, which need to be addressed. First, Guttman and co-workers showed that the acetamido groups of the glycan moiety can retain some deuterium after quenching, digestion, and LC separation.[73] Thus, direct comparisons between peptides with different numbers of acetamido groups cannot be made unless the measured HX kinetics are adjusted to account for this excess deuteration. In cases where glycopeptides have the same number of acetamido groups, this particular factor is not a limiting issue. Second, it is unknown whether glycosylation has an effect on chemical exchange at amide sites near the glycan. Acetamido groups include the two core N-acetyl glucosamine sugars and the modified asparagine/glutamine side chain hydrogens. In another study, it was observed that complex, high mannose and hybrid glycans of IgG1 and IgG2 retained excess deuterium in the glycopeptides that was proportional to the amount of acetamido groups. In our study, the HM-Fc (Man8-Man12) and Man5-Fc all have three acetamido groups: two GlcNAcs and one modified Asn side chain. GlcNAc-Fc has two acetamido groups: one GlcNAc and one modified Asn side chain. The non-glycosylated N297Q-Fc has no glycans. In

principle, the observed HX could be adjusted for HX in the glycan acetamido groups. This trend is apparent in the roughly 0.4 Da mass increase as seen in Supplemental Table 4.2 as the number of glycan acetamido groups increases from zero to two to three. However, if there are differences in back-exchange between peptides with different glycoforms, the comparisons become problematic. A final complication is that the HM IgG1-Fc is a distribution of 8 to 12 mannose residues at the glycosylation site on each chain. The majority of heavy chains carry the Man8 glycan, as characterized in a previous study.[31] Our ability to interpret hydrogen exchange results in the case of the high mannose glycoforms is more limited because of the heterogeneity of glycosylation on the adjacent chain. Effectively, the observed HX kinetics for any high mannose glycopeptide is averaged across all high mannose forms (Man8-Man12) on the other half of the Fc.

Finally, in all of the previous studies as well as our work, HX differences in specific regions of the C_H2 domains were observed as a consequence of different glycosylation, however in our studies with IgG1-Fc, we also observed additional differences in the C_H2-C_H3 interface (residues 306-348, peptides 24-27) and in the C_H3 domains that were not previously reported with mAbs. Again, there was a trend where the backbone flexibility of Man5-Fc was greater than HM-Fc near the C_H2-C_H3 domain interface. On the other hand, decreasing the glycan to GlcNAc-Fc and removal of the glycan with N297Q-Fc increased the backbone flexibility in this region to a much greater degree than the effect observed with Man5-Fc. Increase in flexibility in the C_H2-C_H3 interface (especially at L317 and N318) was also observed recently in a deglycosylated Herceptin which supports destabilization and increased flexibility of Fc by increased C_H2-C_H3 interface breathing motions upon deglycosylation.[62] Another region where we observed the highest increase in backbone flexibility upon deglycosylation of the IgG1-Fc

were residues 300-306 (peptides 20-23). Changes in this region were not reported in other HX-MS measurements of other non-glycosylated mAbs,[54,62] but upon environmental stress, this region might be one of the aggregation hots spots in mAbs (see above).

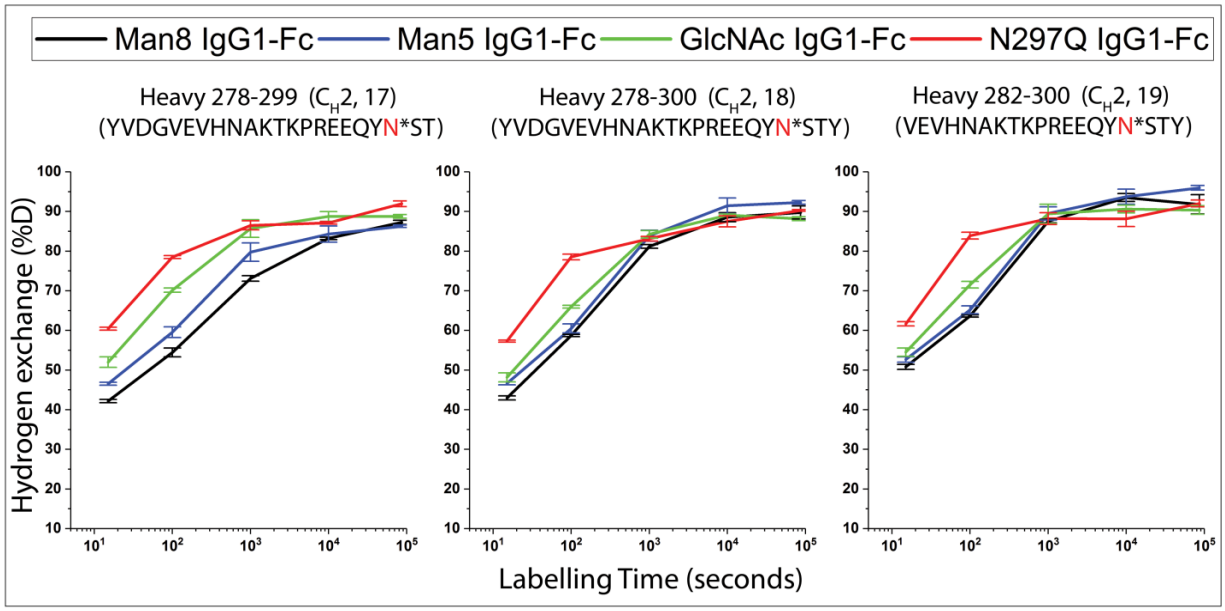

Figure 4.1: Trends in the HX kinetics of 3 different peptides containing the N-linked Asn297 glycosylation site located in the four different well-defined IgG1-Fc glycoforms. The extent of HX has been corrected for back-exchange using deuteration controls as defined by equation (1). Error bars represent sample standard deviation from three independent HX measurements.

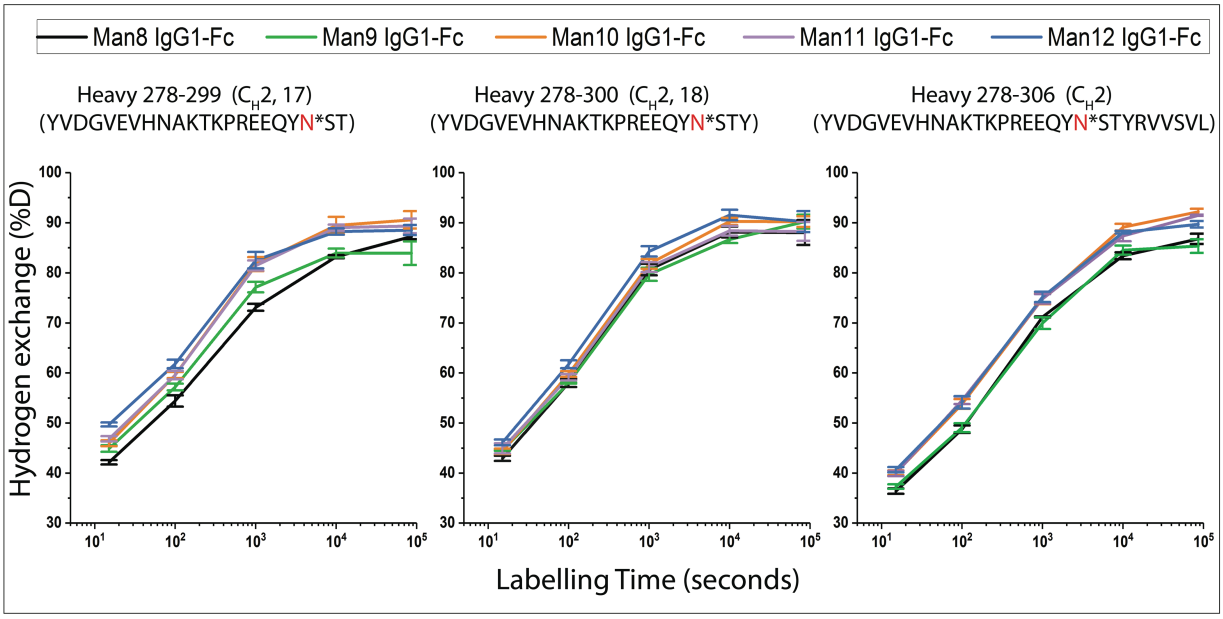

Figure 4.2: Trends in the HX kinetics of 3 different peptides containing different high mannose oligosaccharide structures at the N-linked Asn297 glycosylation site in the high mannose IgG1-Fc glycoform. The extent of HX has been corrected for back-exchange using deuteration controls as defined by equation (1). Error bars represent sample standard deviation from three independent HX measurements.

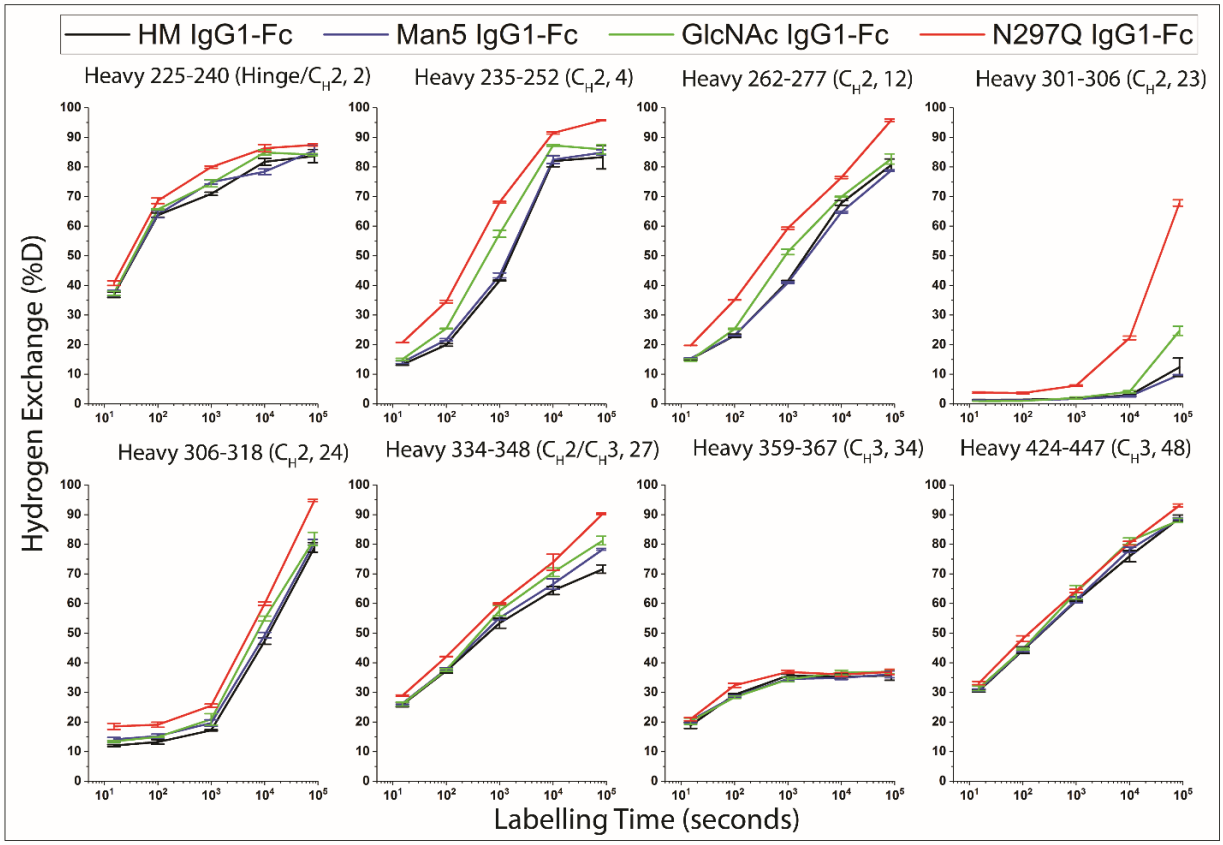

Figure 4.3: Differences in the HX kinetics of 8 representative peptides found in the four well-defined IgG1-Fc glycoforms in different regions distal from the N-linked Asn297 glycan attachment site. The extent of HX has been corrected for back-exchange using deuteration controls as defined by equation (1). Error bars represent sample standard deviation from three independent HX measurements.

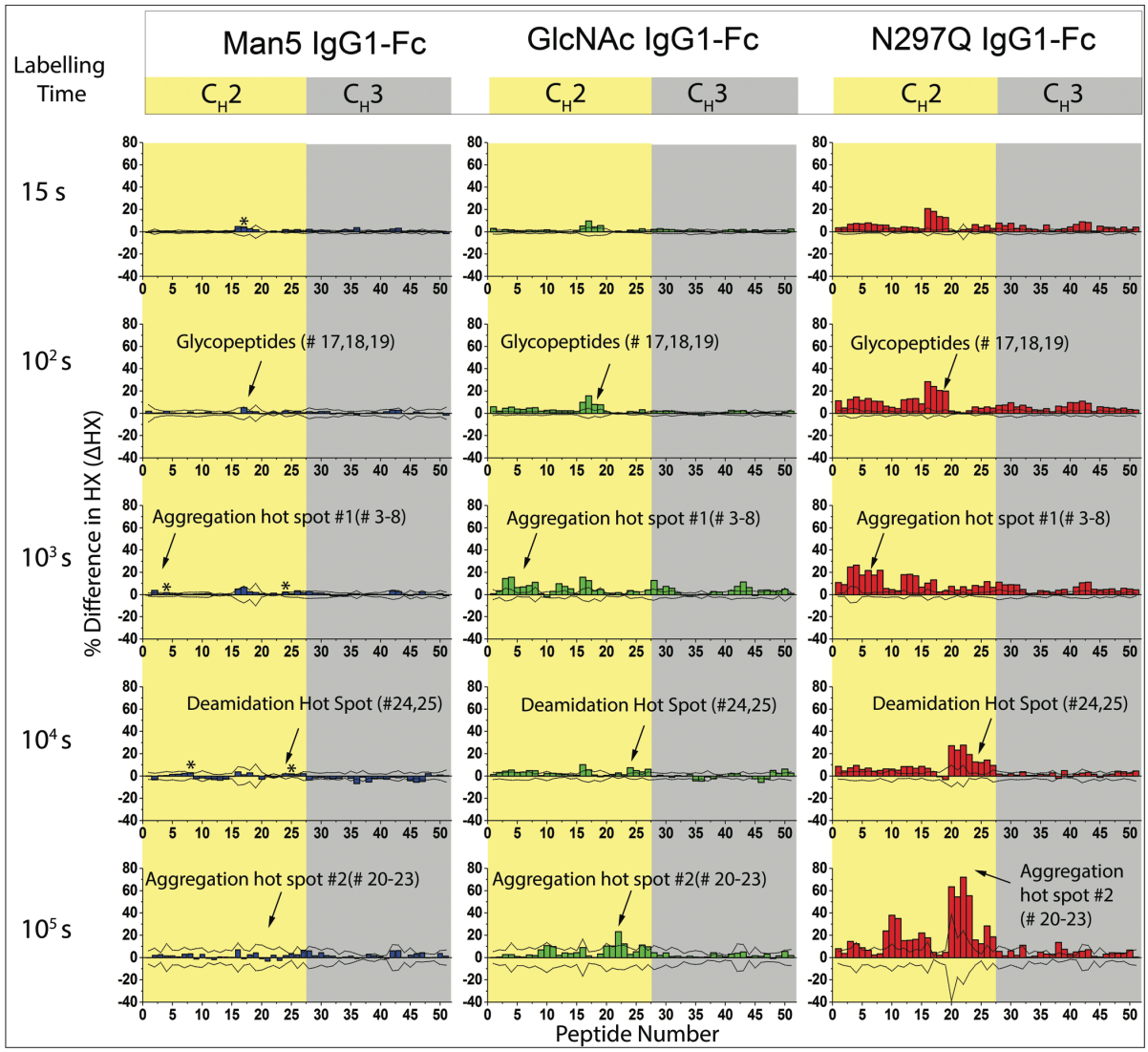

Figure 4.4: Differential deuterium uptake of 51 peptides at five HX times Differential HX in 51 peptides of three different IgG1-Fc glycoforms compared to the high mannose IgG1-Fc control. ΔHX in Man5-IgG1-Fc (blue), GlcNAc-IgG1-Fc (green), and N297Q-IgG1-Fc (red) relative to HM-IgG1-Fc at pH 6.0 calculated as defined by equation (2) is shown. For the HM-IgG1-Fc glycopeptides (peptide # 17, 18 and 19) data are shown for the most abundant form, Man8. The peptides are indexed from N- to C-terminus. The corresponding locations and sequences are listed in the supporting information in Supplementary Table 4.1. The yellow region denotes the C_H2 domain; the grey region denotes the C_H3 domain. One peptide, 27, spanning both the

domains, is shown in C_H2 domain. Each bar represents an average of three independent HX measurements. The dashed lines define the limit of statistical significance as described in the Methods section. The regions of interest to correlate with previously published stability and receptor binding data are as follows: Glycopeptide (peptides 17-19 at 10^2 s), Aggregation hot spot #1 (peptides 3-8, at 10^3 s), Aggregation hot spot #2 (peptides 20-23, at 10^5 s) and Deamidation hot spot (peptides 24,25 at 10^4 s). The above regions of interest are pointed out at particular labelling times that showed the largest differences in HX. * denote the peptides from the important regions that showed significant differences, but are not clearly visible due to the scale of the plot.

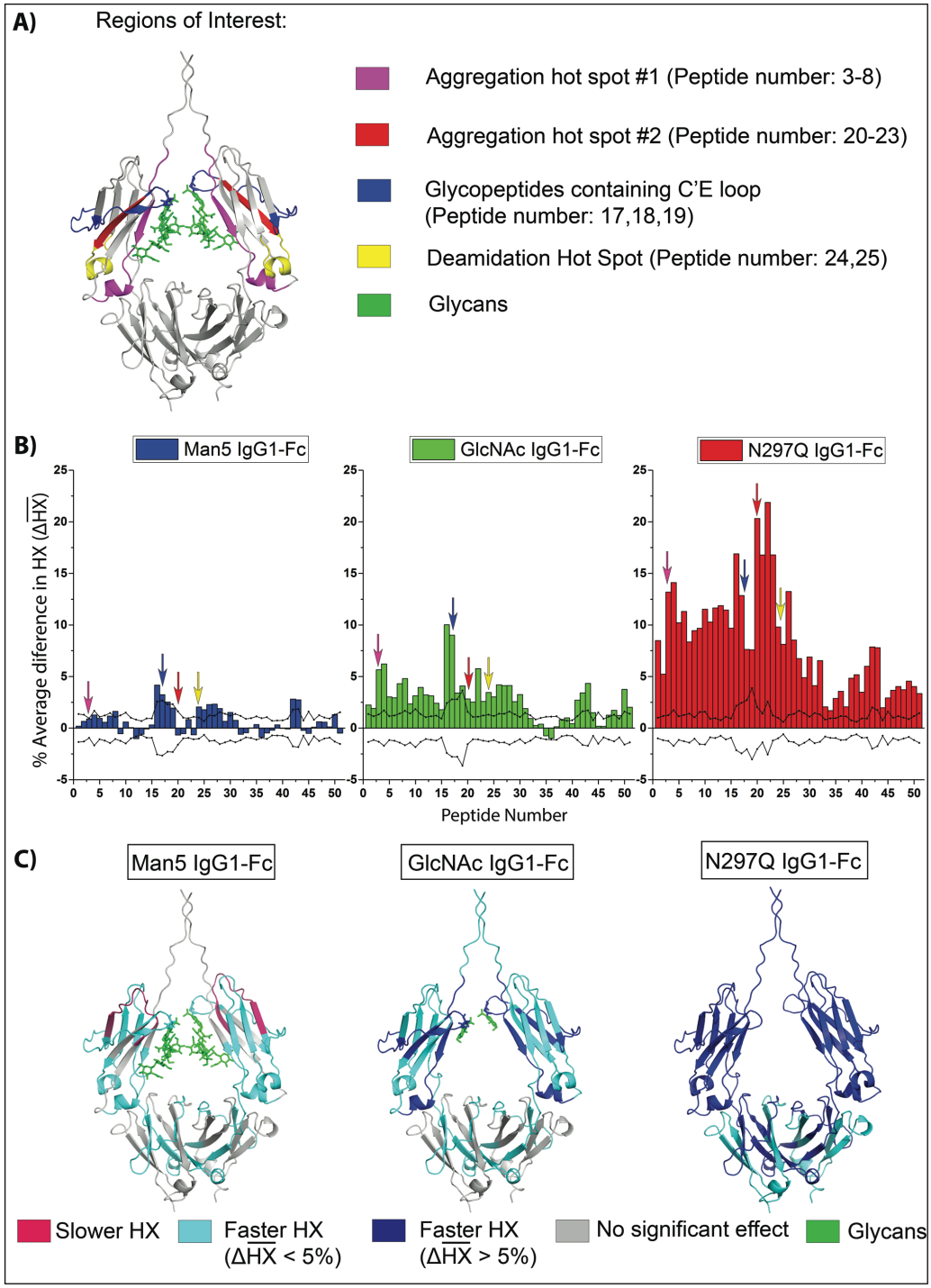

Figure 4.5: Averaged per-peptide trends in altered HX kinetics relative to the high mannose glycoform. A) Regions of interest as mentioned in Figure 4.4 are mapped on to a homology model B) HX kinetics of Man5-Fc (blue), GlcNAc-Fc (green) and N297Q-Fc (red) with respect to HM-Fc. $\Delta\overline{HX}$ represents an average of the deuterium differences at all HX times, normalized

for peptide length by using deuteration controls as defined by equation (3). The dashed lines represent the threshold for statistical significance as detailed in the Methods section as defined by equation. The arrows represent the regions of interest. C) Statistically significant $\Delta\overline{HX}$ in dark blue, cyan and pink colors is mapped onto a homology model indicating areas of strongly increased local flexibility where $\Delta\overline{HX} > 5\%$, weakly increased local flexibility where $\Delta\overline{HX} < 5\%$ and decreased local flexibility, respectively as compared to the high mannose glycoform. The homology model is based on PDB 1HZH.[64]

Supplementary Table 4.1: Identity of peptic peptides of IgG1-Fc based on Eu numbering system.[7-9]

Peptide Number	Starting AA number	Ending AA number	AA Sequence	Fc Domain
1	225	234	TCPPCPAPEL	Hinge
2	225	240	TCPPCPAPELLGGPSV	Hinge-C_H2
3	235	251	LGGPSVFLFPPKPKDTL	C_H2
4	235	253	LGGPSVFLFPPKPKDTLM	C_H2
5	241	251	FLFPPKPKDTL	C_H2
6	241	252	FLFPPKPKDTLM	C_H2
7	242	251	LFPPKPKDTL	C_H2
8	242	252	LFPPKPKDTLM	C_H2
9	253	260	ISRTPEVT	C_H2
10	253	261	ISRTPEVTC	C_H2
11	253	262	ISRTPEVTCV	C_H2
12	262	277	VVVDVSHEDPEVKFNW	C_H2
13	263	277	VVDVSHEDPEVKFNW	C_H2
14	264	277	VDVSHEDPEVKFNW	C_H2
15	266	277	VSHEDPEVKFNW	C_H2
16	278	293	YVDGVEVHNAKTKPRE	C_H2
17	278	299	YVDGVEVHNAKTKPREEQYN*ST	C_H2
18	278	300	YVDGVEVHNAKTKPREEQYN*STY	C_H2
19	282	300	VEVHNAKTKPREEQYN*STY	C_H2
20	300	305	YRVVSV	C_H2
21	300	306	YRVVSVL	C_H2
22	301	305	RVVSV	C_H2
23	301	306	RVVSVL	C_H2
24	306	318	LTVLHQDWLNGKE	C_H2
25	307	318	TVLHQDWLNGKE	C_H2
26	319	333	YKCKVSNKALPAPIE	C_H2
27	334	348	KTISKAKGQPREPQV	C_H2/ C_H3
28	349	358	YTLPPSRDEL	C_H3
29	349	364	YTLPPSRDELTKNQVS	C_H3
30	349	356	YTLPPSRDELTKNQVSL	C_H3
31	349	366	YTLPPSRDELTKNQVSLT	C_H3
32	357	365	ELTKNQVSL	C_H3
33	359	365	TKNQVSL	C_H3
34	359	367	TKNQVSLTC	C_H3
35	368	376	LVKGFYPSD	C_H3
36	368	380	LVKGFYPSDIAVE	C_H3
37	369	376	VKGFYPSD	C_H3
38	369	379	VKGFYPSDIAV	C_H3

39	369	380	VKGFYPSDIAVE	C_H3
40	377	380	IAVE	C_H3
41	377	390	IAVEWESNGQPENN	C_H3
42	377	398	IAVEWESNGQPENNYKTTPPVL	C_H3
43	381	398	WESNGQPENNYKTTPPVL	C_H3
44	392	398	KTTPPVL	C_H3
45	399	404	DSDGSF	C_H3
46	405	423	FLYSKLTVDKSRWQQGNVF	C_H3
47	411	425	TVDKSRWQQGNVFSC	C_H3
48	424	447	SCSVMHEALHNHYTQKSLSLSPGK	C_H3
49	426	447	SVMHEALHNHYTQKSLSLSPGK	C_H3
50	429	447	HEALHNHYTQKSLSLSPGK	C_H3
51	441	447	LSLSPGK	C_H3

Supplementary Table 4.2: Measured deuterium content in fully deuterated controls in three glycopeptides (# 17, 18, and 19) of IgG1-Fc glycoforms.

Note: The numbers of acetamido groups in each type of N-glycan are shown. The average values and standard deviations are in units of Da and were obtained from triplicate measurements. See Supplemental Table S1 for the amino acid composition of each peptide.

		Deuterium content (Da)		
Type of Glycan	**Number of acetamido groups**	**Peptide Number 17**	**Peptide Number 18**	**Peptide Number 19**
Man8-Fc	3	12.2 ± 0.1	12.0 ± 0.1	10.8 ± 0.2
Man5-Fc	3	12.1 ± 0.6	12.0 ± 0.3	10.7 ± 0.7
GlcNAc-Fc	2	11.0 ± 0.4	11.5 ± 0.2	10.4 ± 0.2
N297Q-Fc	0	10.9 ± 0.1	11.1 ± 0.1	9.6 ± 0.1

4.5 References

1. Zhang X, Wang Y 2016. Glycosylation Quality Control by the Golgi Structure. J Mol Biol 428(16):3183-3193.

2. Wong CH 2005. Protein glycosylation: new challenges and opportunities. The Journal of organic chemistry 70(11):4219-4225.

3. Walsh G, Jefferis R 2006. Post-translational modifications in the context of therapeutic proteins. Nat Biotech 24(10):1241-1252.

4. Khoury GA, Baliban RC, Floudas CA 2011. Proteome-wide post-translational modification statistics: frequency analysis and curation of the swiss-prot database. Scientific reports 1:90.

5. Walsh G 2014. Biopharmaceutical benchmarks 2014. Nat Biotech 32(10):992-1000.

6. Volkin DB, Hershenson S, Ho RJY, Uchiyama S, Winter G, Carpenter JF 2015. Two Decades of Publishing Excellence in Pharmaceutical Biotechnology. Journal of pharmaceutical sciences 104(2):290-300.

7. Edelman GM, Cunningham BA, Gall WE, Gottlieb PD, Rutishauser U, Waxdal MJ 1969. The covalent structure of an entire gammaG immunoglobulin molecule. Proceedings of the National Academy of Sciences of the United States of America 63(1):78-85.

8. Abhinandan KR, Martin AC 2008. Analysis and improvements to Kabat and structurally correct numbering of antibody variable domains. Mol Immunol 45(14):3832-3839.

9. Béranger S, Martinez-Jean, C., Bellahcene, F., Lefranc, M.-P. 2001. Correspondence between the IMGT unique numbering for C-DOMAIN, the IMGT exon numbering, the Eu and Kabat numberings: Human IGHG. IMGT®, the international ImMunoGeneTics information system®.

10. Vidarsson G, Dekkers G, Rispens T 2014. IgG subclasses and allotypes: from structure to effector functions. Frontiers in immunology 5:520.

11. Irani V, Guy AJ, Andrew D, Beeson JG, Ramsland PA, Richards JS 2015. Molecular properties of human IgG subclasses and their implications for designing therapeutic monoclonal antibodies against infectious diseases. Mol Immunol 67(2 Pt A):171-182.

12. Quast I, Peschke B, Lunemann JD 2017. Regulation of antibody effector functions through IgG Fc N-glycosylation. Cellular and molecular life sciences : CMLS 74(5):837-847.

13. Jensen PF, Larraillet V, Schlothauer T, Kettenberger H, Hilger M, Rand KD 2015. Investigating the interaction between the neonatal Fc receptor and monoclonal antibody variants by hydrogen/deuterium exchange mass spectrometry. Molecular & cellular proteomics : MCP 14(1):148-161.

14. Wuhrer M, Stam JC, van de Geijn FE, Koeleman CA, Verrips CT, Dolhain RJ, Hokke CH, Deelder AM 2007. Glycosylation profiling of immunoglobulin G (IgG) subclasses from human serum. Proteomics 7(22):4070-4081.

15. Huhn C, Selman MH, Ruhaak LR, Deelder AM, Wuhrer M 2009. IgG glycosylation analysis. Proteomics 9(4):882-913.

16. Jefferis R 2009. Glycosylation as a strategy to improve antibody-based therapeutics. Nature reviews Drug discovery 8(3):226-234.

17. Jefferis R 2012. Isotype and glycoform selection for antibody therapeutics. Archives of biochemistry and biophysics 526(2):159-166.

18. Jefferis R 2016. Posttranslational Modifications and the Immunogenicity of Biotherapeutics. Journal of immunology research 2016:5358272.

19. Liu L 2015. Antibody Glycosylation and Its Impact on the Pharmacokinetics and Pharmacodynamics of Monoclonal Antibodies and Fc-Fusion Proteins. Journal of pharmaceutical sciences 104(6):1866-1884.

20. Shinkawa T, Nakamura K, Yamane N, Shoji-Hosaka E, Kanda Y, Sakurada M, Uchida K, Anazawa H, Satoh M, Yamasaki M, Hanai N, Shitara K 2003. The absence of fucose but not the presence of galactose or bisecting N-acetylglucosamine of human IgG1 complex-type oligosaccharides shows the critical role of enhancing antibody-dependent cellular cytotoxicity. The Journal of biological chemistry 278(5):3466-3473.

21. Reusch D, Tejada ML 2015. Fc glycans of therapeutic antibodies as critical quality attributes. Glycobiology 25(12):1325-1334.

22. Caaveiro JM, Kiyoshi M, Tsumoto K 2015. Structural analysis of Fc/FcgammaR complexes: a blueprint for antibody design. Immunological reviews 268(1):201-221.

23. Higel F, Seidl A, Sorgel F, Friess W 2016. N-glycosylation heterogeneity and the influence on structure, function and pharmacokinetics of monoclonal antibodies and Fc fusion

proteins. European journal of pharmaceutics and biopharmaceutics : official journal of Arbeitsgemeinschaft fur Pharmazeutische Verfahrenstechnik eV 100:94-100.

24. Alsenaidy MA, Jain NK, Kim JH, Middaugh CR, Volkin DB 2014. Protein comparability assessments and potential applicability of high throughput biophysical methods and data visualization tools to compare physical stability profiles. Frontiers in Pharmacology 5:39.

25. Majumdar R, Manikwar P, Hickey JM, Samra HS, Sathish HA, Bishop SM, Middaugh CR, Volkin DB, Weis DD 2013. Effects of salts from the Hofmeister series on the conformational stability, aggregation propensity, and local flexibility of an IgG1 monoclonal antibody. Biochemistry 52(19):3376-3389.

26. Wang W, Singh S, Zeng DL, King K, Nema S 2007. Antibody structure, instability, and formulation. Journal of pharmaceutical sciences 96(1):1-26.

27. Wang W, Vlasak J, Li Y, Pristatsky P, Fang Y, Pittman T, Roman J, Wang Y, Prueksaritanont T, Ionescu R 2011. Impact of methionine oxidation in human IgG1 Fc on serum half-life of monoclonal antibodies. Molecular immunology 48(6):860-866.

28. More AS, Toprani VM, Okbazghi SZ, Kim JH, Joshi SB, Middaugh CR, Tolbert TJ, Volkin DB 2016. Correlating the Impact of Well-Defined Oligosaccharide Structures on Physical Stability Profiles of IgG1-Fc Glycoforms. Journal of pharmaceutical sciences 105(2):588-601.

29. Mozziconacci O, Okbazghi S, More AS, Volkin DB, Tolbert T, Schoneich C 2016. Comparative Evaluation of the Chemical Stability of 4 Well-Defined Immunoglobulin G1-Fc Glycoforms. Journal of pharmaceutical sciences 105(2):575-587.

30. Alsenaidy et al. 2013. High-Throughput Biophysical Analysis and Data Visualization of Conformational Stability of an IgG1 Monoclonal Antibody After Deglycosylation. Journal of pharmaceutical sciences.

31. Okbazghi SZ, More AS, White DR, Duan S, Shah IS, Joshi SB, Middaugh CR, Volkin DB, Tolbert TJ 2016. Production, Characterization, and Biological Evaluation of Well-Defined IgG1 Fc Glycoforms as a Model System for Biosimilarity Analysis. Journal of pharmaceutical sciences 105(2):559-574.

32. Fang J, Richardson J, Du Z, Zhang Z 2016. Effect of Fc-Glycan Structure on the Conformational Stability of IgG Revealed by Hydrogen/Deuterium Exchange and Limited Proteolysis. Biochemistry 55(6):860-868.

33. Visser J, Feuerstein I, Stangler T, Schmiederer T, Fritsch C, Schiestl M 2013. Physicochemical and functional comparability between the proposed biosimilar rituximab

GP2013 and originator rituximab. BioDrugs : clinical immunotherapeutics, biopharmaceuticals and gene therapy 27(5):495-507.

34. Schiestl M, Stangler T, Torella C, Cepeljnik T, Toll H, Grau R 2011. Acceptable changes in quality attributes of glycosylated biopharmaceuticals. Nature biotechnology 29(4):310-312.

35. Pais DA, Carrondo MJ, Alves PM, Teixeira AP 2014. Towards real-time monitoring of therapeutic protein quality in mammalian cell processes. Current opinion in biotechnology 30:161-167.

36. Montacir O, Montacir H, Eravci M, Springer A, Hinderlich S, Saadati A, Parr MK 2017. Comparability study of Rituximab originator and follow-on biopharmaceutical. Journal of pharmaceutical and biomedical analysis 140:239-251.

37. Kunert R, Reinhart D 2016. Advances in recombinant antibody manufacturing. Applied Microbiology and Biotechnology 100:3451-3461.

38. Frenzel A, Hust M, Schirrmann T 2013. Expression of Recombinant Antibodies. Frontiers in immunology 4:217.

39. Li F, Vijayasankaran N, Shen A, Kiss R, Amanullah A 2010. Cell culture processes for monoclonal antibody production. mAbs 2(5):466-477.

40. Goetze AM, Liu YD, Zhang Z, Shah B, Lee E, Bondarenko PV, Flynn GC 2011. High-mannose glycans on the Fc region of therapeutic IgG antibodies increase serum clearance in humans. Glycobiology 21(7):949-959.

41. Raju S 2003. Glycosylation variations with expression systems. BioProcess International 1:44-53.

42. Pacis E, Yu M, Autsen J, Bayer R, Li F 2011. Effects of cell culture conditions on antibody N-linked glycosylation—what affects high mannose 5 glycoform. Biotechnology and bioengineering 108(10):2348-2358.

43. Raju TS 2008. Terminal sugars of Fc glycans influence antibody effector functions of IgGs. Current opinion in immunology 20(4):471-478.

44. Kim S, Song J, Park S, Ham S, Paek K, Kang M, Chae Y, Seo H, Kim H-C, Flores M 2017. Drifts in ADCC-related quality attributes of Herceptin®: Impact on development of a trastuzumab biosimilar. mAbs 9(4):704-714.

45. Sha S, Agarabi C, Brorson K, Lee DY, Yoon S 2016. N-Glycosylation Design and Control of Therapeutic Monoclonal Antibodies. Trends in biotechnology 34(10):835-846.

46. Shi HH, Goudar CT 2014. Recent advances in the understanding of biological implications and modulation methodologies of monoclonal antibody N-linked high mannose glycans. Biotechnology and bioengineering 111(10):1907-1919.

47. Wang W, Singh SK, Li N, Toler MR, King KR, Nema S 2012. Immunogenicity of protein aggregates—Concerns and realities. International Journal of Pharmaceutics 431(1–2):1-11.

48. Sola RJ, Griebenow K 2009. Effects of glycosylation on the stability of protein pharmaceuticals. Journal of pharmaceutical sciences 98(4):1223-1245.

49. Chen W, Kong L, Connelly S, Dendle JM, Liu Y, Wilson IA, Powers ET, Kelly JW 2016. Stabilizing the CH2 Domain of an Antibody by Engineering in an Enhanced Aromatic Sequon. ACS chemical biology 11(7):1852-1861.

50. Chirino AJ, Mire-Sluis A 2004. Characterizing biological products and assessing comparability following manufacturing changes. Nat Biotechnol 22(11):1383-1391.

51. Federici M, Lubiniecki A, Manikwar P, Volkin DB 2013. Analytical lessons learned from selected therapeutic protein drug comparability studies. Biologicals 41(3):131-147.

52. Lubiniecki A, Volkin DB, Federici M, Bond MD, Nedved ML, Hendricks L, Mehndiratta P, Bruner M, Burman S, Dal MP, Kline J, Ni A, Panek ME, Pikounis B, Powers G, Vafa O, Siegel R 2011. Comparability assessments of process and product changes made during development of two different monoclonal antibodies. Biologicals 39(1):9-22.

53. Kim JH, Joshi SB, Tolbert TJ, Middaugh CR, Volkin DB, Smalter Hall A 2016. Biosimilarity Assessments of Model IgG1-Fc Glycoforms Using a Machine Learning Approach. Journal of pharmaceutical sciences 105(2):602-612.

54. Houde D, Arndt J, Domeier W, Berkowitz S, Engen JR 2009. Characterization of IgG1 Conformation and Conformational Dynamics by Hydrogen/Deuterium Exchange Mass Spectrometry. Analytical chemistry 81(7):2644-2651.

55. Houde D, Peng Y, Berkowitz S, Engen J 2010. Post-translational Modifications Differentially Affect IgG1 Conformation and Receptor Binding. Molecular and Cellular Proteomics.

56. Iacob RE, Bou-Assaf GM, Makowski L, Engen JR, Berkowitz SA, Houde D 2013. Investigating monoclonal antibody aggregation using a combination of H/DX-MS and other biophysical measurements. Journal of pharmaceutical sciences 102(12):4315-4329.

57. Arora J, Hu Y, Esfandiary R, Sathish HA, Bishop SM, Joshi SB, Middaugh CR, Volkin DB, Weis DD 2016. Charge-mediated Fab-Fc interactions in an IgG1 antibody induce reversible self-association, cluster formation, and elevated viscosity. mAbs 8(8):1561-1574.

58. Majumdar R, Esfandiary R, Bishop SM, Samra HS, Middaugh CR, Volkin DB, Weis DD 2015. Correlations between changes in conformational dynamics and physical stability in a mutant IgG1 mAb engineered for extended serum half-life. mAbs 7(1):84-95.

59. Mo J, Yan Q, So CK, Soden T, Lewis MJ, Hu P 2016. Understanding the Impact of Methionine Oxidation on the Biological Functions of IgG1 Antibodies Using Hydrogen/Deuterium Exchange Mass Spectrometry. Analytical chemistry 88(19):9495-9502.

60. Manikwar P, Majumdar R, Hickey JM, Thakkar SV, Samra HS, Sathish HA, Bishop SM, Middaugh CR, Weis DD, Volkin DB 2013. Correlating excipient effects on conformational and storage stability of an IgG1 monoclonal antibody with local dynamics as measured by hydrogen/deuterium-exchange mass spectrometry. Journal of pharmaceutical sciences 102(7):2136-2151.

61. Tsuchida D, Yamazaki K, Akashi S 2016. Comprehensive Characterization of Relationship Between Higher-Order Structure and FcRn Binding Affinity of Stress-Exposed Monoclonal Antibodies. Pharmaceutical research 33(4):994-1002.

62. Pan J, Zhang S, Chou A, Borchers CH 2016. Higher-order structural interrogation of antibodies using middle-down hydrogen/deuterium exchange mass spectrometry. Chem Sci 7(2):1480-1486.

63. Glasoe PK, Long FA 1960. Use Of Glass Electrodes To Measure Acidities In Deuterium Oxide1,2. The Journal of Physical Chemistry 64(1):188-190.

64. Saphire EO, Parren PW, Pantophlet R, Zwick MB, Morris GM, Rudd PM, Dwek RA, Stanfield RL, Burton DR, Wilson IA 2001. Crystal structure of a neutralizing human IGG against HIV-1: a template for vaccine design. Science 293(5532):1155-1159.

65. Busby SA, Chalmers MJ, Griffin PR 2007. Improving digestion efficiency under H/D exchange conditions with activated pepsinogen coupled columns. International Journal of Mass Spectrometry 259(1):130-139.

66. Arora J, Joshi SB, Middaugh CR, Weis DD, Volkin DB 2017. Correlating the Effects of Antimicrobial Preservatives on Conformational Stability, Aggregation Propensity, and Backbone Flexibility of an IgG1 mAb. Journal of pharmaceutical sciences 106(6):1508-1518.

67. 2017. Toth et. al. Manuscript in preparation.

68. Majumdar R, Manikwar P, Hickey JM, Arora J, Middaugh CR, Volkin DB, Weis DD 2012. Minimizing carry-over in an online pepsin digestion system used for the H/D exchange mass spectrometric analysis of an IgG1 monoclonal antibody. Journal of the American Society for Mass Spectrometry 23(12):2140-2148.

69. Mechref Y 2012. Use of CID/ETD mass spectrometry to analyze glycopeptides. Current protocols in protein science Chapter 12:Unit 12.11.11-11.

70. Hinneburg H, Stavenhagen K, Schweiger-Hufnagel U, Pengelley S, Jabs W, Seeberger PH, Silva DV, Wuhrer M, Kolarich D 2016. The Art of Destruction: Optimizing Collision Energies in Quadrupole-Time of Flight (Q-TOF) Instruments for Glycopeptide-Based Glycoproteomics. Journal of the American Society for Mass Spectrometry 27(3):507-519.

71. Krapp S, Mimura Y, Jefferis R, Huber R, Sondermann P 2003. Structural Analysis of Human IgG-Fc Glycoforms Reveals a Correlation Between Glycosylation and Structural Integrity. Journal of Molecular Biology 325(5):979-989.

72. Borrok MJ, Jung ST, Kang TH, Monzingo AF, Georgiou G 2012. Revisiting the role of glycosylation in the structure of human IgG Fc. ACS chemical biology 7(9):1596-1602.

73. Guttman M, Scian M, Lee KK 2011. Tracking hydrogen/deuterium exchange at glycan sites in glycoproteins by mass spectrometry. Analytical chemistry 83(19):7492-7499.

74. Wu H, Kroe-Barrett R, Singh S, Robinson AS, Roberts CJ 2014. Competing aggregation pathways for monoclonal antibodies. FEBS letters 588(6):936-941.

75. Chennamsetty N, Helk B, Voynov V, Kayser V, Trout BL 2009. Aggregation-prone motifs in human immunoglobulin G. J Mol Biol 391(2):404-413.

76. Majumdar R, Middaugh CR, Weis DD, Volkin DB 2015. Hydrogen-deuterium exchange mass spectrometry as an emerging analytical tool for stabilization and formulation development of therapeutic monoclonal antibodies. Journal of pharmaceutical sciences 104(2):327-345.

77. Liu YD, van Enk JZ, Flynn GC 2009. Human antibody Fc deamidation in vivo. Biologicals : journal of the International Association of Biological Standardization 37(5):313-322.

78. Wang L, Amphlett G, Lambert JM, Blattler W, Zhang W 2005. Structural characterization of a recombinant monoclonal antibody by electrospray time-of-flight mass spectrometry. Pharmaceutical research 22(8):1338-1349.

79. Sinha S, Zhang L, Duan S, Williams TD, Vlasak J, Ionescu R, Topp EM 2009. Effect of protein structure on deamidation rate in the Fc fragment of an IgG1 monoclonal antibody. Protein science : a publication of the Protein Society 18(8):1573-1584.

80. Chelius D, Rehder DS, Bondarenko PV 2005. Identification and characterization of deamidation sites in the conserved regions of human immunoglobulin gamma antibodies. Analytical chemistry 77(18):6004-6011.

81. Correia IR 2010. Stability of IgG isotypes in serum. mAbs 2(3):221-232.

82. Liu H, Gaza-Bulseco G, Faldu D, Chumsae C, Sun J 2008. Heterogeneity of monoclonal antibodies. Journal of pharmaceutical sciences 97(7):2426-2447.

83. 2017. Gamage et al. Manuscript in preparation.

84. Hanson QM, Barb AW 2015. A perspective on the structure and receptor binding properties of immunoglobulin G Fc. Biochemistry 54(19):2931-2942.

85. Subedi GP, Barb AW 2016. The immunoglobulin G1 N-glycan composition affects binding to each low affinity Fc gamma receptor. mAbs 8(8):1512-1524.

86. Mimura Y, Church S, Ghirlando R, Ashton PR, Dong S, Goodall M, Lund J, Jefferis R 2000. The influence of glycosylation on the thermal stability and effector function expression of human IgG1-Fc: properties of a series of truncated glycoforms. Molecular Immunology 37:697-706.

87. Subedi GP, Barb AW 2015. The Structural Role of Antibody N-Glycosylation in Receptor Interactions. Structure 23(9):1573-1583.

88. Subedi GP, Hanson QM, Barb AW 2014. Restricted motion of the conserved immunoglobulin G1 N-glycan is essential for efficient FcgammaRIIIa binding. Structure 22(10):1478-1488.

89. Yu M, Brown D, Reed C, Chung S, Lutman J, Stefanich E, Wong A, Stephan J-P, Bayer R 2012. Production, characterization and pharmacokinetic properties of antibodies with N-linked Mannose-5 glycans. mAbs 4(4):475-487.

90. Hristodorov D, Fischer R, Linden L 2013. With or without sugar? (A)glycosylation of therapeutic antibodies. Molecular biotechnology 54(3):1056-1068.

91. Feige MJ, Nath S, Catharino SR, Weinfurtner D, Steinbacher S, Buchner J 2009. Structure of the murine unglycosylated IgG1 Fc fragment. J Mol Biol 391(3):599-608.

92. Crispin M, Bowden TA, Coles CH, Harlos K, Aricescu AR, Harvey DJ, Stuart DI, Jones EY 2009. Carbohydrate and domain architecture of an immature antibody glycoform exhibiting enhanced effector functions. J Mol Biol 387(5):1061-1066.

Chapter 5 Summary, Conclusions and Future work

5.1 Overview

The process and formulation development of protein biopharmaceutical such as monoclonal antibodies (mAbs) is a long, complex and expensive endeavor. The main characteristics of mAbs which make their development challenging are 1) their large molecular weight combined with their complex, fragile and heterogeneous (due to PTMs) primary and higher order structures, 2) complex production using living cells that we have limited control and knowledge of, 3) multifaceted behaviors and interaction with other molecules in the human system, and 4) limitation of the analytical tools used to characterize them.[1-3] It is required for the manufacturers of novel biologics and biosimilars to prove to the regulatory authorities that all necessary studies have been conducted and their product is biologically active and safe and efficacious for use in an identified patient population.[4] Hence, it is of utmost importance to make an effort in improving our understanding about the physicochemical properties and develop better analytical tools for studying these molecules to achieve minimum risk for their utilization as therapeutics. Each mAb biologic or biosimilar product has different structural characteristics, a glycosylation patterns and stability profiles by virtue of different variables during their development such as raw materials, cell lines, manufacturing procedures, formulations, container closures, delivery devices, etc.

It is well known that N-glycosylation affects the structure, stability and can severely impact the safety and therapeutic efficacy of mAb drug candidates, hence monitoring and controlling them in a drug product is crucial. Multiple attempts have been made to control and characterize the type and content of glycosylation heterogeneity in biologics. Currently, HPLC-MS techniques are the most popular for glycosylation profiling and primary structure analysis of mAbs and research is ongoing in developing new and sensitive analytical instruments for their

characterization. However, studying the impact of glycosylation on higher order structure of mAbs has remained a challenge due to complexity of the glycosylation and the need for multiple and improved biophysical characterization tools to accesses all aspects of their complex HOS especially in case of comparability and biosimilarity assessments.[2] Therefore, biophysical analysis of mAbs in attempt to investigate the impact of glycosylation during their formulation development and in comparability/biosimilarity exercises is necessary and was the main focus of this PhD thesis project.

5.2 Chapter summaries and future work

5.2.1 Chapter 2

The well-defined glycoforms of IgG1-Fc produced in this work serve as model proteins to develop novel analytical tools for comparability and biosimilarity assessments. Additionally, this study provides improved understanding of the impact of N-glycosylation on higher order structure and stability profile of IgG1-Fc proteins in different formulations. Four homogenous, well-defined glycoforms of IgG1-Fc (HM-Fc, Man5-Fc, GlcNAc-Fc and N297Q-Fc) were achieved using genetically modified yeast cells and *in vitro* enzymatic synthesis. Routinely used low resolution, higher throughput biophysical tools for formulation development in the biopharmaceutical industry, like PEG precipitation along with UV, intrinsic and extrinsic fluorescence spectroscopy, as well as DSC and turbidity were employed for extensive physical stability characterization of these glycoforms to evaluate their solubility, tertiary structure, overall conformation, and aggregation propensity, respectively. The information provided by these techniques was relatively low in molecular resolution; where in the signals were an average value of all the conformations of these proteins. Such data sets still served as a strong foundation,

from which more detailed biophysical analysis was developed to monitor subtle changes in HOS upon glycosylation which was by exposing the proteins to a wide range of stresses. Thus, conformational stability is used as a sensitive surrogate for probing for subtle differences in HOS between the different IgG1-Fc glycoforms.

Forced degradation studies expose the molecules to extreme conditions and allows for detection of subtle higher order differences in a short amount of time. In our studies, we exposed the four IgG1-Fc glycoforms to a wide range of pH (4-7.5 with 0.5 unit increments) and temperature conditions (from 25°C-90°C with 1.25°C increments). These studies showed differences in physical stability with respect to glycosylation across the different glycoforms. We observed that the physical stability profile of IgG1-Fc glycoforms showed a trend of decreasing stability with decreasing the glycan size. Physical stability of the HM-Fc and Man5-Fc was the highest, followed by GlcNAc-Fc, and the least stability was observed for N297Q-Fc. It was also observed that the GlcNAc-Fc and N297Q-Fc showed higher aggregation propensities above pH 5. Further, the forced degradation studies allowed us to develop stability indicating assays (intrinsic and extrinsic fluorescence spectroscopy as well as OD350 turbidity) which required least amount of material and successfully detected subtle changes in HOS of these proteins. These high throughput techniques developed in this study can be essential tools in early candidate selection and assessing developability of mAbs where only small amounts of material are available. Further, the above stability indicating assays were utilized for monitoring the physical stability of various mixtures of these glycoforms (in Chapter 3) and also can be employed for future long-term stability studies of these four glycoforms. Additionally, the forced degradation studies allowed us to monitor the stability of these four glycoforms in two different formulations (contain NaCl and sucrose) and helped us to select a better formulation.

A large amount of data was generated from these forced degradation studies in two different formulations over large pH and temperature conditions, which was utilized to develop data visualization tools (like EPD and radar charts) to make relative comparisons of the physical stability profile of the IgG1-Fc glycoforms. These tools present a complimentary approach to study and compare the HOS changes in these glycoproteins and offer a more efficient way to compare a large stability data sets obtained from multiple and various analytical techniques. Further, we utilized the EPD and radar charts to compare the physical stability of these four glycoforms of IgG1-Fc in two different formulations. This data visualization approach could be applied to comparability exercises or biosimilarity where the products are compared pre and post changes such as process and formulation changes or when the biosimilar formulation might be different than the originator, respectively.

In terms of future work, although the biophysical stability data sets, along with EPD and radar charts analysis, showed subtle differences between these proteins, it will be interesting to correlate these forced degradation studies with real time stability studies of these glycoforms by the same or different analytical tools for monitoring the physicochemical stability during storage. In addition, a major analytical challenge for the utility of these novel data visualization tools for comparability and biosimilarity applications will be their ability to define the precision of EPD's phase transitions and radar chart's clusters for incorporating the degree of variability observed during data collection and this could be addressed in future work. Finally, this approach of producing well-defined IgG Fc glycoforms from yeast and *in vitro* enzyme synthesis can be utilized in future to prepare more human like complex glycoforms like G0, G0F, G2F, G2 and sialic acid. The HOS analysis of full length mAbs as a function of Fc N-glycosylation should also be studied; however, it can be complicated by glycosylation present in Fab regions of certain

mAbs. It would be interesting in future studies to see if N-glycosylation in Fc can affect the antigen binding of these glycoforms in their Fab domains.

5.2.2 Chapter 3

After initial qualitative comparisons of HOS and physical stability profiles of the four IgG1-Fc glycoforms, the next goal was to develop a quantitative comparative mathematical model to assess biosimilars vs originator molecules. As a step to achieve that, the four well-defined model glycoforms of IgG1-Fc showing a wide range of biophysical (studied in Chapter 2), chemical and biological (studied in other KU laboratories) properties were mixed in various proportions to potentially mimic heterogeneity in glycosylation that may be observed in biosimilar vs. originator drug products. Seven mixtures were prepared and were predicted to have subtle and evident differences in receptor binding and physicochemical properties. The study in Chapter 2 allowed us to understand the properties of the individual well-defined glycoforms beforehand, and hence we were able to optimize the properties of mixtures and expected them to show subtle (90% mixtures of HM-Fc with Man5-Fc, GlcNAc-Fc and N297Q-Fc) or evident differences (50% mixtures of HM-Fc with Man5-Fc, GlcNAc-Fc and N297Q-Fc). Another complex mixture was prepared which had 25% of all the four glycoforms of IgG1-Fc. The previously studied individual four well-defined IgG1-Fc glycoforms in Chapter 2 were utilized as controls in this study. Many of the physical characterization stability indicating assays that were developed in Chapter 2 were utilized in this study to investigate the ability of these techniques to successfully detect the expected higher order structural differences between these mixtures. These studies demonstrated high sensitivity of PEG precipitation solubility assay and DSC for distinguishing between the mixtures at two different pH conditions (4.5 and 6.0). Stress condition at pH 4.5 allowed monitoring the differences in the mixtures to a greater extent than

pH 6.0. All the biophysical data sets generated from these studies are being utilized by the Deed laboratory at KU, to develop a mathematical model, which will be able to predict biosimilarity quantitatively. The ability to accurately predict differences between the mixtures showed the importance of these routinely used high-throughput techniques in evaluating comparability and biosimilarity and indeed these form the foundation of comparability exercises. As mentioned by the FDA "the more comprehensive and robust the comparative structural and functional characterization is, the stronger the scientific justification for a selective and targeted approach to animal and/or clinical testing." [4] We see that this array of biophysical techniques were able to detect changes in the mixtures of different glycoforms that were not subtle, but still can be useful in comparative biosimilarity exercises.

In terms of future work, mAb biosimilars are more complex and have multiple distributions of glycoforms, along with the entire molecule vs an antibody fragment, and can be formulated in different excipients. These variables could make it difficult for the global biophysical tools to distinguish between subtle differences of a biosimilar and an innovator. It will be interesting to see if the above biophysical characterization tools can identify and characterize excipients-related impurities in these glycoform mixtures and their ability to critically assess the differences in detail. It should be noted that changes in N-glycosylation patterns might lead to measurable changes in biological activity but might not lead to changes is HOS. Also, subtle HOS changes due to different glycans might not be detected by biophysical techniques.[5] Hence, in such cases were biophysical tools are not sensitive to demonstrate any changes, more advanced and high resolution tools like HX-MS and NMR spectroscopy could find utility as described in the next chapter of this thesis work.

5.2.3 Chapter 4

Lastly, a higher resolution technique (HX-MS) was utilized to study the HOS of these glycoforms. HX-MS provides understanding of dynamics of proteins which can be correlated with physicochemical stability and biologically activity of mAbs. However, the relation between N-glycosylation, dynamics and stability of mAbs is complex and is often difficult to elucidate due to the heterogeneous nature of glycosylation.[6] Previously, not all changes in mAb glycosylation were shown to correspond to changes in dynamics, stability and biological activity making it difficult to correlate these attributes with glycosylation.[6] However, it is well known that complete removal of N-linked oligosaccharides severely affect a mAb's biological properties and stability although the underlying mechanism is unclear.[7] This dissertation contributed towards exploring the mechanisms of changes in physical stability of IgG1-Fc (studied in Chapter 2) as a function of well-defined N-glycosylation by studying changes in local backbone dynamics of these glycoforms. The results were also correlated to physical stability results obtained from Chapter 2 along with chemical stability and biological function data (FcγRIIIa receptor binding data) of these glycoforms studied in other KU laboratories.

It was found that sequential truncation of N-glycans resulted in a trend of increased backbone flexibility of the IgG1-Fc most probably due to loss of multiple contacts with the protein backbone. We demonstrated that sequentially decreasing the glycan size from high mannose (Man8-Man12) to Man5, GlcNAc and non-glycosylated increased the backbone flexibility of IgG1-Fc molecules. The trends observed included Man5-Fc showing similar and relatively lowest flexibility of the glycoforms, intermediate increase in flexibility was shown by GlcNAc-Fc, and the non-glycosylated N297Q-Fc showed highest increase in flexibility of the IgG1-Fc (as compared to HM-Fc). However, high mannose glycans (Man8-12) showed sequential increase in flexibility if the C'E loop glycopeptide with increase in mannose content,

and was probably caused by steric effects of these bulky glycans, which weakened the interaction between the glycan and C_H2 domain as previously seen in sialic acid glycoforms of IgG2-Fc.[8]

Previously, increase in conformational flexibility was observed in a region in the C_H2 domain of mAbs in the presence of excipients[3] and salts[9], which was recognized as an aggregation hot spot.[9] In this study, we found increase in flexibility of this aggregation hot spot region in the C_H2 domains of GlcNAc and N297Q-Fc that make these glycoforms more susceptible to aggregation and conformational destabilization. We also identified another region that showed increase in flexibility with decrease in glycan size (in GlcNAc and N297Q-Fc) that might contribute to the aggregation (aggregation hot spot 2) of these glycoforms. This region, in spite of showing increased flexibility in the presence of excipients and salts, it was not recognized as an aggregation hot spot in previous studies with mAbs.[3,9]

Interestingly, results from FcγRIIIa binding data of these four glycoforms (studied in Tolbert lab at KU) were compared with these flexibility results and showed a correlation of decreased binding[10] with increase in flexibility in the receptor binding peptide (C'E loop) as the glycans were truncated. Chemical stability results of these four glycoforms from the Schoneich laboratory at KU, showed a complicated relationship with flexibility. Decreased rate and extent of deamidation of Asn-315 was observed with increased glycan size (in HM-Fc and Man5-Fc)[11] while we saw least flexibility of the Asn315 containing peptide in HM-Fc and Man5-Fc. However, rate of conversion of Trp-277 into glycine hydroperoxide was increased with increase in glycan size (highest for HM-Fc and Man5-Fc, lowest for GlcNAc and non-glycosylated N297Q-Fc IgG1-Fc),[11] while we saw lower flexibility in the Trp-277 peptide as the glycan size increased (in HM and Man5-Fc). These results are complicated by the potential of a different

impurity profile across the purified glycoform preparations due to differences in glycosylation (e.g., trace metal ion content). This possibility should be considered in future work.

This study improves our understanding of N-glycosylation and its impact on chemical stability, physical stability, biological activity and flexibility of these well-defined IgG1-Fc glycoforms. In terms of future work, flexibility trends of the four glycoforms of IgG1-Fc observed from this study can also be applied to full length mAbs of the same IgG subclass of IgG as well as other subclasses as they have almost identical amino acid sequences (except a few amino acid residues) in the N-glycosylation site with the Fc domain. This approach should also be utilized further for studying complex and well-defined glycoforms of full length mAbs that showed subtle differences in physical stability but significant differences in Fc ɣ receptor binding.

It was observed previously that even though forced degradation studies showed differences between complex glycoforms and aglycosylated IgG mAbs, their long term stability was not affected by glycosylation.[12,13] Hence, changes in physical and chemical stability and receptor binding of different glycoforms of mAbs can be explored upon long-term storage and/or stressed conditions in a variety of excipients containing liquid formulations. This future work may help better explain and understand the inter-relationships between changes in real time protein stability with respect to glycosylation from the outlook of local dynamics, physicochemical stability and biological activity.

Although, higher resolution analytical tools like HX-MS have not been routinely utilized especially in early stages of protein drug formulation development due to their high cost and requirement of highly specialized expertise, the increased utility of HX-MS in protein formulation development has been demonstrated in this work and other work from our

laboratories.[14] It is also been shown to be valuable in high priority activities like lot-to-lot comparisons as well as comparability and biosimilarity assessments.[15] Even though utilization of higher resolution-tools to find subtle changes in HOS of mAbs for comparability and biosimilarity assessments provides state-of-the-art structural information of a protein molecule in a pharmaceutical dosage form, a lot of time and resources are still needed, not only to make HX-MS more accessible for routine pharmaceutical development, but also to figure out the clinical consequences, if any, of these structural differences.[1] The holistic approach to study local flexibility with respect to physicochemical stability and biological activity of well-defined IgG1-Fc glycoforms described in this work shows the promise of HX-MS as a tool for protein formulation development as well as comparability and biosimilarity assessment of glycosylated full length mAbs.

5.3 References

1. Houde DJ, Berkowitz SA. 2015. Chapter 14 - Biophysical Characterization: An Integral Part of the "Totality of the Evidence" Concept. Biophysical Characterization of Proteins in Developing Biopharmaceuticals, ed., Amsterdam: Elsevier. p 385-396.

2. Berkowitz SA, Engen JR, Mazzeo JR, Jones GB 2012. Analytical tools for characterizing biopharmaceuticals and the implications for biosimilars. Nature reviews Drug discovery 11(7):527-540.

3. Manikwar P, Majumdar R, Hickey JM, Thakkar SV, Samra HS, Sathish HA, Bishop SM, Middaugh CR, Weis DD, Volkin DB 2013. Correlating excipient effects on conformational and storage stability of an IgG1 monoclonal antibody with local dynamics as measured by hydrogen/deuterium-exchange mass spectrometry. Journal of pharmaceutical sciences 102(7):2136-2151.

4. 2015. U.S. Food and Drug Administration. Guidance for Industry- Scientific Considerations in Demonstrating Biosimilarity to a Reference Product.

5. Houde DJ, Berkowitz SA. 2015. Chapter 2 - Biophysical Characterization and Its Role in the Biopharmaceutical Industry. Biophysical Characterization of Proteins in Developing Biopharmaceuticals, ed., Amsterdam: Elsevier. p 23-47.

6. Houde D, Peng Y, Berkowitz S, Engen J 2010. Post-translational Modifications Differentially Affect IgG1 Conformation and Receptor Binding. Molecular and Cellular Proteomics.

7. Subedi GP, Barb AW 2015. The Structural Role of Antibody N-Glycosylation in Receptor Interactions. Structure 23(9):1573-1583.

8. Fang J, Richardson J, Du Z, Zhang Z 2016. Effect of Fc-Glycan Structure on the Conformational Stability of IgG Revealed by Hydrogen/Deuterium Exchange and Limited Proteolysis. Biochemistry 55(6):860-868.

9. Majumdar R, Manikwar P, Hickey JM, Samra HS, Sathish HA, Bishop SM, Middaugh CR, Volkin DB, Weis DD 2013. Effects of salts from the Hofmeister series on the conformational stability, aggregation propensity, and local flexibility of an IgG1 monoclonal antibody. Biochemistry 52(19):3376-3389.

10. Okbazghi SZ, More AS, White DR, Duan S, Shah IS, Joshi SB, Middaugh CR, Volkin DB, Tolbert TJ 2016. Production, Characterization, and Biological Evaluation of Well-Defined IgG1 Fc Glycoforms as a Model System for Biosimilarity Analysis. Journal of pharmaceutical sciences 105(2):559-574.

11. Mozziconacci O, Okbazghi S, More AS, Volkin DB, Tolbert T, Schoneich C 2016. Comparative Evaluation of the Chemical Stability of 4 Well-Defined Immunoglobulin G1-Fc Glycoforms. Journal of pharmaceutical sciences 105(2):575-587.

12. Jung ST, Kang TH, Kelton W, Georgiou G 2011. Bypassing glycosylation: engineering aglycosylated full-length IgG antibodies for human therapy. Current opinion in biotechnology 22(6):858-867.

13. Hristodorov D, Fischer R, Linden L 2013. With or without sugar? (A)glycosylation of therapeutic antibodies. Molecular biotechnology 54(3):1056-1068.

14. Majumdar R, Middaugh CR, Weis DD, Volkin DB 2015. Hydrogen-deuterium exchange mass spectrometry as an emerging analytical tool for stabilization and formulation development of therapeutic monoclonal antibodies. Journal of pharmaceutical sciences 104(2):327-345.

15. Fang J, Doneanu C, Alley WR, Jr., Yu YQ, Beck A, Chen W 2016. Advanced assessment of the physicochemical characteristics of Remicade(R) and Inflectra(R) by sensitive LC/MS techniques. mAbs 8(6):1021-1034.